Biodiversity and spatial ecology of arctic sponge grounds in the Nordic Seas

Heidi Kristina Meyer

Thesis for the degree of Philosophiae Doctor (PhD)
University of Bergen, Norway
2022

UNIVERSITY OF BERGEN

Biodiversity and spatial ecology of arctic sponge grounds in the Nordic Seas

Heidi Kristina Meyer

Thesis for the degree of Philosophiae Doctor (PhD)
at the University of Bergen

Date of defense: 17.06.2022

Year: 2022

Title: Biodiversity and spatial ecology of arctic sponge grounds in the Nordic Seas

Name: Heidi Kristina Meyer

Print: Skipnes Kommunikasjon / University of Bergen

To Hans Tore Rapp and his love of sponges

Table of Contents

Scientific environment

This PhD project was funded as a four-year position at the University of Bergen. The work presented in this thesis was carried out at the Department of Biological Sciences in the Deep-Sea Biology research group and as part of the Center for Deep Sea Research at the University of Bergen. The work was part of the European Union's Horizon 2020 research and innovation programme "SponGES: Deep-sea sponge ground ecosystems of the North Atlantic, an integrated approach towards their preservation and sustainable exploitation", grant agreement number 679849. The University of Rhode Island hosted a BIIGLE 2.0 server for the video annotation conducted in **Paper 4**.

UNIVERSITY OF BERGEN
Faculty of Mathematics and Natural Sciences

Acknowledgements

I am beyond thankful for my incredible supervision team, who has been supportive and encouraging throughout my entire PhD. This project took me around the world, from a conference in Colombia to a course in Svalbard to days at sea in the Arctic, and none of that would have been possible without the support and encouragement of my main supervisor, Hans Tore Rapp. You were inclusive since the first day we met, and you welcomed me with open arms when I flew to Bergen for my interview. You encouraged me to participate in conferences and classes that took me away from Bergen and emphasized the importance of taking time away from work to enjoy the company of family and friends and pursue my hobbies. Our time together was too short, but I am grateful for every second of it. Thank you for giving me the chance to work with you and to learn more about these amazing communities.

Henrik Glenner stepped in as my new main supervisor at the University of Bergen when the world felt like it was ending. You always had your door open to me when I needed to chat about everything and nothing, whether it had to do with my project or random questions that popped up during the day. I've shared many laughs with you (over many cups of coffee), and I am so glad to be able to work with you more. Thank you for your wisdom and afternoon chats.

All my other supervisors (Andy, Martyn, Joana, and Ellen) have been so helpful throughout this journey, and while you may not be at the University of Bergen (anymore), you never failed to support me and provide me with the guidance I needed for this project. If it was not for Andy and Martyn during my masters at Bangor University, I would have never been introduced to the amazing world of arctic sponge grounds. Andy, you have given me so many opportunities and have been a constant support since we started working together. You have helped me grow as a scientist and person and I am so happy to have been able to work with you over these last 6 years. Martyn, you were the first person I really knew when I moved to Bergen and have always allowed me to come to you for any question I had about work, PhD expectations, and life. You have been a major support system throughout my PhD, and

I knew I could come to you for anything. Thank you for encouraging my ramblings and questions, teaching me about cool oceanographic systems that influence the sponges we know and love, and for just being there when I needed someone to talk to. I especially appreciate your help and support in the final leg of this work. Joana and Ellen, your support and guidance has been so valuable throughout these years. You encouraged me to reach for opportunities, provided incredible resources, and were always there to help when I needed it. You never cease to amaze me with how a strong woman in science can look like, and I am constantly in awe of your drive and accomplishments. You inspire me to be better and I thank you for that.

A special thanks to the Deep-Sea Biology research group (Mari, Tone, Pedro, David, Solveig, Anita, Anna, Ida, Runar, Hasan, Petra, Francesca, Francisca, Adriana, Jon, Achim, Emily, Katharina, Victoria)! Our coffee breaks, social gatherings, and overall comradery has been a saving grace throughout these years. You welcomed me into the group with open arms and fun discussions. Our group is what exactly what I imagined a healthy research group to be. Special shout-out to Mari, Tone, and Pedro for answering my constant questions about sponges and megabenthic communities on AMOR, especially in the last few months. Thank you, Francisca, for being a mentor throughout the PhD and being there to talk when things were tough. Thank you, David, for always being up for talking about popular culture, books, games, and art, I value our conversations and laughs. Thank you, Ida, for the support in the last few weeks of the PhD, I appreciate everything you have done for me.

Thank you to all the great early career researchers in the SponGES project, you are all so inspiring and I am so happy to have been able to meet you and collaborate with you. I hope we can celebrate our accomplishments together in person someday soon. Thank you to the members of the SponGES team who helped me grow as a researcher. To the Dungeons and Scientists group, thank you for the fun nights of escaping science by adventuring into the cold unknown or descending into the deep below.

I would like to thank my family and friends for their constant support during this adventure. To my mom for always being there for me when I needed to talk and for supporting my decisions me even when we live so far away from each other. To Hanna, thank you for the deep talks, fun walks, spooky movie nights, and for being a great and compassionate friend. And finally, to Martin. I am so happy to have you and Nellie in my life and to have your encouragement during this journey. You always advocated for me to do what was best for myself and took care of me when life was tough. You have been there for me during the best and worst parts of my PhD, and I am beyond grateful to have you in my life. You are amazing, you are my rock, and I appreciate you. Thank you for your support, kindness, humor, and everything you do.

I am so grateful for everyone I have met along my journey. Thank you all.

Bergen, April 2022
Heidi Kristina Meyer

Summary

Sponge grounds are biogenic habitats formed by large structure-forming sponges in the deep-sea. They are biodiversity hotspots because they provide associated fauna a place of refuge, additional substratum, foraging areas, and can act as nursery grounds for many demersal fish. Sponge grounds have a global distribution, though there has been an increased focus in the North Atlantic in recent years due to the Horizon 2020 funded SponGES project. While there are a variety of sponge ground types based on their main sponge composition (monospecific and multispecific) or distribution (temperate, boreal, and arctic), there has been relatively little scientific focus on arctic sponge grounds, in terms of biodiversity, community ecology, and distribution. With potential imposing threats (e.g., climate change, bottom fishing, deep-sea mining) to arctic deep-sea communities such as arctic sponge grounds, there is a clear need to form a baseline understanding of these communities and their spatial ecology.

The main aims of this thesis were to fill the current knowledge gaps of arctic sponge ground biodiversity and spatial ecology in the Nordic Seas. More specifically, this project aimed to: 1) describe the megafauna composition and diversity of arctic sponge grounds to improve on their current habitat classification; 2) examine biotic interactions occurring within the sponge grounds to evaluate the ecological services arctic sponge grounds provide; 3) investigate the spatial distribution of arctic sponge grounds and the characterising megafauna to identify how communities are distributed on a seascape and how megafauna are assembled within a habitat; and 4) explore the primary abiotic drivers that influence the distribution and community structure of arctic sponges grounds and their inhabitants in order to understand what conditions sponge grounds need to form and thrive.

This thesis provides the first description of the oceanographic setting of Schulz Bank, a seamount on the Arctic Mid-Ocean Ridge used as a case study site for majority of the thesis and evaluates how the oceanographic conditions benefit the communities the seamount supports (**Paper 1**). The visual data collected from remotely operated vehicles (ROV) at various sites allowed us to test and refine annotation and statistical

methodology that can be employed in future research for characterising benthic communities, exploring their distribution, and identifying their abiotic drivers (**Papers 2–4)**. Furthermore, this thesis further highlights the potential of using AUVs for habitat mapping at small scales (<10 m) by identifying the fine-scale spatial patterns of arctic sponge ground fauna for the first time and visualizing how megafauna are assembled within their habitat **(Paper 2)**.

The work presented in the thesis forms a baseline understanding of the different types of arctic sponge grounds on Schulz Bank and builds on the limited scientific understanding of arctic sponge ground community and spatial ecology. Based on the results of this thesis, various new arctic megabenthic communities (biotopes), comprised of vulnerable marine ecosystem (VME) characterising taxa, were classified and are being proposed to the habitat classification system, European Nature Information System (EUNIS). These classifications can further improve habitat mapping and species distribution modelling capabilities of arctic megabenthic communities in the future. The extensive annotation of visual data identified key ecological roles that the sponge grounds provide to the associated megafauna, which can be further evaluated. Our work enhances the current understanding of abiotic drivers that influence arctic sponge ground distribution, although there is still a clear need to further build on this knowledge. Furthermore, our findings show that Schulz Bank is a prime candidate for protection due to its diverse and vulnerable communities, the ecological services the communities provide, and the relatively pristine condition the seamount is currently in. The work from this thesis has improved the understanding of sponge ground community and spatial ecology and developed tools and datasets that have been used in other work in the field. This thesis shows that arctic sponge grounds are important habitats in the Nordic Seas and highlights the need to form a baseline understanding of arctic benthic communities, especially in light of potential anthropogenic disturbances in the future.

Abbreviations and Terminology

AMOR – Arctic Mid-Ocean Ridge

AUV – Autonomous underwater vehicle

BIIGLE – Bio-Image Indexing and Graphical Labeling Environment

CTD – Conductivity, temperature, depth

HMA sponges – Sponges with high microbial abundance

LMA sponges – Sponges with low microbial abundance

MPA – Marine protection area

Monospecific sponge ground – sponge grounds characterised by a single sponge species

Multispecific sponge ground – sponge grounds characterised by multiple sponge species

Ostur – Sponge ground primarily dominated by sponges of the *Geodia* genera, either in abundance or biomass or both

ROV – Remotely operated vehicle

Spicule mat – Carpet-like substratum made up of dead sponges

Visual data – Video or imagery footage collected from ROV or AUV surveys

VME – Vulnerable marine ecosystem

List of publications

Paper 1

Roberts, E.M., Mienis, F., Rapp, H.T., Hanz, U., **Meyer, H.K.**, Davies, A.J. (2018). Oceanographic setting and short-timescale environmental variability at an Arctic seamount sponge ground. Deep-Sea Research I, 138, 98–113. https://doi.org/10.1016/j.dsr.2018.06.007.

Paper 2

Meyer, H.K., Roberts, E.M., Rapp, H.T., and Davies, A.J. (2019). Spatial patterns of arctic sponge ground fauna and demersal fish are detectable in autonomous underwater vehicle (AUV) imagery. Deep-Sea Research I, 153:103137. https://doi.org/10.1016/j.dsr.2019.103137.

Paper 3

Meyer, H.K., Roberts, E.M., Mienis, F., and Rapp, H.T. (2020). Drivers of megabenthic community structure in one of the world's deepest silled-fjords, Sognefjord (Western Norway). Frontiers in Marine Science, 7:393. https://doi.org/10.3389/fmars.2020.00393.

Paper 4

Meyer H.K., Davies, A.J, Roberts, E.M., Xavier, J.R., Ribeiro, P.A., Glenner, H., and Rapp, H.T. Beyond the tip of the seamount: Distinct megabenthic communities found beyond the charismatic summit sponge ground on an arctic seamount (Schulz Bank, Arctic Mid-Ocean Ridge). Submitted to Deep-Sea Research I.

1. Introduction

1.1 A brief introduction to sponges (phylum Porifera)

Sponges (phylum Porifera Grant, 1836) are filter-feeding invertebrates found in all bodies of water: freshwater and marine, Arctic to Antarctic, and from the intertidal zone to the deepest parts of the ocean. There are currently more than 9,000 species described, though it is estimated to be more than 15,000 species alive, with four classes: Demospongiae Sollas, 1885, Hexactinellida Schmidt, 1870, Calcarea Bowerbank, 1862, and Homoscleromorpha Bergquist, 1978 (van Soest et al., 2012). They are considered generally sessile fauna, though there has been indications that sponges can move (Bond and Harris, 1988; Kahn et al., 2020; Morganti et al., 2021), and may leave behind spicule trails as they attempt to find more suitable conditions (Morganti et al., 2021).

Sponges filter the surrounding water column for food and nutrients, through pores covering their bodies called ostia, and expel the filtered water out of a larger hole known as the osculum (Degnan et al., 2015). Some species of large structure-forming sponges (*Geodia* spp.) have been estimated to have an average daily filtration rate more than 250 L of seawater per sponge wet weight (kg) in *in situ* experiments and from 350 to 600 L of seawater per sponge wet weight (kg) in laboratory experiments (Kutti et al., 2013; Leys et al., 2018). When upscaled to an area with dense sponge coverage (~135,000 km^2), the sponge filtration rates have been modelled to be approximately 56.1 million litres of seawater daily (Pham et al., 2019), and consume more than 60 tons of organic carbon a day. Sponges contribute to bentho-pelagic coupling through this filtering process by extracting nutrients from the water column, further recycling dissolved organic matter into particulate matter consumed by detritivores (Bart et al., 2021; de Goeij et al., 2013; Hanz, 2021).

Sponges also host a diverse microbiome and specific microorganisms are consistently associated with specific sponge species (Taylor et al., 2007). The sponge microbiome can influence the types of compounds produced by the sponge, and can lead to new sources of novel bioactive compounds (Steffen et al., 2021, 2022 and

references therein). In general, there are two groups of sponge-microbe associations, which are referred to as high microbial abundance (HMA) and low microbial abundance (LMA) sponges. In the deep-sea, examples of HMA sponges would be demosponges of the *Geodia* genus and LMA sponges would be the hexactinellid *Schaudinnia rosea* (Fristedt, 1887) or the demosponge *Lissodendoryx (Lissodendoryx) complicata* (Hansen, 1885) (Busch et al., 2020; Steffen et al., 2022). These microbial associations are thought to influence the position in the trophic food web and feeding mechanisms. LMA sponges have been observed at the top of the food web whereas HMA sponges have a unique trophic position (Hanz, 2021). Furthermore, LMA sponges internally recycles nutrients and accumulates dissolved organic material from the water column before transfering detritus to the associated megafauna. HMA sponges, on the other hand, use their microbial associates to utilize dissolved inorganic and organic carbon (Bart et al., 2021; Hanz, 2021), and may even be able to break down and use ancient detritus as a food source (Morganti et al., 2022).

1.2 Sponge grounds of the North Atlantic

Sponge grounds are benthic communities made up of aggregations of large structure-forming sponges, and are known to form continuous or semi-continuous habitats (Beazley et al., 2013). While there is not a clear quantitative metric that classifies what constitutes a sponge ground based on the area or volume, studies have indicated the presence of sponge grounds are when the structure-forming sponges constitute up to 90% of non-fish biomass in trawl data (Klitgaard and Tendal, 2004), extend over at least 25m^2 (OSPAR, 2008), occur every 1 to 30 m^2 (ICES, 2009), or have 0.5 to 1 sponge per 1 m^2 in video-based surveys (Hogg et al., 2010; Kutti et al., 2013). But as of yet, there is no agreed upon definition and further exploration is needed to help parameterize our understanding of what constitutes a sponge ground.

There are different types of sponge grounds based on their distribution and composition of the main structure-forming sponges. Sponge grounds can be made up of multiple different structure-forming sponge taxa (multispecific) or one sponge species forming the habitat structure (monospecific). Multispecific sponge grounds in the North

Atlantic are often comprised of a mixture of demosponges (tetractinellid) and glass sponges (hexactinellid), such as those found in Davis Strait or in the Arctic (Beazley et al., 2013; Klitgaard and Tendal, 2004; Murillo et al., 2018). In some cases, there can be up to 50 different sponge species present in these sponge grounds (Klitgaard and Tendal, 2004). Examples of monospecific sponge grounds are the *Vazella pourtalesii* (Schmidt, 1870) sponge ground in Emerald Basin (Beazley et al., 2018; Hawkes et al., 2019), the *Pheronema carpenteri* (Thomson, 1869) sponge ground found on Porcupine Seabight (Rice et al., 1990), or the *Poliopogon amadou* Thomson, 1877 sponge ground on the Great Meteor seamount (Xavier et al., 2015).

Sponge grounds in the North Atlantic can also be classified as temperate, boreal, and arctic sponge grounds. The differences in these types of sponge grounds are based on the dominating sponge taxa, the specific water masses they occur in, and the general latitudes, although some sponge ground types may occur above or below their respective latitude belt (Klitgaard and Tendal, 2004; Hogg et al., 2010; Maldonado et al., 2016). Examples of temperate grounds are those formed by *V. pourtalesii* or *P. carpenteri*. These grounds are generally found within the 25–60˚ latitude belt. The *V. pourtalesii* grounds form on coarse sediment from 100–600 m depth on the eastern Scotian Shelf (Beazley et al., 2018; Hawkes et al., 2019; Maldonado et al., 2016). *Pheronema carpenteri* fields are found on muddy bottoms from 650–1550 m depth from the south of Iceland to the west of Scotland to the Azores and Morocco (Howell et al., 2016; Maldonado et al., 2016; Rice et al., 1990).

Boreal and arctic sponge grounds in the North Atlantic tend to be dominated by tetractinellid sponges of the genera *Geodia*, *Stelletta*, or *Stryphnus* (Klitgaard and Tendal, 2004; Maldonado et al., 2016). They have commonly been referred been to as ‘ostur’ or ‘cheese bottoms’ by fishers in the past (Klitgaard and Tendal, 2001). They form within the 40–75˚ latitude belt, from 150–1700 m depth on gravel or coarse sedimented bottoms (Maldonado et al., 2016). These types of sponge grounds are found from the western Barents Sea to south of Greenland to Newfoundland, and from Spitzbergen to the Canadian Archipelago to the Davis Strait and to northern Iceland and the Denmark strait (Klitgaard and Tendal, 2004). Boreal sponge grounds are

characterised by *Geodia barretti* Bowerbank, 1858, *Geodia macandrewii* Bowerbank, 1858, *Geodia atlantica* (Stephens, 1915), *Geodia phlegraei* (Sollas, 1880), *Stryphnus ponderosus* (Bowerbank, 1866), and *Stelletta normani* Sollas, 1880. Arctic sponge grounds are dominated by *Geodia hentscheli* Cárdenas, Rapp, Schander & Tendal, 2010, *Geodia parva* Hansen, 1885, *Stelletta rhaphidiophora* Hentschel, 1929 and the hexactinellid, *Schaudinnia rosea*. Arctic sponge grounds occur in the Arctic Basin, Davis Strait, Denmark Strait, and off East Greenland, and while they generally form separately from the boreal counterparts, there are cases where both sponge ground types are inhabiting the same region (e.g., Davis Strait and Denmark Strait) (Murillo et al., 2018).

1.2.1 Arctic sponge grounds

There have been few published studies on arctic sponge grounds specifically, thus our knowledge of the megafauna composition, sponge ground ecology, distribution, and abiotic drivers is extremely limited. Much of what we do know has been acquired during large-scale sponge ground studies or studies focused primarily on the dominant structure-forming sponges (Cárdenas et al., 2013; Klitgaard and Tendal, 2004; Murillo et al., 2018). From previous studies, arctic sponge grounds are characterised by hexactinellids (genera *Asconema*, *Trichasterina*, *Schaudinnia*, and *Scyphidium*), large demosponges (genera *Geodia* and *Stelletta*), and smaller demosponges (genera *Craniella* and *Thenea*) (Figure 1) (Cárdenas et al., 2013; Klitgaard and Tendal, 2004; Maldonado et al., 2016; Murillo et al., 2018). Klitgaard and Tendal (2004) found that *Geodia hentscheli, G. parva,* and *Stelletta rhaphidiophora*, with a frequent presence of *Schaudinnia rosea*, were discriminate sponges for arctic sponge grounds in the Northeast Atlantic, and Murillo et al. (2018) identified *G. hentscheli* and *S. rhaphidiophora* to be indicator species of arctic sponge grounds in the Canadian Arctic. Murillo et al. (2018) also determined that *Chondrocladia (Chondrocladia) grandis* (Verrill, 1879), *Bathydorus* sp. nov, and *Lissodendoryx (Lissodendoryx) complicata* are characteristic of arctic slope communities.

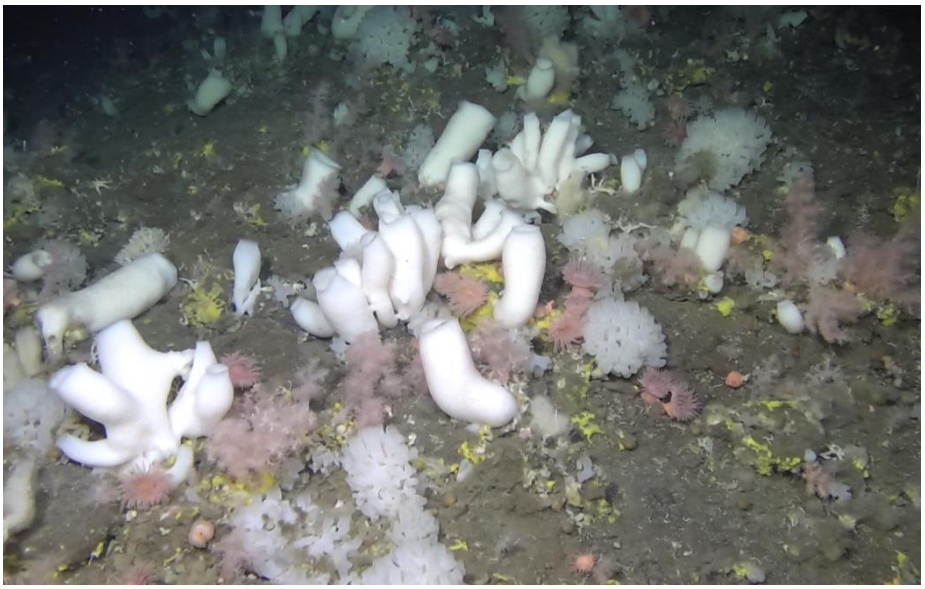

Figure 1. Arctic sponge ground on the summit of Schulz Bank, Arctic Mid-Ocean Ridge. Photo credits: SponGES project and University of Bergen, Norway.

The knowledge and documentation of associated megafauna of arctic sponge grounds is also relatively limited. From what we know from Klitgaard and Tendal (2004), arctic sponge grounds likely have the similar associated fauna composition as their boreal counterparts, where associated epifaunal groups consists of encrusting sponges, hydroids, zoantharians, bryozoans and ascidians. However, the authors also state that there needs to be more *in situ* investigations of the biological roles of sponge grounds to identify how sponge grounds are being utilized by other megafauna (Klitgaard and Tendal, 2004). A study by Henrich et al. (1992) describes the benthic communities on Vesteris Bank, a seamount in the Central Greenland Sea, where the summit is dominated by arctic sponge ground-forming sponges. Here, in addition to the large structure-forming sponges, smaller sponges, endobenthic ascidians, actiniarians, serpulid polychaetes, brittle stars, and sea stars were noted as associated megafauna. A more recent study of bedrock walls dominated by *G. hentscheli*, *G. parva*, and *S. rhaphidiophora* at the inactive vent field site, Mohn's Treasure, found the associated megafauna to be sponges, decapods, and crinoids (Ramirez-Llodra et al., 2020). In the Central Arctic Basin, arctic sponge grounds found on extinct volcanoes had glass and

calcareous sponges, bryozoan colonies, serpulid polychaetes, octocorals, shrimps, and echinoderms inhabiting the sponge grounds (Morganti et al., 2022).

1.3 Sponge grounds as biodiversity hotspots

1.3.1 Enhanced biodiversity

The structurally-complex biogenic habitats formed by sponges have been known to improve local biodiversity (Beazley et al., 2013; Bett and Rice, 1992; Hawkes et al., 2019; Hogg et al., 2010; Kenchington et al., 2013), by acting as a refuge from predators, substratum for settling organisms, foraging areas, and nursery and spawning grounds for a variety of taxa. In addition, sponge grounds can increase niche availability and habitat heterogeneity, and act as microhabitats for smaller organisms (Beazley et al., 2013; Buhl-Mortensen et al., 2010; Janussen and Tendal, 2007; McIntyre et al., 2016).

Diversity and density of associated megafauna has been shown to be higher within sponge grounds compared to nearby non-sponge ground localities (Beazley et al., 2013, 2015; Hawkes et al., 2019). A study by Hawkes et al. (2019) showed the mean number of species and mean density of associated megafauna to be significantly higher in the presence of *Vazella pourtalesii* compared to when the sponge was absent. Here, the average associated megafauna density was about four times higher in the presence of *V. pourtalesii* compared to when the sponge was absent. Similar findings have been observed in *Geodia* dominated sponge grounds in the Northwest Atlantic, where the mean density was three times higher in the presence of large structure-forming sponges compared to when they were absent (Beazley et al., 2015; Hawkes et al., 2019).

1.3.2 Biogenic structures and microhabitats

The morphology of the structure-forming sponges allows for invertebrates to use them as microhabitats (Klitgaard and Tendal, 2004), by settling directly on their surface or within their oscular cavities. Klitgaard (1995) found more than 240 macrofauna species living in or on common North Atlantic structure-forming sponge species. Specifically, some species of tetractinellids are known to host epibionts on their surface, such as the

encrusting sponge *Hexadella dedritifera* Topsent, 1913 commonly found on *G. parva* (Cárdenas et al., 2013). Bett and Rice (1992) theorized that many taxa use sponges as perches to gain access to enhanced food supply in the upper water columns. This was observed in a recent study where soft corals were positioned on large *Geodia* in the Central Arctic Ocean (Morganti et al., 2022). Sponges with larger oscules are also known to have taxa residing within their osculum, such as the isopod *Caecognathia robusta* (G. O. Sars, 1879) commonly found within *G. hentscheli* (Figure 2) (Cárdenas et al., 2013) or rock crabs and redfish found inside *V. pourtalesii* (Hawkes et al., 2019).

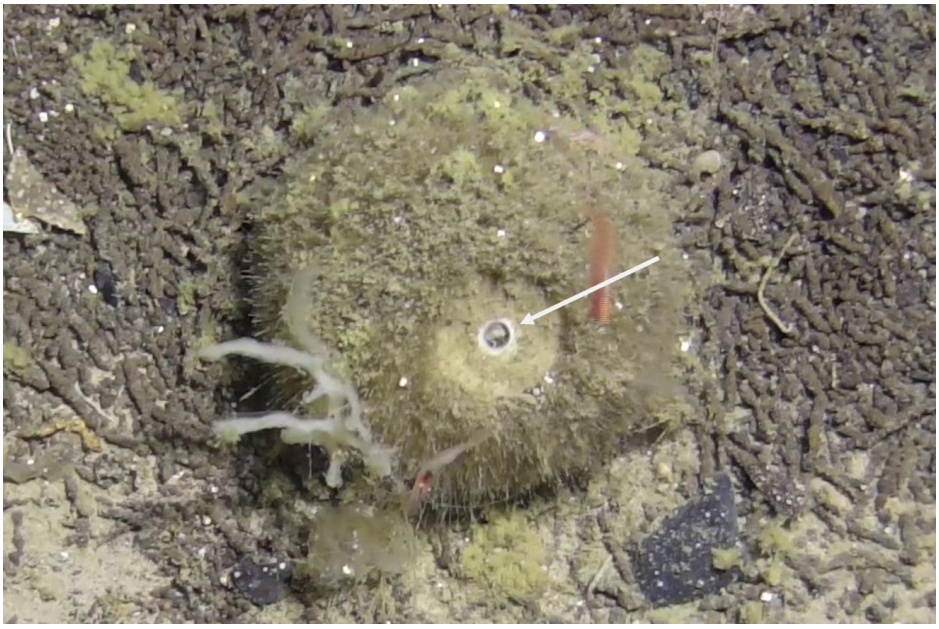

Figure 2. *Geodia hentscheli* with an isopod residing in the osculum (indicated by the white arrow). Photo credits: SponGES project and University of Bergen, Norway.

The sponges themselves produce a carpet-like substratum known as a 'spicule mat' when they die (Barthel et al., 1996; Bett and Rice, 1992; Klitgaard and Tendal, 2004), or shed their spicules while they move around the seafloor (Morganti et al., 2021). Spicule mats can be made up of centuries-old deceased sponges and the spicules can be used to indicate the age of the sponge ground through sediment samples (Murillo et al., 2016). These spicule mats can also be relatively thick, and some areas had documented spicule mats to be more than 10 cm thick (Henrich et al., 1992). Sessile fauna have been known to use spicule mat as substratum to settle on or reside within

(Bett and Rice, 1992), and it is not uncommon to find small or juvenile sponges, burrowing ascidians, nematodes, or polychaetes within spicule mat samples. Areas with the presence of spicule mat have been known to have increased megafaunal diversity compared to areas without, where Bett and Rice (1992) found the associated megafauna density in the presence of spicule mats to be nearly tenfold higher than areas without.

1.3.3 Fish nurseries

Fish and cephalopods have been observed using sponge grounds as nursery areas, where they lay their eggs either within the sponge oscule or directly on the spicule mat (Barthel, 1997; Bell, 2008; Kenchington et al., 2013; Klitgaard and Tendal, 2004). Barthel (1997) documented high densities of fish eggs, sometimes more than 8000 eggs, in the suboscular cavity of hexactinellid sponges of the genus *Rossella*. These eggs were not attached to any other substratum or within any other taxa, suggesting they have a preference for the *Rossella* sponges. Kenchington et al. (2013) noted egg cases belonging to the deep-sea cat shark, *Apristurus profundorum* (Goode & Bean, 1896) are regularly distributed around sponge grounds. Other studies have also documented juvenile fish associated with large sponges (Freese and Wing, 2003; Rooper et al., 2019), likely as a way to avoid predators. Overall, it appears that sponge grounds provide a safe refuge for many demersal fish to lay their eggs or rear the juveniles.

1.4 Spatial distribution of sponge grounds

1.4.1 Broad-scale distribution

Due to the numerous services provided by sponge grounds, there has formed a desire to understand and map the distribution of sponge grounds. Klitgaard and Tendal (2004) conducted an extensive and detailed survey of sponge grounds in the North Atlantic using data collected from bottom sampling methods (trawl, dredge, and sledge), from East Greenland to Northern Norway to Spitzbergen. This massive undertaking improved our knowledge of sponge ground distribution in the North Atlantic. Other broad-scale distribution surveys have been conducted in the eastern Canadian Arctic (Dinn et al., 2020; Murillo et al., 2018), the Northwest Atlantic (Murillo et al., 2012),

and Northeast Atlantic (Kazanidis et al., 2019; Vad et al., 2020). From these types of surveys, it was found that sponge grounds tend to form in fjords, continental shelves, slopes, ridges, and seamounts (Maldonado et al., 2016) and are thought to be distributed along specific water masses (Klitgaard and Tendal, 2004).

Since Klitgaard and Tendal (2004), there has been a rise in studies predicting the current distribution of sponge grounds over broad-scales (Beazley et al., 2018; Burgos et al., 2020; Howell et al., 2016; Knudby et al., 2013; Liu et al., 2021). Kernel density estimations have also been used to identify areas with dense aggregations of large structure-forming sponges to better describe their local and regional distribution (Kenchington et al., 2014). However, very few studies have included arctic sponge grounds either explicitly or separately in their studies (Howell et al., 2016; Knudby et al., 2013). This is likely due to the paucity of information on arctic sponge grounds, making the development of accurate models difficult to obtain. Furthermore, while some studies have produced outputs with low predictive power for arctic sponge grounds specifically (Liu et al., 2021), others have predicted arctic sponge ground-forming sponges to have high suitability along the Arctic Mid-Ocean Ridge (AMOR) and in the Norwegian and Greenland seas below 1500 m (Burgos et al., 2020). In order to enhance scientific understanding and the predictive capabilities of arctic sponge ground distribution over broad scales, it is clear that more research on arctic sponge grounds is needed.

1.4.2 Site-specific distribution

Many studies have performed site-specific surveys (e.g., seamounts, canyons, ridges, etc.) of sponge grounds better understand their local distribution and the drivers that influence their formation at a smaller scale (Beazley et al., 2013; Bett and Rice, 1992; Hawkes et al., 2019; Kutti et al., 2013; McIntyre et al., 2016; Morganti et al., 2022; Powell et al., 2018; Ramiro-Sánchez et al., 2019; Rice et al., 1990). In these areas, sponge grounds tend to form where there is irregular topography, with internal wave activity and increased bottom currents, such as shelf plateaus, shelf edges, bank sides, and on upper slopes.

For arctic sponge grounds specifically, there have been limited site-specific studies to date. For example, arctic sponge grounds have been described on the summits of arctic seamounts (Henrich et al., 1992; Morganti et al., 2022), where they formed on dense spicule mats at the summit and extended as far as 1000 m deep. Sponges that resemble arctic sponge ground-forming sponges were also described on bedrock walls at an inactive sulphide mound on AMOR as deep as 2385 m (Ramirez-Llodra et al., 2020), however the sponges observed in the study were not identified beyond morphospecies level (e.g., Demospongiae sp. 1). Apart from the listed studies, few surveys have investigated arctic sponge grounds specifically and occurrence data for arctic sponge grounds have been limited.

1.4.3 Fine-scale spatial patterns

Few studies have looked at the fine-scale spatial patterns of benthic communities (e.g., how the assemblages occur, where fauna have settled and their proximity to other conspecifics or species, etc.), even rarer are studies focused on sponge grounds. However, fine-scale spatial patterns and morphology can reveal much about the ecology and interactions occurring within a community based on the position of sessile fauna (Mitchell and Harris, 2020), such as larval dispersal, intra and inter-specific interactions, and access to food in the water column. For example, Mitchell and Harris (2020) used Spatial Point Process Analyses to detect competition between two octocoral species and habitat association between an octocoral species and hexactinellid species within the “Forest of the Weird”, a seamount sponge community in the Pacific Ocean. In addition to inferring biotic interactions, they were able to examine how abiotic drivers were influencing the fine-scale spatial patterns of the megafauna. In that study, they examined how megafaunal density increased with habitat heterogeneity, which corresponded to increased current speeds, and observed sponge mortality was likely a result of sponge disease (Mitchell and Harris, 2020). To date, there has been no examination of the fine-scale spatial relationships found within arctic sponge grounds.

1.5 Abiotic drivers of sponge grounds

The knowledge of the abiotic drivers influencing sponge ground formation and distribution is still limited, especially for the different types of grounds (and respective structure-forming species). Knudby et al. (2013) found that water mass characteristics (e.g., minimum salinity, temperature, depth) and bottom current speeds were major drivers for predicting sponge ground presence. When looking at geodiid-dominated grounds, the authors considered minimum salinity and depth to be the most important variable for predicting the species' presence (Knudby et al., 2013). Depth, however, does not necessarily influence a species distribution as it can be considered a proxy for many other variables and is strongly correlated with temperature, salinity, and water pressure (Burgos et al., 2020; Howell et al., 2016, 2010; McArthur et al., 2010). Therefore, to truly understand which drivers influences a species formation and distribution, it is important to look beyond geographical factors like depth, latitude, and longitude, and more towards the ecologically relevant variables that would fundamentally impact species distribution (e.g., temperature, bottom currents, dissolved oxygen, organic matter, food availability, etc.) (Burgos et al., 2020; Howell et al., 2010, 2016; McArthur et al., 2010).

Bottom current speed and the influence of internal waves are suspected to influence where sponge grounds form (Davison et al., 2019; Hanz et al., 2021; Klitgaard and Tendal, 2001, 2004). Areas with high hydrodynamic mixing and fluxes (e.g., areas with internal waves or accelerated local currents) are thought to influence transport of larval recruitment and the access of food and nutrients to filter-feeding organisms, thus leading to a higher accumulation of such taxa (Klitgaard and Tendal, 2004; McIntyre et al., 2016; Muñoz et al., 2012). Steep slopes subjected to the influence of internal waves are also supplied with additional resources like food particles and nutrients as the internal waves lead to increased turbulent mixing over the community (Hanz et al., 2021). Knudby et al. (2013) found that sponge grounds occurred in areas where the maximum bottom current speed was greater than 0.1 m s^{-1}. The increased current speed is suspected to influence sessile invertebrate distribution at a fine scale, where larval

dispersal and food supply are dependent on water flow (Bell et al., 2016; Howell et al., 2016).

Substratum characteristics and composition also play a large role in the composition and distribution of benthic communities (including sponge grounds) at a local scale (Bell et al., 2016; Sánchez et al., 2009). Larval attachment capability and selectivity is directly influenced by the availability and type of suitable substratum (Bell et al., 2016). For example, Bell et al. (2016) found that demosponges are associated with exposed rock, whereas hexactinellids show a preference towards more heterogeneous substratum. Furthermore, the authors note that sponge species richness was greater in areas that contained hard substrata with patches of soft sediment (Bell et al., 2016). Vertical rock walls are known to have increased current flow, which can provide beneficial conditions for filter- and suspension-feeding taxa (Buhl-Mortensen et al., 2020; Clark et al., 2010; Flach et al., 1998; Meyer et al., 2014) . Sponges are particularly sensitive to sedimentation clogging their filtration system (Bell et al., 2015; Kutti et al., 2015; Tjensvoll et al., 2013; Wurz et al., 2021), therefore areas with heavy sedimentation or resuspension of material can be detrimental to sponge survival. This is especially the case for sponges subjected to high sedimentation over long periods of time. However, some species of sponge have mechanisms to either pass sediment slowly through its filtration system or "sneeze" unwanted material out of their pores (Cummings et al., 2020; Hoffmann et al., 2004; Kahn et al., 2020), making it possible for them to withstand short periods of elevated sedimentation.

Looking at arctic sponge ground-forming species (*Geodia hentscheli* and *G. parva*), it is thought that temperature was the most important variable for the species' distribution (Burgos et al., 2020; Howell et al., 2016; Klitgaard and Tendal, 2004). These sponges tend to occur at temperature and salinity ranges of -1.76 to 8 °C and 34.8 to 35.5 ppt (Bett, 2012; Cárdenas et al., 2013; Klitgaard and Tendal, 2004; Murillo et al., 2018). Murillo et al. (2018) suggests that arctic sponge ground-forming species have narrow environmental niches and found them to be influenced by bottom temperature, depth, and summer primary production. The authors predicted that arctic sponge grounds are likely found between ~450 and 1395 m depth if the conditions are right.

However, apart from the study by Murillo et al. (2018) in the Canadian Arctic and the predictive distribution modelling study by Burgos et al. (2020), not much is known about the key abiotic drivers that influence the formation and distribution arctic sponge grounds in the North Atlantic.

1.6 Conservation status and vulnerability

1.6.1 Conservation status

As documented in **Section 1.3**, sponge grounds provide numerous ecological functions and are considered of conservational importance under Annex V of the Oslo-Paris (OSPAR) convention for the Protection of Marine Environment of the Northeast Atlantic (Howell et al., 2016; OSPAR, 2008). They are also classified as vulnerable marine ecosystems (VMEs) due to their fragility, long-life spans, and the structurally complex habitats they form (FAO, 2009; Hogg et al., 2010; OSPAR, 2008). Deep-sea sponges are generally long-living and can take decades to grow (Leys and Lauzon, 1998; Prado et al., 2021), which implies they probably have slow recovery rates after external disturbances. And since sponge grounds are regularly found on seamounts or ridges (which are common demersal fisheries and potential deep-sea mining targets) (Clark et al., 2010; Hogg et al., 2010), the likelihood of them being impacted by anthropogenic disturbances is high.

The classification of sponge grounds as VMEs has resulted in the closure of areas to demersal fishing until appropriate management and conservation measures have been established to reduce adverse impacts on the VMEs (FAO, 2009; Howell et al., 2016; Murillo et al., 2012; UNGA, 2006). However, these protection attempts have been slow to establish, and globally only 7.74% of the global oceans are within a marine protection area (MPA) as of 2020 (UN, 2021). Furthermore, there are few MPAs solely for sponge grounds (OSPAR, 2010), although some established MPAs do incorporate sponge grounds such as the Trænadypet coral MPA off the Northern Norwegian continental shelf (Kutti et al., 2013) or Rosemary Bank off the coast of Scotland (McIntyre et al., 2016). This is likely due to the limited information regarding the spatial distribution and

species composition of sponge grounds to date. Even with the increased effort on mapping sponge ground distribution (both current and predicted) in the North Atlantic (Beazley et al., 2021; Klitgaard and Tendal, 2004; Knudby et al., 2013; Liu et al., 2021), there is still limited knowledge regarding arctic sponge ground distributions. Therefore, it is important to improve our understanding of sponge ground distribution, community composition, and environmental drivers to aid in the implementation of appropriate management strategies. These efforts will help reduce the impact of anthropogenic disturbances on biologically important communities, like sponge grounds, in the future.

1.6.2 The effects of bottom-trawling

The most obvious threat to sponge grounds is the demersal fisheries industry (Hogg et al., 2010). Bottom trawling may be especially detrimental to sponge ground communities due to their slow recovery rate and fragility (Leys and Lauzon, 1998; Murillo et al., 2012). This can directly impact sponges through removing, damaging, fragmenting, dislodging, and crushing the sponges (and associated fauna) as bottom trawls pass over (Clark et al., 2016; Colaço et al., 2022). Indirect impacts can occur when resuspended material gets lodged in the sponge's filtration system which can reduce their filtration rates and cause smothering (see **section 1.5** for impact of sedimentation) (Hogg et al., 2010; Martín et al., 2014). Studies have shown considerable decrease in biomass and density in sponge grounds that were impacted by bottom trawling (Vieira et al., 2020), where a well-known *Pheronema carpenteri* ground showed a reduction in density from 1.09 to 0.03 ind. m^{-2} after being subjected to bottom fishing activity in recent decades. Furthermore, the sizes of sponges may also be affected by bottom trawling where intensely trawled areas have been shown to have smaller sponges than those with lower trawling efforts (Colaço et al., 2022).

Unfortunately, the slow recovery rate of structure-forming sponges makes it difficult for sponge grounds to recover adequately to their pre-disturbed state (especially over a short timescale). Without a comprehensive understanding of the life history traits of the sponges and the biotic interactions between the sponges and the associated taxa, it becomes difficult to know the true impact bottom trawling really has

on the specific community or how much time is needed for it to recover (Clark et al., 2019; Lotze et al., 2011; Vieira et al., 2020). If recovery was not possible or took place over an extended period of time, changes in ecosystem functioning or reduction in local biodiversity may occur due to the loss of available habitat or substratum for the associated megafauna to use (Bell, 2008; Colaço et al., 2022).

1.6.3 The impact of climate change

Like most marine communities, deep-sea communities are suspected to have distribution shifts towards higher latitudes and deeper waters as the current habitat conditions become unsuitable with climate change (Beazley et al., 2021; Morato et al., 2020). Structure-forming sponges typically require a set of specific favourable conditions in order to form dense aggregations (Beazley et al., 2021), and changes to the environmental conditions (e.g., increasing temperature, water mass structure, ocean acidification, etc.) can impact where the sponges (and their subsequent communities) can thrive. Increasing water temperatures can have severe impacts on the benthic organisms and structure-forming sponges, where temperature increase has been linked to disease susceptibility (Luter and Webster, 2017), compromised physiological fitness (Scanes et al., 2018), decreased pumping rates (Bell et al., 2018); and changes in suitable habitats (Beazley et al., 2021; Morato et al., 2020).

However, some structure-forming sponges have been shown to withstand large fluctuations in environmental conditions. For example, *Vazella pourtalesii* can withstand varying bottom temperature ranges of 8°C (from 4–12°C) in the Emerald Basin and is adapted to warmer conditions since it is also found in subtropical waters (Beazley et al., 2018, 2021). Because *V. pourtalesii* has a wide thermal tolerance, it was projected to have an increased range of suitable habitat, where predictions showed a northward shift and into deeper waters with the worst-case climate change scenario (Beazley et al., 2021). On the other hand, some structure-forming sponges find short-term environmental fluctuations to be detrimental to their health (González-Aravena et al., 2019).

Arctic sponges are thought to exhibit a narrow environmental niche (Murillo et al., 2018), and it is suspected that cold-adapted sponges may be most at risk for habitat loss as they reach their latitudinal and depth limits (Beazley et al., 2021; González-Aravena et al., 2019). Hindcast models have already displayed a change in environmental conditions in areas with arctic sponge grounds since 1948 (Samuelsen et al., 2022), where trends of changing temperatures and frequencies of anomalous events were modelled at sponge ground sites across the North Atlantic and Arctic. However, due to the limited research done on arctic sponge grounds, it has been difficult to accurately predict suitable habitats for future conditions (Liu et al., 2021).

1.6.4 The threat of deep-sea mining

Another threat to deep-sea sponge grounds is the potential for deep-sea mining in neighbouring areas. As mentioned before, sponge grounds are often found on seamounts or ridges, which are topographic features that may become targets for deep-sea mining in the future. This is because many seamounts and ridge systems are in proximity to hydrothermal vent fields that contain valuable mineral deposits like seafloor massive sulphide deposits or the seamounts themselves may have manganese crusts that may be targeted in the future (Boschen et al., 2015; Clark et al., 2010, 2021).

Since deep-sea mining is an emerging threat, not much information is available on how mining will impact benthic communities (both at targeted localities and nearby). It is believed the impacts will be similar (if not worse) to what has been observed with bottom trawling (Clark et al., 2010). Possible impacts are toxicity or smothering from sediment plumes produced while mining (see Vad et al., 2021 and references therein). Elevated sediment suspension has been linked to impacted physiological processes like silicate uptake, cellular stability and metabolic activity for *Geodia* sponges (Scanes et al., 2018). Furthermore, it is suspected that these sediment plumes can be transported away from the mining location, meaning that adjacent communities could be endangered if adequate regulations are not in place (Dunn et al., 2018; Ramiro-Sánchez et al., 2019). Therefore, to truly evaluate how deep-sea mining may impact benthic

communities, like arctic sponge grounds, there needs to be a baseline understanding of the communities' ecology and distribution before mining begins.

1.7 Using visual surveys to investigate the deep-sea

The deep-sea is difficult and expensive to survey as it is not as accessible as coastal or shelf habitats. Traditionally, physical extraction methods like trawling, dredging, and using benthic sledges were the main way to survey deep-sea communities like sponge grounds (Hogg et al., 2010), and are still used today. The collection of physical samples allow for biomass and biodiversity measurements, evaluation of species distribution, and identification of fauna to higher taxonomic levels (Biber et al., 2014; Hogg et al., 2010; Knudby et al., 2013; Murillo et al., 2012). Unfortunately, these methods can be damaging to vulnerable communities, like sponge grounds, and ultimately may result in slow recovery capabilities of the structure-forming sponges (see **Section 1.6.2**).

To overcome these difficulties and limit the amount of disturbance caused by physical extractive methods, visual surveying methods have become more common over the years, especially for sampling sensitive communities like sponge grounds (Beazley et al., 2013, 2015; Hawkes et al., 2019; Morganti et al., 2021, 2022). These methods include drop cameras, towed video surveys, autonomous underwater vehicles (AUVs), remotely operated vehicles (ROVs), and manned-submersibles (Biber et al., 2014; McIntyre et al., 2015). Visual surveys can provide estimations of biodiversity and biomass (Copeland et al., 2013; Grizzle et al., 2008; McIntyre et al., 2015, 2016; Rice et al., 1990; Savini et al., 2014), measure faunal growth (Prado et al., 2021), examine organismal behaviour (e.g., sponge trails, fish nursery, etc.) (Morganti et al., 2021; Purser et al., 2022), evaluate species distributions (as ground truthing techniques) (Van Audenhaege et al., 2021), identify anthropogenic material (e.g., plastics, ghost nets, ship falls) (Singh et al., 2007), and discover changes in substratum type (Bridges et al., 2021; Copeland et al., 2013; Savini et al., 2014). Although visual surveys can have some limitations that extraction surveys do not have (e.g., taxonomic resolution), visual surveys do provide a window into the deep-sea.

1.7.1 Autonomous underwater vehicles

Autonomous underwater vehicles (AUVs) are autonomous submersibles used to map the benthos without requiring active human involvement (Wynn et al., 2014). While following a pre-programmed course, they can collect a variety of data (e.g., images, multibeam bathymetry, water column properties, etc.) and are capable of manoeuvring across difficult terrain or inaccessible areas (Singh et al., 2017; Wynn et al., 2014). AUVs are beneficial because they do not require active human interaction (which can minimize sampling bias), can survey at a pre-programmed speed and altitude, and can be fitted with other oceanographic instruments to collect a variety of data during the survey. AUVs are generally less 'invasive' than other underwater surveying systems (e.g., ROVs or towed cameras), because they tend to use strobe lighting rather than floodlights and are relatively quiet (Morris et al., 2014; Pizarro and Singh, 2003). Furthermore, AUVs have the potential to cover large areas and produce extensive photomosaics (Singh et al., 2004), which can then be used to investigate spatial relationships based on how fauna are assembled in the mosaic (Ludvigsen et al., 2007).

However, the drawbacks of using AUVs for sampling deep-sea communities are that they may have power constraints that result in low lighting power, cannot collect samples to confirm identifications, or detect sudden obstructions (e.g., infrequent boulders) that can damage the AUV, especially if the AUV surveys are close to the seabed in order to record high-resolution seafloor imagery (Singh et al., 2004; Wynn et al., 2014).

Using AUVs could be an optimum way for surveying sensitive communities and mapping out their spatial patterns with a consistent camera angle, altitude, and speed. Yet very few surveys have used AUVs to study deep-sea sponge grounds (Powell et al., 2018), and none have used AUVs to survey arctic sponge grounds before.

1.7.2 Remotely operated vehicles

Remotely operated vehicles (ROVs) are unmanned submersibles tethered to research vessels and operate under direct human control. ROVs allow for the exploration,

interaction, and observation of the marine environment (Hogg et al., 2010; Macreadie et al., 2018; Wynn et al., 2014). They can be fitted with CTDs, multi-beam echosounders, side-scan sonars, high-definition cameras, and other tools necessary to achieve defined goals. During research dives, they can conduct long exploration and survey transects with high video resolution, collect physical samples from the seafloor and water column, navigate delicate landscapes, and conduct experiments like deploying chambers to examine the respiration of fauna or operate blade cores for studying infauna communities. High-resolution images collected from ROV video transects can be used to recreate deep-sea habitats through 3D models or photomosaics (Marsh et al., 2013; Mitchell and Harris, 2020; Singh et al., 2004, 2007).

However, the use of ROVs for benthic habitat mapping can be problematic at times for a variety of reasons. There are risks of sampling bias if there is a focus on specific phyla or charismatic areas. The manual adjustments of the ROVs can cause excessive residual movements and sediment suspension that may obscure the footage or damage the surveying area (Marsh et al., 2013). If the lasers, which are used for scaling, are turned off mid-survey, there may be difficulties in estimating areas, densities, or biomass in the surveyed region. The noise produced by ROVs can also deter mobile taxa (e.g., fish or cephalopods) and the continuous use of flood lights may impact organisms highly adapted to dark environments (Biber et al., 2014; Morris et al., 2014). And because the ROVs are tethered to the research vessel above, their spatial range and mobility is limited (Morris et al., 2014).

When it comes to sponge grounds, ROV surveys have provided insight into the community structure (Bo et al., 2012; Ríos et al., 2018), population and recovery status after bottom trawl impact (Colaço et al., 2022; Morrison et al., 2020), reproductive strategies (Teixidó et al., 2006), and mortality dynamics (Mitchell and Harris, 2020). Overall, ROVs have been a useful tool for surveying sponge grounds, although few have surveyed arctic sponge grounds (Morganti et al., 2021, 2022).

2. Study Objectives

The introduction highlights the clear knowledge gaps in the current community and spatial ecology of arctic sponge grounds. Much of the current literature have focused on the main structure-forming sponges (primarily of the *Geodia* genera), where the sponge ground ecological function and their associated megafauna remains largely unknown, especially for arctic sponge grounds. Furthermore, there is still limited information regarding the distribution and drivers of arctic sponge grounds. With increasing threats of bottom trawling, climate change, deep-sea mining, and other anthropogenic impacts, it is crucial to form a comprehensive understanding of these vulnerable marine ecosystems. The results presented in this thesis are meant to reduce this knowledge gap and can be further used to generate accurate habitat maps, model their predicted distribution, and implement effective management strategies for the future.

The overarching goal of this PhD thesis was to describe the **biodiversity**, **community composition**, and **spatial ecology** of arctic sponge grounds over varying spatial scales through the use of visual data. To achieve this goal, the project aimed to:

1. Describe the megafauna composition and diversity of arctic sponge grounds and other deep-sea benthic communities in the Nordic Seas.
2. Examine biotic interactions occurring within arctic sponge grounds between the structure-forming and associated taxa.
3. Investigate the spatial distribution of megafauna and communities over varying scales (site-specific and fine-scale).
4. Explore the primary abiotic drivers of the main megafauna and community structure over varying scales.

3. Materials and methods

The specific methodology is presented in detail in the respective papers (**Papers 1 – 4**). However, descriptions of the different case study sites, underwater surveying systems, and video annotation methods and software are provided below.

3.1 Case study sites

Multi-disciplinary research cruises were carried out as part of the SponGES project on the *RV G.O Sars* at Schulz Bank and Sognefjord during the summers of 2016 to 2018 (Figure 3). Visual surveys were conducted using the AUV *Hugin1000* and ROV *Ægir6000*. In addition to the visual surveys, physical specimens were collected during the cruises either through research trawls or during the ROV dives.

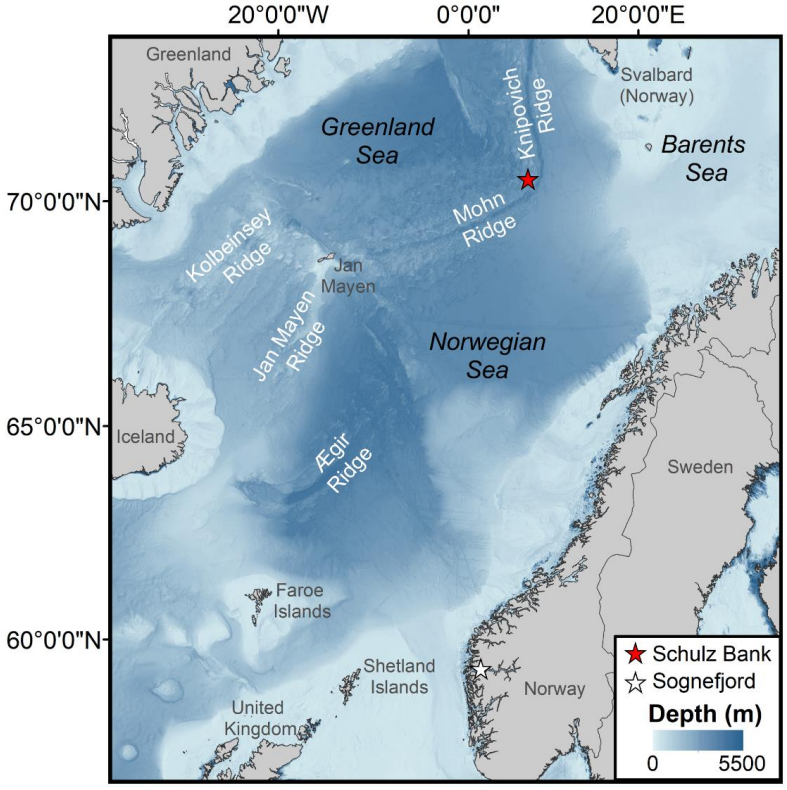

Figure 3. Map of the thesis case study sites (Schulz Bank (red) and Sognefjord (white)) surveyed during the SponGES cruises in the summers of 2016–2018 on the *RV G.O Sars*. Digital bathymetry with a resolution of 1/16 x 1/16 arc min was extracted from EMODnet Bathymetry Consortium (2020).

3.1.1 Schulz Bank – Arctic Mid-Ocean Ridge

The majority of the work in this thesis was either conducted on or included data from Schulz Bank (**Papers 1, 2, 4**), a seamount on the Arctic Mid-Ocean Ridge (AMOR). AMOR is an ultraslow-spreading ridge system made up of six ridge sections - Ægir, Jan Mayen, Kolbeinsey, Mohn, Knipovich, and Gakkel (Pedersen et al., 2021). It has a length of 4000 km and extends from the east of Iceland along Ægir Ridge to north of Svalbard into the Polar Basin at Gakkel Ridge (Johnson and Heezen, 1967; Pedersen et al., 2021).

Schulz Bank, previously referred to as 'Schulz Massive' (Tangen, 2011; Torkildsen, 2013), 'Schultz Massif' (**Paper 1**), or 'Schultz Massive' (Cárdenas et al., 2011, 2013; Cárdenas and Rapp, 2015) is located at the transition point from Mohn Ridge to Knipovich Ridge, at the interface between the Greenland and Norwegian Seas (Hopkins, 1991). It has a depth range of 580 m at the summit to 2700 m at the base. Three water masses surround Schulz Bank: the Norwegian Atlantic Water (salinity > 35, temperature > 2 °C) sits above the seamount; the Norwegian Arctic Intermediate Water (salinity ≈ 34.88, temperature ≈ 0.5 °C) interacts with the summit and slopes; and the Norwegian Deep Water (salinity ≈ 34.92, temperature ≈ -0.5 °C) occurs on the slopes and base (Hopkins, 1991; **Paper 1**). A complete description of the Schulz Bank oceanographic setting that has been further expanded on in **Paper 1** and by Hanz et al. (2021).

3.1.2 Sognefjord – Western Norway

Sognefjord is in Western Norway and Norway's longest (205 km) and deepest (1308 m) silled-fjord. The deep basin simulates deep-sea conditions, making Sognefjord a prime deep-sea laboratory that is more accessible than the oceanic deep-sea. Sognefjord was selected as a case-study site for **Paper 3** to test and refine the video annotation methodology that would be used in **Paper 4.**

The fjord is subjected to three water-masses (Storesund et al., 2017), where brackish water (salinity ≤ 33) dominates the surface (top 10 m), well-oxygenated

intermediate water (salinity 33–35) flows in and out of the fjord below the surface layer (10 m) to the sill-depth (170 m), and below this, dense Atlantic water (salinity ≥ 35) fills the fjord basin. The basin water is renewed every ~8 years (Buhl-Mortensen et al., 2020). Bottom conditions have been consistently reported to be ~7.4 °C (Witte et al., 2003), and oxygen concentration generally decreases with increasing water depth and distance into the fjord (Storesund et al., 2017).

3.2 Underwater surveying systems

All visual data used in this thesis was collected during the Horizon 2020 SponGES project cruises from 2016 to 2018 (Figure 4a). The imagery data annotated in **Paper 2** was collected by the AUV *Hugin1000* in 2016 (Figure 4b). The video footage annotated in **Papers 1, 3, and 4**, as well as in Morrison et al. (2020), was collected using the ROV *Ægir6000* from 2016 to 2018 (Figure 4c).

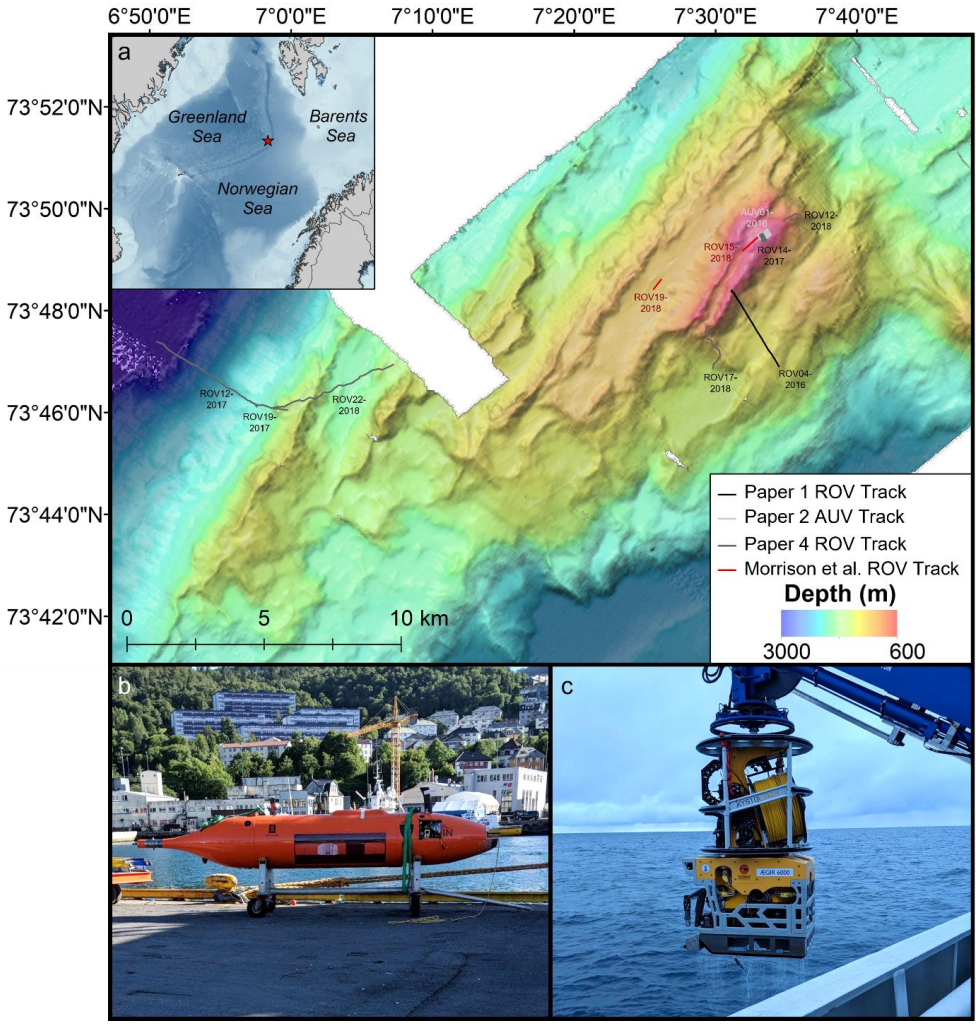

Figure 4. a) Schulz Bank bathymetric map with inset showing location on the AMOR in relation to Greenland, Svalbard, and Norway. The lines indicate locations of the visual surveys used in Papers 1, 2, 4, and Morrison et al. (2020). Bathymetric map provided by the Centre for Deep Sea Research, University of Bergen, Norway. This figure is an updated version of ***Figure 1*** seen in **Paper 4**. b) The autonomous underwater vehicle *Hugin1000* used for surveying the Schulz Bank summit in 2016. c) Deployment of the remotely operated vehicle *Ægir6000* during the 2018 SponGES cruise. Photo credits for b and c: Heidi Kristina Meyer.

3.2.1 AUV *Hugin1000*

Images annotated in **Paper 2** were collected from the Schulz Bank summit in 2016 by the Kongsberg AUV, *Hugin1000* (Figure 4b). *Hugin1000* is an AUV designed and manufactured by Kongsberg Maritime and owned by the Norwegian Defence Research Establishment (FFI). It has a length and diameter of 5.27 m and 0.75 m, respectively,

and weighs 1200 kg out of water. While *Hugin1000* has a depth rating of 3000 m depth, it currently operates up to 1000 m. For the study, *Hugin1000* was fitted with a SAIV SD208 dual conductivity, temperature, and depth (CTD) system, synthetic aperture sonar HISAS 1030, multibeam echosounder EM 2040, and a TileCam optical camera with a 10-megapixel resolution and 10 GB h^{-1} collection rate separated by ~1 m to a LED light bar containing 720 LEDS (Hagen, 2014). The AUV surveyed at an average speed of 1.54 ms^{-1}, with a maximum speed of 3.08 ms^{-1}.

Hugin1000 was deployed at the summit of Schulz Bank to map the summit sponge ground and generate a photomosaic of the scanned area. The AUV followed a pre-determined track that had a total of 47 overlapping lines with a length of ~435 m to maximize the surveying area, covering an area of 0.123 km^2 from 577–600 m depth. The images collected in the survey all contained the date, AUV depth, seafloor depth, altitude, slant range, ground range, heading, speed, and coordinates; and the CTD fitted to the AUV collected the *in-situ* water depth, temperature, and salinity.

3.2.2 ROV *Ægir6000*

The ROV *Ægir6000* (Figure 4c) was used to survey Schulz Bank and Sognefjord during the summers of 2016–2018 (**Papers 1, 3, and 4**). *Ægir6000* is a work-class ROV from Kystdesign AS (Haugesund, Norway). It has the dimensions of 2.75 x 1.70 x 1.65 m, with a load capacity of 400 kg. While it has a depth rating of 6000 m, it can currently operate up to 4700 m. *Ægir6000* has two Imenco Spinner II Shark Wide Angle 3G HD-SDI zoom cameras, where one is positioned at the top of the ROV, and the other is positioned toward the center of the ROV, directly above the lasers. The cameras have a zoom capacity of 30x, 72° diagonally and 65° horizontally angle of view, and a resolution of 1080p at 60fps. The videos collected from the center camera were annotated based on its relative positioning to the lasers and that the camera was more consistently down-ward facing during the surveys (**Papers 1, 3, and 4**). Lasers were not consistently on for **Papers 1 and 3**, but for **Paper 4**, the lasers had an average separation of 16 cm throughout all dives selected for the study.

3.3 Annotation methodology and software

There are challenges that come from multiple people annotating visual data from the same location or videos (e.g., inconsistent fauna identification, differences in annotation resolution, etc.) (Durden et al., 2016), and it is important to develop tools to reduce errors that may arise. Therefore, to ensure that video annotation was consistent between projects using visual data from the Schulz Bank, a workshop was conducted in 2019 to define methodological standards and procedures with other members of the SponGES project consortium. The methodology decided in the workshop was used for **Papers 4** and Morrison et al. (2020), and similar methodology for image selection and annotation was used for **Paper 3**. For these papers, all images were cropped in RStudio to maintain consistent field of views and exclude marring around the image edges. Images were cropped using the package "Magick" version 2.6.0 (Ooms, 2021). The cropping code used for all the images selected in **Papers 3 and 4**, as well as in Morrison et al. (2020), was: image_crop(test,"1500x1000+250+150"), where the numbers in the brackets represent the horizontal image size, vertical image size, cropping position on the horizontal axis, and cropping position on the vertical axis, respectively. Images selected for annotation had an image area between 1.5 to 6.5 m^2, downward facing camera, and no blurring or obstruction in field of view (e.g., sediment cloud, ROV arm, etc).

To ensure the risk of spatial autocorrelation was reduced, the images used in **Papers 1, 3, and 4** were extracted at time specific intervals (5 minute, 30 seconds, and 1 minute, respectively), whereas for **Paper 2**, the images were extracted pseudo randomly based on spatial separation between neighbouring images.

All fauna above approximately 1 cm in size were counted and identified to the lowest possible taxonomic resolution. Encrusting and branching taxa were counted based on their encrusting or branching group, due to the difficulty in identifying individuals of these taxa. Because organisms, especially sponges, are difficult to identify without physical specimens, in some cases they were identified to morphotaxa rather than to species level (e.g., Small globular demosponge 1). In **Paper 4**, the morphotaxa level was further refined to use open taxonomic nomenclature based on the

suggestions by Horton et al. (2021) so each morphotaxa had a specific OTU number to not be confused with other taxa (e.g., 'small globular sponge 123' in **Paper 4** rather than 'Demospongiae spp.' in **Paper 2** or 'small demosponge' in Morrison et al. (2020)).

In **Papers 3 and 4** and Morrison et al. (2020), a grid was overlayed on the images to be able to document the percent cover of the substrata. Substratum type for larger grain sizes (e.g., gravel, boulders, cobbles, etc.) was largely based on the Wentworth (1922) substrata categories, and grain size smaller than 1 cm was categorised as 'soft bottom'.

The majority of the annotation took place in ImageJ (**Papers 1, 2, 3**) as it was open-source, freely available, and can be used with most image types (Gomes-Pereira et al., 2016). However, ImageJ is labour intensive and can be prone to errors and oversight when checking fauna identifications and counts. This is due to ImageJ requiring the use of a spreadsheet software (e.g., Microsoft Excel) and manually checking annotations. Therefore, it was deemed problematic for annotating images from multiple ROV dives, and we switched to BIIGLE 2.0 when access to a secure BIIGLE 2.0 server became available (hosted through Dr. Andrew Davies at the University of Rhode Island). Hereafter, the annotation of visual data for **Paper 4** moved to BIIGLE. BIIGLE 2.0 is a more suitable annotation system for annotating multiple ROV dives because it has improved the management of annotations and allows for checking and changing annotations with ease (Gomes-Pereira et al., 2016; Langenkämper et al., 2017; Zurowietz et al., 2021). Furthermore, it is an optimal software for collaborating internationally as it is all online and every user can have specific roles (e.g., admin, guest, expert, editor).

4. Key results and discussion

The work presented in this thesis provides a comprehensive description of arctic sponge ground megafaunal composition and ecology in the Nordic Seas. The main findings and conclusions of each study presented in this thesis are described in the respective papers. The short-term oceanographic setting and first description of sponge distribution and abundance trends on Schulz Bank are provided in **Paper 1**. A detailed description of the prominent megafauna and their fine-scale spatial patterns on the summit of Schulz Bank was presented in **Paper 2**. The annotation and statistical methodology that would be used in future work was tested and refined in **Paper 3** by investigating megabenthic communities and their abiotic drivers in Sognefjord. A complete description the megafauna communities and their general distribution, depth range, and dominant substratum from base to summit of Schulz Bank was provided in **Paper 4**.

4.1 Megabenthic communities

While the general sponge composition on Schulz Bank was briefly described in **Paper 1**, the first detailed description of the sponge ground community structure on the summit of Schulz Bank was provided in **Paper 2** (Figure 5a). The summit sponge ground was characterised by large hexactinellids (*Schaudinnia rosea, Trichasterina borealis* Schulze, 1900*,* and *Scyphidium septentrionale* Schulze, 1900) and demosponges (*Geodia parva, Stelletta rhaphidiophora*, *Lissodendoryx (Lissodendoryx) complicata*), as well as smaller demosponges (*Hexadella dedritifera, Craniella infrequens* (Carter, 1876), *Polymastia thielei* Koltun, 1964*, Stylocordyla borealis* (Lovén, 1868), *Hemigellius* sp., and other unidentified demosponges), ascidians, anemones, soft corals (*Gersemia rubiformis* (Ehrenberg, 1834)), and echinoderms (*Tylaster willei* Danielssen & Koren, 1881). The demersal fish found on the summit were the Arctic skate (*Amblyraja hyperborea*), roughhead grenadier (*Macrourus berglax* Lacepède, 1801), and Greenland halibut (*Reinhardtius hippoglossoides* (Walbaum, 1792)). The descriptions made in **Paper 2** were supported and further expanded on in **Paper 4** to include all megafauna larger than 1 cm in the community descriptions. From this, we

observed variations in species composition from the top of the summit to the upper slopes, where *Asconema foliatum* (Fristedt, 1887) and *Thenea valdiviae* were present in high densities on the sloping regions of the summit sponge ground. The community composition of the primary sponges making up the summit sponge ground is consistent to the findings in other studies (Cárdenas et al., 2013; Klitgaard and Tendal, 2004; Maldonado et al., 2016; Murillo et al., 2018).

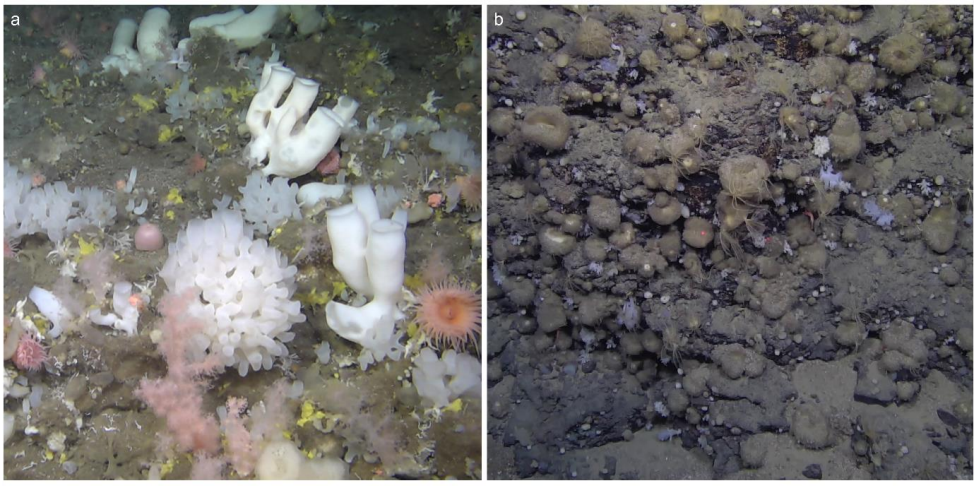

Figure 5. Arctic sponge grounds on the Schulz Bank, Arctic Mid-Ocean Ridge. a) Summit sponge ground characterised by glass sponges (*Asconema foliatum, Schaudinnia rosea*, *Scyphidium septentrionale,* and *Trichasterina borealis*), demosponges (*Geodia parva* and *Stelletta rhaphidiophora*), soft corals (*Gersemia rubiformis*), anemones, and ascidians. b) Sponge dominated bedrock wall dominated by demosponges (*Geodia parva*, *Geodia hentscheli*, and *Stelletta rhaphidiophora*), crinoids (*Poliometra prolixa*), and decapods (*Bythocaris leucopis*). Photo credits: SponGES project and University of Bergen, Norway.

Another arctic sponge community dominated by *G. hentscheli* and *G. parva* was found on bedrock walls in the deeper regions of Schulz Bank in **Paper 4** (Figure 5b). This type of sponge ground has not yet been described in detail in previous literature, although a similar community was documented on Mohn's Treasure, an inactive sulphide mound just south of Schulz Bank (Ramirez-Llodra et al., 2020). Arctic sponge grounds have generally been considered to form only on soft bottom from 150 to 1700 m depth (Burgos et al., 2020; Maldonado et al., 2016), whereas this community was documented mainly on bedrock walls beyond 1500 m. *Geodia hentscheli, G. parva,* and *S. rhaphidiophora* were identified to be the main structure-forming sponges, with the major associated taxa being sponges (Aphrocallistidae, *Lissodendoryx*

(Lissodendoryx) sp., *Amphidiscella monai* Tabachnick & Lévi, 1997, unidentified axinellids, and encrusting sponges), crinoids (*Poliometra prolixa* (Sladen, 1881)), decapods (*Bythocaris leucopis* GO Sars, 1879), and the occasional fish (*Lycenchelys sarsii* (Collett, 1871), *Lycodes frigidus* Collett, 1879, *Paraliparis bathybius* (Collett, 1879), and *Rhodichthys regina* Collett, 1879).

In addition to the main sponge grounds on the Schulz Bank, the slopes and base had distinct communities as well (**Paper 4**). Dense ophiuroid aggregations covered the coarse-sedimented upper slopes and rocky outcrops contained the occasional sponge or scalpelid (*Catherinum striolatum* (Sars G.O., 1877)), which was also observed by Morrison et al. (2020). Patchy aggregations of *Neohela* sp. burrows were present in much of the soft-sedimented regions of Schulz Bank. The base of the seamount had concentrated fields of the stalked crinoid, *Bathycrinus carpenterii* (Danielssen & Koren, 1877), and the rocky outcrops here were normally covered in large sponges like *Caulophacus (Caulophacus) arcticus* (Hansen, 1885), *Amphidiscella monai*, or unidentified axinellids.

Besides describing the Schulz Bank benthic megafaunal communities, we also provided the first description of benthic megafaunal communities in Sognefjord in recent years (Christiansen, 1993), although it must be noted that Buhl-Mortensen et al. (2020) independently released a chapter on the benthic biotopes in Sognefjord at the same time **Paper 3** was published. The benthic communities on Schulz Bank (**Papers 2 and 4**) shared similarities in functional groups with the communities in Sognefjord (**Paper 3**). Like Schulz Bank, Sognefjord has vertical walls that are dominated by filter feeding taxa such as encrusting sponges and bivalves (**Paper 3)**. *Asconema* aff. *foliatum* was also discovered for the first time on the vertical cliffs in Sognefjord. This sponge closely resembles *Asconema foliatum*, which is a prominent sponge species in the Schulz Bank summit ground (**Paper 4**) and thought to occur in cooler waters off Northern Norway or on AMOR. In Sognefjord, the sponge was found on vertical walls below 800 m depth (**Paper 3**), in the homogeneous basin waters where the average temperature and salinity (7.5°C and 35.06 psu) is generally higher than the conditions on the Schulz Bank summit (0.5 °C and 34.88). Soft bottom communities in Sognefjord

were characterised by echinoderms, seapens and burrowing taxa, which have similar functional groups to the megafauna in the soft bottom communities on Schulz Bank.

4.2 Biotic interactions

The biotic interactions described in this section were mainly based on observations made during the annotation of the ROV visual data (Figure 6). To truly understand the extent of biotic interactions at play within the sponge grounds, more robust studies are needed.

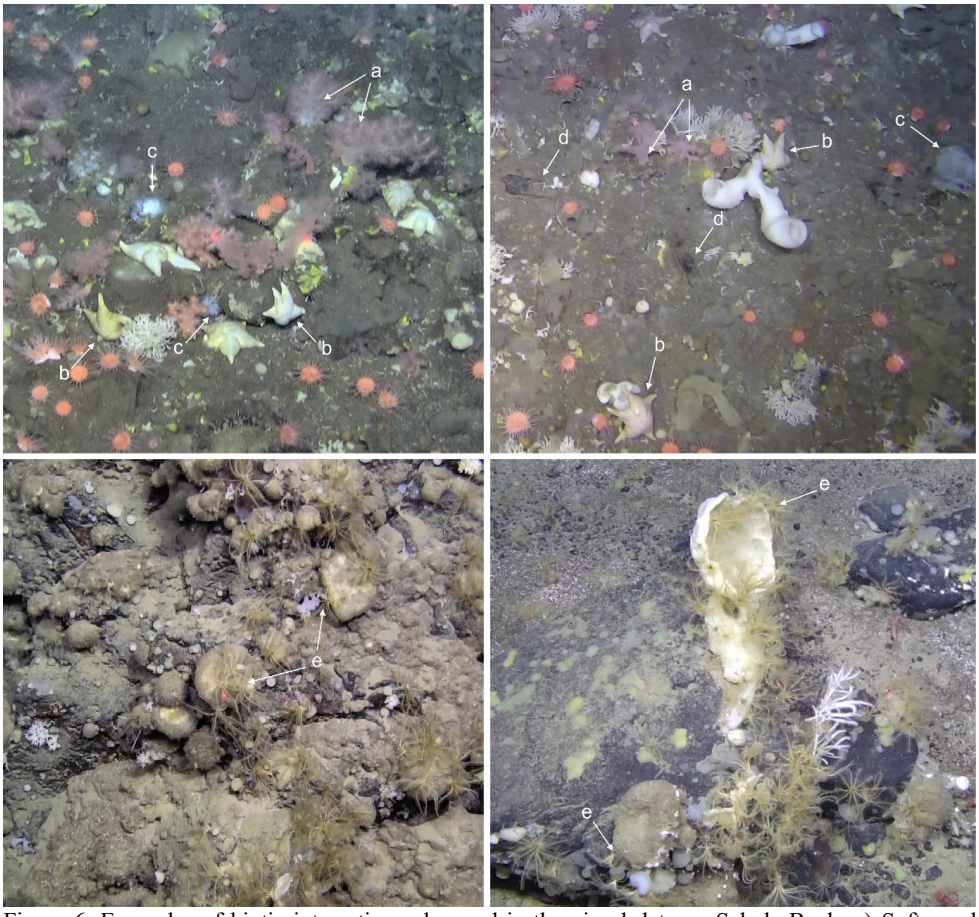

Figure 6. Examples of biotic interactions observed in the visual data on Schulz Bank. a) Soft coral (*Gersemia rubiformis*) growing directly on the large demosponges. b) Seastars (*Tylaster willei*) predating on large demosponges and hexactinellids. c) Blue biofilm growing on demosponges. d) Arctic skate (*Amblyraja hyperborea*) egg case settled directly on the summit sponge ground spicule mat. e) Crinoids (*Poliometra prolixa*) perched on large demosponges. Photo credits: SponGES project, University of Bergen.

4.2.1 Sessile invertebrates settling on sponges

The large demosponges served as a perch or substratum for different invertebrates (**Paper 4**) (Figure 6a and 6e), which has been noted previously in other sponge grounds (Bett and Rice, 1992; Morganti et al., 2022; Rice et al., 1990). At the summit, the soft corals (*Gersemia rubiformis*) were positioned directly on top of the large demosponges, which was also observed in the Central Arctic Ocean summit sponge grounds (Morganti et al., 2022). This type of interaction appeared to be restricted to the summit, where on the upper slopes, *Gersemia* was regularly observed directly on the soft sediment even though large demosponges were present. It is not uncommon for sponges to provide substratum for other sessile invertebrates, and it has been suggested that structure-forming sponges (or other organisms that provide elevated biogenic habitats) help other sessile fauna access food particles from enhanced water currents higher in the bottom boundary layer (Buhl-Mortensen et al., 2010). The change in position for *Gersemia* from the large demosponges on the top of the summit to directly on the seafloor surface on the slopes could be due to the interaction with the bottom currents along the seamount. The soft corals may be using the large demosponges as a perch to gain access to food supply into the bottom boundary layer above the summit, whereas elevated currents on the slopes supply enough food to the soft corals without the need to be positioned higher in the water column.

Crinoids were also observed settled directly on the large hexactinellids and demosponges on the bedrock walls in the deeper regions of Schulz Bank. This could be tied into increased feeding efficiency, as crinoids have been previously observed settling directly on the oscular rim of large hexactinellids in Antarctica (McClintock et al., 2005). Alternatively, current speeds tend to be higher around bedrock walls, and like the soft corals, the crinoids may be using the large sponges as means to get better access to food.

4.2.2 Predation on structure-forming sponges

On numerous occasions, seastars predating on the large sponges were observed on Schulz Bank and Sognefjord (Figure 6b) (**Paper 2–4**). Spongivory by seastars is not an

an uncommon occurrence (Mah, 2020; McClintock et al., 2005; Wulff, 2006), and similar observations were made by Morganti et al. 2022. Because this interaction was commonly observed in the Schulz Bank summit sponge ground, we collected seastars in the midst of predating on large hexactinellids for further analysis. Based on compound-specific isotope analyses, it appears the large sponges are an important food source for both seastars and urchins on Schulz Bank (Hanz, 2021). However, while demersal fish are also known to predate on sponges elsewhere (Wulff, 2006), Hanz (2021) found no indication that the demersal fish in the vicinity fed on the sponges at all.

In some cases, we noted demosponges covered in a blueish white biofilm (Figure 6c), which was suspected to be a result of the predation and similar observations were made by Morganti et al. (2022). Samples of the biofilm were collected by Morganti and Slaby, who confirmed the material to be of microbial origin (Morganti and Slaby pers. comm and unpublished data), and they theorized the biofilm formed as the sponge decays and the seastars feed on the decaying sponges. However, sponges are known to produce chemical defences in response to predation (McClintock et al., 2005; Molinski and Faulkner, 1988; Thoms et al., 2007; Thoms and Schupp, 2008; Wulff, 2006), and some sponges are capable of producing wound-activated defences in a matter of seconds in response to predation (Thoms and Schupp, 2008). Furthermore, the sponges that were covered in the biofilm were also HMA sponges (Busch et al., 2020), which have high microbial abundances and a diverse associated microbial community. Therefore, it might be possible that the biofilm is produced by the large demosponges to use their microbial associates for deterring the seastars as they wound the sponge, though this theory requires investigation where physical samples are collected for further analyses.

4.2.3 Schulz Bank summit sponge ground as a fish nursery

Paper 2 documented high densities of Arctic skate (*Amblyraja hyperborea*) egg cases distributed around the survey area (summit of Schulz Bank) (Figure 6d), with adults and the occasional hatchling (where hatchlings are considered to have a total length <20 cm (Climent, 2021)) in the vicinity. To the best of our knowledge, this is the first

documented case of *A. hyperborea* using arctic sponge grounds as nursery grounds, particularly since their life-history traits have been relatively unknown (Climent, 2021). Previous studies have found *A. hyperborea* nurseries around cold seeps off the coast of Northern Norway (Sen et al., 2019) and have highlighted potential nurseries along outer shelf regions or canyons (Climent, 2021).

When analysing the ROV video footage for **Paper 4**, these egg cases were only observed on the summit (from 580–760 m), suggesting that the summit is the only area of the seamount used as a nursery ground for the *A. hyperborea*. In addition, egg cases were observed on the summit in visual data collected over multiple years (AUV imagery from 2016, ROV footage from 2017 and 2018), indicating that *A. hyperborea* have been repeatedly choosing to lay their eggs here over time. *Amblyraja hyperborea* were observed as deep as 1626 m depth in the video footage and possibly deeper as they are known to predate on *Lycodes frigidis* (Byrkjedal et al., 2015), a eelpout species common on the deeper regions of Schulz Bank below 1500 m. Therefore, *A. hyperborea* is not restricted to only the summit, but likely chooses to use the summit sponge ground as a nursery area to lay their eggs.

4.3 Spatial distribution

4.3.1 Fine-scale spatial patterns on Schulz Bank summit

Paper 2 is the first study to investigate the fine-scale spatial patterns of arctic sponge ground megafauna using the neighbour-based kernel density estimation approach. Here, we found that most of the taxa displayed random spatial patterns, which indicates no clear influences at the survey area spatial scale (Mitchell and Harris, 2020). However, some taxa displayed clear spatial preference within the sample area, particularly with the soft coral (*Gersemia rubiformis*) and branching sponge (*Lissodendoryx (Lissodendoryx) complicata*) having nearly opposite spatial preferences. It is unclear what is influencing their spatial patterns at such fine scales, but possible drivers could be biotic (e.g., competition or interaction) or abiotic (e.g., topographic or

hydrodynamic) based on the positioning on the summit edge to the steep slopes (see **Paper 1**), possibly influencing the delivery of food (Davies et al., 2009).

Variation in species assemblage within the summit sponge ground were also observed in **Paper 4** where we documented changes in the main sponge composition from the top of the summit to the upper slopes. On the gently sloping summit, the large hexactinellids and demosponges were more prominent, but on the steeply sloping summit edges, delicate branching sponges, soft corals, and smaller demosponges seemed to dominate. Towards the lower region of the summit sponge ground, where soft sediment was more frequent, stalked sponges were regularly observed with the occasional large demosponge and hexactinellid. These fine-scale variations of the spatial patterns and faunal assemblages could be due to biotic interactions or abiotic drivers based on the availability of food for the taxa, which were not evaluated in the thesis.

4.3.2 Sponge ground and structure-forming sponge distribution on Schulz Bank

The first documentation of the distribution and relative density (ind. image^{-1}) trends of the sponges on the Schulz Bank were documented in **Paper 1**, where species richness and relative sponge density generally increased with decreasing water depths (from ~1300–650 m depth). From this study, there formed a general assumption that the summit sponge ground was the most dense and diverse community on Schulz Bank, which was also suggested in **Paper 2**. However, a more robust annotation and analyses was conducted for **Paper 4** and extended the scope of the survey from the base to summit rather than just the summit and upper slopes (**Papers 1–2).** Therefore, the assumption that the summit was the densest community was not necessarily correct, as the bedrock-wall sponge grounds had comparable densities to the summit sponge ground.

The range of the summit sponge ground was initially thought to extend to approximately 700 m (**Paper 1 and 2**), but it was revealed that the summit sponge ground has a continuous presence from 580 to ~1050 m, with a patchy distribution until

~1265 m (**Paper 4**). **Paper 1** initially notes that the bedrock-wall sponge grounds formed around 1000–1400 m; however, results from **Paper 4** show these communities were mainly found from 1550–2400 m.

The hexactinellids that characterised the summit sponge ground only occurred on the summit region (580–1275 m) (**Paper 4**), where they had the highest density on the top of the summit (Figure 7). The other large structure-forming sponges found in the summit sponge ground were *Geodia hentscheli, G. parva,* and *Stelletta rhaphidiophora,* (580–2175 m), and *Lissodendoryx (Lissodendoryx) complicata* (580–2490 m). While the large demosponges (*G. hentscheli*, *G. parva*, and *S. rhaphidiophora*) were present on the summit sponge ground, they occurred in greater densities on the bedrock walls in the lower slopes. However, the density of *L. (L.) complicata* was greatest in the southwestern area of the Schulz Bank summit and spiked again on the bedrock walls. The unidentified axinellid was found only in the deeper regions of Schulz Bank (1630–2725 m).

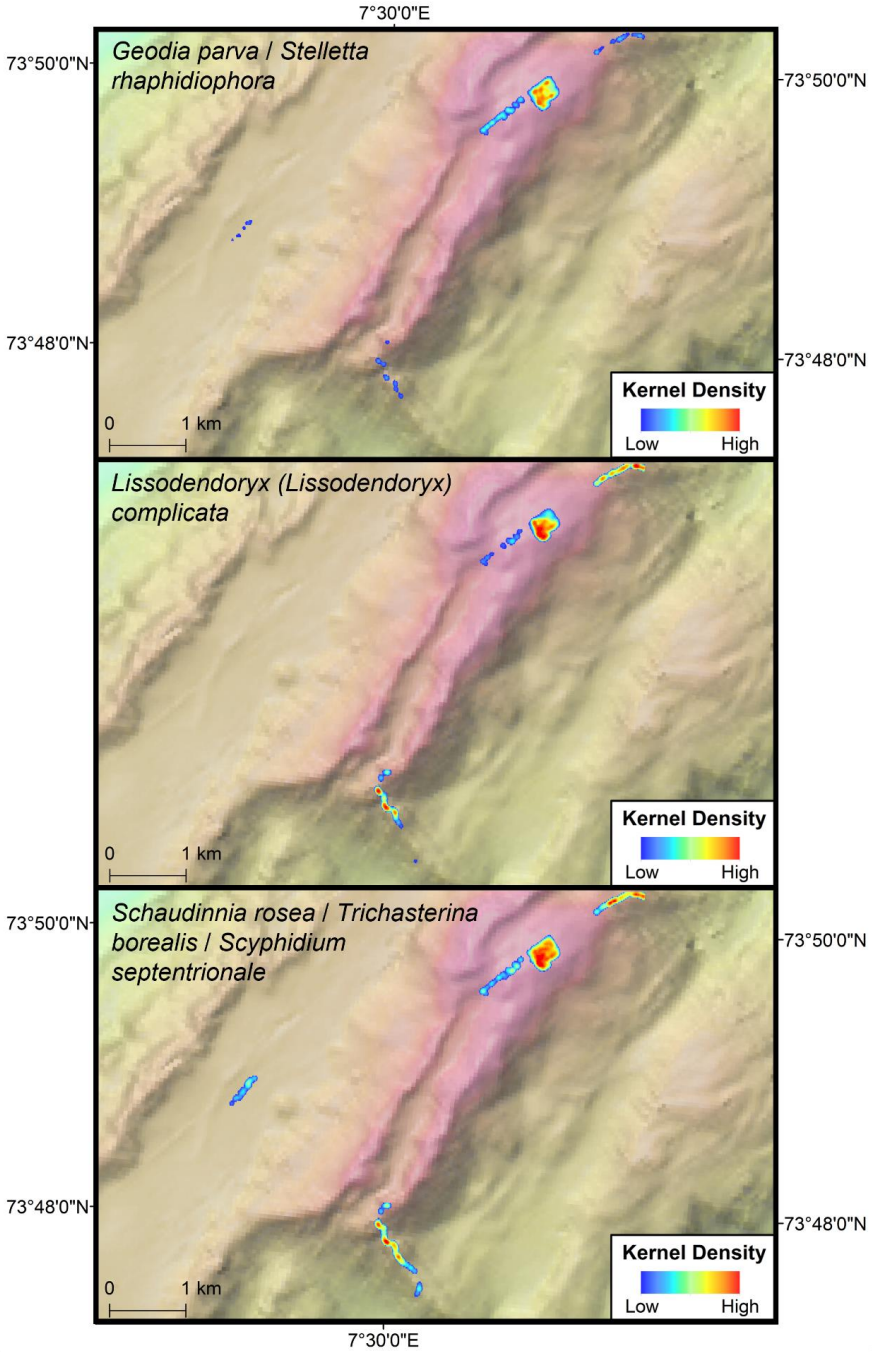

Figure 7. Kernel density estimation plots of a subset of prominent structure-forming sponges on Schulz Bank determined from the *Hugin 1000* and *Ægir 6000* visual data. Kernel density values are normalised by the maximum densities occurring for each species from base to summit, with a selected search radius of 50 m to include neighbouring data points. This figure is an updated version of ***Figure 4*** in **Paper 2** to include faunal densities from **Paper 4** and Morrison et al. (2020). *Continued.*

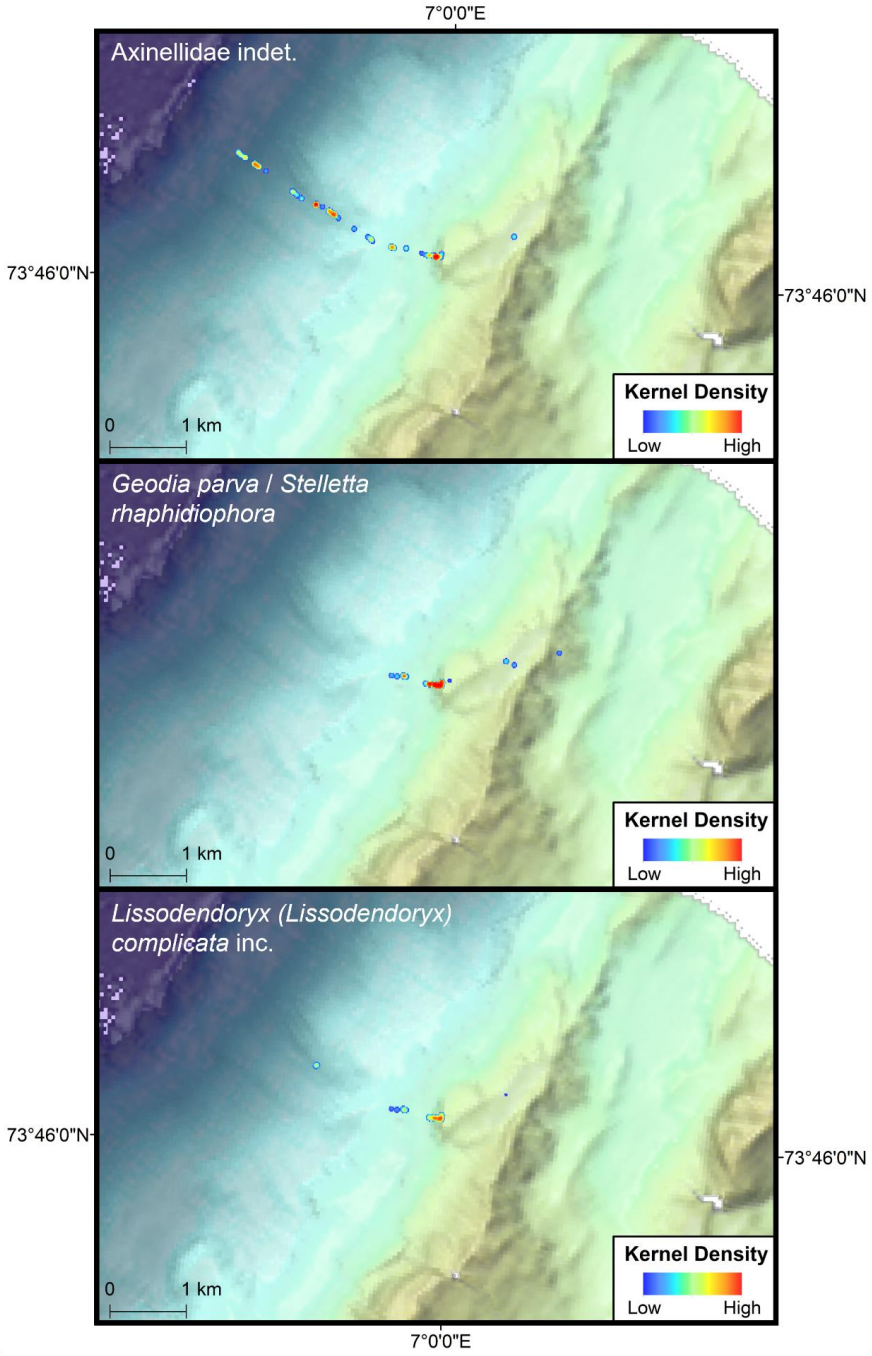

Figure 7. *Continued.*

4.3.3 Arctic sponge ground distribution in the North Atlantic

While the work in this thesis did not specifically investigate the broad-scale distribution of arctic sponge grounds, the results can be used to build on other studies. Roberts et al. (2021) suggested that sponge ground-forming species (*Geodia*) are not always found strictly within specific temperature and salinity ranges but tend to occur along certain water masses, and subsequently, current pathways. Their study indicates that arctic sponge ground-forming species occur in the Nordic Seas along the East Greenland, Jan Mayen, and East Icelandic Currents, and correspond with the Deep Western Boundary Current in the Northwest Atlantic (along with the boreal species). Predicted species distribution models have also predicted high likelihood of occurrence of arctic sponge ground taxa (*G. hentscheli* and *G. parva*) along AMOR and off the eastern Greenland shelf (Burgos et al., 2020). Therefore, future studies investigating the broad-scale distribution of arctic sponge grounds should turn their focus along these current pathways and various points along AMOR and the eastern Greenland shelf.

At AMOR specifically, arctic sponge grounds or arctic sponge ground taxa have been documented as far north as the Central Arctic Ocean (Morganti et al., 2021, 2022) and as far south as the Northeast Iceland Shelf (Roberts et al., 2021). However, there has been limited research efforts on the Knipovich Ridge (Pedersen et al., 2021) and the therefore the megabenthic communities on this AMOR section are largely unknown. It is, however, possible that similar communities found on Schulz Bank would be found all along the ridge system. However, further investigation is needed to truly understand the extent of arctic sponge ground distribution, their drivers, and the connectivity between the communities on AMOR.

4.4 Potential abiotic drivers

The main abiotic drivers of arctic sponge grounds and structure-forming sponges are still largely unknown due to the limited research done on arctic sponge grounds and require further investigation. Identifying the key abiotic drivers can help build more accurate habitat maps and species distribution models that can be used in the future.

Following the submission of this thesis, a major aim for future work is to build on the work done in this thesis and further investigate the abiotic drivers for arctic sponge ground formation and distribution on AMOR.

4.4.1 The influence of internal waves and bottom currents

The first description of the short-term oceanographic setting on Schulz Bank was provided in **Paper 1**. Just above or at the summit of Schulz Bank (~300–650 m), there are elevated levels of dissolved oxygen, with peaks of turbidity and chlorophyll around 300 m, indicating an intermediate nepheloid layer at this depth and possibly an important food source for the summit sponge ground. This layer also coincides with the Norwegian Arctic Intermediate Water, where the lower boundary of this water mass reaches the top of the summit. Diurnal/semi-diurnal tidal forcing is probably important to the summit sponge ground, where the summit experienced regular temperature and dissolved oxygen fluctuations brought on by internal waves, which was further examined by Hanz et al. (2021). The internal waves were suspected to regularly subject the summit to warmer, oxygen-enriched water from the Norwegian Arctic Intermediate Water and bring in a supply of inorganic nutrients and dissolved inorganic carbon from the Upper Norwegian Deep Water positioned below the summit (**Paper 1**).

The summit sponge ground on Schulz Bank was identified to have critical slopes (Hanz et al., 2021), which are areas where the bottom topography slope matches the slope of an incoming internal wave energy ray. Areas with critical slopes tend to have enhanced localised internal tidal currents, shear, turbulence, and mixing. These tidal currents on Schulz Bank were hypothesized to resuspend suspended particulate matter that may act as an important food source for the sponges (**Paper 1**). This was further supported by the findings of Hanz (2021), who suggested the large hexactinellids mainly relied on the resuspended particulate matter (and other food sources like bacteria) and recycled nutrients; whereas the large demosponges likely utilized dissolved organic matter more than the resuspended particulate matter (Bart et al., 2021; Hanz, 2021).

The enhanced currents at the summit may also be influencing the fine-scale spatial patterns of the megafauna in summit sponge ground, where the summit was observed to be periodically subjected to high current speeds (up to 72 cm s^{-2}) in the winter (Hanz et al., 2021). When investigating the influence of the *in-situ* abiotic variables on the fine-scale community patterns in **Paper 2**, we found the summit area to be too homogeneous to clearly discern any main environmental drivers for the species richness and megafaunal abundance. There was, however, an apparent relationship with the narrow depth range (~580 to 590 m) for some of the megafauna, which could be due to the proximity to the steeper slopes around the edges of the sampling area and correspond with faster current speeds or enhanced mixing (Davies et al., 2009; Mitchell and Harris, 2020).

While the abiotic drivers were not specifically investigated in **Paper 4**, the different communities did appear to occur within specific depth ranges and on certain substrata. Suitable available substratum is an important resource for sponges (Barthel and Gutt, 1992; Barthel and Tendal, 1993; Buhl-Mortensen et al., 2012; Williams et al., 2010), and it appears that available (hard) substratum may play a role on the Schulz Bank, particularly in the deeper regions. Beyond the summit sponge ground, we found exposed bedrock walls or rocky outcrops to be regularly inhabited by filter- and suspension-feeding taxa (**Paper 4**), similar functional groups to what was observed in **Paper 3** on the vertical rock walls of Sognefjord. Vertical walls are generally known to be areas with increased current speeds, low sedimentation, and high presence of hard substrata, which further improves food supply and available substrata for sessile fauna to use with the reduced chance of smothering (Buhl-Mortensen et al., 2020; Clark et al., 2010; Flach et al., 1998; Meyer et al., 2014). However, bottom current speeds were not measured for the base and lower slopes of Schulz Bank in previous studies (Hanz et al., 2021). That said, CTD casts from 2016 show a steady increase in turbidity from 1500 to 2700 m indicating increased suspended matter in the water column (unpublished data) and may act an important food source for the filter- and suspension-feeding fauna below this depth.

4.4.2 Broad associations with water masses

The formation and distribution of arctic sponge ground taxa has been regularly proposed to be influenced by specific water masses (Howell et al., 2016; Klitgaard and Tendal, 2004), and arctic sponge ground fauna have been found to have broad associations with generally cool, fresh, and dense water masses (Roberts et al., 2021). This was supported in predictive species distribution models that found low temperature and salinity (as proxy for cool and fresh water masses) to be the most important variable influencing the distribution of arctic sponge ground fauna (Burgos et al., 2020; Murillo et al., 2018). It is uncertain why these species occur along the specific water masses or currents, but one theory is that larval dispersal is constrained by density stratification or current shear (Roberts et al., 2021), thus limiting their distribution to the specific water masses or currents. In areas that contain both boreal and arctic sponge ground-forming sponges (e.g., Davis Strait and Denmark Strait) are thought to be influenced by the turbulent mixing or entrainment of both Atlantic and Arctic water masses, which may allow for the right conditions for both sponge ground types to occur.

At a more site-specific scale, the interface between the Norwegian Arctic Intermediate Water and the Upper Norwegian Deep Water on the Schulz Bank summit is thought to be important for the sponge grounds' survival (**Paper 1**). This is possibly due to the regular fluctuations of temperature and dissolved oxygen through the internal waves or the internal waves supplying food to the sponges. However, these conditions may not always be needed for arctic sponge grounds to form and thrive. Morganti et al. (2022) found dense arctic sponge grounds on seamounts in the Central Arctic Ocean, where bottom currents seemed slow and food availability was poor. Regardless of the difficult environmental conditions, dense aggregations of sponges were seemingly thriving, and suspected to be surviving off fossil detritus from extinct seep communities (Morganti et al., 2022). These vast difference in abiotic conditions where dense arctic sponge communities occur really raises the question on what variables are actually needed to support arctic sponge ground communities.

The importance of water mass structure on megabenthic communities was also highlighted in **Paper 3**, where depth (as proxy for unmeasured variables), dissolved oxygen and salinity were noted to be important variables for the megabenthic communities. However, unlike Schulz Bank, Sognefjord has relatively little mixing of the water masses (Buhl-Mortensen et al., 2020), due to the infrequent renewal events of the basin. This has resulted in homogeneous and food poor conditions in the Sognefjord basin. As such, the benthic communities in the fjord basin have likely adapted to the stable and poor food quality over time. This may indicate that replenishment of dissolved oxygen and food quality may not be as important for the survival of some deep-sea benthic communities (Levin, 2002; Zhulay et al., 2021). Or at the very least, some deep-sea benthic communities may survive in low-oxygenated and/or food scarce conditions for long periods of time.

5. Broader relevance and future research

The work presented in this thesis builds on the current understanding of the biodiversity and spatial ecology of arctic sponge grounds and other megabenthic communities on AMOR and can be used as baseline studies to evaluate how the communities may change in the future. This work has a broader relevance in terms of understanding how arctic sponge grounds may be impacted by climate change, deep-sea mining, and other anthropogenic disturbances. In addition, it bridges key research gaps in the knowledge of arctic megabenthic communities.

5.1 The future of climate change in the Arctic Ocean

Benthic communities globally are going to be impacted by climate change, and polar communities are most at risk. With increasing warming of the Arctic comes the distribution shifts of southern species that will likely replace the established arctic communities (Thomas et al., 2022). Occurrences of 'Atlantification' have already been observed in marine communities in the Arctic, where the northerly expansion of Atlantic water has allowed typically boreal Atlantic species to now withstand previously arctic conditions (Lind et al., 2018; Renaud et al., 2012; Tarling et al., 2022). Seasonality and the timing of primary production are also expected to change in the Arctic, which will likely impact the ecosystem functioning (e.g., nutrient cycling, carbon storage, benthic-pelagic coupling, trophic interactions, etc.) of benthic communities, like arctic sponge grounds (Morata et al., 2020; Solan et al., 2020).

The implications of climate change on AMOR are still largely unknown, however changes in oceanographic conditions have already been seen nearby. The Schulz Bank is located at the interface between Norwegian Sea and Greenland Sea and is influenced by three main water masses: Norwegian Atlantic Water, Intermediate Arctic Water, and Norwegian Deep-Water. The nearby Barents Sea is experiencing weaker stratification of Atlantic Water, more vertical mixing and an increased upward heat flux (Lind et al., 2018; Tuerena et al., 2022), which is leading to a reduction of sea ice cover in the summer and winter seasons. As warming increases and sea ice cover is

reduced, less freshwater input from ice melt is transferred into the cooler (and fresher) Arctic intermediate layers (Lind et al., 2018). As such, water inflow from the Barents Sea into the Arctic Ocean is becoming warmer and more saline (Lind et al., 2018), and consequently, the warmer water is then fed back into the Nordic Seas along AMOR. In the Greenland Sea, the water column structure is also changing and the deep convection previously occurring here has greatly reduced (Moore et al., 2015; Somavilla et al., 2013). This reduction in the deep convection is now directly impacting the formation of deep water in the Greenland Basin. Warmer and more saline water is now present in the Greenland Sea where the deep water was previously relatively cool and fresh compared to the Norwegian Deep Water (Swift et al., 1983). In addition to this, the findings from Somavilla et al. (2013) suggests that the increased warming of the Greenland Sea is a direct result of the changes occurring in advection in the Arctic Ocean.

The changes in the Barents Sea and Greenland Sea with climate change are likely going to have direct ramifications for the sponge grounds on Schulz Bank (and along AMOR). Changes in the water mass structure on AMOR may occur in the future, as the stratification and vertical mixing between the three water masses may be impacted or reduced (Lind et al., 2018). These changes may result in unfavourable conditions for the sponges' survival or negatively influence their distribution. This is particularly concerning since it was theorized that the larvae of arctic sponges are constrained within the specific water masses through the density stratification (Roberts et al., 2021), and alterations to the water mass density could impact their distribution. Environmental changes from the past have already been modelled in studies, where temperature fluctuations and environmental anomalies were projected for sites with sponge grounds (Samuelsen et al., 2022). Currently it is not clear how arctic sponge grounds will be impacted by climate change in the future, particularly because there have been limited research on these communities previously. Therefore, enhanced sampling efforts and more focused species distribution studies are required to better understand how arctic sponge grounds and their suitable habitats will be influenced by climate change.

5.2 Benthic communities and the impact of deep-sea mining on AMOR

The Norwegian bottom area exclusive economic zone (EEZ) encompasses much of AMOR, including Schulz Bank (Oljedirektoratet, 2021; Pedersen et al., 2021). Recently, the Norwegian Government has tasked the Norwegian Petroleum Directorate with mapping AMOR to identify areas with mineral deposits (seafloor massive sulphide deposits and manganese crusts), with a current focus on Mohn Ridge based on the knowledge of both active and inactive hydrothermal sites (e.g., Loki's Castle, Mohn's Treasure, Fåvne, and Ægir) and unexplored seamounts (Pedersen et al., 2010b, 2010a, 2021; Pedersen and Bjerkgård, 2016). While there has been an increased surveying effort to reduce the knowledge gap on the biology (both macro and microbiology) at vent sites on AMOR (Eilertsen et al., 2018, 2020; Jaeschke et al., 2012; Kongsrud et al., 2017; Pedersen et al., 2010a; Ramirez-Llodra et al., 2020; Schander et al., 2010), there is still a lot to learn from the communities not only within the vent fields, but also those from outside their immediate vicinity. Despite the limited information regarding the benthic communities on AMOR and their potential vulnerability, Norway will likely be opening for mining exploration in the coming years (estimated to be as early as 2023) (Oljedirektoratet, 2021).

While Schulz Bank is not going to be directly targeted by deep-sea mining efforts, it is located near Mohn's Treasure and Loki's Castle Vent Field, the former having a higher chance to be targeted by the deep-sea mining industry due to its presumed inactivity. It is still uncertain how deep-sea mining will impact megabenthic communities, like arctic sponge grounds, but based on the signs of little recovery after being trawled (Morrison et al., 2020), it is likely the sponge grounds will be vulnerable to disturbances caused by deep-sea mining as well. Having baseline studies, like what was presented throughout this thesis, is critical for understanding how communities will be impacted by future anthropogenic disturbances, like deep-sea mining. Yet, it is clear that more baseline research is needed of the benthic communities on AMOR, especially in areas that have yet to be surveyed, like most of Knipovich Ridge (Pedersen et al., 2021).

5.3 UN Ocean Decade

The work presented in this thesis falls within the scope of the UN Ocean Decade Sustainable Development Goal (SDG) 14 – Life below Water, particularly SDG 14.a, which aims to improve scientific knowledge of marine habitats, scientific research capacity, and access and transfer of marine technology (IOC-UNESCO, 2021). Throughout the thesis, we improved the global scientific understanding of arctic sponge grounds biodiversity and spatial ecology on AMOR (a largely unexplored region) (**Papers 1, 2, and 4**), enhanced research capacity by training and collaborating with other international researchers through the H2020 SponGES project (**Papers 1–4**; Morrison et al., 2020; Roberts et al., 2021), and we expanded on the access and transfer of marine technology by providing accessible data (through submitting our datasets to the World Data Center PANGAEA; **Papers 1, 2, 3**) which have since been used in other research activities (Liu et al., 2021).

In addition, this work also contributes to SDG 14.c by providing a significant contribution to the application of conservation for Schulz Bank (IOC-UNESCO, 2021). The result of this thesis demonstrates that Schulz Bank hosts diverse sponge ground communities that provide numerous ecological services to other local marine organisms and should be considered for marine protection (**Papers 2 and 4**). In addition, the tools developed in this work was used to highlight that the sponge grounds on Schulz Bank are vulnerable and slow to recover from anthropogenic disturbances (Morrison et al., 2020), further enhancing their need for protection.

Since 2020, only 7.74% of the global ocean are within marine protected areas (UN, 2021). And to date, there is only one area on AMOR that is considered a marine protection area – Jan Mayen (Marine Protection Atlas, accessed 12 January 2022). However, there has been a request to implement a protection area around Schulz Bank submitted for consideration during a consultation between the Norwegian parliament and scientific community in recent years (Ribeiro pers. comm, 2022). To date, it is not clear if any decision has been made at this point in time.

6. Conclusion

The work presented in this thesis further improves our knowledge of arctic sponge ground biodiversity and spatial ecology and forms a baseline understanding of arctic sponge ground communities in the Nordic Seas. The main conclusions of this thesis are as follows:

- Schulz Bank is subjected to three water masses, where two of the water masses directly interact with the summit of the seamount through internal waves **(Paper 1)**. Furthermore, the summit is below a nepheloid layer and the interaction with the internal waves may enhance food supply to the filter- and suspension-feeding megafauna.

- There are two different types of sponge grounds comprised of the characterising arctic sponges on the Schulz Bank (**Paper 2** and **Paper 4**):
    - The summit sponge ground is mainly characterised by large hexactinellid and demosponges with other sponges, ascidians, cnidarians, echinoderms, and demersal fish present throughout the sponge ground. This sponge ground occurred on spicule mat from 580 to 1060 m depth, with patchy distribution to 1265 m.
    - The bedrock-wall sponge grounds are characterised by large demosponges with other sponges, crinoids, and decapods present throughout sponge ground. This ground occurred on bedrock walls from 1550 to 2400 m depth, with the occasional presence on soft bottom.

- The structure-forming sponges interact with many of the associated fauna (**Paper 4**), where the sponges provide additional substratum to sessile invertebrates, act as a food source for echinoderms, and offer microhabitats for smaller crustaceans. In addition, **Paper 2** documented the first known case of the largely understudied Arctic skate using sponge grounds as a nursery area based on the high density of egg cases found on the summit and observations of both adult and hatchlings in the vicinity.

- The Schulz Bank megafauna communities shares similarities with Sognefjord megabenthic communities in terms of functional groups, particularly on the vertical walls (**Papers 3 and 4**). Using inland or easy to access locations like deep fjords can act as a laboratory that simulate deep-sea environments. These locations allow researchers to learn more about functional trait assemblages, investigate the influences of abiotic conditions on deep megabenthic communities, and evaluate how environmental fluctuations or climate change will impact the community assemblages in the future.

- Visual surveying techniques (e.g., AUVs) are a useful tool to map the fine-scale spatial patterns within a community (**Paper 2**). The spatial patterns detected can be further used to investigate how biotic and abiotic variables are influencing the megafaunal spatial patterns and how species are assembled within a community.

- The abiotic drivers of arctic sponge grounds still need further investigation. However, based on results from this thesis and other work performed within the scope of the SponGES project, it is likely that internal waves, bottom currents, and water masses play an important role in the distribution of these communities, either in terms of larval dispersal, food availability, and evolved tolerances.

7. References

Bart, M. C., Hudspith, M., Rapp, H. T., Verdonschot, P. F. M., and de Goeij, J. M. (2021). A deep-sea sponge loop? Sponges transfer dissolved and particulate organic carbon and nitrogen to associated fauna. *Front. Mar. Sci.* 8, 1–12. doi:10.3389/fmars.2021.604879.

Barthel, D. (1997). Fish eggs and pentacrinoids in Weddell Sea hexactinellids: Further examples for the structuring role of sponges in Antarctic benthic ecosystems. *Polar Biol.* 17, 91–94. doi:10.1007/s003000050110.

Barthel, D., and Gutt, J. (1992). Sponge associations in the eastern Weddell Sea. *Antarct. Sci.* 4, 137–150. doi:10.1017/S0954102092000221.

Barthel, D., and Tendal, O. S. (1993). The sponge association of the abyssal Norwegian-Greenland Sea: Species composition, substrate relationships and distribution. *Sarsia* 78, 83–96. doi:10.1080/00364827.1993.10413524.

Barthel, D., Tendal, O. S., and Thiel, H. (1996). A wandering population of the hexactinellid sponge *Pheronema carpenteri* on the continental slope off Morocco, Northwest Africa. *Mar. Ecol.* 17, 603–616. doi:10.1111/j.1439-0485.1996.tb00420.x.

Beazley, L. I., Kenchington, E. L., Murillo, F. J., and Sacau, M. D. M. (2013). Deep-sea sponge grounds enhance diversity and abundance of epibenthic megafauna in the Northwest Atlantic. *ICES J. Mar. Sci.* 70, 1471–1490. doi:10.1093/icesjms/fst124.

Beazley, L., Kenchington, E., Murillo, F. J., Brickman, D., Wang, Z., Davies, A. J., Roberts, E. M., and Rapp, H. T. (2021). Climate change winner in the deep sea? predicting the impacts of climate change on the distribution of the glass sponge *Vazella pourtalesii*. *Mar. Ecol. Prog. Ser.* 657, 1–23. doi:10.3354/meps13566.

Beazley, L., Kenchington, E., Yashayaev, I., and Murillo, F. J. (2015). Drivers of epibenthic megafaunal composition in the sponge grounds of the Sackville Spur, northwest Atlantic. *Deep. Res. Part I Oceanogr. Res. Pap.* 98, 102–114. doi:10.1016/j.dsr.2014.11.016.

Beazley, L., Wang, Z., Kenchington, E., Yashayaev, I., Rapp, H. T., Xavier, J. R., Murillo, F. J., Fenton, D., and Fuller, S. (2018). Predicted distribution of the glass sponge *Vazella pourtalesii* on the Scotian Shelf and its persistence in the face of climatic variability. *PLoS One* 13, 1–29. doi:10.1371/journal.pone.0205505.

Bell, J. B., Alt, C. H. S., and Jones, D. O. B. (2016). Benthic megafauna on steep slopes at the northern mid-Atlantic ridge. *Mar. Ecol.* 37, 1290–1302. doi:10.1111/maec.12319.

Bell, J. J. (2008). The functional roles of marine sponges. *Estuar. Coast. Shelf Sci.* 79, 341–353. doi:10.1016/j.ecss.2008.05.002

Bell, J. J., Bennett, H. M., Rovellini, A., and Webster, N. S. (2018). Sponges to be winners under near-future climate scenarios. *Bioscience* 68, 955–968. doi:10.1093/biosci/biy142.

Bell, J. J., McGrath, E., Biggerstaff, A., Bates, T., Bennett, H., Marlow, J., et al. (2015). Sediment impacts on marine sponges. *Mar. Pollut. Bull.* 94, 5–13. doi:10.1016/j.marpolbul.2015.03.030.

Bett, B. J. (2012). JNCC Report 472: Seafloor biotope analysis of the deep waters of

the SEA4 region of Scotland ' s seas. Southampton.

Bett, B. J., and Rice, A. L. (1992). The influence of hexactinellid sponge (*Pheronema carpenteri*) spicules on the patchy distribution of macrobenthos in the porcupine seabight (Bathyal ne atlantic). *Ophelia* 36, 217–226. doi:10.1080/00785326.1992.10430372.

Biber, M. F., Duineveld, G. C., Lavaleye, M. S., Davies, A. J., Bergman, M. J., and van den Beld, I. M. (2014). Investigating the association of fish abundance and biomass with cold-water corals in the deep Northeast Atlantic Ocean using a generalised linear modelling approach. *Deep. Res. Part II Top. Stud. Oceanogr.* 99, 134–145. doi:10.1016/j.dsr2.2013.05.022.

Bo, M., Bertolino, M., Bavestrello, G., Canese, S., Giusti, M., Angiolillo, M.,Pansini, M., and Taviani, M. (2012). Role of deep sponge grounds in the Mediterranean Sea: A case study in southern Italy. *Hydrobiologia* 687, 163–177. doi:10.1007/s10750-011-0964-1.

Bond, C., and Harris, A. K. (1988). Locomotion of sponges and its physical mechanism. *J. Exp. Zool.* 246, 271–284. doi:10.1002/jez.1402460307.

Boschen, R. E., Rowden, A. A., Clark, M. R., Barton, S. J., Pallentin, A., and Gardner, J. P. A. (2015). Megabenthic assemblage structure on three New Zealand seamounts: Implications for seafloor massive sulfide mining. *Mar. Ecol. Prog. Ser.* 523, 1–14. doi:10.3354/meps11239.

Bridges, A. E. H., Barnes, D. K. A., Bell, J. B., Ross, R. E., and Howell, K. L. (2021). Benthic Assemblage Composition of South Atlantic Seamounts. *Front. Mar. Sci.* 8, 1–18. doi:10.3389/fmars.2021.660648.

Buhl-Mortensen, L., Buhl-Mortensen, P., Dolan, M. F. J., Dannheim, J., Bellec, V., and Holte, B. (2012). Habitat complexity and bottom fauna composition at different scales on the continental shelf and slope of northern Norway. *Hydrobiologia* 685, 191–219. doi:10.1007/s10750-011-0988-6.

Buhl-Mortensen, L., Buhl-Mortensen, P., Glenner, H., Båmstedt, U., and Bakkeplass, K. (2020). The inland deep sea—benthic biotopes in the Sognefjord. *Seafloor Geomorphol. as Benthic Habitat*, 355–372. doi:10.1016/b978-0-12-814960-7.00019-1.

Buhl-Mortensen, L., Vanreusel, A., Gooday, A. J., Levin, L. A., Priede, I. G., Buhl-Mortensen, P., et al. (2010). Biological structures as a source of habitat heterogeneity and biodiversity on the deep ocean margins. *Mar. Ecol.* 31, 21–50. doi:10.1111/j.1439-0485.2010.00359.x

Burgos, J. M., Buhl-Mortensen, L., Buhl-Mortensen, P., Ólafsdóttir, S. H., Steingrund, P., Ragnarsson, S., and Skagseth, Ø. (2020). Predicting the Distribution of Indicator Taxa of Vulnerable Marine Ecosystems in the Arctic and Sub-arctic Waters of the Nordic Seas. *Front. Mar. Sci.* 7, 1–25. doi:10.3389/fmars.2020.00131.

Busch, K., Hanz, U., Mienis, F., Mueller, B., Franke, A., Roberts, E. M., Rapp, H. T. and Hentschel, U. (2020). On giant shoulders: How a seamount affects the microbial community composition of seawater and sponges. *Biogeosciences* 17, 3471–3486. doi:10.5194/bg-17-3471-2020.

Byrkjedal, I., Christiansen, J. S., Karamushko, O. V., Langhelle, G., and Lynghammar, A. (2015). Arctic skate *Amblyraja hyperborea* preys on remarkably large glacial

eelpouts *Lycodes frigidus*. *J. Fish Biol.* 86, 360–364. doi:10.1111/jfb.12554.

Cárdenas, P., and Rapp, H. T. (2015). Demosponges from the Northern Mid-Atlantic Ridge shed more light on the diversity and biogeography of North Atlantic deep-sea sponges. *J. Mar. Biol. Assoc. United Kingdom* 95, 1475–1516. doi:10.1017/S0025315415000983.

Cárdenas, P., Rapp, H. T., Klitgaard, A. B., Best, M., Thollesson, M., and Tendal, O. S. (2013). Taxonomy, biogeography and DNA barcodes of *Geodia* species (Porifera, Demospongiae, Tetractinellida) in the Atlantic boreo-arctic region. *Zool. J. Linn. Soc.* 169, 251–311. doi:10.1111/zoj.12056.

Cárdenas, P., Xavier, J. R., Reveillaud, J., Schander, C., and Rapp, H. T. (2011). Molecular phylogeny of the Astrophorida (Porifera, *Demospongiae*^{p}) reveals an unexpected high level of spicule homoplasy. *PLoS One* 6. doi:10.1371/journal.pone.0018318.

Christiansen, B. (1993). A television and photographic survey of megafaunal abundance in Central Sognefjorden, western Norway. *Sarsia* 78, 1–8. doi:10.1080/00364827.1993.10413515.

Clark, M. R., Althaus, F., Schlacher, T. A., Williams, A., Bowden, D. A., and Rowden, A. A. (2016). The impacts of deep-sea fisheries on benthic communities: A review. *ICES J. Mar. Sci.* 73, i51–i69. doi:10.1093/icesjms/fsv123.

Clark, M. R., Bernardino, A. F., Roberts, J. M., Narayanaswamy, B. E., Snelgrove, P. V. R., and Tuhumwire, J. T. (2021). "The Second World Ocean Assessment," in *The Second World Ocean Assessment* (New York: United Nations), 439–451.

Clark, M. R., Bowden, D. A., Rowden, A. A., and Stewart, R. (2019). Little evidence of benthic community resilience to bottom trawling on seamounts after 15 years. *Front. Mar. Sci.* 6, 1–16. doi:10.3389/fmars.2019.00063.

Clark, M. R., Rowden, A. A., Schlacher, T., Williams, A., Consalvey, M., Stocks, K. I., Rogers, A. D., O'Hara, T. D., White, M., Shank, T. M., and Hall-Spencer, J. M. (2010). The ecology of seamounts: structure, function, and human impacts. *Ann. Rev. Mar. Sci.* 2, 253–278. doi:10.1146/annurev-marine-120308-081109.

Climent, R. L. (2021). Distribution, reproductive ecology, and colouration of the Arctic skate *Amblyraja hyperborea* (Collett, 1879) in the North Atlantic Ocean. MSc Thesis.

Colaço, A., Rapp, H., Campanyà-Llovet, N., and Pham, C. K. (2022). Bottom trawling in sponge grounds of the Barents Sea (Arctic Ocean): A functional diversity approach. *Deep Sea Res. Part I Oceanogr. Res. Pap.* 183, 103742. doi:10.1016/j.dsr.2022.103742.

Copeland, A., Edinger, E., Devillers, R., Bell, T., LeBlanc, P., and Wroblewski, J. (2013). Marine habitat mapping in support of Marine Protected Area management in a subarctic fjord: Gilbert Bay, Labrador, Canada. *J. Coast. Conserv.* 17, 225–237. doi:10.1007/s11852-011-0172-1.

Cummings, V. J., Beaumont, J., Mobilia, V., Bell, J. J., Tracey, D., Clark, M. R., and Barr, N. (2020). Responses of a common New Zealand coastal sponge to elevated suspended sediments: Indications of resilience. *Mar. Environ. Res.* 155, 104886. doi:10.1016/j.marenvres.2020.104886.

Davies, A. J., Duineveld, G. C. A., Lavaleye, M. S. S., Bergman, M. J. N., and Van Haren, H. (2009). Downwelling and deep-water bottom currents as food supply

mechanisms to the cold-water coral *Lophelia pertusa* (Scleractinia) at the Mingulay Reef Complex. *Limnol. Oceanogr.* 54, 620–629. doi:10.4319/lo.2009.54.2.0620.

Davison, J. J., van Haren, H., Hosegood, P., Piechaud, N., and Howell, K. L. (2019). The distribution of deep-sea sponge aggregations (Porifera) in relation to oceanographic processes in the Faroe-Shetland Channel. *Deep. Res. Part I Oceanogr. Res. Pap.* 146, 55–61. doi:10.1016/j.dsr.2019.03.005.

de Goeij, J. M., van Oevelen, D., Vermeij, M. J. A., Osinga, R., Middelburg, J. J., de Goeij, A. F., and Admiraal, W. (2013). Surviving in a marine desert : the sponge loop retains resources within coral reefs. *Science.* 342, 6154, 108–110. doi:10.1126/science.1241981.

Degnan, B., Larroux, C., Calcino, A., Taylor, K., Nakanishi, N., and Degnan, S. M. (2015). "Porifera," in *Evolutionary development biology of Invertebrates 1*, ed. A. Wanninger (Wein: Springer-Verlag), 65–106. doi:10.1007/978-3-7091-1862-7_1.

Dinn, C., Zhang, X., Edinger, E., and Leys, S. P. (2020). Sponge communities in the eastern Canadian Arctic: species richness, diversity and density determined using targeted benthic sampling and underwater video analysis. *Polar Biol.* 43, 1287–1305. doi:10.1007/s00300-020-02709-z.

Dunn, D. C., Van Dover, C. L., Etter, R. J., Smith, C. R., Levin, L. A., Morato, T., Colaço, A., Dale, A. C., Gerbruk, A. V., Gjerde, K. M., Halpin, P. N., Howell, K. L., Johnson, D., Perez, J. A. A., Ribeiro, M. C., Stuckas, H., Weaver, P., and SEMPIA Workshop Participants (2018). A strategy for the conservation of biodiversity on mid-ocean ridges from deep-sea mining. *Sci. Adv.* 4, 1–16. doi:10.1126/sciadv.aar4313.

Durden, J. M., Bett, B. J., Schoening, T., Morris, K. J., Nattkemper, T. W., and Ruhl, H. A. (2016). Comparison of image annotation data generated by multiple investigators for benthic ecology. *Mar. Ecol. Prog. Ser.* 552, 61–70. doi:10.3354/meps11775.

Eilertsen, M. H., Dahlgren, T. G., and Rapp, H. T. (2020). A new species of *Osedax* (Siboglinidae: Annelida) from colonization experiments in the Arctic deep sea. *Front. Mar. Sci.* 7. doi:10.3389/fmars.2020.00443.

Eilertsen, M. H., Georgieva, M. N., Kongsrud, J. A., Linse, K., Wiklund, H., Glover, A. G., et al. (2018). Genetic connectivity from the Arctic to the Antarctic: *Sclerolinum contortum* and *Nicomache lokii* (Annelida) are both widespread in reducing environments. *Sci. Rep.* 8, 1–13. doi:10.1038/s41598-018-23076-0.

EMODnet Bathymetry Consortium (2020). EMODnet Digital Bathymetry (2020). doi:10.12770/bb6a87dd-e579-4036-abe1-e649cea9881a. Available online at: https://www.emodnet-bathymetry.eu/data-products/acknowledgement-in-publications

FAO (2009). International guidelines for the management of deep-sea fisheries in the High Seas. Rome.

Flach, E., Lavaleye, M., De Stigter, H., and Thomsen, L. (1998). Feeding types of the benthic community and particle transport across the slope of the N.W. European Continental Margin (Goban Spur). *Prog. Oceanogr.* 42, 209–231. doi:10.1016/S0079-6611(98)00035-4.

Freese, J. L. J., and Wing, B. L. B. (2003). Juvenile red rockfish, *Sebastes* sp., associations with sponges in the Gulf of Alaska. *Mar. Fish. Rev.* 65, 38–42.

Available at: http://aquaticcommons.org/9733/.

Gomes-Pereira, J. N., Auger, V., Beisiegel, K., Benjamin, R., Bergmann, M., Bowden, D., Buhl-Mortensen, P., De Leo, F. C., Dionísio, G., Durden, J. M., and Edwards, L. (2016). Current and future trends in marine image annotation software. *Prog. Oceanogr.* 149, 106–120. doi:10.1016/j.pocean.2016.07.005.

González-Aravena, M., Kenny, N. J., Osorio, M., Font, A., Riesgo, A., and Cárdenas, C. A. (2019). Warm temperatures, cool sponges: The effect of increased temperatures on the Antarctic sponge Isodictya sp. *PeerJ* 2019, 1–34. doi:10.7717/peerj.8088.

Grizzle, R. E., Brodeur, M. A., Abeels, H. A., and Greene, J. K. (2008). Bottom habitat mapping using towed underwater videography: Subtidal oyster reefs as an example application. *J. Coast. Res.* 24, 103–109. doi:10.2112/06-0672.1.

Hagen, P. E. (2014). Multi-sensor pipeline inspection with AUV. 55. Available at: http://www.oceanologyinternational.com.

Hanz, U. (2021). Biological hotspots in the deep-sea: Environmental controls and interactions in deep-sea sponge and coral assemblages. PhD Thesis.

Hanz, U., Roberts, E. M., Duineveld, G., Davies, A. J., van Haren, H., Rapp, H. T., Reighart, G. J., and Mienis, F. (2021). Long – term observations reveal environmental conditions and food supply mechanisms at an Arctic deep-sea sponge ground. *J. Geophys. Res. Ocean.* 126, 1–18. doi:10.1029/2020JC016776.

Hawkes, N., Korabik, M., Beazley, L., Rapp, H. T., Xavier, J. R., and Kenchington, E. (2019). Glass sponge grounds on the Scotian Shelf and their associated biodiversity. *Mar. Ecol. Prog. Ser.* 614, 91–109. doi:10.3354/meps12903.

Henrich, R., Hartmann, M., Reitner, J., Schäfer, P., Freiwald, A., Steinmetz, S., et al. (1992). Facies belts and communities of the arctic Vesterisbanken Seamount (Central Greenland Sea). *Facies* 27, 71–103. doi:10.1007/BF02536805.

Hoffmann, F., Rapp, H. T., Pape, T., Peters, H., and Reitner, J. (2004). Sedimentary inclusions in the deep-water sponge *Geodia barretti* (Geodiidae, Demospongiae) from the Korsfjord, western Norway. *Sarsia* 89, 245–252. doi:10.1080/00364820410002451.

Hogg, M. M., Tendal, O. S., Conway, K. W., Pomponi, S. A., van Soest, R. W. M., Gutt, J., Krautter, M., and Roberts, J. M. (2010). *Deep-sea sponge grounds Regional Seas*.

Hopkins, T. S. (1991). The GIN Sea-A synthesis of its physical oceanography and literature review 1972-1985. *Earth Sci. Rev.* 30, 175–318. doi:10.1016/0012-8252(91)90001-V.

Horton, T., Marsh, L., Bett, B. J., Gates, A. R., Jones, D. O. B., Benoist, N. M. A., Pfeifer, S., Simon-Lledó, E., Durden, J. M., Vandepitte, L., and Appeltans, W. (2021). Recommendations for the Standardisation of Open Taxonomic Nomenclature for Image-Based Identifications. *Front. Mar. Sci.* 8. doi:10.3389/fmars.2021.620702.

Howell, K. L., Davies, J. S., and Narayanaswamy, B. E. (2010). Identifying deep-sea megafaunal epibenthic assemblages for use in habitat mapping and marine protected area network design. *J. Mar. Biol. Assoc. United Kingdom* 90, 33–68. doi:10.1017/S0025315409991299.

Howell, K. L., Piechaud, N., Downie, A. L., and Kenny, A. (2016). The distribution of

deep-sea sponge aggregations in the North Atlantic and implications for their effective spatial management. *Deep. Res. Part I Oceanogr. Res. Pap.* 115, 203–220. doi:10.1016/j.dsr.2016.07.005.

ICES (2009). Report of the ICES-NAFO Joint Working Group on Deep-Water Ecology (WGDEC), 9–13 March 2009, vol. 23, p. 94. ICES CM 2009\ACOM.

IOC-UNESCO (2021). The United Nations Decade of Ocean Science for Sustainable Development (2021-2030) Implementation Plan. *IOC Ocean Decad. Ser.* 19, 56.

Jaeschke, A., Jørgensen, S. L., Bernasconi, S. M., Pedersen, R. B., Thorseth, I. H., and Früh-Green, G. L. (2012). Microbial diversity of Loki's Castle black smokers at the Arctic Mid-Ocean Ridge. *Geobiology* 10, 548–561. doi:10.1111/gbi.12009.

Janussen, D., and Tendal, O. S. (2007). Diversity and distribution of Porifera in the bathyal and abyssal Weddell Sea and adjacent areas. *Deep. Res. Part II Top. Stud. Oceanogr.* 54, 1864–1875. doi:10.1016/j.dsr2.2007.07.012.

Johnson, G. L., and Heezen, B. C. (1967). The Arctic mid-oceanic ridge [6]. *Nature* 215, 724–725. doi:10.1038/215724a0.

Kahn, A. S., Pennelly, C. W., McGill, P. R., and Leys, S. P. (2020). Behaviors of sessile benthic animals in the abyssal northeast Pacific Ocean. *Deep. Res. Part II Top. Stud. Oceanogr.* 173, 104729. doi:10.1016/j.dsr2.2019.104729.

Kazanidis, G., Vad, J., Henry, L. A., Neat, F., Berx, B., Georgoulas, K., and Roberts, J. M. (2019). Distribution of deep-sea sponge aggregations in an area of multisectoral activities and changing oceanic conditions. *Front. Mar. Sci.* 6, 1–15. doi:10.3389/fmars.2019.00163.

Kenchington, E., Murillo, F. J., Lirette, C., Sacau, M., Koen-Alonso, M., Kenny, A., Ollerhead, N., Wareham, V., and Beazley, L. (2014). Kernel density surface modelling as a means to identify significant concentrations of vulnerable marine ecosystem indicators. *PLoS One* 9. doi:10.1371/journal.pone.0109365.

Kenchington, E., Power, D., and Koen-Alonso, M. (2013). Associations of demersal fish with sponge grounds on the continental slopes of the northwest Atlantic. *Mar. Ecol. Prog. Ser.* 477, 217–230. doi:10.3354/meps10127.

Klitgaard, A. B. (1995). The fauna associated with outer shelf and upper slope sponges (Porifera, Demospongiae) at the Faroe Islands, northeastern Atlantic. *Sarsia* 80, 1–22. doi:10.1080/00364827.1995.10413574.

Klitgaard, A. B., and Tendal, O. S. (2001). " Ostur " - " cheese bottoms " - sponge dominated areas in Faroese shelf and slope areas. *Mar. Biol. Investig. Assem. benthic Invertebr. from Faroe Islands*, 13–21.

Klitgaard, A. B., and Tendal, O. S. (2004). Distribution and species composition of mass occurrences of large-sized sponges in the northeast Atlantic. *Prog. Oceanogr.* 61, 57–98. doi:10.1016/j.pocean.2004.06.002.

Knudby, A., Kenchington, E., and Murillo, F. J. (2013). Modeling the distribution of *Geodia* sponges and sponge grounds in the Northwest Atlantic. *PLoS One* 8, 1–20. doi:10.1371/journal.pone.0082306.

Kongsrud, J. A., Eilertsen, M. H., Alvestad, T., Kongshavn, K., and Rapp, H. T. (2017). New species of Ampharetidae (Annelida: Polychaeta) from the Arctic Loki Castle vent field. *Deep. Res. Part II Top. Stud. Oceanogr.* 137, 232–245. doi:10.1016/j.dsr2.2016.08.015.

Kutti, T., Bannister, R. J., and Fosså, J. H. (2013). Community structure and ecological

function of deep-water sponge grounds in the Traenadypet MPA-Northern Norwegian continental shelf. *Cont. Shelf Res.* 69, 21–30. doi:10.1016/j.csr.2013.09.011.

Kutti, T., Bannister, R. J., Fosså, J. H., Krogness, C. M., Tjensvoll, I., and Søvik, G. (2015). Metabolic responses of the deep-water sponge *Geodia barretti* to suspended bottom sediment, simulated mine tailings and drill cuttings. *J. Exp. Mar. Bio. Ecol.* 473, 64–72. doi:10.1016/j.jembe.2015.07.017.

Langenkämper, D., Zurowietz, M., Schoening, T., and Nattkemper, T. W. (2017). BIIGLE 2.0 - browsing and annotating large marine image collections. *Front. Mar. Sci.* 4, 1–10. doi:10.3389/fmars.2017.00083.

Levin, L. A. (2002). Deep-Ocean life where oxygen is scarce. *Am. Sci.* 90, 436–444. doi:10.1511/2002.33.756.

Leys, S. P., Kahn, A. S., Fang, J. K. H., Kutti, T., and Bannister, R. J. (2018). Phagocytosis of microbial symbionts balances the carbon and nitrogen budget for the deep-water boreal sponge *Geodia barretti*. *Limnol. Oceanogr.* 63, 187–202. doi:10.1002/lno.10623.

Leys, S. P., and Lauzon, N. R. J. (1998). Hexactinellid sponge ecology: growth rates and seasonality in deep water sponges. *J. Exp. Mar. Bio. Ecol.* 230, 111–129. doi:10.1016/S0022-0981(98)00088-4.

Lind, S., Ingvaldsen, R. B., and Furevik, T. (2018). Arctic warming hotspot in the northern Barents Sea linked to declining sea-ice import. *Nat. Clim. Chang.* 8, 634–639. doi:10.1038/s41558-018-0205-y.

Liu, F., Daewel, U., Samuelsen, A., Brune, S., Hanz, U., Pohlmann, H., Baehr, J., and Schrum, C. (2021). Can environmental conditions at north Atlantic deep-sea habitats be predicted several years ahead? ——Taking sponge habitats as an example. *Front. Mar. Sci.* 8, 1–22. doi:10.3389/fmars.2021.703297.

Lotze, H. K., Coll, M., Magera, A. M., Ward-Paige, C., and Airoldi, L. (2011). Recovery of marine animal populations and ecosystems. *Trends Ecol. Evol.* 26, 595–605. doi:10.1016/j.tree.2011.07.008.

Ludvigsen, M., Sortland, B., Johnsen, G., and Singh, H. (2007). Underwater Photo Mosaics. *Oceanography* 20, 140–149.

Luter, H. M., and Webster, N. S. (2017). "Sponge disease and climate change," in *Climate Change, Ocean Acidification and Sponges: Impacts Across Multiple Levels of Organization*, eds. J. L. Carballo and J. J. Bell, 1–452. doi:10.1007/978-3-319-59008-0.

Macreadie, P. I., McLean, D. L., Thomson, P. G., Partridge, J. C., Jones, D. O. B., Gates, A. R., Benfield, M. C., Collin, S. P., Booth, D. J., Smith, L. L., and Techera, E (2018). Eyes in the sea: unlocking the mysteries of the ocean using industrial, remotely operated vehicles (ROVs). *Sci. Total Environ.* 634, 1077–1091. doi:10.1016/j.scitotenv.2018.04.049.

Mah, C. L. (2020). New species, occurrence records and observations of predation by deep-sea Asteroidea (Echinodermata) from the North Atlantic by NOAA ship *Okeanos Explorer*. *Zootaxa* 4766, 201–260. doi:10.11646/zootaxa.4766.2.1.

Maldonado, M., Aguilar, R., Bannister, R. J., Bell, J. J., Conway, K. W., Dayton, P. K., Díaz, C., Gutt, J., Kelly, M., Kenchington, E. L. and Leys, S. P. (2016). "Sponge Grounds as Key Marine Habitats: A Synthetic Review of Types, Structure,

Functional Roles, and Conservation Concerns," in *Marine Animal Forests* (Springer International Publishing), 1–39. doi:10.1007/978-3-319-17001-5_24-1.

Marine Protection Atlas, Marine Conservation Insitute. Svalbard and Jan Mayen Marine Protected Areas. Accessed 12 January 2022. Downloaded from: https://mpatlas.org/countries/SJM

Marsh, L., Copley, J. T., Huvenne, V. A. I., Tyler, P. A., and the Isis ROV Facility (2013). Getting the bigger picture: using precision Remotely Operated Vehicle (ROV) videography to acquire high-definition mosaic images of newly discovered hydrothermal vents in the Southern Ocean. *Deep. Res. Part II Top. Stud. Oceanogr.* 92, 124–135. doi:10.1016/j.dsr2.2013.02.007.

Martín, J., Puig, P., Masqué, P., Palanques, A., and Sánchez-Gómez, A. (2014). Impact of bottom trawling on deep-sea sediment properties along the flanks of a submarine canyon. *PLoS One* 9. doi:10.1371/journal.pone.0104536.

McArthur, M. A., Brooke, B. P., Przeslawski, R., Ryan, D. A., Lucieer, V. L., Nichol, S., et al. (2010). On the use of abiotic surrogates to describe marine benthic biodiversity. *Estuar. Coast. Shelf Sci.* 88, 21–32. doi:10.1016/j.ecss.2010.03.003.

McClintock, J. B., Amsler, C. D., Baker, B. J., and van Soest, R. W. M. (2005). Ecology of Antarctic marine sponges: an overview. *Integr. Comp. Biol.* 45, 359–368. doi:10.1093/icb/45.2.359.

McIntyre, F. D., Drewery, J., Eerkes-Medrano, D., and Neat, F. C. (2016). Distribution and diversity of deep-sea sponge grounds on the Rosemary Bank Seamount, NE Atlantic. *Mar. Biol.* 163, 1–11. doi:10.1007/s00227-016-2913-z.

McIntyre, F. D., Neat, F., Collie, N., Stewart, M., and Fernandes, P. G. (2015). Visual surveys can reveal rather different "pictures" of fish densities: comparison of trawl and video camera surveys in the Rockall Bank, NE Atlantic Ocean. *Deep. Res. Part I Oceanogr. Res. Pap.* 95, 67–74. doi:10.1016/j.dsr.2014.09.005.

Meyer, K. S., Soltwedel, T., and Bergmann, M. (2014). High biodiversity on a deep-water reef in the eastern Fram Strait. *PLoS One* 9, 1–16. doi:10.1371/journal.pone.0105424.

Mitchell, E. G., and Harris, S. (2020). Mortality , population and community dynamics of the glass sponge dominated community " The Forest of the Weird " from the Ridge Seamount, Johnston Atoll, Pacific Ocean. *Front. Mar. Sci.* 7, 1–21. doi:10.3389/fmars.2020.565171.

Molinski, T. F., and Faulkner, D. J. (1988). An antibacterial pigment from the sponge *Dendrilla Membranosa*. *Tetrahedron Lett.* 29, 2137–2138.

Moore, G. W. K., Vage, K., Pickart, R. S., and Renfrew, I. A. (2015). Decreasing intensity of open-ocean convection in the Greenland and Iceland Seas. *Nat. Clim. Chang.* 5, 877–882. doi:10.1038/nclimate2688.

Morata, N., Michaud, E., Poullaouec, M. A., Devesa, J., Le Goff, M., Corvaisier, R., and Renaud, P. E. (2020). Climate change and diminishing seasonality in Arctic benthic processes. *Philos. Trans. R. Soc. A Math. Phys. Eng. Sci.* 378. doi:10.1098/rsta.2019.0369.

Morato, T., González-Irusta, J. M., Dominguez-Carrió, C., Wei, C. L., Davies, A., Sweetman, A. K., Taranto, G. H., Beazley, L., García-Alegre, A., Grehan, A., and Laffargue, P. (2020). Climate-induced changes in the suitable habitat of cold-water corals and commercially important deep-sea fishes in the North Atlantic. *Glob.*

Chang. Biol. 26, 2181–2202. doi:10.1111/gcb.14996.

Morganti, T. M., Purser, A., Rapp, H. T., German, C. R., Jakuba, M. V., Hehemann, L., Blendl, J., Slaby, B. M., and Boetius, A. (2021). *In situ* observation of sponge trails suggests common sponge locomotion in the deep central Arctic. *Curr. Biol.* 31, R368–R370. doi:10.1016/j.cub.2021.03.014.

Morganti, T. M., Slaby, B. M., de Kluijver, A., Busch, K., Hentschel, U., Middelburg, J. J., Grotheer, H., Mollenhauer, G., Dannheim, J., Rapp, H. T., and Purser, A. (2022). Giant sponge grounds of Central Arctic seamounts are associated with extinct seep life. *Nat. Commun.* doi:10.1038/s41467-022-28129-7.

Morris, K. J., Bett, B. J., Durden, J. M., Huvenne, V. A. I., Milligan, R., Jones, D. O. B., McPhail, S., Robert, K., Bailey, D. M., and Ruhl, H. A. (2014). A new method for ecological surveying of the abyss using autonomous underwater vehicle photography. *Limnol. Oceanogr. Methods* 12, 795–809. doi:10.4319/lom.2014.12.795.

Morrison, K. M., Meyer, H. K., Roberts, E. M., Rapp, H. T., Colaço, A., and Pham, C. K. (2020). The first cut is the deepest: trawl effects on a deep-sea sponge ground are pronounced four years on. *Front. Mar. Sci.* 7, 1–13. doi:10.3389/fmars.2020.605281.

Muñoz, P. D., Sayago-Gil, M., Patrocinio, T., González-Porto, M., Murillo, F. J., Sacau, M., González, E., Fernández, G., and Gago, A. (2012). Distribution patterns of deep-sea fish and benthic invertebrates from trawlable grounds of the Hatton Bank, north-east Atlantic: Effects of deep-sea bottom trawling. *J. Mar. Biol. Assoc. United Kingdom* 92, 1509–1524. doi:10.1017/S002531541200015X.

Murillo, F. J., Kenchington, E., Lawson, J. M., Li, G., and Piper, D. J. W. (2016). Ancient deep-sea sponge grounds on the Flemish Cap and Grand Bank, northwest Atlantic. *Mar. Biol.* 163, 1–11. doi:10.1007/s00227-016-2839-5.

Murillo, F. J., Kenchington, E., Tompkins, G., Beazley, L., Baker, E., Knudby, A., and Walkusz, W. (2018). Sponge assemblages and predicted archetypes in the eastern Canadian Arctic. *Mar. Ecol. Prog. Ser.* 597, 115–135. doi:10.3354/meps12589.

Murillo, F. J., Muñoz, P. D., Cristobo, J., Ríos, P., González, C., Kenchington, E., and Serrano, A. (2012). Deep-sea sponge grounds of the Flemish Cap, Flemish Pass and the Grand Banks of Newfoundland (Northwest Atlantic Ocean): distribution and species composition. *Mar. Biol. Res.* 8, 842–854. doi:10.1080/17451000.2012.682583.

Oljedirektoratet (2021). Åpningsprosess for undersøkelse og utvinning av havbunnsmineraler på norsk kontinentalsokkel Forslag til program for konsekvensutredning etter havbunnsmineralloven. 38.

Ooms, J. (2021). magick: Advanced Graphics and Image-Processing in R. R package version 2.6.0. https://CRAN.R-project.org/package=magick.

OSPAR (2008). OSPAR List of Threatened And/or Declining Species and Habitats (Reference Number: 2008-6). London.

OSPAR (2010). Background Document for Deep-sea sponge aggregations Biodiversity Series. London. Available at: http://www.ospar.org/v_publications/browse.asp?preset=1&menu=00080800000000_000000_000000&v0_0=Background+Document+for+Deep-sea+sponge+aggregations&v1_0=n_code,title,language,ISBNNumber,YearOfPub

lication,SeriesName,Summary,publicationnumber&v2_0=&v0_1=&v1.

Pedersen, R. B., and Bjerkgård, T. (2016). "Sea-Floor Massive Sulphides in Arctic Waters," in *Mineral Resources In The Arctic 1*, 209–216.

Pedersen, R. B., Olsen, B. R., Barreyre, T., Bjerga, A., Denny, A., Heggernes Eilertsen, M., Fer, I., Haflidason, H., Hestetun, J. T., Jørgensen, S., Ribeiro, P. A., Steen, I. H., Stubseid, H., Tandberg, A. H. S., and Thorseth, I. (2021). Fagutredning mineralressurse i Norskehavet landskapstrekk, naturtyper og benthiske økosystemer. Bergen.

Pedersen, R. B., Rapp, H. T., Thorseth, I. H., Lilley, M. D., Barriga, F. J. A. S., Baumberger, T., Flesland, K., Fonseca, R., Früh-Green, G. L., and Jorgensen, S. L. (2010a). Discovery of a black smoker vent field and vent fauna at the Arctic Mid-Ocean Ridge. *Nat. Commun.* 1. doi:10.1038/ncomms1124.

Pedersen, R. B., Thorseth, I. H., Nygård, T. E., Lilley, M. D., and Kelley, D. S. (2010b). "Hydrothermal Activity at the Arctic Mid-Ocean Ridges," in *Diversity of Hydrothermal Systems on Slow Spreading Ocean Ridges*, eds. P. A. Rona, C. W. Devey, J. Dyment, and B. J. Murton, 67–89. doi:10.1029/2008GM000783.

Pham, C. K., Murillo, F. J., Lirette, C., Maldonado, M., Colaço, A., Ottaviani, D., and Kenchington, E. (2019). Removal of deep-sea sponges by bottom trawling in the Flemish Cap area: conservation, ecology and economic assessment. *Sci. Rep.* 9. doi:10.1038/s41598-019-52250-1.

Pizarro, O., and Singh, H. (2003). Toward large-area mosaicing for underwater scientific applications. *IEEE J. Ocean. Eng.* 28, 651–672. doi:10.1109/JOE.2003.819154.

Powell, A., Clarke, M. E., Fruh, E., Chaytor, J. D., Reiswig, H. M., and Whitmire, C. E. (2018). Characterizing the sponge grounds of Grays Canyon, Washington, USA. *Deep. Res. Part II Top. Stud. Oceanogr.* 150, 146–155. doi:10.1016/j.dsr2.2018.01.004.

Prado, E., Cristobo, J., Rodríguez-Basalo, A., Ríos, P., Rodríguez-Cabello, C., and Sánchez, F. (2021). *In situ* Growth Rate Assessment of the Hexactinellid Sponge *Asconema setubalense* Using 3D Photogrammetric Reconstruction. *Front. Mar. Sci.* 8, 1–16. doi:10.3389/fmars.2021.612613.

Purser, A., Hehemann, L., Boehringer, L., Tippenhauer, S., Wege, M., Bornemann, H., et al. (2022). A vast icefish breeding colony discovered in the Antarctic. *Curr. Biol.*, 1–9. doi:10.1016/j.cub.2021.12.022.

Ramirez-Llodra, E., Hilario, A., Paulsen, E., Costa, C. V., Bakken, T., Johnsen, G., and Rapp, H. T. (2020). Benthic communities on the Mohn's Treasure Mound: implications for management of seabed mining in the Arctic Mid-Ocean Ridge. *Front. Mar. Sci.* 7, 1–12. doi:10.3389/fmars.2020.00490.

Ramiro-Sánchez, B., González-Irusta, J. M., Henry, L.-A., Cleland, J., Yeo, I., Xavier, J. R., Carreiro-Silva, M., Sampaio, Í., Spearman, J., Victorero, L., and Messing, C.G. (2019). Characterization and mapping of a deep-sea sponge ground on the Tropic Seamount (Northeast Tropical Atlantic): implications for spatial management in the High Seas. *Front. Mar. Sci.* 6, 1–19. doi:10.3389/fmars.2019.00278.

Renaud, P. E., Berge, J., Varpe, O., Lønne, O. J., Nahrgang, J., Ottesen, C., and Hallanger, I. (2012). Is the poleward expansion by Atlantic cod and haddock

threatening native polar cod, *Boreogadus saida*? *Polar Biol.* 35, 401–412. doi:10.1007/s00300-011-1085-z.

Rice, A. L., Thurston, M. H., and New, A. L. (1990). Dense aggregations of a hexactinellid sponge, *Pheronema carpenteri*, in the Porcupine Seabight (northeast Atlantic Ocean), and possible causes. *Prog. Oceanogr.* 24, 179–196.

Ríos, P., Aguilar, R., Torriente, A., Muñoz, A., and Cristobo, J. (2018). Sponge grounds of *Artemisina* (Porifera, demospongiae) in the Iberian Peninsula, ecological characterization by ROV techniques. *Zootaxa* 4466, 95–123. doi:10.11646/zootaxa.4466.1.10.

Roberts, E. M., Bowers, D. G., Meyer, H. K., Samuelsen, A., Rapp, H. T., and Cárdenas, P. (2021). Water masses constrain the distribution of deep-sea sponges in the North Atlantic Ocean and Nordic Seas. *Mar. Ecol. Prog. Ser.* 659, 75–96. doi:10.3354/meps13570.

Rooper, C. N., Goddard, P., and Wilborn, R. (2019). Are fish associations with corals and sponges more than an affinity to structure? Evidence across two widely divergent ecosystems. *Can. J. Fish. Aquat. Sci.* 76, 2184–2198. doi:10.1139/cjfas-2018-0264.

Samuelsen, A., Schrum, C., Yumruktepe, V. Ç., Daewel, U., and Roberts, E. M. (2022). Environmental Change at Deep-Sea Sponge Habitats Over the Last Half Century : A Model Hindcast Study for the Age of Anthropogenic Climate Change. *Front. Mar. Sci.* 9:737164, 1–17. doi:10.3389/fmars.2022.737164.

Sánchez, F., Serrano, A., and Ballesteros, M. G. (2009). Photogrammetric quantitative study of habitat and benthic communities of deep Cantabrian Sea hard grounds. *Cont. Shelf Res.* 29, 1174–1188. doi:10.1016/j.csr.2009.01.004.

Savini, A., Vertino, A., Marchese, F., Beuck, L., and Freiwald, A. (2014). Mapping cold-water coral habitats at different scales within the Northern Ionian Sea (Central Mediterranean): an assessment of coral coverage and associated vulnerability. *PLoS One* 9. doi:10.1371/journal.pone.0087108.

Scanes, E., Kutti, T., Fang, J. K. H., Johnston, E. L., Ross, P. M., and Bannister, R. J. (2018). Mine waste and acute warming induce energetic stress in the deep-sea sponge *Geodia atlantica* and coral *Primnoa resedeaformis*; results from a mesocosm study. *Front. Mar. Sci.* 5, 1–14. doi:10.3389/fmars.2018.00129.

Schander, C., Rapp, H. T., Kongsrud, J. A., Bakken, T., Berge, J., Cochrane, S., Oug, E., Byrkjedal, I., Todt, C., Cedhagen, T., and Fosshagen, A. (2010). The fauna of hydrothermal vents on the Mohn Ridge (North Atlantic). *Mar. Biol. Res.* 6, 155–171. doi:10.1080/17451000903147450.

Sen, A., Himmler, T., Hong, W. L., Chitkara, C., Lee, R. W., Ferré, B., Lepland, A., and Knies, J. (2019). Atypical biological features of a new cold seep site on the Lofoten-Vesterålen continental margin (northern Norway). *Sci. Rep.* 9, 1–14. doi:10.1038/s41598-018-38070-9.

Singh, H., Howland, J., and Pizarro, O. (2004). Advances in Large-Area Photomosaicking. 29, 872–886.

Singh, H., Maksym, T., Wilkinson, J., and Williams, G. (2017). Inexpensive, small AUVs for studying ice-covered polar environments. *Sci. Robot.* 2. doi:10.1126/scirobotics.aan4809.

Singh, H., Roman, C., Pizarro, O., Eustice, R., and Can, A. (2007). Towards high-

resolution imaging from underwater vehicles. *Int. J. Rob. Res.* 26, 55–74. doi:10.1177/0278364907074473.

Solan, M., Archambault, P., Renaud, P. E., and März, C. (2020). The changing Arctic Ocean: consequences for biological communities, biogeochemical processes and ecosystem functioning. *Philos. Trans. R. Soc. A Math. Phys. Eng. Sci.* 378. doi:10.1098/rsta.2020.0266.

Somavilla, R., Schauer, U., and Budéus, G. (2013). Increasing amount of Arctic Ocean deep waters in the Greenland Sea. *Geophys. Res. Lett.* 40, 4361–4366. doi:10.1002/grl.50775.

Steffen, K., Indraningrat, A. A. G., Erngren, I., Haglöf, J., Becking, L. E., Smidt, H., Yashayaev, I., Kenchington, E., Pettersson, C., Cárdenas, P., and Sipkema, D. (2022). Oceanographic setting influences the prokaryotic community and metabolome in deep-sea sponges. *Sci. Rep.* 12, 1–16. doi:10.1038/s41598-022-07292-3.

Steffen, K., Laborde, Q., Gunasekera, S., Payne, C. D., Rosengren, K. J., Riesgo, A., Goransson, U., and Cárdenas, P. (2021). Barrettides: A peptide family specifically produced by the deep-sea sponge *Geodia barretti*. *J. Nat. Prod.* 84, 3138–3146. doi:10.1021/acs.jnatprod.1c00938.

Storesund, J. E., Sandaa, R. A., Thingstad, T. F., Asplin, L., Albretsen, J., and Erga, S. R. (2017). Linking bacterial community structure to advection and environmental impact along a coast-fjord gradient of the Sognefjord, western Norway. *Prog. Oceanogr.* 159, 13–30. doi:10.1016/j.pocean.2017.09.002.

Swift, J. H., Takahashi, T., and Livingston, H. D. (1983). Contribution of the Greenland and Barents Seas To the Deep Water of the Arctic Ocean. *J. Geophys. Res.* 88, 5981–5986. doi:10.1029/JC088iC10p05981.

Tangen, S (2011). A taxonomic inventory of Demospongiae occurring at abyssal depths on an arctic seamount, the Schulz Massive. MSc Thesis.

Tarling, G. A., Freer, J. J., Banas, N. S., Belcher, A., Blackwell, M., Castellani, C., Cook, K. B., Cottier, F. R., Daase, M., Johnson, M. L., and Last, K. S. (2022). Can a key boreal *Calanus* copepod species now complete its life-cycle in the Arctic? Evidence and implications for Arctic food-webs. *Ambio* 51, 333–344. doi:10.1007/s13280-021-01667-y.

Taylor, M. W., Radax, R., Steger, D., and Wagner, M. (2007). Sponge-associated microorganisms: evolution, ecology, and biotechnological potential. *Microbiol. Mol. Biol. Rev.* 71, 295–347. doi:10.1128/mmbr.00040-06.

Teixidó, N., Gili, J. M., Uriz, M. J., Gutt, J., and Arntz, W. E. (2006). Observations of asexual reproductive strategies in Antarctic hexactinellid sponges from ROV video records. *Deep. Res. Part II Top. Stud. Oceanogr.* 53, 972–984. doi:10.1016/j.dsr2.2006.02.008

Thomas, D. N., Arévalo-Martínez, D. L., Crocket, K. C., Große, F., Grosse, J., Schulz, K., Sühring, R., and Tessin, A. (2022). A changing Arctic Ocean. *Ambio* 51, 293–297. doi:10.1007/s13280-021-01677-w.

Thoms, C., and Schupp, P. J. (2008). Activated chemical defense in marine sponges-a case study on *Aplysinella rhax*. *J. Chem. Ecol.* 34, 1242–1252. doi:10.1007/s10886-008-9518-z.

Thoms, C., Schupp, P. J., Custodio, M. R., Lobo-Hajdu, G., Hajdu, E., and Muricy, G.

(2007). Chemical defense strategies in sponges: a review. *Porifera Res. biodiversity, Innov. Sustain. [Serie Livros 28]*, 627–637.

Tjensvoll, I., Kutti, T., Fosså, J. H., and Bannister, R. J. (2013). Rapid respiratory responses of the deep-water sponge *Geodia barretti* exposed to suspended sediments. *Aquat. Biol.* 19, 65–73. doi:10.3354/ab00522.

Torkildsen, M. M. (2013). Diversity of hexactinellid sponges (Porifera, Hexactinellida) on an arctic seamount, the Schulz Massive. MSc Thesis.

Tuerena, R. E., Mahaffey, C., Henley, S. F., de la Vega, C., Norman, L., Brand, T., Sanders, T., Debyser, M., Dähnke, K., Braun, J., and März, C. (2022). Nutrient pathways and their susceptibility to past and future change in the Eurasian Arctic Ocean. *Ambio* 51, 355–369. doi:10.1007/s13280-021-01673-0.

UN (2021). The Sustainable Development Goals Report 2021. New York.

UNGA (2006). Resolution 61/105 Sustainable fisheries, including through the 1995 Agreement for the Implementation of the Provisions of the United Nations Convention on the Law of the Sea of 10 December 1982 relating to the Conservation and Management of Straddling Fish Stocks and Highly Migratory Fish Stocks, and related instruments. UNGA A/RES/61/105.

Vad, J., Barnhill, K. A., Kazanidis, G., and Roberts, J. M. (2021). *Human impacts on deep-sea sponge grounds: Applying environmental omics to monitoring*. 1st ed. Elsevier Ltd. doi:10.1016/bs.amb.2021.08.004.

Vad, J., Kazanidis, G., Henry, L. A., Jones, D. O. B., Gates, A. R., and Roberts, J. M. (2020). Environmental controls and anthropogenic impacts on deep-sea sponge grounds in the Faroe-Shetland Channel, NE Atlantic: The importance of considering spatial scale to distinguish drivers of change. *ICES J. Mar. Sci.* 77, 451–461. doi:10.1093/icesjms/fsz185.

Van Audenhaege, L., Broad, E., Hendry, K. R., and Huvenne, V. A. I. (2021). High-Resolution vertical habitat mapping of a deep-sea cliff offshore Greenland. *Front. Mar. Sci.* 8, 1–18. doi:10.3389/fmars.2021.669372.

van Soest, R. W. M., Boury-Esnault, N., Vacelet, J., Dohrmann, M., Erpenbeck, D., de Voogd, N. J., Santodomingo, N., Vanhoorne, B., Kelly, M., and Hooper, J.N. (2012). Global diversity of sponges (Porifera). *PLoS One* 7. doi:10.1371/journal.pone.0035105.

Vieira, R. P., Bett, B. J., Jones, D. O. B., Durden, J. M., Morris, K. J., Cunha, M. R., Trueman, C. N., and Ruhl, H. A. (2020). Deep-sea sponge aggregations (*Pheronema carpenteri*) in the Porcupine Seabight (NE Atlantic) potentially degraded by demersal fishing. *Prog. Oceanogr.* 183. doi:10.1016/j.pocean.2019.102189.

Wentworth, C. K. (1922). A Scale of grade and class terms for clastic sediments. *J. Geol.* 30, 377–392. doi:10.1086/622910.

Williams, A., Schlacher, T. A., Rowden, A. A., Althaus, F., Clark, M. R., Bowden, D. A., Stewart, R., Bax, N. J., Consalvey, M., and Kloser, R. J. (2010). Seamount megabenthic assemblages fail to recover from trawling impacts. *Mar. Ecol.* 31, 183–199. doi:10.1111/j.1439-0485.2010.00385.x.

Witte, U., Aberle, N., Sand, M., and Wenzhöfer, F. (2003). Rapid response of a deep-sea benthic community to POM enrichment: an in-situ experimental study. *Mar. Ecol. Prog. Ser.* 251, 27–36. doi:10.3354/meps251027.

Wulff, J. L. (2006). Ecological interactions of marine sponges. *Can. J. Zool.* 84, 146–166. doi:10.1139/z06-019.

Wurz, E., Beazley, L., MacDonald, B., Kenchington, E., Rapp, H. T., and Osinga, R. (2021). The hexactinellid deep-water sponge *Vazella pourtalesii* (Schmidt, 1870) (Rossellidae) copes with temporarily elevated concentrations of suspended natural sediment. *Front. Mar. Sci.* 8, 1–15. doi:10.3389/fmars.2021.611539.

Wynn, R. B., Huvenne, V. A. I., Le Bas, T. P., Murton, B. J., Connelly, D. P., Bett, B. J., Ruhl, H. A., Morris, K. J., Peakall, J., Parsons, D. R., and Sumner, E. J. (2014). Autonomous Underwater Vehicles (AUVs): Their past, present and future contributions to the advancement of marine geoscience. *Mar. Geol.* 352, 451–468. doi:10.1016/j.margeo.2014.03.012.

Xavier, J. R., Tojeira, I., and van Soest, R. W. M. (2015). On a hexactinellid sponge aggregation at the Great Meteor seamount (North-east Atlantic). *J. Mar. Biol. Assoc. United Kingdom* 95, 1389–1394. doi:10.1017/S0025315415000685.

Zhulay, I., Bluhm, B. A., Renaud, P. E., Degen, R., and Iken, K. (2021). Functional pattern of benthic epifauna in the Chukchi Borderland, Arctic deep sea. *Front. Mar. Sci.* 8, 1–20. doi:10.3389/fmars.2021.609956.

Zurowietz, M., Nattkemper, T. W., and Salem, S. I. (2021). Current Trends and Future Directions of large scale image and video annotation: observations from four years of BIIGLE 2.0. *Front. Mar. Sci.* 8, 760036. doi:10.3389/fmars.2021.760036.

Publications

Paper 1

Deep-Sea Research Part I 138 (2018) 98–113

Contents lists available at ScienceDirect

Deep-Sea Research Part I

journal homepage: www.elsevier.com/locate/dsri

Oceanographic setting and short-timescale environmental variability at an Arctic seamount sponge ground

E.M. Roberts[a,*], F. Mienis[b], H.T. Rapp[c], U. Hanz[b], H.K. Meyer[c], A.J. Davies[a]

[a] School of Ocean Sciences, Bangor University, Menai Bridge, Anglesey LL59 5AB, UK
[b] NIOZ Royal Netherlands Institute for Sea Research and Utrecht University, Department of Ocean Sciences, P.O. Box 59, 1790 AB Den Burg, Texel, The Netherlands
[c] Department of Biology and K.G. Jebsen Centre for Deep Sea Research, University of Bergen, P.O. Box 7803, N-5020 Bergen, Norway

ARTICLE INFO

Keywords:
Sponges
Seamounts
Mid-ocean ridge
Deep sea
Hexactinellida
Astrophorida

ABSTRACT

Mass occurrences of large sponges, or 'sponge grounds', are found globally in a range of oceanographic settings. Interest in these grounds is growing because of their ecological importance as hotspots of biodiversity, their role in biogeochemical cycling and bentho-pelagic coupling, the biotechnological potential of their constituent sponges, and their perceived vulnerability to physical disturbance and environmental change. Little is known about the environmental conditions required for sponges to persist and for grounds to form, and very few studies have explicitly characterised and interpreted the importance of oceanographic conditions. Here, results are presented of the first observational oceanographic campaign at a known sponge ground on the Schultz Massif Seamount (SMS; Arctic Mid-Ocean Ridge, Greenland / Norwegian Seas). The campaign consisted of water column profiling and short-term deployment of a benthic lander. It was supported by multibeam echosounder bathymetry and remotely operated vehicle video surveys. The seamount summit hosted several environmental factors potentially beneficial to sponges. It occurred within relatively nutrient-rich waters and was regularly flushed from above with slightly warmer, oxygen-enriched Norwegian Arctic Intermediate Water. It was exposed to elevated suspended particulate matter levels and oscillating currents (with diurnal tidal frequency) likely to enhance food supply and prevent smothering of the sponges by sedimentation. Elevated chlorophyll *a* concentration was observed in lenses above the summit, which may indicate particle retention by seamount-scale circulation patterns. High sponge density and diversity observed on the summit is likely explained by the combination of several beneficial factors, the coincidence of which at the summit arises from interaction between seamount geomorphology, hydrodynamic regime, and water column structure. Neighbouring seamounts along the mid-ocean ridge are likely to present similarly complex oceanographic settings and, as with the SMS, associated sponge ground ecosystems may therefore be sensitive to changes over a particularly broad range of abiotic factors.

1. Introduction

Mass occurrences of large sponges, or 'sponge grounds', are found globally, including in fjords, on continental shelves and slopes, and in the deep sea at mid-ocean ridges and seamounts (Barthel, 1992; Whitney et al., 2005; Hogg et al., 2010; Murillo et al., 2012; Bo et al., 2012; Cathalot et al., 2015; Maldonado et al., 2015). At sponge grounds, sponges dominate the benthic macrofauna in terms of body size and abundance (Hogg et al., 2010), and often account for the majority of invertebrate biomass (Klitgaard and Tendal, 2004; Murillo et al., 2012; Maldonado et al., 2015). Beyond this, considerable variability exists between prevailing 'types' of sponge ground (in terms of distribution, community composition, and species richness), and current understanding of these ecosystems is limited such that even a simple, quantitative framework of sponge ground definitions does not yet exist. Sponge grounds occurring in the deep sea have received relatively little scientific attention, in contrast to cold-water coral reefs, for example, which have been studied extensively in recent decades (see Freiwald and Roberts, 2005).

Interest in deep-sea sponge grounds has been growing, driven by three main factors. Firstly, sponges possess significant biotechnological and biomedical potential. Their anatomical structures have inspired biomimetic lines of research and their secondary metabolites are a valuable source of potentially useful bioactive compounds (e.g., Belarbi et al., 2003; Sundar et al., 2003; Ehrlich et al., 2010; Leal et al., 2012; Dudik et al., 2018). Secondly, sponge grounds are ecologically

* Corresponding author.
E-mail address: emyr.roberts@bangor.ac.uk (E.M. Roberts).

https://doi.org/10.1016/j.dsr.2018.06.007
Received 19 January 2018; Received in revised form 8 May 2018; Accepted 11 June 2018
Available online 12 June 2018

important. They are increasingly recognised as hotspots of biodiversity and biomass in the deep sea (Klitgaard, 1995; Beazley et al., 2013). They form complex biogenic habitats (sponge structures + 'spicule mat' substrate (Bett and Rice, 1992)), where there is a general paucity of such structural habitat (Buhl-Mortensen et al., 2010). These provide refuge, foraging, spawning, and nursery grounds for fish (Kenchington et al., 2013; Kutti et al., 2015), and create an abundance of microhabitats for sponge-associated invertebrates (Barthel, 1992; Bett and Rice, 1992; Herrnkind et al., 1997; Freese and Wing, 2003, and references therein; Henkel and Pawlik, 2005; Amsler et al., 2009; Maldonado et al., 2015). Sponge grounds also play important roles in biogeochemical cycling and bentho-pelagic coupling (Gatti, 2002; Pile and Young, 2006; Bell, 2008; Hoffmann et al., 2009; De Goeij et al., 2013; Kutti et al., 2013). Thirdly, deep-sea sponges are thought to be vulnerable to physical disturbance and environmental change (Hogg et al., 2010). This is in need of assessment to ensure adequate protection, mitigation, and sustainable exploitation measures are in place. Sponges may take millennia to form grounds (Murillo et al., 2016a), be very slow-growing (Pusceddu et al., 2014), and reproduce infrequently (Klitgaard and Tendal, 2004). Deep-sea sponge grounds have recently been classified as a 'habitat under immediate threat and / or decline' by the OSPAR Commission (OSPAR, 2008), and a 'vulnerable marine ecosystem (VME)' by the Food and Agriculture Organisation of the United Nations (FAO, 2009).

Despite a growing body of research highlighting the functional significance of deep-sea sponge grounds, little is known about the environmental conditions required for sponges to persist, and for sponge grounds to form at specific locations. This is fundamentally important information for the assessment of their vulnerability and response to disturbance and climate change. Several authors have commented on the importance of various hydrographic variables. A number have emphasised the need for stable bottom conditions in terms of temperature and salinity (Klitgaard and Tendal, 2004; Murillo et al., 2016a), or relate the presence of sponges to that of a particular water mass or current system in the study region (Barthel et al., 1996; Klitgaard and Tendal, 2004; Murillo et al., 2012; Beazley et al., 2015; van Haren et al., 2017). Murillo et al. (2012) report the temperature and salinity ranges (3.38 – 3.84 °C; 34.85 – 34.90‰) experienced by sponge grounds dominated by large astrophorid demosponges off Newfoundland, Canada. They note that these conditions, provided by the Labrador Current, may be suitable for the sponges' persistence, but other factors must influence the finer-scale patterns of distribution in this region (Murillo et al., 2012). Modelling studies have implicated silicate concentration, and near-bed temperature and salinity (amongst other factors) as important drivers of broad-scale sponge ground distribution in the North Atlantic (Knudby et al., 2013; Howell et al., 2016). The availability of a suitable substrate for settlement, growth, and development seems likely to influence local-scale sponge distribution, though there is apparent variability in substrate requirements for different sponge species (Klitgaard and Tendal, 2004; c.f. Murillo et al., 2016a, 2016b). Water column turbidity has also been proposed as a factor limiting the distribution of sponge grounds (Klitgaard and Tendal, 2004). Excessive suspended particulate matter (particularly inorganic) loads are believed to clog the filtration systems of some sponges and therefore render some locations unviable for colonisation (Klitgaard and Tendal, 2004).

Hydrodynamical phenomena are frequently invoked as mechanisms explaining the presence of a sponge ground. Rice et al. (1990) considered the theoretical possibility that near-bed tidal currents are locally enhanced by interaction between the flow and the bed slope. A resonance-type intensification of the local currents is believed to occur at locations where internal tides (internal waves of tidal frequency) would typically be generated (Sandstrom, 1975; New, 1988; Huthnance, 1989), and it was hypothesised that these enhanced near-bed currents would resuspend (or maintain in near-bed suspension) flocculent phytodetrital material and improve food supply to a downslope population of sponges (Rice et al., 1990). Different authors also place emphasis on the importance of internal tides, focussing instead on current enhancement by incident / reflecting internal tides propagating along water mass boundaries that impinge upon seabed features (e.g., slopes and seamounts), and the acceleration of local currents, the generation of turbulence, and the induction of various flow patterns by interactions between prevailing current regimes and irregular seabed topography have been proposed to be important at various spatial scales (Genin et al., 1986; Klitgaard and Tendal, 2004; McIntyre et al., 2016; van Haren et al., 2017). The importance of enhanced currents to sponge grounds is typically outlined in terms of improved food / larval supply and the prevention of smothering by settling suspended sediments. The idea that such currents are useful in inducing a passive flow through sponges that reduces the metabolic cost of pumping (Leys et al., 2011) has been thus far overlooked. Although sponge grounds are frequently found on sloped or irregular topography, leading to speculation about the predominance of hydrodynamic influence, McIntyre et al. (2016) note that they are also reported from relatively flat areas (e.g., Tromsøflaket in the Western Barents Sea (Klitgaard and Tendal, 2004; and personal observation) and Hatton Basin in the Northeast Atlantic (Durán Muñoz et al., 2011)).

Very few studies have explicitly set out to characterise and interpret the importance of oceanographic conditions at deep-sea sponge grounds. Genin et al. (1986) measured the current regime at the Jasper Seamount in the Eastern Pacific, which hosts an abundant and diverse fauna dominated by suspension feeders such as sponges and corals. They noted that abundance peaked at sites of flow acceleration (i.e., at topographic peaks), and they attributed this to flow conditions that are favourable either through a 'settlement pathway' (i.e., an enhanced supply of larval recruits per unit time) or a 'feeding pathway' (i.e., an enhanced supply of potential food per unit time) (Genin et al., 1986). White (2003) measured currents in the Porcupine Seabight (west of Ireland) at both locations of sponge presence and absence. Their measurements supported the hypothesis of Rice et al. (1990) that the sponges (the hexactinellid *Pheronema carpenteri*) favour locations adjacent to regions of enhanced near-bed tidal currents (where they benefit from the advection of resuspended material in the bottom boundary layer), but probably cannot tolerate the highest currents found locally (White, 2003). Whitney et al. (2005) examined the oceanographic conditions at hexactinellid sponge reefs occurring at the heads of shelf canyons off Canada's west coast. These authors identified up-canyon transport of water rich in nutrients (particularly silicates) and suspended matter as important in explaining sponge reef presence, and noted that conditions may be favourable in several other respects also (e.g., appropriate ranges of dissolved oxygen, temperature, and salinity, and the prevalence of moderate, tidally-modulated near-bed currents that increase food supply to, and food residency times near, the sponges and prevent smothering by sedimentation) (Whitney et al., 2005). Beazley et al. (2015) investigated the hydrographic conditions associated with dense sponge grounds on the Sackville Spur in the Northwest Atlantic and concluded that their presence could potentially be attributed to a warm, salty remnant of the Irminger Current residing over the slope in that area.

No comprehensive oceanographic survey studies of deep-sea sponge ground localities currently exist for the Northeast Atlantic - Arctic region, despite there being numerous, widely distributed sponge grounds in the area (Klitgaard and Tendal, 2004). Such studies, though descriptive, offer valuable insight into the physical setting and environmental requirements of marine ecosystems. Studies of this type relating to cold-water coral reefs, for example, have identified food supply mechanisms (Davies et al., 2009, 2010) and improved understanding of the ideal conditions for their growth and development (Mienis et al., 2007). The purpose of the current paper is to present the results of the first short-duration, high temporal resolution, observational oceanographic campaign at a cold-water sponge ground (*sensu* Klitgaard and Tendal (2004) on the Schultz Massif Seamount (SMS) of the Arctic Mid-

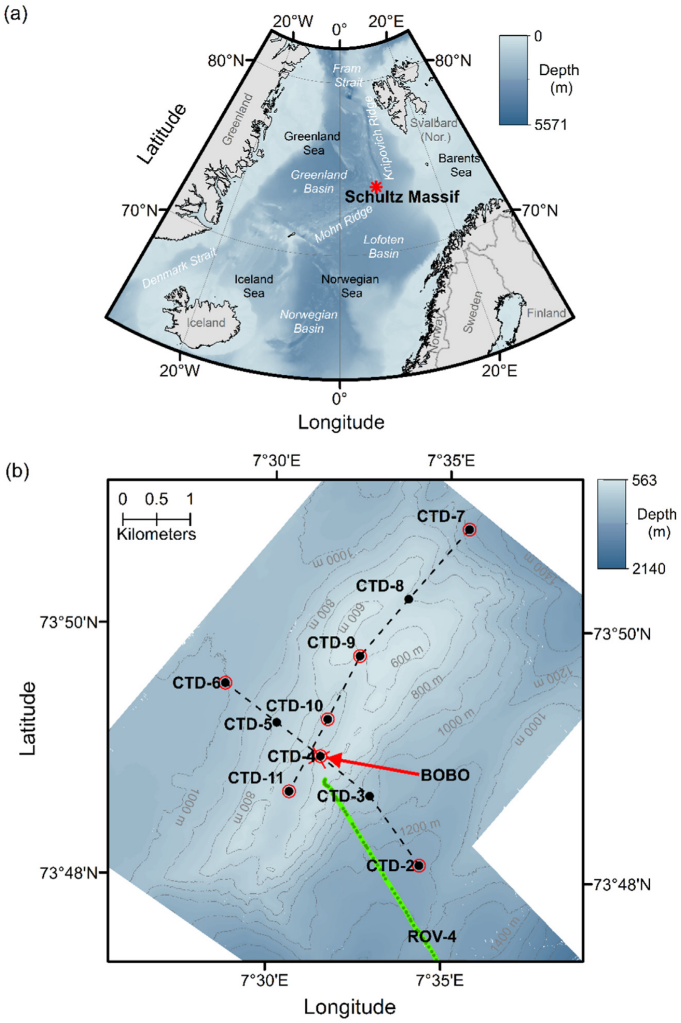

Fig. 1. The Schultz Massif Seamount (SMS) study site. (a) shows the location of the SMS in the Nordic Seas region (polar stereographic map projection; 30 arc-second bathymetry from General Bathymetric Chart of the Oceans 2014 (Weatherall et al., 2015); coastline data from NOAA's Global Self-consistent, Hierarchical, High-resolution Shoreline Database (Wessel and Smith, 1996)). (b) shows bathymetry at the SMS from multibeam echosounder data (EM 302; spatial resolution = 10 m). Conductivity, temperature, and depth (CTD) profile stations are indicated by solid black circles, and transects by dashed lines. Water sampling (rosette sampler) is indicated with additional red outer circles. The Bottom Boundary Benthic Lander (BOBO) is denoted by a red cross. The bright green line shows the ROV video transect analysed; darker green dots indicate the positions of still images extracted for the analysis.

Ocean Ridge. The campaign consisted of a water column profiling survey and a c. 3 day deployment of a benthic lander, and was supported by multibeam echosounder bathymetry and remotely operated vehicle (ROV) video data collection. The oceanographic setting and short-timescale environmental variability experienced by the sponges is described. A peak in sponge density and diversity was observed towards the seamount summit, and explanations for this observation are considered in light of the oceanographic data collected.

2. Materials and methods

2.1. Study site

The Schultz Massif (73° 50′ N, 7° 34′ E) is a seamount located at the Arctic Mid-Ocean Ridge (AMOR), a 4000 km long, ultraslow-spreading ridge extending northwards from north of Iceland into the Polar Basin (Bruvoll et al., 2009). It is situated at a bend in the ridge at which the Mohn Ridge transitions into the Knipovich Ridge (Fig. 1(a)). It has a broadly elliptical shape in plan view, with its major axis oriented northeast-southwest (Fig. 1(b)), and rises from abyssal depths of more than 2500 m in adjacent basins to depths of 560–600 m at the summit. A trough of approximately 100 m depth and 500 m width bisects the summit and is aligned with the major axis described above. The lower slope of the seamount is dominated by soft sediments (mainly calcareous foraminifera) with some rocky outcrops and areas covered by pillow lavas. At intermediary parts of the slope soft sediments are still dominant, but rocky outcrops and walls are common. Approaching the summit there are still some rocky outcrops; sediments have a high content of sponge spicules. In the upper 100 m of the seamount a spicule mat is present that is up to 20 cm thick.

Estimating the seamount's dimensions is complicated, as it belongs to a ridge system. Based on bathymetry data collected (Fig. 1(b)), a major axis of 10 km and a minor axis of 4 km appear appropriate. The deepest contours relating to this footprint are 1400–1500 m deep. We use these values in later calculations. However, they represent lower bound estimates and larger values could also be considered appropriate (e.g., 15 km × 6 km, > 2000 m depth at the base), based on coarser resolution bathymetry datasets and depending on the criteria applied to

define the seamount's extent. The effects of using larger estimates in calculations have been considered (see Section 4).

The SMS lies at the nominal boundary between the Greenland and Norwegian Seas, two of the three Nordic Seas (the Iceland Sea being the third). These seas host two-way advective exchange between the Polar Sea and the North Atlantic Ocean, and they act as primary sites of water mass formation and transformation, producing waters that feed into the deep North Atlantic Ocean as dense overflows across the Greenland-Scotland Ridge (Dickson and Brown, 1994; Mauritzen, 1996; Hansen and Østerhus, 2000). The physical oceanography of the Nordic Seas is described in Hopkins (1991), and the surface circulation is fairly well known. Polar Water, of low temperature and salinity, enters the region primarily as a surface water mass (Greenland Polar Water) in a southward flowing current (the East Greenland Current) that travels through the western side of the Fram Strait and along the eastern Greenland Shelf (Hopkins, 1991). North Atlantic Water, which is warmer and of higher salinity, enters from the south, also as a surface water mass (Norwegian Atlantic Water, NwAtW), in the northwards flowing and variously branched Norwegian Atlantic Current (Orvik and Niiler, 2002). Nordic Sea water masses can thus be considered mixtures of Polar Water, North Atlantic Water, and locally-formed / -modified deep water(s) (Carmack and Aagaard, 1973). Key water masses in the vicinity of the SMS are likely to include Norwegian Deep Water (NwDW), Upper Norwegian Deep Water (uNwDW), Norwegian Arctic Intermediate Water (NwArIW), and NwAtW (defined above), though the influence of Greenland Basin water masses cannot be ruled out (Hopkins, 1991). Understanding of the circulation of intermediate and deep water masses is being continually revised, as more and better physical data become available. There is some evidence that Norwegian intermediate and deep water masses have an advective origin (i.e., as opposed to significant local production), in contrast to those in the Greenland and Iceland Seas (Hopkins, 1991; Jeansson et al., 2017).

The AMOR is a significant bathymetric feature in the Nordic Seas. It influences circulation patterns and water exchange between adjacent basins / seas (Mauritzen, 1996). Orvik and Niiler (2002) demonstrated that the western-most branch of the Norwegian Atlantic Current consists of a jet steered by topography such as the Mohn and Knipovich Ridges (Orvik and Niiler, 2002). The SMS is a prominent feature in the ridge system, and is likely to be subject to (and contribute towards the creation of) a complex oceanographic setting. It may be influenced by such topographically-steered deep currents. Hydrodynamical modelling efforts have predicted that semi-diurnal tidal constituents dominate diurnal constituents in terms of tidal elevation in the vicinity of the SMS (Lyard, 1997). In terms of tidal current velocity the reverse situation can occur, with diurnal tidal currents dominating (Kowalik and Proshutinsky, 1993, and references therein). Several of these authors note strong local responses to diurnal tidal forcing in the velocity field of the Northeast Atlantic - Arctic region. Harmonic constants and tidal predictions (elevations and currents) determined for the SMS from regional barotropic inverse tidal solutions using the Oregon State University Tidal Inversion Software (OTIS; Egbert and Erofeeva, 2002) corroborate the importance of diurnal tides to the velocity field (see Section 3 and Supplementary material).

The sponge ground at the SMS has been the subject of several research cruises by the University of Bergen (UiB) since 2008. Biological sampling by means of ROV, epibenthic sledges, bottom trawls, and cores, supported by high-definition video imagery, has revealed seemingly rich and undisturbed benthic communities dominated mostly by sponges, anthozoans, and ascidians (see Torkildsen (2013), as well as Cárdenas et al. (2013), Hestetun et al. (2017), and Plotkin et al. (2017) for dominating sponge taxa).

2.2. Fieldwork campaign

A multi-disciplinary research cruise to the SMS was conducted using the *RV G.O. Sars* (Norwegian Institute of Marine Research and UiB) from 18th to 26th June 2016. The present study focusses on physical and biogeochemical data collected during this cruise, particularly those from the deployment of a benthic lander and from water column profiling and sampling. Acoustic maps of the seamount bathymetry and high-definition video imagery of its benthic environments and fauna (captured using an ROV) have been used primarily to supplement existing knowledge on the site.

2.2.1. Acoustic mapping

The bathymetry of the SMS was mapped using an EM 302 multibeam echosounder system (Kongsberg Maritime AS, Kongsberg, Norway). The EM 302 has a nominal sonar frequency of 30 kHz and uses 288 beams (per swath) over a maximum angular coverage of 150° (beam spacing was equidistant). This system is well suited to mapping bathymetry in deep water, down to depths of 7000 m. Mapping of the seamount summit and flanks was achieved in four parallel survey lines (aligned approximately northeast to southwest), and the resulting bathymetric data (gridded to 10 m spatial resolution) were used to select a site for the benthic lander deployment and to plan the water column profiling survey strategy.

2.2.2. ROV video imagery and water sampling

ROV Ægir 6000 (Kystdesign AS, Haugesund, Norway) is a 95 kW remotely operated vehicle (dimensions: 2.75 × 1.70 × 1.65 m) rated to 6000 m water depth, owned by UiB. It has considerable scientific payload capacity (400 kg) and can be deployed with various suites of modular sensors and sampling equipment. High-definition video footage of benthic communities on the SMS was recorded during base-to-summit transects from several directions and during targeted biological sampling for taxonomic and other studies.

For the present work, imagery from video transect ROV-4 (see Fig. 1) was analysed. The transect ran approximately south-east to north-west, spanned a depth range of 1313–658 m (i.e., approaching the summit), and took 8 h to complete. Still images were extracted from the footage at 5 min intervals and analysed to obtain estimates of species richness and abundance for the major taxonomic groups present amongst the large epifauna observed. ROV altitude (or 'flying height') varied over the transect. For consistency, images captured when ROV altitude was outside the range 1–3 m were not included in the analysis. 16 images were disregarded for this reason, out of 72 'under-way' images available. It was not possible to reliably provide quantities per unit area, but values 'per image' are sufficient to demonstrate relative changes / trends over depth, as is required for this study (particularly for sponges (phylum Porifera) as a group). More in-depth analysis of the video transect data will be presented in a forthcoming publication.

The ROV was fitted with small Niskin bottles (3 L sample volumes), which were used to opportunistically sample water near the seamount summit. Sub-samples were taken for dissolved inorganic carbon and nutrient concentration analysis, and were handled according to the procedures outlined in Section 2.4. below.

2.2.3. Near-bed observations

A free-falling, autonomous 'Bottom Boundary' Benthic Lander (BOBO; van Weering et al., 2000) was deployed near the seamount summit (73° 48.960′ N, 7° 31.408′ E, at 669 m water depth) on the 20th June 2016 for a period slightly longer than 3 days. It was equipped with instruments set to log time series observations of several key oceanographic parameters, including water temperature, salinity, dissolved oxygen concentration, and current velocity. In the present study, a short-leg lander configuration (i.e., relative to the original design) was employed.

The scientific payload of the BOBO Lander included the following instruments: (1) an SBE 16 Seacat conductivity and temperature (CT) Sensor (Sea-Bird Electronics Inc., Washington, USA), mounted at 2 m above the seabed (mab) upon deployment; (2) a Rinko I fast response optical dissolved oxygen sensor (JFE Advantech Co. Ltd., Hyogo,

Japan), mounted at 2 mab; (3) an upward-looking 300 kHz acoustic Doppler current profiler (ADCP) (Teledyne RDI Inc., California, USA), mounted at 2.2 mab; and (4) a high-definition video camera (Sony Corp., Tokyo, Japan) with LED illumination, directed at the seabed just outside the footprint of the lander and mounted at 0.7 mab. Sensors were programmed with a 5 min sampling interval, with the exception of the video camera, which was programmed to record 30 s of footage every 15 min.

The lander also hosted a programmable, autonomous particulate sampler (Phytoplankton Sampler (PPS), McLane Research Laboratories Inc., Massachusetts, USA). This was programmed to pump 24 individual in situ water samples, in time series, through pre-combusted, pre-weighed glass microfibre filters (47 mm diameter Whatman GF/F, nominal pore size 0.7 μm, GE Healthcare UK Ltd., UK) for the determination of suspended particulate matter (SPM) concentration by gravimetric analysis (after Strickland and Parsons, 1972). The programme was scheduled to begin shortly after lander deployment, with a sample volume of 7.5 L being filtered every 2 h at a flow rate of 125 mL min^{-1}. Owing to battery failure and filter paper damage, only 10 reliable samples were obtained over the first 22 h and the resulting values were averaged to obtain a near-bed SPM estimate for comparison with water column concentrations.

2.2.4. Water column profiling

Water column profiling at the SMS was conducted along two transects: across the seamount's ridge-like summit, and along the summit ridge (Fig. 1(b)). Each transect consisted of 5 CTD stations. The across-ridge CTD transect commenced at 04:02 h UTC on the 22nd June 2016 at the south-eastern end of the transect (CTD-2 in Fig. 1(b)), and was completed by 09:06 h UTC. The along-ridge transect commenced at 07:18 h UTC on the 23rd June 2016 at the north-eastern end of the transect (CTD-7 in Fig. 1(b)), and was completed by 11:41 h UTC. Profiling was carried out using a conductivity, temperature, depth (CTD) system (SBE-9, manufactured by Sea-Bird Electronics Inc., Washington, USA) with additional sensors including a dissolved oxygen sensor (SBE-43, also by Sea-Bird), a turbidity sensor (Seapoint Sensors Inc., New Hampshire, USA), and a fluorometer (AquaTracka III, manufactured by Chelsea Technologies Group Ltd., UK). At all stations, the CTD unit was lowered to approximately 10 – 20 mab and raised before moving on to the next station. The CTD system was installed on a rosette water sampler (consisting of twelve 10 L Niskin water bottles). Water samples were collected at selected stations (those indicated by solid black circles with red outer rings in Fig. 1(b)) and depths (typically near-bed, mid-water column, and chlorophyll *a* maximum / surface) for a suite of analyses, including the determination of inorganic nutrient (PO_4^{3-}, NO_3^- + NO_2^-, Si), dissolved inorganic carbon (DIC), and suspended particulate matter (SPM) concentrations (see Section 2.4.). CTD-1 was an off-seamount reference station, approximately 20 km to the southeast of the SMS (73° 38.896′ N, 7° 52.734′ E, 2462 m water depth), which was sampled (profiles and water samples) on the 20th June 2016 at 07:55 h UTC. All reported CTD depth values were estimated from measured pressures using equations from Fofonoff and Millard (1983).

2.3. Particle motion analysis of video footage

Owing to component failure within the ADCP, video footage from the lander was analysed instead to infer the nature of the current regime from recorded particle motion. 326 videos were captured sequentially over the course of the lander deployment. Each video was converted into 'stacks' of individual image frames (1920 × 1080 pixels), such that 300 frames were produced per video (i.e., 10 frames per second of footage). A smaller region (180 × 500 pixels) was extracted from the top right corner of each frame for further analysis, as this area consistently contained clearly identifiable particles.

Coordinates (in pixels from the image origin) and frame numbers were obtained for the start and end of the trajectories of up to 10 particles per video using the image processing software ImageJ (Schneider et al., 2012). Assuming linear paths and constant speeds, particle speeds and directions were calculated using Pythagoras' Theorem (for distance travelled, in pixels), frames elapsed (as a proxy for travel time), and trigonometric relations (to determine direction). Average particle speed was determined for each video by calculating the arithmetic mean of the individual particle speeds (i.e., scalar averaging), whilst average particle direction was determined as a unit vector average (see Gilhousen, 1987).

Average particle speeds were converted from units of 'pixels per frame' to relative units by normalising all values by the maximum observed over the deployment period. More meaningful physical units could not be obtained because the camera set-up lacked a means of determining spatial scale accurately (e.g., parallel lasers of known separation). Direction determined in the way described refers to particle motion occurring in the plane of the images only (i.e., no particle motion towards or away from the camera was quantified). We used the convention that 0° relates to vertical motion upwards, 180° relates to downwards motion, 90° relates to lateral motion towards the right of the image, and 270° relates to motion towards the left. It was not possible to relate these directions to a geographic coordinate system (e.g., to estimate flow direction).

Some qualitative criteria were applied to the selection of particles to analyse. Brighter, clearer particles were preferentially selected, as these could be more easily 'tracked'. Particles that exhibited an obvious change in diameter over their trajectories were deemed likely to possess a component of motion in the axis perpendicular to the plane of the image (i.e., towards or away from the camera) and were thus ignored (motion in this axis could not be resolved precisely). Any particles with curved or spiralling trajectories were ignored, since straight-line travel was assumed in calculations. Approximately 12% of the videos failed to provide 10 particle trajectories for analysis (the minimum number of trajectories analysed for any one video was 3).

2.4. Water sample analyses

In situ water samples were collected at several stations, as described in Section 2.2.4. For every sampled depth, two times 5 L of seawater were immediately filtered over pre-combusted (450 °C; 4 h), pre-weighed (balance precision = ± 0.01 mg) GF/F filters (47 mm diameter; 0.7 μm nominal pore size) under an applied vacuum for the determination of SPM concentration by gravimetric analysis. After filtration, filters were flushed with 100 mL of purified water to dissolve salt crystals, and were then stored at − 20 °C until further analysis at NIOZ. In the laboratory, filters were freeze-dried (-12 h; Vaco 5 (Zirbus Technology GmbH, Germany)) and re-weighed in order to calculate the total mass of suspended matter in each water sample.

Additional samples were taken from the Niskin bottles for the determination of dissolved inorganic carbon (DIC) and nutrient concentrations (i.e., phosphate (PO_4^{3-}), ammonium (NH_4^+ - not presented), nitrate (NO_3^-), nitrite (NO_2^-), and silicate (Si)). These were collected in 50 mL Nalgene bottles, which had been rinsed three times with water from the relevant Niskin bottles before filling. After sampling on deck, samples were filtered through 0.2 μm polycarbonate membrane filters (Whatman Nuclepore). Those samples intended for nutrient analysis were immediately sub-sampled into two vials, one of which was used for PO_4^{3-}, NH_4^+, NO_3^-, and NO_2^- determination (stored at −20 °C) and the other for Si determination (stored at 4 °C). Nutrient concentrations were determined by colorimetric analyses in the NIOZ laboratory using a QuAAtro Continuous Segmented Flow Analyser (Seal Analytical Ltd., UK). Measurements were made simultaneously on four channels: PO_4^{3-}, NH_4^+, NO_2^-, and NO_3^- and NO_2^- combined. Si concentrations were analysed in separate runs of the QuAAtro system. All measurements were calibrated against standards diluted to known nutrient concentrations with low nutrient seawater (LNSW). The LNSW

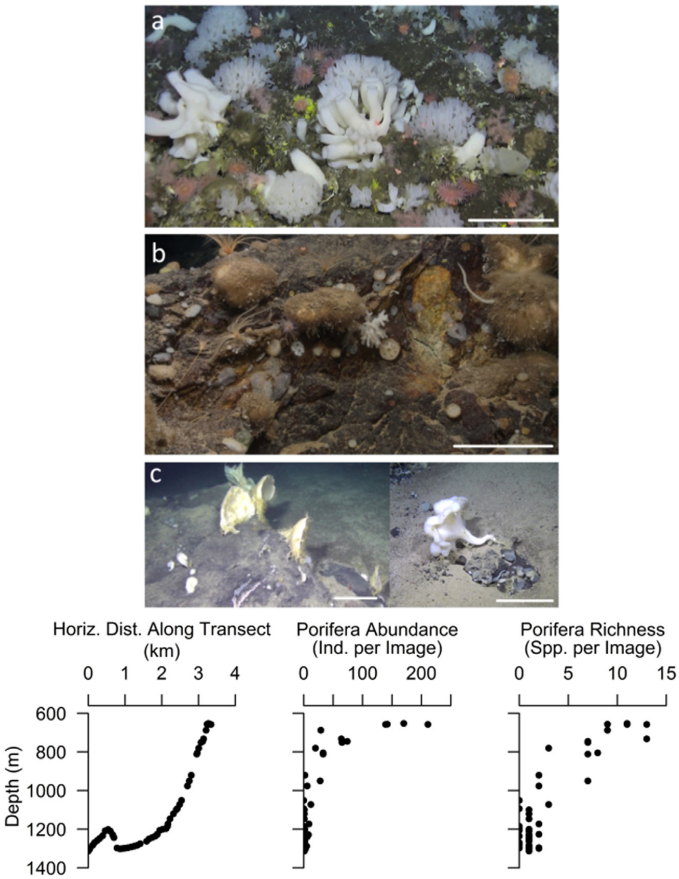

Fig. 2. Sponge-dominated communities found along a depth gradient on the Schultz Massif Seamount. (a) shows the typical sponge community in the summit area (560–700 m depth), dominated by *Schaudinnia rosea* (coarse branching sponge) and *Asconema foliata* (delicate branching sponge) growing on a dense layer of spicule mat and living tetractinellid sponges (*Geodia parva*, *G. hentscheli*, and *Stelletta rhaphidiophora*). (b) shows the seamount flank (at ~1000–1400 m depth), dominated by *Geodia hentscheli* (brownish, massive) and the polymastid *Spinularia njordi* (disc-shaped). (c) shows an unidentified Axinellidae (left) and *Caulophacus arcticus* (right), two common representatives of the sponges found on hard substrates in deeper areas around the base of the seamount. All scale bars represent 0.3 m. Plots beneath the images show depth profiles of total abundance and species richness of sponges (phylum Porifera), as determined from ROV video transect analysis.

was in the salinity range of the stations at the SMS (approximately 35 psu) to ensure calibration standards were of equivalent ionic strength to samples and hence negate salt effects. Each run of the system produced a calibration curve with a correlation coefficient of at least 0.9999 for 10 calibration points, but typically 1.0000 for linear chemistry. A freshly-diluted, mixed nutrient standard, containing silicate, phosphate, and nitrate (a so-called 'nutrient cocktail'), was measured in every run, as a guide to monitor the performance of the standards.

Filtered seawater samples intended for DIC determination were transferred into glass vials already containing 15 μL $HgCl_2$ (mercury chloride). The vials were filled with a convex meniscus before being capped and stored upside down in a refrigerator. Samples were analysed on a Traacs 800 Auto-Analyser (Seal Analytical Ltd., formerly Technicon) following the methodology described in Stoll et al. (2001).

3. Results

3.1. Sponge ground characteristics from biological sampling

Variation was observed in the composition and distribution of sponge-dominated communities along a depth gradient (i.e., summit, slope, and base) on the seamount. The summit and shallower areas (560–700 m water depth) were inhabited mainly by dense aggregations of hexactinellid sponges (*Schaudinnia rosea*, *Trichasterina borealis*, *Scyphidium septentrionale*, and *Asconema foliata*) (see also Torkildsen, 2013) along with tetractinellids (*Geodia parva*, *G. hentscheli*, and *Stelletta rhaphidiophora*) (Cárdenas et al., 2013) growing on a mixed substrate dominated by spicule mats (Fig. 2(a)). The slope was largely dominated by *G. hentscheli*, polymastiids, and various encrusting sponges growing on hard substrates (Fig. 2(b)). Deeper areas (> 2000 m depth) were dominated by the demosponges *Spinularia sarsi*, *Tentorium semisuberites*, and *Thenea abyssorum* (Barthel and Tendal, 1993; Plotkin et al., 2017) on soft sediments, along with the hexactinellid sponges *Caulophacus arcticus* and *Asconema megaatrialia* and dense aggregations of unidentified Axinellidae on hard substrates (mainly pillow lava) (Torkildsen, 2013; this study, Fig. 2(c)). The dominating sponge fauna found on the SMS represent a core group of ground-forming species shared by a number of seamounts along this ridge system.

ROV video transect analysis (ROV-4) revealed trends of increasing species richness and total abundance with decreasing water depth (i.e., increasing elevation up the seamount) for the phylum Porifera (plots in Fig. 2), which clearly dominated the large epifauna. Similar trends were observed in ROV transects from different directions, and more in-depth analysis of these data will be presented in a forthcoming article. The summit sponge aggregations were particularly dense and diverse, and the seabed there is largely covered by surficial spicule mats of several centimetres thickness (~10–20 cm thick - data not presented in this article).

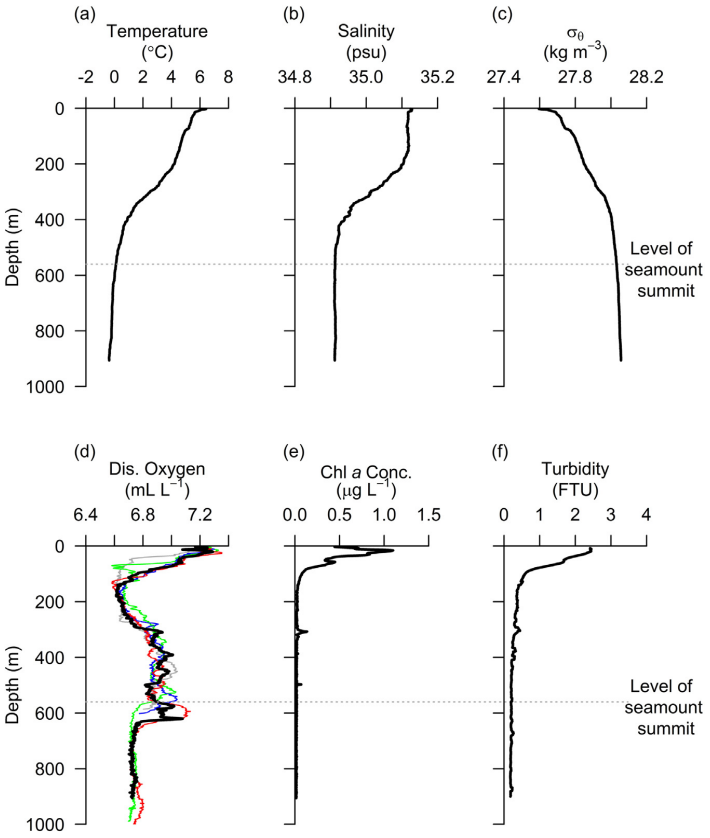

Fig. 3. Vertical profiles of (a) water temperature, (b) salinity, (c) potential density anomaly (σ_θ), (d) dissolved oxygen concentration, (e) chlorophyll a concentration, and (f) turbidity from CTD Station 3. Dissolved oxygen profiles from several other CTD stations are also plotted in panel (d) (coloured lines) to illustrate the variability observed in the position of the local maximum near the level of the seamount summit.

3.2. Oceanographic setting from water column profiling

Representative water depth profiles of key oceanographic parameters are shown in Fig. 3. Profiles were similar across all seamount stations (i.e., CTD-2 to −11). A permanent thermocline and halocline are clearly discernible in panels (a) and (b), respectively, between approximately 200 and 400 m. There is also evidence of seasonal stratification occurring near the surface.

Dissolved oxygen concentration (Fig. 3(d)) exhibited a sub-surface maximum in the upper water column (~25 m depth). This was coupled with maxima in both fluorescence and turbidity (panels (e) and (f)), suggesting a productive surface layer most likely benefitting from oxygenated water and, at least in its upper range, light availability. A broad zone of reduced oxygen concentration was present, centred on the base of the surface layer (~200 m). Below this zone, a layer of elevated oxygen concentration was observed between 300 and 650 m. Within the oxygen-enriched layer, a peak in oxygen concentration was consistently observed to coincide approximately with the level of the adjacent seamount summit. Spatio-temporal variability in the position of this peak over the survey is illustrated in Fig. 3(d) by the inclusion of oxygen profiles from a number of other CTD stations.

In several profiles (particularly CTDs 3, 4, and 7–11), secondary peaks in fluorescence were apparent at the upper boundary of the oxygen-enriched layer (~300 m; Fig. 3(e)). Close inspection reveals associated peaks in turbidity (Fig. 3(f)), likely indicating the presence of a lens (or lenses) of water with elevated suspended matter content or a thin intermediate nepheloid layer (INL). No similar features were observed at the off-seamount reference station (CTD-1). Note that the turbidity profile in Fig. 3(f) has been smoothed to remove spikes caused by large individual particles and/or instrument noise. Profiles of chlorophyll *a* concentration and turbidity are shown together for all CTD stations in Supplementary Figs. S1 and S2. High surface values have been omitted (i.e., 200–1000 m depth plotted) to allow the use of an appropriate horizontal axis scale for inspecting the smaller, secondary peaks. The square of the Brunt-Väisälä buoyancy frequency, N^2 (a measure of stratification stability), is also shown. The chlorophyll and turbidity peaks at~300 m coincide with peaks in N^2. The lenses of suspended matter appear to have occurred at a local increase in vertical density gradient (also seen in Fig. 3(c)) associated with the transition to the oxygen-enriched layer / intermediate water mass.

The permanent thermocline and halocline were also observed at approximately 200–400 m depth in the across-ridge CTD transect (Fig. 4(a) and (b)). The oxygen-enriched layer, apparent in Fig. 3, spans the entire transect and has a near-constant thickness of approximately 300 m (Fig. 4(c)). The lower boundary of this layer was just above the level of the bed (at the ridge crest), though the transect did not cross the absolute summit of the seamount, which was almost 100 m shallower. Lenses of water with elevated fluorescence levels are evident above the

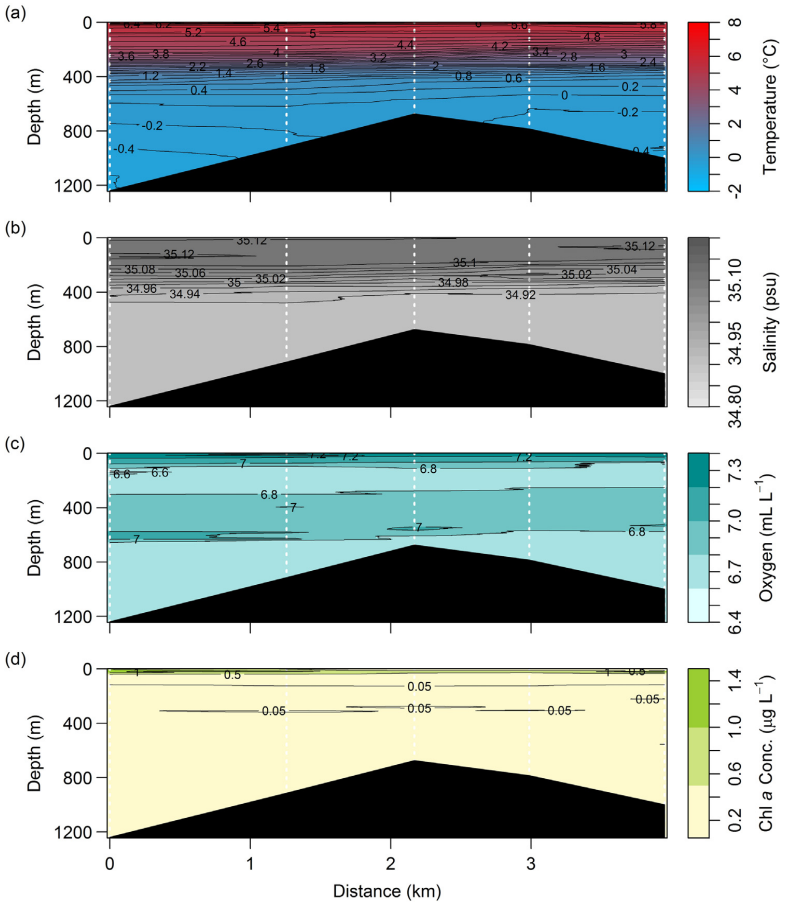

Fig. 4. Cross-sectional distribution of (a) water temperature, (b) salinity, (c) dissolved oxygen concentration, and (d) chlorophyll a concentration from the across-ridge water column profiling transect (south-east to north-west).

ridge crest (Fig. 4(d)) at the upper boundary of the oxygen-enriched layer. Cross-sections from the along-ridge CTD transect exhibit similar features and are shown in Fig. 5. Notably this transect bisected the seamount summit, crossing topography of greater elevation, and so convergence of the oxygen-enriched layer upon the summit is apparent. In both cross-sections there is evidence of the vertical displacement of isotherms in the mid-water column (~300–600 m) from station to station. Such displacements indicate either a modification of the water column structure by the seamount or baroclinic tidal perturbations captured over the course of each CTD transect. In the along-ridge salinity and dissolved oxygen cross-sections (Fig. 5(b) and (c)) horizontal gradients present in surface waters (< 200 m) may indicate a frontal scenario.

A potential temperature-salinity (θ-S) diagram was produced (Fig. 6) using all CTD profiles collected in the vicinity of the seamount (i.e., CTD-2 – 11). For each profile, the top 100 m of data were removed because temperature and salinity are influenced by surface processes at these depths (rather than simply the mixing and advection of water masses) and cannot be considered to behave conservatively. The θ-S diagram shows the influence of 3 principal water masses: (1) Norwegian Atlantic Water (NwAtW – $\theta > 2\,^{\circ}C$, $S > 35$ psu); (2) Norwegian Arctic Intermediate Water (NwArIW – $\theta \approx 0.5\,^{\circ}C$, $S \approx 34.88$ psu); and (3) Upper Norwegian Deep Water (uNwDW – $\theta \approx -0.5\,^{\circ}C$, $S \approx 34.92$ psu) (Hopkins, 1991; Blindheim and Østerhus, 2005). Since NwAtW has its origins in the North Atlantic, North Atlantic Water (NAtW) with $\theta > 8\,^{\circ}C$ and $S > 35.3$ psu is its warmest, highest salinity end member (not shown). The coldest end member influencing water mass structure in this region is likely to be Norwegian Deep Water (NwDW - $\theta \approx -1.05\,^{\circ}C$, $S \approx 34.91$ psu) (Hopkins, 1991; Blindheim and Østerhus, 2005). The influence of NwArIW occurred at depths corresponding to the oxygen-enriched layer (i.e., between 300 and 600 m).

Depth profiles of inorganic nutrient concentrations (PO_4^{3-}, $NO_3^- + NO_2^-$, Si) and dissolved inorganic carbon (DIC) at SMS are shown in Fig. 7. They combine values from water samples taken during the CTD survey and during ROV dives near the summit. Nutrient concentrations in the surface layer were low, indicating depletion by phytoplankton. They increased, whilst dissolved oxygen decreased, with depth in the surface layer. This likely reflects the combined effects of decreasing phytoplankton photosynthesis, growth, and nutrient uptake with depth and of oxygen depletion and nutrient enhancement by microbial respiration and remineralisation processes near the base of the surface layer. The zone of reduced oxygen concentration at this level (discussed above) is likewise accounted for. Nutrient concentrations and DIC continued to increase with increasing water depth: they were high

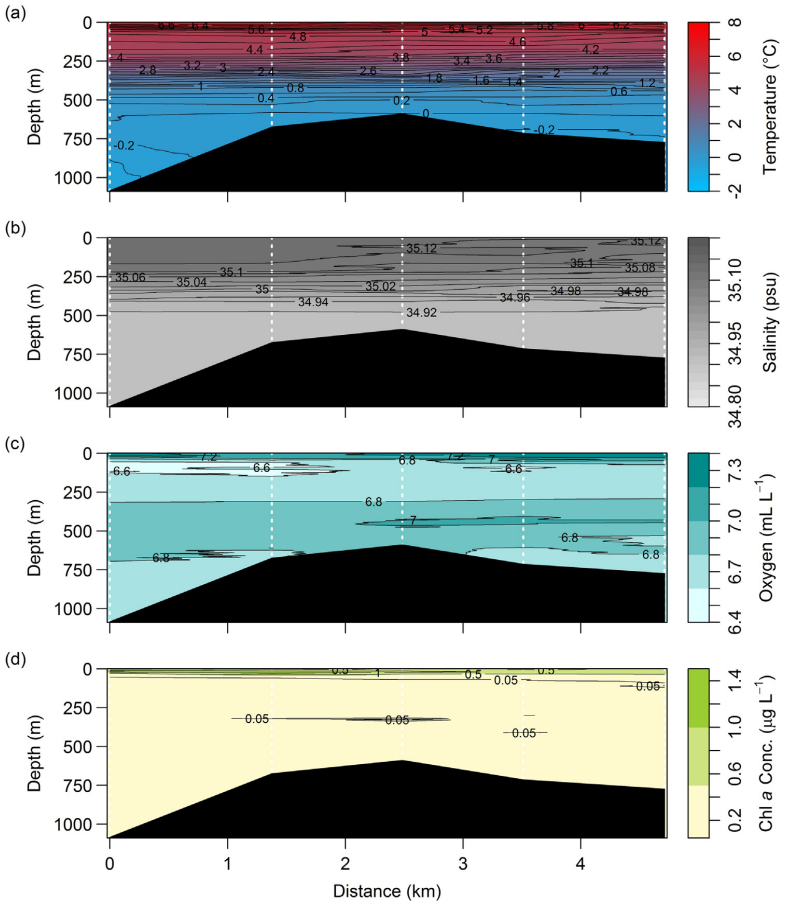

Fig. 5. Cross-sectional distribution of (a) water temperature, (b) salinity, (c) dissolved oxygen concentration, and (d) chlorophyll a concentration from the along-ridge water column profiling transect (north-east to south-west).

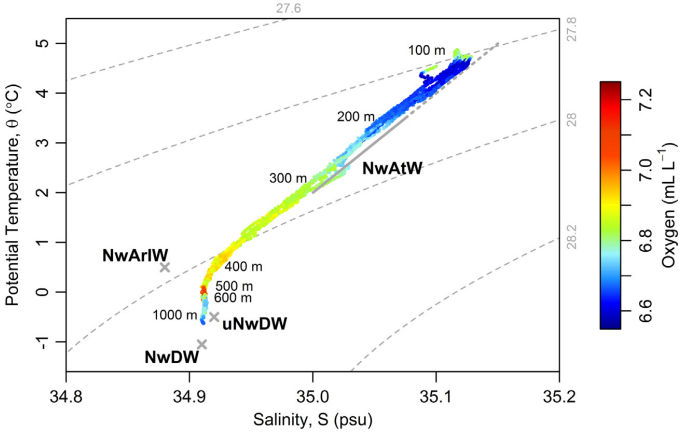

Fig. 6. Potential temperature-salinity (θ-S) diagram showing the water mass structure in the vicinity of the Schultz Massif Seamount (June 2016). Dissolved oxygen concentrations are overlaid. Norwegian Atlantic Water (NwAtW), Norwegian Arctic Intermediate Water (NwArIW), Upper Norwegian Deep Water (uNwDW), and Norwegian Deep Water (NwDW) characteristics are shown using a thick grey line and grey crosses, respectively (values from Hopkins (1991) and Blindheim and Østerhus (2005)). Dashed grey curves are isopycnals (labelled with potential density anomaly, σ_θ, values).

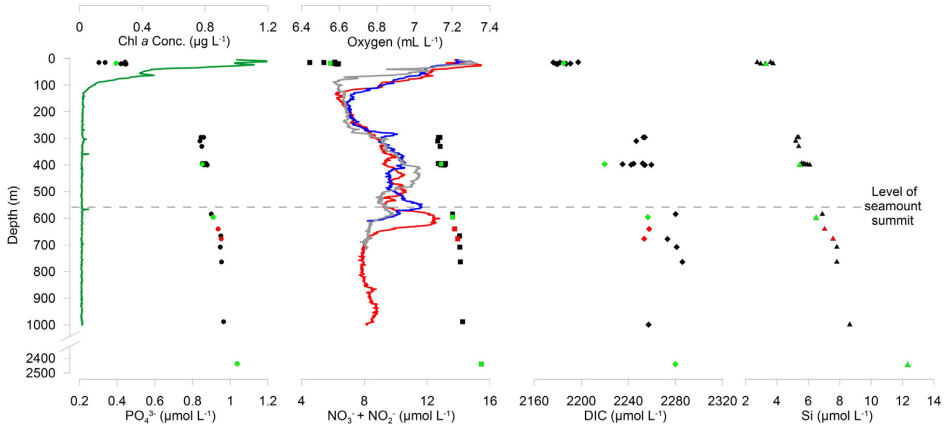

Fig. 7. Vertical profiles of inorganic nutrient concentrations (PO_4^{3-}, NO_3^- + NO_2^-, Si) and dissolved inorganic carbon (DIC) at the Schultz Massif Seamount. Near-seamount values have been combined (black symbols) and are presented with those from opportunistic water sampling during ROV dives to the summit (red points). Values from the deeper, off-seamount reference station (CTD-1) are also included (bright green points). A chlorophyll a profile (CTD-2; green line) and several dissolved oxygen profiles (CTD-2, −4, and −10; red, blue, and grey lines, respectively) are plotted to provide context.

(relative to surface waters) in the NwArIW (400–600 m), and slightly higher still in the uNwDW (> 600 m).

Fig. 8 shows depth profiles of SPM at the SMS. All profiles show elevated SPM in the surface layer (~1.5–2 mg L^{-1}), likely the result of surface productivity. SPM values were generally smaller at 300–400 m water depth (~1 mg L^{-1}), and similar values were observed in deeper waters (at the bottom of profiling casts). An average value for near-bed (0.6 mab) SPM concentration was determined to be 3.2 mg L^{-1} (range: 2.4–4.2 mg L^{-1}) using data from the McLane particulate sampler installed on the benthic lander (value shown in Fig. 8 for comparison).

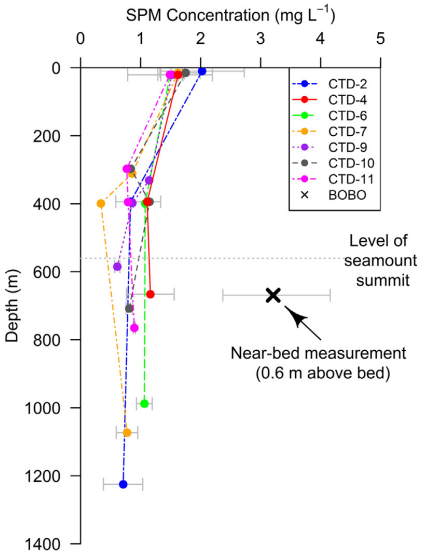

Fig. 8. Vertical profiles of suspended particulate matter (SPM) concentration at the Schultz Massif Seamount. An average near-bed value (i.e., 0.6 mab), determined using data from the benthic lander, is also shown for comparison. Error bars represent the data range for mean-averaged points, and are thus not shown for those depths at which single samples (rather than duplicates) were obtained.

Near-bed SPM appeared considerably elevated when compared with values at equivalent depths in adjacent water column profiles. This is indicative of local / near-field particulate resuspension by near-bed currents. Elevated levels of SPM in bottom waters are not clearly detectable in the depth profiles, as the CTD-Rosette unit was rarely permitted to approach the bed to within 10 m.

3.3. Near-bed time series data from the benthic lander

Time series data recorded by the BOBO lander are shown in Fig. 9. Regular, in-phase fluctuations were observed in water temperature and dissolved oxygen concentration (Fig. 9(a) and (b)). Each consisted of (1) a 'jump-relax' event (shaded grey in Fig. 9) characterised by an initial step-increase and a gradual decline (exhibiting a secondary, less pronounced local maximum) and (2) a short period of lower temperature and dissolved oxygen (typically exhibiting reduced temporal variability in both parameters). For the two entire cycles captured in the record, the period was 25.7 and 26.7 h (measured from step-increase to step-increase). Further (partial) cycles can be discerned at the start and end of the record.

The temperature and dissolved oxygen signals had a fixed-phase relationship with periodic variations in near-bed suspended particle speeds and particularly directions (Fig. 9(c) and (d)), as determined from video analysis. Change of particle direction coincided with the step-increases in temperature and dissolved oxygen, and the particles continued in that direction (left to right, laterally in the benthic boundary layer) during the gradual relaxation of these parameters. Particle direction reversed (right to left) for the duration of the short 'reduced-variability' stages, with the result that the periodic variations in particle direction were somewhat asymmetric (particles travelled for longer in one direction than in the reverse). Particle speeds were generally elevated during the longer 'jump-relax' stage, exhibiting two peaks during these periods. They were typically lower during the shorter 'reduced-variability' stage. The data derived from lander video analysis in this paper are subject to several limitations (see Section 2) but offer qualitative insight. Taking particle speed and direction as proxies for current speed and direction, the fixed-phase relationship with temperature and dissolved oxygen suggests a hydrodynamical phenomenon is responsible for the temporal behaviour of these parameters. Diurnal tidal forcing is likely important, given the periods between successive 'jumps' and the periodicity of the particle direction

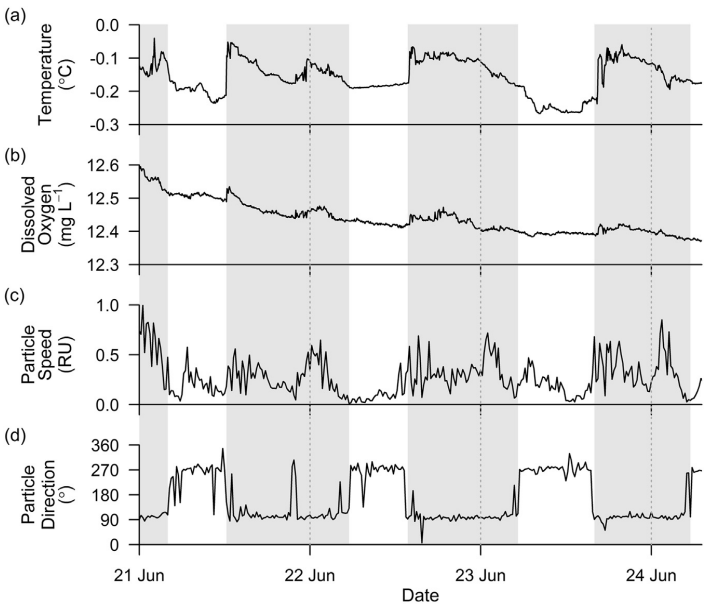

Fig. 9. Time series data from the Bottom Boundary (BOBO) Benthic Lander deployed near the seamount summit for c. 3 days in June 2016. Panels show (a) water temperature, (b) dissolved oxygen concentration, (c) suspended particle speed, and (d) suspended particle direction (0° = up (in the video footage); 180° = down; 90° = towards the right; 270° = towards the left; see Section 2). Grey-shaded areas highlight 'jump-relax' events in temperature and dissolved oxygen and associated features in particle speed and direction (see text).

behaviour, but this does not preclude the influence of higher frequency signals. For example, the secondary local maxima in temperature and dissolved oxygen (i.e., those peaks that are not 'jump'-like), and associated peaks in particle speed, occurring throughout the record could indicate the influence of shorter period tidal constituents or inertial motions.

To support near-bed flow information inferred from video analysis, data were extracted from a regional barotropic inverse tidal solution using the Oregon State University Tidal Inversion Software (OTIS – 'Iceland' domain; Egbert and Erofeeva, 2002). Harmonic constants for key tidal constituents at the SMS are shown in Table S1, and tidal current amplitudes indicate that diurnal constituents are indeed likely to dominate the local velocity field. In fact, the importance of the luni-solar diurnal tidal constituent (K_1) relative to the principal lunar semi-diurnal constituent (M_2) appears to increase in the vicinity of the SMS (Fig. S3). Tidal current predictions from OTIS for the SMS at the time of the lander observations show encouragingly similar patterns to those in the dataset inferred from analysis of the lander video (see Fig. S4(b-d)), including strong asymmetry in the current direction signal (Fig. S4(d)). Predicted current speeds from OTIS appear too low, however, being almost 3 cm s^{-1} at peak flow. This is likely owing to the depth-averaged, barotropic nature of the model, which does not capture baroclinic components that may be contributing to the observed tidal currents. The limitations of the particle motion analysis (Section 2.3) have prevented presentation of flow information in typical physical units in this article. However, based on features visible in the video footage, estimated peak flow speeds are of the order of 25 cm s^{-1} for this window of observation, and are indicative of enhanced flows at the SMS summit.

The temperatures immediately before and after the largest 'jump' in the lander record were extracted (−0.21 °C and −0.05 °C, respectively) and compared to adjacent CTD profiles, in order to determine the depths at which waters of these temperatures typically occur and their vertical separation. These two values were separated by 131 ± 50 m water depth (mean ± SD), averaged across 4 CTD profiles from the nearest stations adjacent to the lander's position (i.e., CTD-3, −5, −10, −11). The cast at CTD-4, nearest the lander site, was not deep enough to capture the full range of temperatures experienced by the lander, and so could not be used for this purpose. This analysis suggests that vertical displacements of water / isotherms by 130 m or more can occur at this location, interacting with the seamount summit with a periodicity of slightly longer than 1 d. The warmest water incident upon the lander site (669 m water depth) was more typically found 72 m higher in the water column (at 597 ± 40 m depth (mean ± SD)), at the base of the layer of NwArIW. The change in water temperature at the time of a 'jump' is fairly rapid, occurring in 15 min or less.

Note that a decreasing trend was apparent in the dissolved oxygen record but, owing to the short duration of the time series, it is unclear whether this can be attributed to longer timescale variability or to gradual acclimatisation of the instrument to a deep-sea environment. The salinity record has been omitted from Fig. 9 because fluctuations in salinity were small to negligible and no clear temporal pattern could be discerned above noise (i.e., short periods of spikey salinity data at step-changes in temperature, most likely the result of thermal-lag induced instrumental error – see Garau et al. (2011)). De-spiking and interpolation of the salinity record could not be achieved with sufficient scientific rigour, but visual inspection confirmed an estimated mean salinity value of 34.91 psu is appropriate. This is consistent with values at the same water depth from the CTD survey.

4. Discussion

The purpose of this study was to characterise the oceanographic setting and short-timescale environmental variability at the SMS in order to identify environmental conditions that sustain and influence a dense sponge ground on its summit. The summit coincided approximately with the lower boundary of an intermediate water mass, believed to be Norwegian Arctic Intermediate Water (NwArIW) (Blindheim, 1990; Hopkins, 1991; Blindheim and Rey, 2004; Jeansson et al., 2017). This had a slightly higher temperature and dissolved oxygen concentration than the deep water mass below (Upper Norwegian Deep Water – uNwDW), to which the seamount flanks were exposed. Time series records from a site just below the seamount summit revealed a series of regular fluctuations in water temperature and dissolved oxygen concentration. These events corresponded with patterns

in reversing near-bed currents, which had a periodicity approximately equal to that of the diurnal tide. Comparison of maximum and minimum temperatures from the time series with temperature profiles from the CTD survey suggests that the fluctuations represent periodic impingement of waters upon the summit that are typically separated by around 130 m depth in the adjacent water column. The warmest water incident upon the lander was typically found 72 m higher in the water column, at the base of the layer of NwArIW. It appears that the summit of the SMS hosts a dynamic environment that is predominantly tidally-forced, a feature common to several sponge-dominated communities described in the scientific literature (see Section 4.2. – *Biological response*).

Other potentially important factors were observed, and are summarised here. Near-bed SPM levels were elevated compared to those in the adjacent water column. Particulate matter was transported laterally in the benthic boundary layer. Its direction of travel underwent frequent reversal, and transport was asymmetric (discussed below). Lenses of water with enhanced chlorophyll *a* concentration were apparent above the seamount summit (at the base of the permanent thermocline / top of the layer of NwArIW). Levels of inorganic nutrients and DIC in uNwDW were slightly elevated compared to NwArIW. Horizontal gradients of salinity and dissolved oxygen concentration were observed at shallow depths during the along-ridge CTD transect (Fig. 5(b) and (c)), possibly indicating the proximity of a front between surface water masses.

Two main questions arise, which are addressed below. What is the dynamical phenomenon responsible for the observed temporal variability in near-bed parameters? How is the observed environmental setting likely to influence sponges on the summit?

4.1. Hydrodynamics

It has not been possible to fully describe the prevailing hydrodynamics at the SMS summit on the basis of a short-term current record, from a single site, containing derived (rather than directly measured) information (see Section 2.3.). However, diurnal tidal forcing appears important. The amplification of diurnal tidal currents at seamount summits and other isolated topographic features is regularly reported in the scientific literature (e.g., Eriksen, 1991; Haidvogel et al., 1993 (and references therein); Brink, 1995; Codiga and Eriksen, 1997). Exactly how seamounts intensify such currents is yet to be clearly established (Kunze and Toole, 1997).

Reflection of incident internal waves has been proposed as one explanatory mechanism (Kunze and Sanford, 1986). The SMS site (latitude: 73° 47′N) is above the critical 'diurnal turning' latitude (~30°N and S) at which the diurnal tidal frequency equals the inertial frequency. Below this critical latitude, diurnal period internal waves are super-inertial and can propagate freely (Kunze and Sanford, 1986; Kulikov et al., 2010). Above it, they are subinertial and cannot do so (Kunze and Sanford, 1986; Kulikov et al., 2010). It is therefore unlikely that diurnal period internal waves from remote sources could be incident upon (and reflected from) the seamount, intensifying near-bed currents. The SMS is < 1° of latitude below the critical 'semi-diurnal turning' latitude (~74.5°N and S for the principal lunar semi-diurnal tidal constituent (M_2)). Semi-diurnal period internal waves are superinertial at the latitude of the SMS and can propagate freely. Thus, incoming semi-diurnal internal waves may potentially contribute to bottom current amplification at the SMS. Although a diurnal signal clearly dominates the timeseries record from the benthic lander, there is some evidence to suggest fluctuations of a higher (possibly semi-diurnal/inertial) frequency. Contribution from the semi-diurnal tide is not unexpected at the latitude of the SMS through mechanisms other than reflection of internal waves. Indeed, several authors have found internal tidal currents to be significantly amplified at near-critical latitudes (such as we have here for the M_2 tide) (Munk and Phillips, 1968; Furevik and Foldvik, 1996; Kulikov et al., 2010).

Baroclinic wave motions that are trapped to seamount topography ('seamount-trapped' topographic waves) are often cited as a mechanism by which oscillating bottom currents may be amplified (Chapman, 1989; Eriksen, 1991; Haidvogel et al., 1993; Brink, 1995; Codiga and Eriksen, 1997). These are believed to be resonantly generated and excited to substantial amplitudes by relatively weak oscillatory flows (e.g., the diurnal tide in many parts of the deep open ocean) (Chapman, 1989; Brink, 1990; Eriksen, 1991; Haidvogel et al., 1993). Internal wave motion generated locally may also persist as 'vortex-trapped' waves (i.e., trapped in circulation patterns existing around the seamount summit) (Kunze and Toole, 1997; White et al., 2007). In both cases, diurnal tidal motions are likely to feature more prominently because the site is above the critical 'diurnal turning' latitude, rendering such motions unable to propagate away freely. Vortex-trapped diurnal internal waves are subject to constraints of scale above about 40°N and S (see Kunze and Toole, 1997), and so seamount-trapped topographic waves of diurnal periodicity may be more likely at the SMS.

The current record obtained in this work suggests asymmetry in tidal transport (i.e., the current flows faster and for longer duration in one direction than in the reverse). Tidal rectification, resulting from non-linear interaction between enhanced tidal currents and steep bathymetry, is a potential explanatory mechanism and one that has been reported for seamounts (Eriksen, 1991; Brink, 1995; White et al., 2007). Asymmetry is also present in the OTIS (barotropic) tidal current predictions for the SMS during the observation period (Fig. S4). The temperature and dissolved oxygen fluctuations in the time series data may be caused either directly by vertical motions associated with seamount-trapped topographic waves (Kunze and Toole, 1997) or as a local consequence of an enhanced tide. In the latter case, topographic acceleration of tidal currents passing over, for example, the strong ridges either side of the lander site may hydraulically generate transient downwelling 'events' downstream of the topographic feature (Davies et al., 2009). This has been shown to influence food supply to other communities of suspension feeders (Davies et al., 2009).

Lenses of water with elevated chlorophyll *a* concentration and turbidity occurring directly above the summit of a seamount, as observed in this study, have been associated with the retention of passive particles by anti-cyclonic (in the Northern Hemisphere) horizontal circulation around the summit and associated secondary circulation in the vertical-radial plane (Goldner and Chapman, 1997; Beckmann and Mohn, 2002). Whilst the existence of such circulation cells at the SMS cannot be confirmed on the basis of this study and it is possible that a broader scale survey may reveal the lenses to be associated with an INL pervading the region, it is noteworthy that tidal rectification (discussed above) has been implicated in driving horizontal circulation at other seamounts (Eriksen, 1991; Brink, 1995; Kunze and Toole, 1997).

Classically, mean circulation patterns over seamounts have been attributed to steady impinging flows (rather than rectified tidal currents), and are explained in terms of Taylor-Proudman dynamics (based on vorticity arguments) (Proudman, 1916; Taylor, 1917). Jet currents, topographically-steered by the AMOR, are thought to exist at depth in the region (Orvik and Niiler, 2002), and could provide the flow required to generate a so-called 'Taylor cap' above the SMS. A Taylor cap is an isolated anti-cyclonic (in the Northern Hemisphere) flow pattern about a seamount.

The ability of the SMS to host a Taylor cap can be explored by calculating three non-dimensional parameters that characterise the flow, stratification, and seamount height: the Rossby number, $R_o = U/fL$ (representing the ratio of advective to rotational effects); the Burger number, $S = NH/fL$ (a measure of the importance of the stratification relative to rotational effects); and the fractional seamount height, $\delta = h_m/H$. In these equations, U is a steady inflow velocity, f the Coriolis frequency, L the seamount horizontal length scale, N the Brunt-Väisälä buoyancy frequency, H the water depth (in the absence of the seamount), and h_m the height of the seamount above the bottom. Given the situation of the SMS on a mid-ocean ridge system, estimating its

horizontal extent is difficult. We employ $L = 7$ km, based on the bathymetry shown in Fig. 1(b) and determined as the average of the major and minor axes of the elliptical seamount footprint (10 km and 4 km, respectively). This represents the lower bound of possible estimates. At the latitude of the SMS, $f = 1.4 \times 10^{-4}$ rad s^{-1}, and the product fL is conveniently close to unity, giving Rossby numbers of $0.05 - 0.3$ for flows (U) of 5–30 cm s^{-1}. The fractional height, δ, of the SMS is sensitive to the values selected for H and h_m, but a range of approaches returns values between 0.6 and 0.8. Selecting an appropriate value for H is also difficult for a seamount rising from a ridge system already elevated relative to adjacent basins. In the discussion that follows, we use $H = 1400$ m and $h_m = 837$ m (i.e., $\delta = 0.6$) for consistency with our estimate of L taken from Fig. 1(b), but larger values could also be considered appropriate. By comparison with the work of Chapman and Haidvogel (1992) (see Fig. 20 in that work), our calculated Rossby numbers span a critical threshold delineating the occurrence (low R_o) and non-occurrence (high R_o) of Taylor caps for seamounts in this height range.

It would appear that the SMS could host a Taylor cap, or what Chapman and Haidvogel (1992) refer to as temporary trapping (a transient cap), under weak, steady flow conditions. A representative length scale, L, for the SMS may be larger than that estimated above. In such a case, smaller R_o values would be returned for the same range of inflow currents, further favouring the possible occurrence of a Taylor cap. The numerical model outputs of Chapman and Haidvogel (1992) were for steady, stratified impinging flows with Burger number $S = 1$, whereas here S is greater (~1.4; calculated using a representative N value from below the permanent pycnocline of 9.6×10^{-4} rad s^{-1}). This will have implications for the critical Rossby number separating the occurrence and non-occurrence of Taylor caps, but is unlikely to alter the broader interpretation that Taylor caps are theoretically possible at the SMS under weak flows. The models were run with the simplifying assumptions of an isolated, smooth, axisymmetric seamount topography and a non-periodic flow regime, which do not hold at the SMS with potential implications for Taylor cap development.

Evidence of the clear isopycnal doming that is expected in association with vortex caps (either Taylor caps or those generated by tidal rectification) over seamounts is not compelling at the SMS (Figs. 4 and 5). Calculating the decay height (H_d) of a hypothetical Taylor cap at the SMS, using the equation fL/N of Brechner Owens and Hogg (1980), gives $H_d = 1021$ m for f, L, and N values as stated above. This suggests that, under steady flow, the SMS could cause local mesoscale variability up to at most~200 m above its summit (i.e., up to the base of the permanent pycnocline). The vertical extent of its influence is likely to be smaller still because it will be truncated further by the higher levels of stratification present above the seamount. This may explain the absence of clear isopycnal doming in the CTD transect data. A hydrographic survey designed to measure currents at various positions on the seamount, quantify the strength and nature of any mean circulation, and determine the relative importance of tidal and steady-flow dynamics would be revealing in this respect.

4.2. Biological response

Sponges living on the SMS summit are likely to benefit from several of the observed factors identified above. The seamount is deep (*sensu* Pitcher et al. (2007)) and situated within very cold waters (i.e., < 0 °C). The summit is periodically flushed with slightly warmer, oxygen-enriched water from the core of Norwegian Arctic Intermediate Water (NwArIW) above, which may boost metabolic processes. Its location at the boundary of two water masses may ensure that the summit sponge ground also benefits from the slightly elevated inorganic nutrient and DIC concentrations of the Upper Norwegian Deep Water (uNwDW) below, supplied through the turbulence and mixing generated by the hydrodynamical processes discussed. Near-bed SPM concentrations are elevated compared with the adjacent water column (probably through local / near-field resuspension by tidal currents), improving food supply to the sponges. Particulates are advected laterally in the benthic boundary layer by oscillating, temporally asymmetric tidal currents, which increase particle residency times near the sponges, whilst also supplying 'fresh' particles and acting to prevent smothering by sedimentation. Furthermore, any retention of passive organic material above the seamount (i.e., the lenses of elevated chl *a* and turbidity) has implications for food supply and recruitment.

The summit of the SMS is assumed to have provided suitable substrate for the initial growth of sponges and, since then, a spicule mat (~10–20 cm thick - data not presented in this article) has developed at the sediment interface, supporting the existence of the sponge ground in the present day. Appropriate substrate availability is a key abiotic factor driving the spatial distribution of sponges (Barthel and Gutt, 1992; Barthel and Tendal, 1993). Investigations that aim to establish the relative importance of different factors to sponge distribution are recommended. These could take the form of correlating changes in sponge density and diversity with depth against changes not only in the oceanographic factors identified in this work but also in other important factors, such as surficial geology and biotic interactions.

Our findings and interpretations are consistent with those of several other authors. Whitney et al. (2005) attributed the persistence of hexactinellid sponge reefs at the heads of shelf canyons to several factors, including the presence of nutrient rich waters, the supply of SPM, and the local prevalence of tidally-modulated near-bed currents that increase particle residency times and prevent smothering of the sponges. Genin et al. (1986), Rice et al. (1990), and White (2003) all highlighted a potential link between enhanced near-bed currents, improved food supply (and/or larval recruit supply, in the case of Genin et al. (1986)), and the occurrence of sponge-dominated communities. Klitgaard and Tendal (2004) discussed the detrimental (smothering) effect of high suspended particulate loads that settle out, which by extension highlights the value to sponge grounds of a current regime that prevents this from occurring. Beazley et al. (2015) concluded that the presence of dense sponge grounds could potentially be attributed to a warmer water mass residing in their study area. Several other authors have related the presence of sponges to that of a specific water mass in the study region (Barthel et al., 1996; Klitgaard and Tendal, 2004; Murillo et al., 2012). Finally, White et al. (2007) noted that the retention of suspended organic material over seamounts could indicate enclosed circulation patterns, which sometimes include a downwelling component likely to be important to benthic organisms located there.

The results presented here identify a subtle interplay between the hydrodynamics of the seamount summit and the water masses located above and below, which may be an important factor in explaining the success of the dense sponge ground occupying the summit. Time series measurements came from a benthic lander positioned 70–80 m below the true summit. Given that the most energetic water motions associated with seamounts are typically concentrated near the very top (Brink, 1989; Chapman, 1989), it is possible that several of the beneficial factors discussed above are further enhanced there.

4.3. Conclusion

Interaction between seamount geomorphology, hydrodynamic regime, and water column structure resulted in several environmental factors that may benefit sponges and help explain enhanced sponge density and diversity at the summit of the SMS. The sponge ground occurred within nutrient-rich waters (NwArIW / uNwDW boundary). It was regularly flushed with warmer, oxygen-enriched water from above (NwArIW). It was also exposed to elevated near-bed SPM levels, and experienced favourable (diurnal tidal) currents that potentially enhance

food supply and prevent smothering by sedimentation. Elevated chlorophyll *a* concentration observed in the mid-water column above the summit may indicate passive particle retention by seamount-scale circulation patterns with further implications for food supply and recruitment.

The primary limitation of the work was that the hydrodynamical setting could not be characterised fully on a summit-wide scale. Furthermore, the observed hydrodynamics may not persist throughout the year, represent the dominant phenomena over longer time scales, or reflect those most important to the sponges. Several longer-term moorings would be required to resolve these questions. Owing to the global diversity in seamount morphology and oceanographic setting, the results of this study cannot be generalised to all seamounts. However, it is likely that they may be generalisable to similar seamounts known to exist along the AMOR. The broad implication is that, if dense seamount sponge grounds (such as that at the SMS) and their associated ecosystems are sustained by the coincidence of multiple beneficial environmental factors acting in synergy at a given location / depth, they may be sensitive to changes across a particularly broad range of abiotic factors (e.g., under climate change, or anthropogenic activities in the deep sea).

Acknowledgements

This research has been performed in the scope of the SponGES project, which received funding from the European Union's Horizon 2020 research and innovation programme under grant agreement No. 679849. This document reflects only the authors' views and the Executive Agency for Small and Medium-sized Enterprises (EASME) is not responsible for any use that may be made of the information it contains. Furu Mienis is supported financially by the Innovational Research Incentives Scheme of the Netherlands Organisation for Scientific Research (NWO-VIDI). A Nuffield research placement scheme supported Bryn Harris, who is thanked for undertaking the lander video analysis. The University of Bergen is thanked for providing ship time for the project. The authors are indebted to Bob Koster and Bernt Olsen, and to the captain and crew of *RV G.O. Sars*. Malen Roberts, David Bowers, and Susan Allender are thanked for their comments on the manuscript. Two anonymous reviewers are thanked for their comments, which led to considerable improvements to this article.

Data availability statement

Datasets presented in this article are available at https://doi.org/10.1594/PANGAEA.891035.

Conflicts of interest

None to declare.

Appendix A. Supporting information

Supplementary material associated with this article can be found in the online version at http://dx.doi.org/10.1016/j.dsr.2018.06.007.

References

Amsler, M.O., McClintock, J.B., Amsler, C.D., Angus, R.A., Baker, B.J., 2009. An evaluation of sponge-associated amphipods from the Antarctic Peninsula. Antarct. Sci. 21 (6), 579–589. http://dx.doi.org/10.1017/S0954102009990356.

Barthel, D., 1992. Do hexactinellids structure antarctic sponge associations? Ophelia 36 (2), 111–118.

Barthel, D., Gutt, J., 1992. Sponge associations in the eastern Weddell Sea. Antarct. Sci. 4 (2), 137–150. http://dx.doi.org/10.1017/S0954102092000221.

Barthel, D., Tendal, O.S., 1993. The sponge association of the abyssal Norwegian-Greenland Sea: species composition, substrate relationships, and distribution. Sarsia 78 (2), 83–96.

Barthel, D., Tendal, O.S., Thiel, H., 1996. A wandering population of the hexactinellid sponge *Pheronema carpenteri* on the continental slope off Morocco, Northwest Africa. Mar. Ecol. 17 (4), 603–616. http://dx.doi.org/10.1111/j.1439-0485.1996.tb00420.x.

Beazley, L.I., Kenchington, E.L., Murillo, F.J., Sacau, M., 2013. Deep-sea sponge grounds enhance diversity and abundance of epibenthic megafauna in the Northwest Atlantic. ICES J. Mar. Sci. 70, 1471–1490. http://dx.doi.org/10.1093/icesjms/fst124.

Beazley, L., Kenchington, E., Yashayaev, I., Murillo, F.J., 2015. Drivers of epibenthic megafaunal composition in the sponge grounds of the Sackville Spur, Northwest Atlantic. Deep-Sea Res. Part I: Oceanogr. Res. Pap. 98, 102–114. http://dx.doi.org/10.1016/j.dsr.2014.11.016.

Beckmann, A., Mohn, C., 2002. The upper ocean circulation at Great Meteor Seamount. Part II: retention potential of the seamount induced circulation. Ocean Dyn. 52 (4), 194–204.

Belarbi, E.H., Contreras Gómez, A., Chisti, Y., García Camacho, F., Molina Grima, E., 2003. Producing drugs from marine sponges. Biotechnol. Adv. 21 (7), 585–598. http://dx.doi.org/10.1016/S0734-9750(03)00100-9.

Bell, J.J., 2008. The functional roles of marine sponges. Estuar. Coast. Shelf Sci. 79 (3), 341–353. http://dx.doi.org/10.1016/j.ecss.2008.05.002.

Bett, B.J., Rice, A.L., 1992. The influence of hexactinellid sponge (*Pheronema carpenteri*) spicules on the patchy distribution of macrobenthos in the Porcupine Seabight (bathyal NE Atlantic). Ophelia 36 (3), 217–226. http://dx.doi.org/10.1080/00785326.1992.10430372.

Blindheim, J., 1990. Arctic intermediate water in the Norwegian sea. Deep Sea Res. Part A Oceanogr. Res. Pap. 37 (9), 1475–1489. http://dx.doi.org/10.1016/0198-0149(90)90138-L.

Blindheim, J., Østerhus, S., 2005. The Nordic Seas, main oceanographic features. In: Drange, H., Dokken, T., Furevik, T., Gerdes, R., Berger, W. (Eds.), The Nordic Seas: An Integrated Perspective. American Geophysical Union, Washington DC, pp. 11–37. http://dx.doi.org/10.1029/158GM03.

Blindheim, J., Rey, F., 2004. Water-mass formation and distribution in the Nordic Seas during the 1990s. ICES J. Mar. Sci. 61 (5), 846–863. http://dx.doi.org/10.1016/j.icesjms.2004.05.003.

Bo, M., Bertolino, M., Bavestrello, G., Canese, S., Giusti, M., Angiolillo, M., Taviani, M., 2012. Role of deep sponge grounds in the Mediterranean Sea: a case study in southern Italy. Hydrobiologia 687 (1), 163–177. http://dx.doi.org/10.1007/s10750-011-0964-1.

Brechner Owens, W., Hogg, N.G., 1980. Oceanic observations of stratified Taylor columns near a bump. Deep Sea Res. Part A Oceanogr. Res. Pap. 27 (12), 1029–1045. http://dx.doi.org/10.1016/0198-0149(80)90063-1.

Brink, K.H., 1989. The effect of stratification on seamount-trapped waves. Deep Sea Res. Part A Oceanogr. Res. Pap. 36 (6), 825–844. http://dx.doi.org/10.1016/0198-0149(89)90031-9.

Brink, K.H., 1990. On the generation of seamount-trapped waves. Deep Sea Res. Part A Oceanogr. Res. Pap. 37 (10), 1569–1582. http://dx.doi.org/10.1016/0198-0149(90)90062-Z.

Brink, K.H., 1995. Tidal and lower frequency currents above Fieberling Guyot. J. Geophys. Res. 100 (C6), 10,817–10,832.

Bruvoll, V., Breivik, A.J., Mjelde, R., Pedersen, R.B., 2009. Burial of the Mohn-Knipovich seafloor spreading ridge by the Bear Island Fan: time constraints on tectonic evolution from seismic stratigraphy. Tectonics 28 (4), 1–14. http://dx.doi.org/10.1029/2008TC002396.

Buhl-Mortensen, L., Vanreusel, A., Gooday, A.J., Levin, L.A., Priede, I.G., Buhl-Mortensen, P., Raes, M., 2010. Biological structures as a source of habitat heterogeneity and biodiversity on the deep ocean margins. Mar. Ecol. 31 (1), 21–50. http://dx.doi.org/10.1111/j.1439-0485.2010.00359.x.

Cárdenas, P., Rapp, H.T., Klitgaard, A.B., Best, M., Thollesson, M., Tendal, O.S., 2013. Taxonomy, biogeography and DNA barcodes of *Geodia* species (Porifera, Demospongiae, Tetractinellida) in the Atlantic boreo-arctic region. Zool. J. Linn. Soc. 169 (2), 251–311. http://dx.doi.org/10.1111/zoj.12056.

Carmack, E., Aagaard, K., 1973. On the deep water of the Greenland Sea. Deep-Sea Res. 20 (8), 687–715. http://dx.doi.org/10.1016/0011-7471(73)90086-7.

Cathalot, C., Van Oevelen, D., Cox, T.J.S., Kutti, T., Lavaleye, M., Duineveld, G., Meysman, F.J.R., 2015. Cold-water coral reefs and adjacent sponge grounds: hotspots of benthic respiration and organic carbon cycling in the deep sea. Front. Mar. Sci. 2 (June), 1–12. http://dx.doi.org/10.3389/fmars.2015.00037.

Chapman, D.C., 1989. Enhanced subinertial diurnal tides over isolated topographic features. Deep Sea Res. Part A Oceanogr. Res. Pap. 36 (6), 815–824. http://dx.doi.org/10.1016/0198-0149(89)90030-7.

Chapman, D.C., Haidvogel, D.B., 1992. Formation of Taylor caps over a tall isolated seamount in a stratified ocean. Geophys. Astrophys. Fluid Dyn. 64 (1–4), 31–65. http://dx.doi.org/10.1080/03091929208228084.

Codiga, D.L., Eriksen, C.C., 1997. Observations of low-frequency circulation and amplified subinertial tidal currents at Cobb Seamount. J. Geophys. Res. 102 (C10), 22,993–23,007.

Davies, A.J., Duineveld, G.C.A., Lavaleye, M.S.S., Bergman, M.J.N., van Haren, H., Roberts, J.M., 2009. Downwelling and deep-water bottom currents as food supply mechanisms to the cold-water coral *Lophelia pertusa* (Scleractinia) at the Mingulay Reef complex. Limnol. Oceanogr. 54 (2), 620–629. http://dx.doi.org/10.4319/lo.2009.54.2.0620.

Davies, A.J., Duineveld, G.C.A., van Weering, T.C.E., Mienis, F., Quattrini, A.M., Seim, H.E., Ross, S.W., 2010. Short-term environmental variability in cold-water coral habitat at Viosca Knoll, Gulf of Mexico. Deep-Sea Res. Part I: Oceanogr. Res. Pap. 57 (2), 199–212. http://dx.doi.org/10.1016/j.dsr.2009.10.012.

De Goeij, J.M., Van Oevelen, D., Vermeij, M.J.A., Osinga, R., Middelburg, J.J., De Goeij, A.F.P.M., Admiraal, W., 2013. Surviving in a marine desert: the sponge loop retains resources within coral reefs. Science 342 (October), 108–110. http://dx.doi.org/10.1126/science.1241981.

Dickson, R.R., Brown, J., 1994. The production of North Atlantic Deep Water: sources, rates, and pathways. J. Geophys. Res. 99 (C6), 12,319–12,341.
Dudik, O., Leonor, I., Xavier, J.R., Rapp, H.T., Pires, R.A., Silva, T.H., Reis, R.L., 2018. Sponge-derived silica for tissue regeneration: bioceramics of deep-sea sponge. Mater. Today. http://dx.doi.org/10.1016/j.mattod.2018.03.025.
Durán Muñoz, P., Murillo, F.J., Sayago-Gil, M., Serrano, A., Laporta, M., Otero, I., Gómez, C., 2011. Effects of deep-sea bottom longlining on the Hatton Bank fish communities and benthic ecosystem, north-east Atlantic. J. Mar. Biol. Assoc. U. Kingd. 91 (4), 939–952. http://dx.doi.org/10.1017/S0025315410001773.
Egbert, G.D., Erofeeva, S.Y., 2002. Efficient inverse modeling of barotropic ocean tides. J. Atmos. Ocean. Technol. 19 (2), 183–204. http://dx.doi.org/10.1175/1520-0426(2002)019<0183:EIMOBO>2.0.CO;2.
Ehrlich, H., Steck, E., Ilan, M., Maldonado, M., Muricy, G., Bavestrello, G., Richter, W., 2010. Three-dimensional chitin-based scaffolds from Verongida sponges (Demospongiae: porifera). Part II: biomimetic potential and applications. Int. J. Biol. Macromol. 47 (2), 141–145. http://dx.doi.org/10.1016/j.ijbiomac.2010.05.009.
Eriksen, C.C., 1991. Observations of amplified flows atop a large seamount. J. Geophys. Res. 96 (C8), 15,227–15,236.
FAO, 2009. International guidelines for the management of deep-sea fisheries in the high seas. Rome.
Fofonoff, N.P., Millard, R.C., 1983. Algorithms for computation of fundamental properties of seawater. Unesco Tech. Pap. Mar. Sci. 44, 1–53.
Freese, J., Wing, B., 2003. Juvenile red rockfish, *Sebastes* sp., associations with sponges in the Gulf of Alaska. Mar. Fish. Rev. 65 (3), 38–42.
Freiwald, A., Roberts, J.M. (Eds.), 2005. Cold-water Corals and Ecosystems. Springer-Verlag, Berlin.
Furevik, T., Foldvik, A., 1996. Stability at M_2 critical latitude in the Barents Sea. J. Geophys. Res. 101 (C4), 8,823–8,837.
Garau, B., Ruiz, S., Zhang, W.G., Pascual, A., Heslop, E., Kerfoot, J., Tintoré, J., 2011. Thermal lag correction on Slocum CTD Glider data. J. Atmos. Ocean. Technol. 28 (9), 1065–1071. http://dx.doi.org/10.1175/JTECH-D-10-05030.1.
Gatti, S., 2002. The role of sponges in High-Antarctic carbon and silicon cycling - a modelling approach. Ber. Polarforsch. Meeresforsch. 434.
Genin, A., Dayton, P.K., Lonsdale, P.F., Spiess, F.N., 1986. Corals on seamount peaks provide evidence of current acceleration over deep-sea topography. Nature 322 (6074), 59–61. http://dx.doi.org/10.1038/324148a0.
Gilhousen, D.B., 1987. A field evaluation of NDBC moored buoy winds. J. Atmos. Ocean. Technol. 4, 94–104.
Goldner, D.R., Chapman, D.C., 1997. Flow and particle motion induced above a tall seamount by steady and tidal background currents. Deep-Sea Res. Part I: Oceanogr. Res. Pap. 44 (5), 719–744. http://dx.doi.org/10.1016/S0967-0637(96)00131-8.
Haidvogel, D.B., Beckmann, A., Chapman, D.C., Lin, R.-Q., 1993. Numerical simulation of flow around a tall isolated seamount. Part II: resonant generation of trapped waves. J. Phys. Oceanogr. 23 (11), 2373–2391. http://dx.doi.org/10.1175/1520-0485(1993)023<2373:NSOFAA>2.0.CO;2.
Hansen, B., Østerhus, S., 2000. North Atlantic-Nordic Seas exchanges. Prog. Oceanogr. 45 (2), 109–208. http://dx.doi.org/10.1016/S0079-6611(99)00052-X.
Henkel, T.P., Pawlik, J.R., 2005. Habitat use by sponge-dwelling brittlestars. Mar. Biol. 146 (2), 301–313. http://dx.doi.org/10.1007/s00227-004-1448-x.
Herrnkind, W.F., Butler IV, M.J., Hunt, J.H., Childress, M., 1997. Role of physical refugia: implications from a mass sponge die-off in a lobster nursery in Florida. Mar. Freshw. Res. 48 (8), 759–770. http://dx.doi.org/10.1071/MF97193.
Hestetun, J.T., Tompkins-Macdonald, G., Rapp, H.T., 2017. A review of carnivorous sponges (Porifera: cladorhizidae) from the Boreal North Atlantic and Arctic. Zool. J. Linn. Soc. 181 (1), 1–69. http://dx.doi.org/10.1093/zoolinnean/zlw022.
Hoffmann, F., Radax, R., Woebken, D., Holtappels, M., Lavik, G., Rapp, H.T., Kuypers, M.M.M., 2009. Complex nitrogen cycling in the sponge *Geodia barretti*. Environ. Microbiol. 11 (9), 2228–2243. http://dx.doi.org/10.1111/j.1462-2920.2009.01944.x.
Hogg, M.M., Tendal, O.S., Conway, K.W., Pomponi, S.A., van Soest, R.W.M., Gutt, J., … Roberts, J.M., 2010. Deep-sea sponge grounds: Reservoirs of biodiversity. UNEP-WCMC Biodiversity Series No. 32. Cambridge.
Hopkins, T.S., 1991. The GIN Sea - A synthesis of its physical oceanography and literature review 1972–1985. Earth-Sci. Rev. 30, 175–318.
Howell, K.L., Piechaud, N., Downie, A.L., Kenny, A., 2016. The distribution of deep-sea sponge aggregations in the North Atlantic and implications for their effective spatial management. Deep-Sea Res. Part I: Oceanogr. Res. Pap. 115, 309–320. http://dx.doi.org/10.1016/j.dsr.2016.07.005.
Huthnance, J.M., 1989. Internal tides and waves near the continental shelf edge. Geophys. Astrophys. Fluid Dyn. 48 (1–3), 81–106.
Jeansson, E., Olsen, A., Jutterström, S., 2017. Arctic Intermediate Water in the Nordic Seas, 1991–2009. Deep-Sea Res. Part I: Oceanogr. Res. Pap. 128 (August), 82–97. http://dx.doi.org/10.1016/j.dsr.2017.08.013.
Kenchington, E., Power, D., Koen-Alonso, M., 2013. Associations of demersal fish with sponge grounds on the continental slopes of the northwest Atlantic. Mar. Ecol. Prog. Ser. 477, 217–230. http://dx.doi.org/10.3354/meps10127.
Klitgaard, A.B., 1995. The fauna associated with the outer shelf and upper slope sponges (Porifera, Demospongiae) at the Faroe Islands, Northeastern Atlantic. Sarsia 80 (1), 1–22. http://dx.doi.org/10.1530/EJE-11-0663.
Klitgaard, A.B., Tendal, O.S., 2004. Distribution and species composition of mass occurrences of large-sized sponges in the northeast Atlantic. Prog. Oceanogr. 61 (1), 57–98. http://dx.doi.org/10.1016/j.pocean.2004.06.002.
Knudby, A., Kenchington, E., Murillo, F.J., 2013. Modeling the distribution of *Geodia* sponges and sponge grounds in the Northwest Atlantic. PLoS One 8 (12), 1–20. http://dx.doi.org/10.1371/journal.pone.0082306.
Kowalik, Z., Proshutinsky, A.Y., 1993. Diurnal tides in the Arctic Ocean. J. Geophys. Res. 98 (C9), 16,449–16,468.
Kulikov, E.A., Rabinovich, A.B., Carmack, E.C., 2010. Variability of baroclinic tidal currents on the Mackenzie Shelf, the Southeastern Beaufort Sea. Cont. Shelf Res. 30, 656–667. http://dx.doi.org/10.1016/j.csr.2009.11.006.
Kunze, E., Sanford, T.B., 1986. Near-inertial wave interactions with mean flow and bottom topography near Caryn Seamount. J. Phys. Oceanogr. 16 (1), 109–120. http://dx.doi.org/10.1175/1520-0485(1986)016<0109:NIWIWM>2.0.CO;2.
Kunze, E., Toole, J.M., 1997. Tidally driven vorticity, diurnal shear, and turbulence atop Fieberling Seamount. J. Phys. Oceanogr. 27 (12), 2663–2693. http://dx.doi.org/10.1175/1520-0485(1997)027<2663:TDVDSA>2.0.CO;2.
Kutti, T., Bannister, R.J., Fosså, J.H., 2013. Community structure and ecological function of deep-water sponge grounds in the Traenadypet MPA - northern Norwegian continental shelf. Cont. Shelf Res. 69, 21–30. http://dx.doi.org/10.1016/j.csr.2013.09.011.
Kutti, T., Fosså, J.H., Bergstad, O.A., 2015. Influence of structurally complex benthic habitats on fish distribution. Mar. Ecol. Prog. Ser. 520, 175–190. http://dx.doi.org/10.3354/meps11047.
Leal, M.C., Puga, J., Serôdio, J., Gomes, N.C.M., Calado, R., 2012. Trends in the discovery of new marine natural products from invertebrates over the last two decades - where and what are we bioprospecting? PLoS One 7 (1), 1–15. http://dx.doi.org/10.1371/journal.pone.0030580.
Leys, S.P., Yahel, G., Reidenbach, M.A., Tunnicliffe, V., Shavit, U., Reiswig, H.M., 2011. The sponge pump: the role of current induced flow in the design of the sponge body plan. PLoS One 6 (12), 1–17. http://dx.doi.org/10.1371/journal.pone.0027787.
Lyard, F.H., 1997. The tides in the Arctic Ocean from a finite element model. J. Geophys. Res. 102 (C7), 15,611–15,638.
Maldonado, M., Aguilar, R., Bannister, R.J., Bell, J.J., Conway, K.W., Dayton, P.K., Young, C.M., 2015. Sponge grounds as key marine habitats: a synthetic review of types, structure, functional roles, and conservation concerns. In: Rossi, S., Bramanti, L., Gori, A., del Valle, C. (Eds.), Marine Animal Forests: The Ecology of Benthic Biodiversity Hotspots. Springer International Publishing, Cham, pp. 1–39. http://dx.doi.org/10.1007/978-3-319-17001-5_24-1.
Mauritzen, C., 1996. Production of dense overflow waters feeding the North Atlantic across the Greenland-Scotland Ridge. Part 1: evidence for a revised circulation scheme. Deep-Sea Res. Part I: Oceanogr. Res. Pap. 43 (6), 769–806.
McIntyre, F.D., Drewery, J., Eerkes-Medrano, D., Neat, F.C., 2016. Distribution and diversity of deep-sea sponge grounds on the Rosemary Bank Seamount, NE Atlantic. Mar. Biol. 163 (6), 1–11. http://dx.doi.org/10.1007/s00227-016-2913-z.
Mienis, F., De Stigter, H.C., White, M., Duineveld, G., De Haas, H., van Weering, T.C.E., 2007. Hydrodynamic controls on cold-water coral growth and carbonate-mound development at the SW and SE Rockall Trough Margin, NE Atlantic Ocean. Deep-Sea Res. Part I: Oceanogr. Res. Pap. 54 (9), 1655–1674. http://dx.doi.org/10.1016/j.dsr.2007.05.013.
Munk, W.H., Phillips, N., 1968. Coherence and band structure of inertial motion in the sea. Rev. Geophys. 6, 447–472.
Murillo, F.J., Durán Muñoz, P., Cristobo, J., Ríos, P., González, C., Kenchington, E., Serrano, A., 2012. Deep-sea sponge grounds of the Flemish Cap, Flemish Pass and the Grand Banks of Newfoundland (Northwest Atlantic Ocean): distribution and species composition. Mar. Biol. Res. 8 (9), 842–854. http://dx.doi.org/10.1080/17451000.2012.682583.
Murillo, F.J., Kenchington, E., Lawson, J.M., Li, G., Piper, D.J.W., 2016a. Ancient deep-sea sponge grounds on the Flemish Cap and Grand Bank, northwest Atlantic. Mar. Biol. 163 (3), 1–11. http://dx.doi.org/10.1007/s00227-016-2839-5.
Murillo, F.J., Serrano, A., Kenchington, E., Mora, J., 2016b. Epibenthic assemblages of the tail of the Grand Bank and Flemish Cap (northwest Atlantic) in relation to environmental parameters and trawling intensity. Deep-Sea Res. Part I: Oceanogr. Res. Pap. 109, 99–122. http://dx.doi.org/10.1016/j.dsr.2015.08.006.
New, A.L., 1988. Internal tidal mixing in the Bay of Biscay. Deep Sea Res. Part A Oceanogr. Res. Pap. 35 (5), 691–709. http://dx.doi.org/10.1016/0198-0149(88)90026-X.
Orvik, K.A., Niiler, P., 2002. Major pathways of Atlantic water in the northern North Atlantic and Nordic Seas toward Arctic. Geophys. Res. Lett. 29 (19), 2-1–2-4. http://dx.doi.org/10.1029/2002GL015002.
OSPAR, 2008. OSPAR list of threatened and/or declining species and habitats (Reference number: 2008-6). London.
Pile, A.J., Young, C.M., 2006. The natural diet of a hexactinellid sponge: benthic-pelagic coupling in a deep-sea microbial food web. Deep-Sea Res. Part I: Oceanogr. Res. Pap. 53 (7), 1148–1156. http://dx.doi.org/10.1016/j.dsr.2006.03.008.
Pitcher, T.J., Morato, T., Hart, P.J.B., Clark, M.R., Haggan, N., Santos, R. (Eds.), 2007. Seamounts: Ecology, Fisheries, and Conservation. Blackwell Publishing Ltd, Oxford.
Plotkin, A., Gerasimova, E., Rapp, H.T., 2017. Polymastiidae (Porifera: Demospongiae) of the Nordic and Siberian Seas. J. Mar. Biol. Assoc. U. Kingd. http://dx.doi.org/10.1017/S0025315417000285.
Proudman, J., 1916. On the motion of solids in a liquid possessing vorticity. Proc. R. Soc. Lond. A92, 408–424.
Pusceddu, A., Bianchelli, S., Martin, J., Puig, P., Palanques, A., Masque, P., Danovaro, R., 2014. Chronic and intensive bottom trawling impairs deep-sea biodiversity and ecosystem functioning. Proc. Natl. Acad. Sci. USA 111 (24), 8861–8866. http://dx.doi.org/10.1073/pnas.1405454111.
Rice, A.L., Thurston, M.H., New, A.L., 1990. Dense aggregations of a hexactinellid sponge, *Pheronema carpenteri*, in the Porcupine Seabight (northeast Atlantic Ocean), and possible causes. Prog. Oceanogr. 24, 179–196.
Sandstrom, H., 1975. On topographic generation and coupling of internal waves. Geophys. Fluid Dyn. 7 (1), 231–270.
Schneider, C.A., Rasband, W.S., Eliceiri, K.W., 2012. NIH Image to ImageJ: 25 years of image analysis. Nat. Methods 9 (7), 671–675. http://dx.doi.org/10.1038/nmeth.

2089.
Stoll, M.H.C., Bakker, K., Nobbe, G.H., Haese, R.R., 2001. Continuous-flow analysis of dissolved inorganic carbon content in seawater. Anal. Chem. 73 (17), 4111–4116. http://dx.doi.org/10.1021/ac010303r.
Strickland, J.D.H., Parsons, T.R., 1972. A practical handbook of seawater analysis, Second Edition. Fisheries Research Board of Canada, Ottawa.
Sundar, V.C., Yablon, A.D., Grazul, J.L., Ilan, M., Aizenberg, J., 2003. Fibre-optical features of a glass sponge. Nature 424 (6951), 899–900. http://dx.doi.org/10.1038/424899a.
Taylor, G.I., 1917. Motions of solids in fluids when the flow is not irrational. Proc. R. Soc. Lond. A93, 99–113.
Torkildsen, M.M., 2013. Diversity of Hexactinellid Sponges (Porifera, Hexactinellida) on an Arctic Seamount, the Schultz Massif. M.Sc. Thesis. University of Bergen.
van Haren, H., Hanz, U., De Stigter, H., Mienis, F., Duineveld, G., 2017. Internal wave turbulence at a biologically rich Mid-Atlantic seamount. PLoS One 12 (12), 1–16. http://dx.doi.org/10.1371/journal.pone.0189720.
van Weering, T., Koster, B., Van Heerwaarden, J., Thomsen, L., Viergutz, T., 2000. New technique for long-term deep seabed studies. Sea Technol. 41 (2), 17–25.
Weatherall, P., Marks, K.M., Jakobsson, M., Schmitt, T., Tani, S., Arndt, J.E., Wigley, R., 2015. A new digital bathymetric model of the world's oceans. Earth Space Sci. 2, 331–345. http://dx.doi.org/10.1002/2015EA000107.
Wessel, P., Smith, W.H.F., 1996. A global, self-consistent, hierarchical, high-resolution shoreline database. J. Geophys. Res.: Solid Earth 101 (B4), 8741–8743. http://dx.doi.org/10.1029/96JB00104.
White, M., 2003. Comparison of near seabed currents at two locations in the Porcupine Sea Bight - implications for benthic fauna. J. Mar. Biol. Assoc. U. Kingd. 83 (4), 683–686. http://dx.doi.org/10.1017/S0025315403007641h.
White, M., Bashmachnikov, I., Aristegui, J., Martins, A., 2007. Physical processes and seamount productivity. In: Pitcher, T.J., Morato, T., Hart, P.J.B., Clark, M.R., Haggan, N., Santos, R.S. (Eds.), Seamounts: Ecology, Fisheries, and Conservation. Blackwell Publishing Ltd, Oxford, pp. 65–84.
Whitney, F., Conway, K., Thomson, R., Barrie, V., Krautter, M., Mungov, G., 2005. Oceanographic habitat of sponge reefs on the Western Canadian Continental Shelf. Cont. Shelf Res. 25 (2), 211–226. http://dx.doi.org/10.1016/j.csr.2004.09.003.

Supplementary material

Oceanographic setting and short-timescale environmental variability at an Arctic seamount sponge ground

E.M. Roberts, F. Mienis, H.T. Rapp, U. Hanz, H.K. Meyer, and A.J. Davies

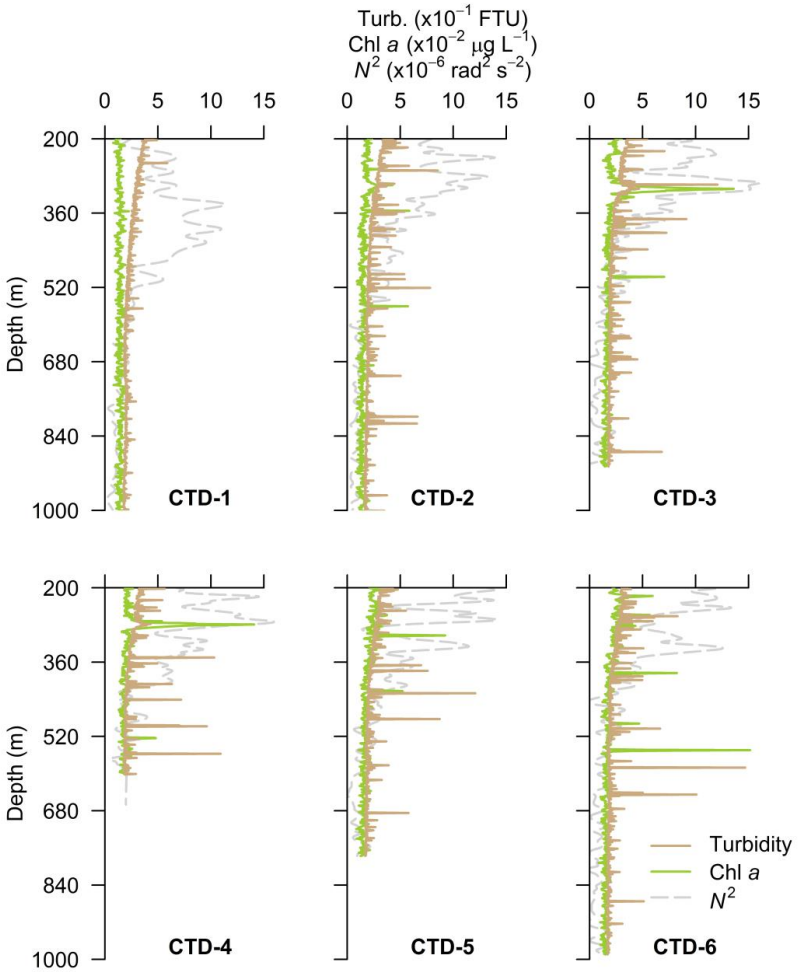

Figure S1 - Vertical profiles of turbidity, chlorophyll *a* concentration, and the square of the Brunt-Väisälä buoyancy frequency, N^2, for CTD stations 1 (off-seamount reference) and 2-6 (across-ridge transect). A reduced vertical range is plotted (i.e., high surface values omitted) to permit inspection of finer scale features at ~300 m depth (see article text).

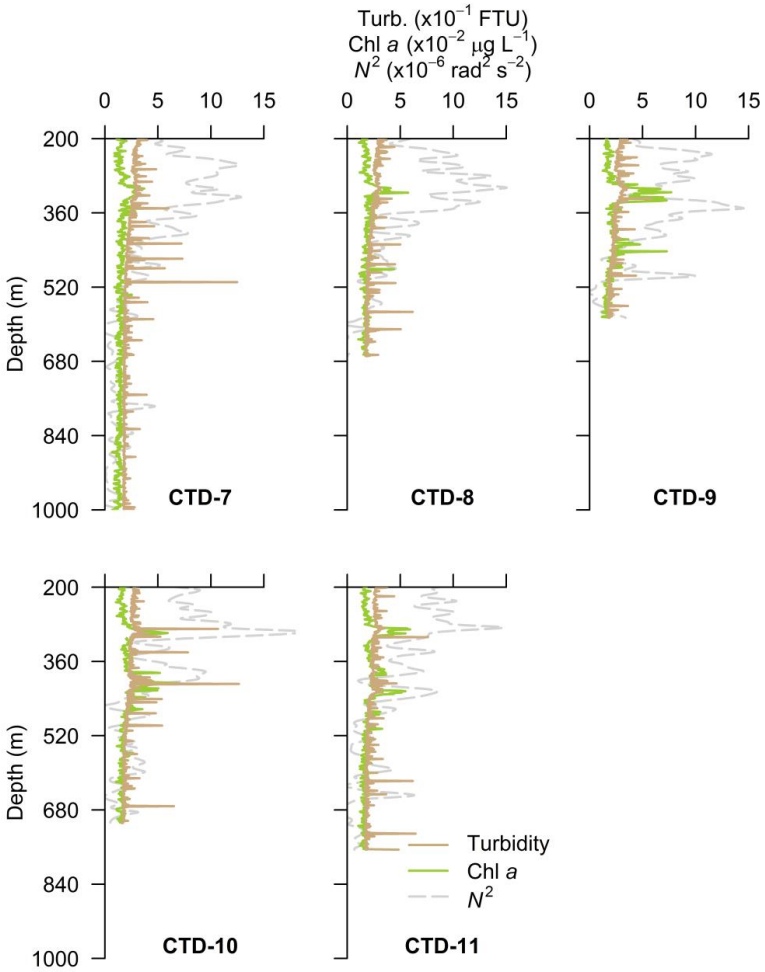

Figure S2 - Vertical profiles of turbidity, chlorophyll *a* concentration, and the square of the Brunt-Väisälä buoyancy frequency, N^2, for CTD stations 7-11 (along-ridge transect). A reduced vertical range is plotted (i.e., high surface values omitted) to permit inspection of finer scale features at ~300 m depth (see article text).

Table S1 – Harmonic constants for important tidal constituents at the benthic lander site (73° 48.960' N, 7° 31.408' E) on the Schultz Massif Seamount, as extracted from regional barotropic inverse tidal solutions obtained with the Oregon State University Tidal Inversion Software (OTIS; Egbert and Erofeeva, 2002). Amplitudes and phases are included for tidal elevation (*z*) and currents (*u* and *v* components; west-east velocity and south-north velocity, respectively). 'Phase' is the phase lag, in degrees, of the constituent in question behind the corresponding constituent at Greenwich. Amp. = amplitude. Bold values (read column-wise) indicate the top two constituents contributing to either elevation or velocity.

Tidal constituent	Symbol	Period (solar hours)	Harmonic constants					
			z (elevation)		*u* (W-E velocity)		*v* (S-N velocity)	
			Amp. (m)	Phase (°)	Amp. (cm s^{-1})	Phase (°)	Amp. (cm s^{-1})	Phase (°)
Semi-diurnal constituents								
Principal lunar semi-diurnal	M_2	12.42	**0.463**	-13.0	**0.549**	63.8	**0.924**	13.3
Principal solar semi-diurnal	S_2	12.00	**0.165**	28.5	0.176	76.5	0.345	32.8
Larger lunar elliptic semi-diurnal	N_2	12.66	0.088	-38.3	0.218	-39.8	0.098	4.5
Luni-solar semi-diurnal	K_2	11.97	0.052	27.9	0.058	-166.0	0.175	55.3
Diurnal constituents								
Luni-solar diurnal	K_1	23.93	0.035	-161.9	**0.763**	-48.7	**1.282**	-123.1
Principal lunar diurnal	O_1	25.82	0.041	61.5	0.109	-86.2	0.244	-155.8
Principal solar diurnal	P_1	24.07	0.012	-167.1	0.186	-51.9	0.352	-122.4
Larger lunar elliptic diurnal	Q_1	26.87	0.015	-6.1	0.013	-131.0	0.040	45.0
Long-period constituents								
Lunar fortnightly	M_f	327.90	0.020	-142.7	0.053	35.9	0.248	-74.8
Lunar monthly	M_m	661.30	0.014	-156.7	0.004	27.7	0.054	-153.0

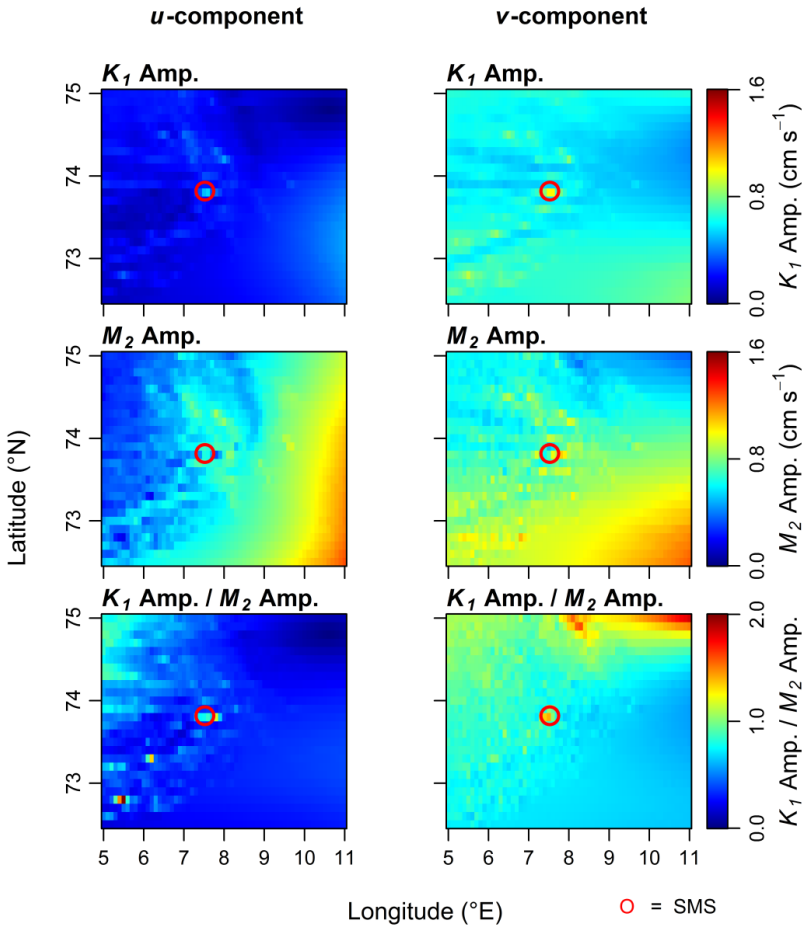

Figure S3 – Tidal current amplitudes for the K_1 and M_2 tidal constituents in the region where the Mohn Ridge transitions into the Knipovich Ridge. Values have been extracted from regional barotropic inverse tidal solutions obtained with the Oregon State University Tidal Inversion Software (OTIS; Egbert and Erofeeva, 2002). *u* and *v* components represent west-east and south-north velocities, respectively. In both cases, K_1 becomes relatively more important near the Schultz Massif Seamount (SMS) (n.b., ratio of K_1 amp. to M_2 amp. plotted in lowest panels).

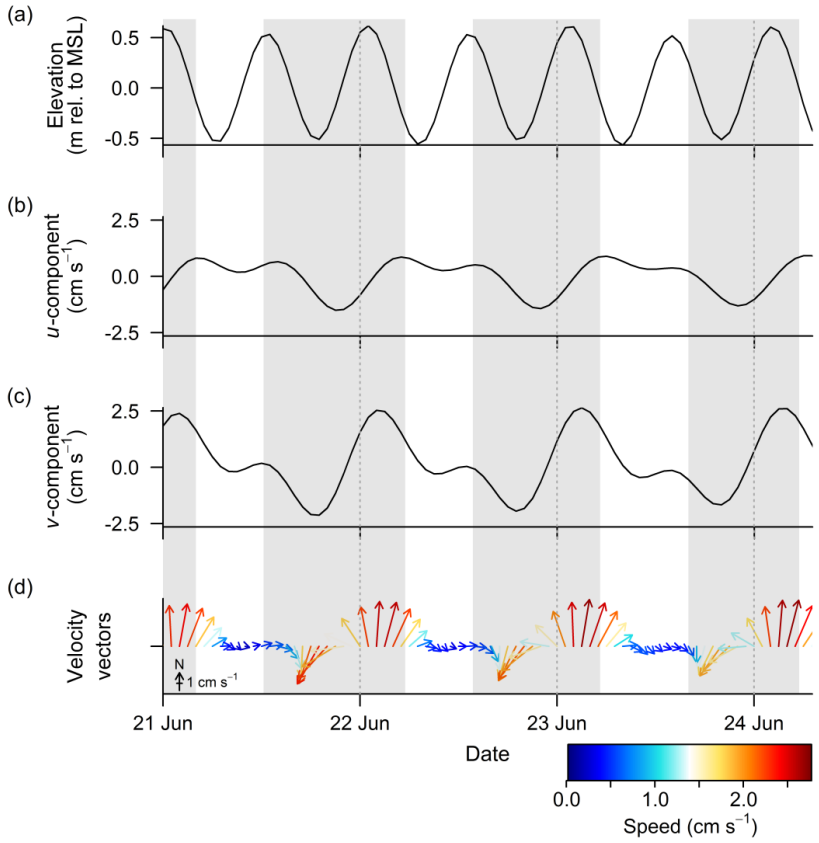

Figure S4 – Predicted tidal elevations (a) and currents (b-d) at the benthic lander site (73° 48.960' N, 7° 31.408' E) on the Schultz Massif Seamount for the period of the time series observations (summer 2016). Predictions are based on regional barotropic inverse tidal solutions obtained with the Oregon State University Tidal Inversion Software (OTIS; Egbert and Erofeeva, 2002). *u* and *v* components of the tidal flow represent west-east and south-north velocities, respectively (+ve *u* = eastwards flow; +ve *v* = northwards flow). Grey-shaded areas indicate the 'jump-relax' events noted in the time series observations from the lander (see article text).

References

Egbert, G. D., & Erofeeva, S. Y. (2002). Efficient Inverse Modeling of Barotropic Ocean Tides. *Journal of Atmospheric and Oceanic Technology*, *19*(2), 183-204. https://doi.org/10.1175/1520-0426(2002)019<0183:EIMOBO>2.0.CO;2

Paper 2

Deep–Sea Research I 153 (2019) 103137

Contents lists available at ScienceDirect

Deep-Sea Research Part I

journal homepage: http://www.elsevier.com/locate/dsri

Spatial patterns of arctic sponge ground fauna and demersal fish are detectable in autonomous underwater vehicle (AUV) imagery

H.K. Meyer [a,*], E.M. Roberts [a,b], H.T. Rapp [a,c], A.J. Davies [b,d]

[a] Department of Biological Sciences and K.G. Jebsen Centre for Deep-sea Research, University of Bergen, P.O. Box 7803, N-5020, Bergen, Norway
[b] School of Ocean Sciences, Bangor University, Menai Bridge, Anglesey, LL59 5AB, UK
[c] NORCE, Norwegian Research Centre, NORCE Environment, Nygårdsgaten 112, 5008, Bergen, Norway
[d] Department of Biological Sciences, University of Rhode Island, Kingston, RI, 02881, USA

ARTICLE INFO

Keywords:
Arctic mid-ocean ridge
Autonomous underwater vehicle
Deep sea
Demersal fish
Seamount
Sponge ground

ABSTRACT

Deep-sea sponge grounds are important habitats that provide several ecosystem services, yet relatively little is known about their distribution and ecology. While most surveys have focused on the broad-scale distribution patterns of sponge grounds (100s–1000s m), only rarely have the finer-scale (<10 m) spatial distribution patterns of the primary organisms been studied. In this study, the autonomous underwater vehicle (AUV) *Hugin 1000* was used to map an area of an arctic sponge ground located on the summit of the Schulz Bank (Arctic Mid-Ocean Ridge), with the aim of detecting small-scale spatial patterns produced by the dominant megafauna. Using low-light cameras to construct a photomosaic comprising of 9,953 images and a virtual quadrat spatial sampling approach, density hotspots of the most prominent megafauna were visualized. The primary megafauna detected were demosponges, hexactinellids, ascidians, cnidarians, echinoderms, and demersal fish species. Most megafauna, like the primary structure-forming sponge species *Geodia parva* and *Stelletta rhaphidiophora,* were distributed evenly throughout the sample area, though species like *Lissodendoryx (Lissodendoryx) complicata* and *Gersemia rubiformis* displayed clear fine-scale spatial preferences. The three demersal fish species, *Macrourus berglax*, *Reinhardtius hippoglossoides*, and *Amblyraja hyperborea*, were uniformly distributed throughout the sample area. Based on the presence of skate egg cases and juveniles within many images, it is likely that the site is being used as a nursery ground for *A. hyperborea*. This study demonstrates the potential of using AUVs to detect fine-scale spatial patterns of the structure-forming sponges and demersal fish species. The use of AUVs for deep-water benthic surveys can help visualize how fauna (e.g. fish) utilise deep-sea habitats, and act as a tool for quantifying individuals through relatively unbiased means (e.g. pre-programmed track, no sampling). Such information is crucial for future conservation and management efforts.

1. Introduction

In the North Atlantic, between the 40° and 75° N latitude belt and depths of 150–1700 m, dense aggregations of large structure-forming sponges primarily of the *Geodia* genera can create habitats known as osturs or sponge grounds (Klitgaard and Tendal, 2004; Maldonado et al., 2016). Sponge grounds tend to form in a continuous or semi-continuous manner due to the patchy spatial distribution patterns of the primary sponge species (Beazley et al., 2013). This has made classifying sponge grounds through quantitative means difficult and led to inconsistencies in their definitions based on sampling techniques. For example, Klitgaard et al. (1997) defined sponge grounds as areas where the sponges make up 90% of the wet weight in non-fish trawl catches. However, in photographic surveys, sponge grounds are generally defined as areas with one sponge occurring every 1–30 m^2 (ICES, 2009), whereas in video-based surveys, they are classified as areas that contain 0.5–1 sponge per m^2 to 1 sponge per 10–30 m^2 (Hogg et al., 2010; Kutti et al., 2013). Regardless of the classification discrepancies, deep-sea sponge grounds have sparked scientific interest in recent years due to the recognition that they can support hotspots of biodiversity where they form structural habitat (Klitgaard and Tendal, 2004; Kutti et al., 2013; Maldonado et al., 2016).

Sponge grounds enhance habitat heterogeneity and biodiversity by providing a number of ecological services (Buhl-Mortensen et al., 2010;

* Corresponding author.
E-mail address: Heidi.Meyer@uib.no (H.K. Meyer).

https://doi.org/10.1016/j.dsr.2019.103137
Received 13 March 2019; Received in revised form 26 September 2019; Accepted 7 October 2019
Available online 10 October 2019

Beazley et al., 2013, 2015; Hawkes et al., 2019). Similar to cold-water coral reefs (e.g. Costello et al., 2005), many fish and invertebrate species appear to exploit sponge grounds as spawning, nursery and foraging grounds, areas of refuge, and additional substrate (Kenchington et al., 2013; Kutti et al., 2013; Hawkes et al., 2019). When actively filtering, sponges recycle carbon, nutrients, and dissolved organic matter back into the environment (de Goeij and van Duyl, 2007; de Goeij et al., 2013; Howell et al., 2016; McIntyre et al., 2016). Through this cycling process, sponge grounds transfer excess energy to upper trophic levels and improve bentho-pelagic coupling (Bell, 2008; Cathalot et al., 2015). The canals, cavities, and porous exterior of sponges generate various microhabitats that are utilised by small organisms for protection against strong currents or predation (Klitgaard and Tendal, 2004; Buhl-Mortensen et al., 2010), and the spicule mats formed from deceased sponges create additional substrate for epibenthic fauna (Bett and Rice, 1992; Beazley et al., 2015; McIntyre et al., 2016). Increasingly, sponge grounds are thought to be highly important to other local fauna similar to cold-water coral reefs (Beazley et al., 2013, 2018; Cathalot et al., 2015; Hawkes et al., 2019). However, there is limited information about the ecology and distribution of deep-sea sponges, particularly at small scales (<10's m).

The majority of studies on deep-sea sponge grounds have investigated the community composition, distribution patterns, and abiotic drivers over broad scales (100's – 1000's m), ranging from topographic features, such as the Flemish Cap (Murillo et al., 2012; Beazley et al., 2013) and Sackville Spur (Beazley et al., 2015), to oceanic regions, such as the Canadian Arctic (Murillo et al., 2018), Northeast Atlantic (Klitgaard and Tendal, 2004), Northwest Atlantic (Knudby et al., 2013), and North Atlantic (Howell et al., 2016). The broad-scale distribution of deep-sea sponge grounds is found to be influenced by a variety of abiotic drivers, such as increased dissolved silicate levels (Howell et al., 2016), low temperatures (Klitgaard and Tendal, 2004; Howell et al., 2016), minimum bottom salinity (Knudby et al., 2013; Beazley et al., 2015), bottom current speed (Beazley et al., 2015), particulate organic carbon flux (Howell et al., 2016), and depth (Knudby et al., 2013; Beazley et al., 2015; Howell et al., 2016). While depth is consistently identified as a top driver for sponge ground distribution over broad-scales (Beazley et al., 2015; Howell et al., 2016), it acts as a proxy for other variables (e.g. temperature, salinity, and water mass). Over such broad scales, environmental conditions and habitat structure will change, and while previous findings provide significant insight into the abiotic variables that vary over large spatial scales, there is very little known about the variables that are important at local scales. As such, there is a clear knowledge gap regarding the drivers of the small-scale patterns observed in the main inhabitants of individual sponge grounds. Understanding these patterns and their respective drivers provides insight into ecological interactions operating within deep-sea ecosystems (Robert et al., 2014).

Given the expected vulnerability of these deep-sea habitats to disturbance and climate change (OSPAR, 2008; FAO, 2009; Hogg et al., 2010), there is an urgent need to identify and map the distribution of primary structure-forming sponge species, and to assess the factors influencing sponge ground formation, persistence, and community composition (Hogg et al., 2010; Kutti et al., 2013; Beazley et al., 2015, 2018; Howell et al., 2016; Roberts et al., 2018). To date, a variety of surveying techniques have been used for these purposes. Traditional extractive methods such as scientific trawling and dredging have been used extensively for large-scale benthic surveys (Klitgaard and Tendal, 2004; Knudby et al., 2013; Morris et al., 2014; McIntyre et al., 2016); however, such methods do not capture the patterns that occur at the fine-scales (i.e. within sponge grounds). Non-extractive methods like visual-based surveys conducted by towed-camera systems or submersibles have become a favoured tool as they allow for continual observations of the benthos and are relatively non-intrusive (Sánchez et al., 2009; Marsh et al., 2013). Photographic surveys can provide abundance estimates for the larger benthic megafauna and are thought to be more realistic than those from extractive methods (Williams et al., 2015). This can help identify areas of specific biological interest (e.g. deep-sea fish species, vulnerable marine ecosystems), community structure, and zonation patterns through finer-scale analysis of georeferenced imagery (Ludvigsen et al., 2007; Marsh et al., 2013). One tool that is gaining in popularity is the creation of photomosaics from imagery data, which make it possible to visualise localised habitat composition and its seafloor extent through quantitative spatial analysis (Sánchez et al., 2009; Robert et al., 2017).

Submersibles like remotely operated vehicles (ROVs) or autonomous underwater vehicles (AUVs) have greatly improved what is currently known about the deep sea (Danovaro et al., 2014). In addition to visualising the seafloor using cameras or acoustic sensors, environmental parameters like temperature, salinity, dissolved oxygen, and depth can be measured simultaneously during the survey (Wynn et al., 2014). ROVs have some benefits over AUVs, for example, they are capable of collecting specimens for taxonomic validation of the video data and surveys can be easily altered by operators when discovering features of interest (Thresher et al., 2014; Howell et al., 2014; Williams et al., 2015). However, they can be influenced by swell and have relatively slow transect speeds (Morris et al., 2014), which can affect altitude, direction, and speed along transects. AUVs, on the other hand, autonomously traverse a specified route within fixed altitude limits (Wynn et al., 2014), minimising human interaction and operator error, giving them an advantage as a survey-tool over ROVs. As such, image-based surveys conducted using AUVs are emerging as an important tool for the exploration of deep-sea habitats and quantitative mapping of benthic megafauna (e.g. Statham et al., 2005; Grasmueck et al., 2006; Kelly et al., 2014; Huvenne et al., 2016).

Previous studies have shown photographic surveys to be a promising means of investigating deep-sea communities such as cold-water coral reefs, hydrothermal vent fields, and sponge grounds (Beazley et al., 2013; Morris et al., 2014; McIntyre et al., 2015; Bell et al., 2016; Milligan et al., 2016; Robert et al., 2017). However, few studies have solely used visual-based surveys for mapping sponge grounds in detail (e.g. Kutti et al., 2013; Hawkes et al., 2019), even fewer with an AUV (e.g. Powell et al., 2018). Additionally, no known study has used AUV imagery to investigate the small-scale spatial patterns produced by individual species within a sponge ground.

In this study, AUV imagery was used to map the spatial patterns of megafauna and demersal fish in an arctic sponge ground on the summit of the Schulz Bank, located on the Arctic Mid-Ocean Ridge. The aims of the study are as follows: (1) detect megafauna (≥1 cm) inhabiting the Schulz Bank sponge ground through AUV imagery; (2) map the fine-scale spatial patterns produced by the most prominent megafauna (≥0.5% of the total abundance); (3) study the influence of the measured abiotic variables on the community patterns and most prominent megafauna; (4) characterise the demersal fish population; and (5) investigate whether this is a potential nursery ground for demersal fish.

2. Materials and methods

2.1. Study area

The Schulz Bank (73° 47′ N, 7° 40′ E), previously reported as the Schultz Massif or Massive (Cárdenas et al., 2011, 2013; Roberts et al., 2018), is a deep-sea seamount located at the Arctic Mid-Ocean Ridge (AMOR) where Mohn's Ridge transitions into the Knipovich Ridge. It rises from water depths greater than 2500 to 560 m at the summit (Fig. 1). The surrounding area has been extensively surveyed in recent years owing to nearby hydrothermal activity, specifically the Loki's Castle vent field (Pedersen et al., 2010; Olsen et al., 2015; Steen et al., 2016). The sponge composition on the Schulz Bank and nearby sponge ground regions are largely dominated by demosponges such as *Geodia parva, G. phlegraei, G. hentscheli, Stelletta rhaphidiophora, Craniella infrequens, Thenea valdivae, Hexadella dedritifera, Polymastia thielei* (Cárdenas

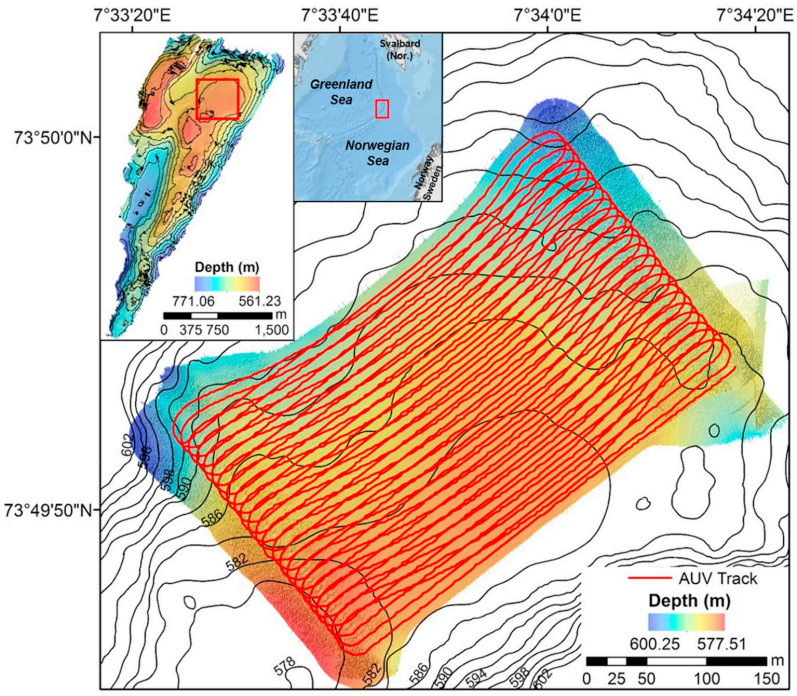

Fig. 1. Multibeam bathymetry of the Schulz Bank summit and the selected sample area. The red box on entire seamount (first inset) indicates the sample area, the second inset shows the location of Schulz Bank on the Arctic Mid-Ocean Ridge. Red lines in the main figure show the *Hugin 1000* track within the sampling area. Bathymetric contours in the sampling area are every 2 m. The black contour lines on the entire seamount (first inset) represent every 20 m. (For interpretation of the references to colour in this figure legend, the reader is referred to the Web version of this article.)

et al., 2011, 2013; Plotkin et al., 2018; Roberts et al., 2018), intermixed with a variety of hexactinellid species such as *Schaudinnia rosea, Scyphidium septentrionale, Trichasterina borealis*, and *Asconema foliata* (Klitgaard and Tendal, 2004; Maldonado et al., 2016; Roberts et al., 2018).

The physical oceanography of the Nordic Seas region is described in Hopkins (1991), Mauritzen (1996) and Hansen and Østerhus (2000). The Schulz Bank is a prominent feature of the AMOR system and is subject to a complex oceanographic setting, as is further described in Roberts et al. (2018). Three main water masses tend to dominate at the Schulz Bank: (1) the surface water mass above the seamount consists of the relatively warm and high salinity Norwegian Atlantic Water; (2) the base and flanks of the seamount are exposed to the colder, fresher Upper Norwegian Deep Water; and (3) an intermediate water mass impinges upon the seamount summit and shallower areas and is likely to be Norwegian Arctic Intermediate Water (Jeansson et al., 2017; Roberts et al., 2018). It may be influenced by topographically-steered deep currents (Orvik and Niiler, 2002), and tidally-driven internal motions are thought to be important to filter feeders inhabiting the summit (Roberts et al., 2018).

For the present study, a gently sloping section of the summit was selected as the primary focus for an in-depth AUV survey (Fig. 1). This had an area of approximately 0.12 km^2 (water depth range: 577–600 m). Soft sediment and a dense spicule mat were characteristic of the substrate on the summit, with little to no visible hard substrate, beyond the occasional boulder.

2.2. Data collection

The seamount was investigated in June 2016 using the RV *G.O. Sars*. Imagery and bathymetric data for the sample area on the summit were collected using AUV *Hugin 1000*. The AUV flew at an average altitude of 5.0 m, with a respective minimum and maximum altitude of 3.8 and 8.5 m, excluding vehicle turns, along a 47 track-line path above the seafloor (Fig. 1). The AUV was fitted with a SAIV SD208 dual conductivity, temperature, and depth (CTD) system, Kongsberg HISAS 1030 synthetic aperture sonar, a Kongsberg EM2040 multibeam echosounder, and a downwards-looking TileCam optical camera. The camera was located approximately 1 m behind the LED light bar (720 LEDs) to reduce the impact of backscattered light. It had a 10-megapixel resolution and a 10-gigabyte hr^{-1} collection rate.

2.3. Environmental data

All spatial data were converted to Universal Transverse Mercator projection (Zone 31° N) to allow for area calculations. EM2040 data was processed with the Reflection AUV post-mission analysis software (version 3.1.0) by Kongsberg Maritime, and the projected bathymetric data of the seamount and sampling area extracted. The final bathymetric grid created had a cell size of 0.1 × 0.1 m. Slope (°), aspect (°), and topographic roughness were calculated from bathymetry using the Digital Elevation Model Surface Tools (Jenness, 2013) within ArcGIS 10.4 (ESRI). *In situ* temperature (°C) and salinity (psu) data obtained from the AUV's CTD system were interpolated using inverse distance weighting (IDW) to create a continuous representation of the conditions on the summit at a resolution of approximately 0.6 × 0.6 m for both variables.

2.4. Image processing

A photomosaic was constructed automatically using Reflection to visualize the sample area and the location of the images to examine the spatial relationships of the fauna, species composition, and community structure of the sponge ground. Images were automatically converted to grey scale by Reflection before stitching successive images together into

a track-line mosaic (Fig. 2). Image area was calculated from Reflection using the AUV position data.

Images were selected for analysis based on the following criteria: (1) AUV altitude was between 4.7 and 5.3 m to maintain image quality (e.g. good scene illumination, consistent altitude, taxonomic resolution, exclude vehicle turns); (2) images were separated by at least 5 m to reduce the risk of using overlapping images that capture the same feature twice (Bell et al., 2016); and (3) images did not display signs of corruption or digital artefacts which could mar interpretation. Image corruption occurred when the Tilecam optical camera wrote over an image with a successive image before the file was completed and stored, thus resulting in an overlap of images on a single file. There were 9,953 images collected by the AUV over 2.78 h, at approximately 1 s intervals. Only 5,611 images (56.4%) fit the criteria and a subset of 430 images were selected for analysis. Images that fit the criteria are hereafter referred to as "optimal images" and the subset of images that were selected for analysis are hereafter referred to as "selected images".

To make sure the selected images were separated by at least 5 m from other selected images, a pseudorandom selection process was conducted whereby selected images separated by 5–20 optimal images were randomly selected along each track-line. The selected images were then checked to ensure they did not contain overlapping features or corruption. Colour versions of the selected images were used to confirm species identification and corruption status. Due to inconsistent illumination, each selected image was overlain with a 2.5×2.0 m digital quadrat, which was placed in the top centre portion of the image to exclude image areas that had poor visibility and allow for quantitative spatial sampling (Fig. 2). Each selected image had an average area of 16.23 m^2 (SD = 0.74 m^2) and was separated from its nearest neighbouring selected images by a mean distance of 9.6 m (SD = 2.44 m). The minimum and maximum distance of separation was 5.56 and 24.83 m, respectively. The mean altitude for both the selected images and optimal images was 4.93 m with a standard deviation (SD) of 0.11, indicating the AUV operated at stable altitude (Morris et al., 2014).

2.5. Identification of fauna

Only epibenthic megafauna and demersal fish visible within the quadrat were enumerated and identified to the lowest taxonomic level possible. Any indication that the sponge ground was being used as a nursery for the demersal fish, such as such as egg cases or juvenile demersal fish, were documented. As is common with imagery analysis, not all fauna were identified to species level due to the relatively low morphological detail visible (Sánchez et al., 2009; Bell et al., 2016). The identifications of the megafauna and demersal fish were quality checked and agreed upon by the authors, and identifications confirmed by physical samples collected from the summit. As a result of the quality check and difficulties in consistent identification of certain species within the selected images, the suspected species *Thenea valdiviae* and *Craniella infrequens* were grouped as 'Demospongiae spp.' and *Schaudinnia rosea, Trichasterina borealis,* and *Scyphidium septentrionale* were grouped as 'Hexactinellida spp.' after the annotation process.

2.6. Demersal fish population

After the initial annotation revealed that the demersal fish and *Amblyraja hyperborea* egg cases were often present outside of the quadrat or in nearby optimal images, a secondary annotation was conducted on all optimal images to assess the demersal fish population and investigate the area as a nursery ground for *A. hyperborea.* All further mentions of the initial annotation and secondary annotation will hereby be referred to as "megafauna survey" and "fish survey", respectively.

All fish and egg cases within the whole optimal image were counted because they were easily identifiable within the images and had a high likelihood of remaining visible even when present outside of the quadrat. In addition, fish were documented as swimming (i.e. appeared in motion, above the substrate, or visible shadow) or non-swimming (i.e. placed directly on the substrate, lack of shadow) in the optimal images. It was also noted if there appeared to be a change in fish behaviour between optimal images that contained the same fish (e.g. non-swimming to swimming between images) (Stoner et al., 2008). To avoid double-counting of the same individual, successive and nearby images within the sample area were checked to ensure the images did not overlap or the individual did not move. Images that contained the same fish individual(s) were dropped from analysis. As it was too difficult to differentiate between decaying and fresh skate eggs, all visible egg cases were counted within an image.

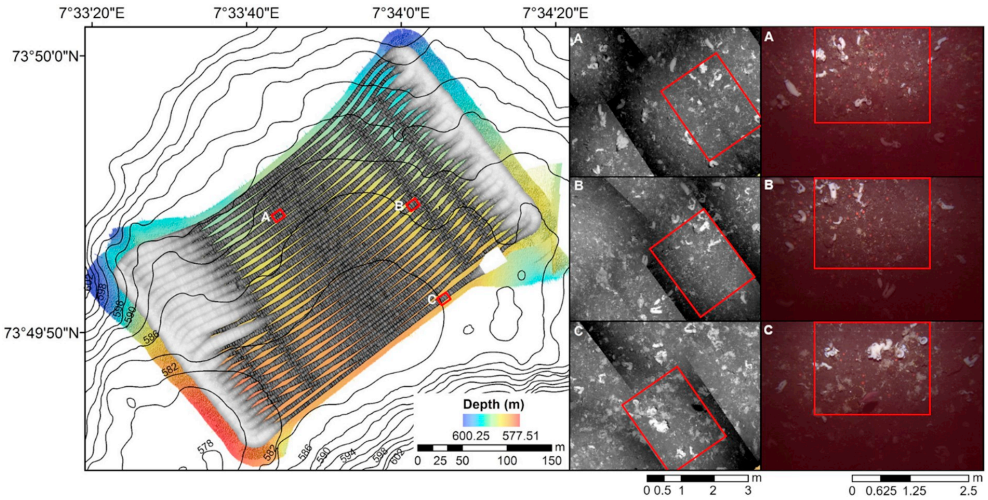

Fig. 2. Photomosaic of the sample area on Schulz Bank with examples of the image mosaic. The labelled red squares on the map indicate the location of example images from the mosaic (second column). The third column show the individual colour image from each area, emphasising the 5 m^2 quadrat used for analysis. (For interpretation of the references to colour in this figure legend, the reader is referred to the Web version of this article.)

2.7. Statistical analysis

2.7.1. Preparation of megafauna data

All taxa with confirmed identities from the quality check were included in the analysis, and taxa that made up ≥0.5% of the total abundance were classified as the "most prominent megafauna". To allow for easier comparison between different surveys, the raw taxon abundance observed in each selected image was converted to density (ind. m^{-2}) (Kutti et al., 2013). All statistical analysis was conducted in RStudio (version 1.1.383; RStudio Team, 2016) unless otherwise specified.

2.7.2. Environmental influence

To determine which, if any, abiotic variables and prominent megafauna densities were correlated, a Spearman's rank correlation coefficient matrix was generated with the package "Hmisc" (version 4.1–1; Harrell Jr., 2018). The *in situ* abiotic conditions demonstrated little variation within the sample area. Depth in the selected images had a range of 579.4–590.8 m and was found to be significantly correlated with temperature, salinity, and topographic roughness, in addition to the majority of the prominent megafauna densities (S1). However, it was selected to remain in the analysis because depth often acts as a proxy for other abiotic variables that were not measured or described in the present study. There were only small differences in temperature and salinity between sampled image locations (0.005–0.078 °C and 35.00–35.04 psu, respectively). Topographic roughness, slope, and aspect also demonstrated little variation, and the overall bottom structure was fairly homogeneous.

Regardless of the apparent homogeneity in abiotic conditions, negative binomial generalized additive models (GAMs) were constructed using R package "mgcv" (version 1.8–24; Wood, 2011) to identify which environmental variables best explained the variance in the community data (e.g. species richness and total megafauna abundance) and the most prominent megafauna abundance data (Zuur et al., 2009). GAMs were selected over a generalized linear models (GLMs) because either not all explanatory variables displayed a linear trend with the community data or most prominent megafauna abundance data, or there was no clear relationship between the response variables and the entire explanatory variables (Zuur et al., 2009). The environmental variables that were included in the GAM analysis were depth (m), temperature (°C), salinity (psu), aspect (°), slope (°), and topographic roughness. Quadrat size was offset to account for the abundance within each quadrat and to obtain estimates that reflected density. Thin plate regression splines were used as smoothing functions applied to each of the abiotic variables (Zuur et al., 2009). To reduce the chance of overfitting of the smooth-functions of the model, a gamma function was used (Zuur et al., 2009).

2.7.3. Sponge ground community and demersal fish patterns

Kernel density estimates (KDEs) were calculated for the most prominent megafauna, demersal fish, and skate egg cases in ArcGIS to visualise their spatial patterns on the summit and identify areas of dense aggregation within the sample area (Kenchington et al., 2014; Beazley et al., 2018). KDE calculations were conducted using a neighbour-based approach that fits a smoothing curve over the data points using the quartic kernel function as described by Silverman (1986). The values of the kernel surfaces overlaying raster cell centres were summed together to generate density estimates for each output raster cell. The smoothing curve is highest at the central point and gradually decreases with the search radius. Therefore, the more data points that fall within the search radius, the more smoothed the output raster becomes. The search radius selected was 20 m to include neighbouring data points for optimal smoothing based on the average neighbour distance between selected images (see section 3.1). The output cell size was 0.6 × 0.6 m and selected based on the resolution of the base map.

Based on the kernel density plots and visible spatial patterns along the depth gradient, regression analysis was conducted on the nine most prominent megafauna to examine the relationship between the density (ind. m^{-2}) and depth (m) using the "car" (version 3.0–2; Fox and Weisberg, 2011) package in R. Regression analyses were also conducted on the demersal fish and skate egg abundances (ind. $image^{-1}$). Taxa that displayed a non-linear trend were analysed with the non-linear least squares function. To check if the relative patterns were preserved after smoothing from the KDE calculations and that over-smoothing had not occurred, regression plots for the prominent megafauna KDEs against depth (m) were compared to the respective density regression plots (S2).

3. Results

3.1. Prominent megafauna

There were 20 morphotypes detected within the selected images (Table 1 and Fig. 3), and were in the following classes: Ascidiacea (1), Hexactinellida (1), Demospongiae (8), Anthozoa (2), Asteroidea (3), Echinoidea (1), Actinopterygii (2), Chondrichtyes (1), and Malacostraca (1). The most prominent megafauna that contributed to ≥0.5% of the total abundance present in the images were ascidians, anemones, demosponges (Demospongiae spp., *Lissodendoryx (Lissodendoryx) complicata*, *Hexadella dedritifera*, *Geodia parva*, *Stelletta raphidiophora*), Hexactinellida spp., and *Gersemia rubiformis*. Mobile fauna such as echinoderms and demersal fish had a low occurrence during the megafauna survey because they were rarely observed within the confines of the quadrat.

3.2. Environmental influence

The GAM analysis showed the measured environmental variables explained relatively little of the variation in species richness (GAM: total deviance explained = 6.74%; S3) or total megafauna abundance (GAM: total deviance explained = 33.14%; S4). Depth most influenced the variability within community patterns (Table 2). Similar trends were observed for the most prominent megafauna data (S5 to S14).

3.3. Sponge ground community patterns

Ascidians were the most abundant taxa within the sample area and present within every image. Their densities were often double that of the

Table 1
Abundance of the prominent megafauna found on the Schulz Bank summit in the megafauna survey.

Phylum	Taxa	Total Abundance
Arthropoda	*Bythocaris* sp. G.O. Sars, 1870	348
Chordata	Ascidiacea spp.	35,952
	Amblyraja hyperborea (Collet, 1879)	4
	Macrourus berglax Lacépède, 1801	42
	Reinhardtius hippoglossoides (Walbaum, 1792)	17
Cnidaria	Actiniaria sp.	19,074
	Gersemia rubiformis (Ehrenberg, 1834)	691
Echinodermata	*Tylaster willei* Danielssen and Koren, 1881	183
	Asteroidea spp.	29
	Solaster spp. Forbes, 1839	8
	Strongylocentrotus sp. Brandt, 1835	78
Porifera	Demospongiae spp.	15,050
	Geodia parva Hansen, 1885	1,713
	Hemigellius sp. Burton, 1932	204
	Hexadella dedritifera Topsent, 1913	5,197
	Hexactinellida spp.	5,489
	Lissodendoryx (Lissodendoryx) complicata (Hansen, 1885)	7,331
	Polymastia thielei Koltun, 1964	251
	Stelletta rhaphidiophora Hentschel, 1929	1,344
	Stylocordyla borealis (Lovén, 1868)	177

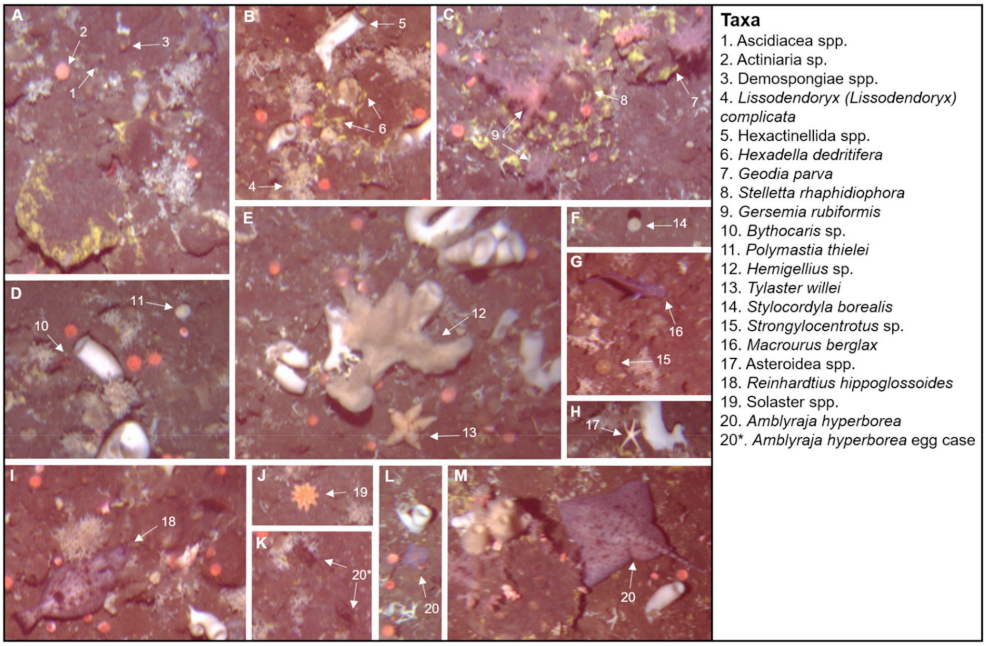

Fig. 3. Examples of megafauna observed on the Schulz Bank summit. Taxa categorized by the most abundant megafauna to the least abundant observed within the megafauna survey.

Table 2
Summary statistics of the generalized additive models fitted to the species richness (S) and total megafaunal abundance (N) (negative binomial distribution, log link). Deviance explained (%) is the percent of null deviance in the data explained by the model. All abiotic variables contained a smoothing function (see S3 and S4).

Response	Explanatory	Deviance Explained (%)	R^2	P-value
Species Richness	Depth (m)	5.05	0.0431	0.001
	Temperature (°C)	1.49	0.0128	0.011
	Salinity (psu)	0.08	−0.0015	0.560
	Slope (°)	0.04	−0.0019	0.670
	Aspect (°)	0.04	−0.0020	0.901
	Topographic Roughness	0.03	−0.0020	0.707
Total Megafauna Abundance	Depth (m)	26.60	0.2580	<0.001
	Temperature (°C)	4.34	0.0406	0.002
	Salinity (psu)	0.15	0.0008	0.419
	Slope (°)	1.62	0.0100	0.335
	Aspect (°)	0.01	−0.2240	0.836
	Topographic Roughness	0.43	0.0012	0.145

next most prominent taxa, the anemones (Table 3). The ascidians were commonly growing directly on the spicule mat and along the edges of large demosponges. They were often used as substrate for other sessile megafauna, predominantly the anemones. Ascidians were more densely aggregated in the deeper north-western region of the sample area (Figs. 4 and 5) and demonstrated a positive correlation with increasing water depth ($R^2 = 0.239$, $p < 0.001$). Unsurprisingly given their co-occurrence with ascidians, the anemones were also significantly correlated with depth ($R^2 = 0.221$, $p < 0.001$), although their density hotspot displayed more signs of patchiness compared to the ascidians (Fig. 4).

Demospongiae spp. had a widespread distribution throughout the sample area and had no significant change in density with depth (Figs. 4 and 5). *Lissodendoryx (Lissodendoryx) complicata* was most densely aggregated in the south-eastern portion of the sample area and its distribution strongly followed the 586 m depth contour (Fig. 4). Deeper than this, the species' density rapidly declined, and occurrences thinned considerably into small patches. Its density demonstrated a statistically significant negative exponential relationship with depth (Nonlinear Least Squares: $p < 0.001$; Fig. 5). Hexactinellida spp. did not exhibit any spatial preference on the summit and were distributed evenly throughout the sample area.

Table 3
Density (ind. m^{-2}) summary of the most prominent megafaunal species within the selected images the taxon was observed in.

Taxa	Number of Images	Minimum	Maximum	Average ± SE
Ascidiacea spp.	430	3.00	40.60	16.52 ± 0.30
Actiniaria sp.	430	2.20	22.20	8.87 ± 0.17
Demospongiae spp.	430	2.00	14.20	7.00 ± 0.11
Lissodendoryx (Lissodendoryx) complicata	419	0.20	11.60	3.50 ± 0.12
Hexactinellida spp.	430	0.40	6.20	2.55 ± 0.05
Hexadella dedritifera	429	0.20	6.20	2.42 ± 0.05
Geodia parva	411	0.20	2.40	0.83 ± 0.02
Stelletta rhaphidiophora	381	0.20	3.20	0.71 ± 0.02
Gersemia rubiformis	244	0.20	2.80	0.57 ± 0.03

The yellow encrusting sponge, *H. dedritifera*, was primarily observed growing on the large demosponges, *G. parva* and *S. rhaphidiophora*. While *G. parva* and *S. rhaphidiophora* were observed in low densities in the present study (Table 3), their large size makes them likely to contribute considerably to the overall megafaunal biomass. The three demosponge species were present throughout the sample area with some signs of spatial patchiness, though only *H. dedritifera* displayed a slight

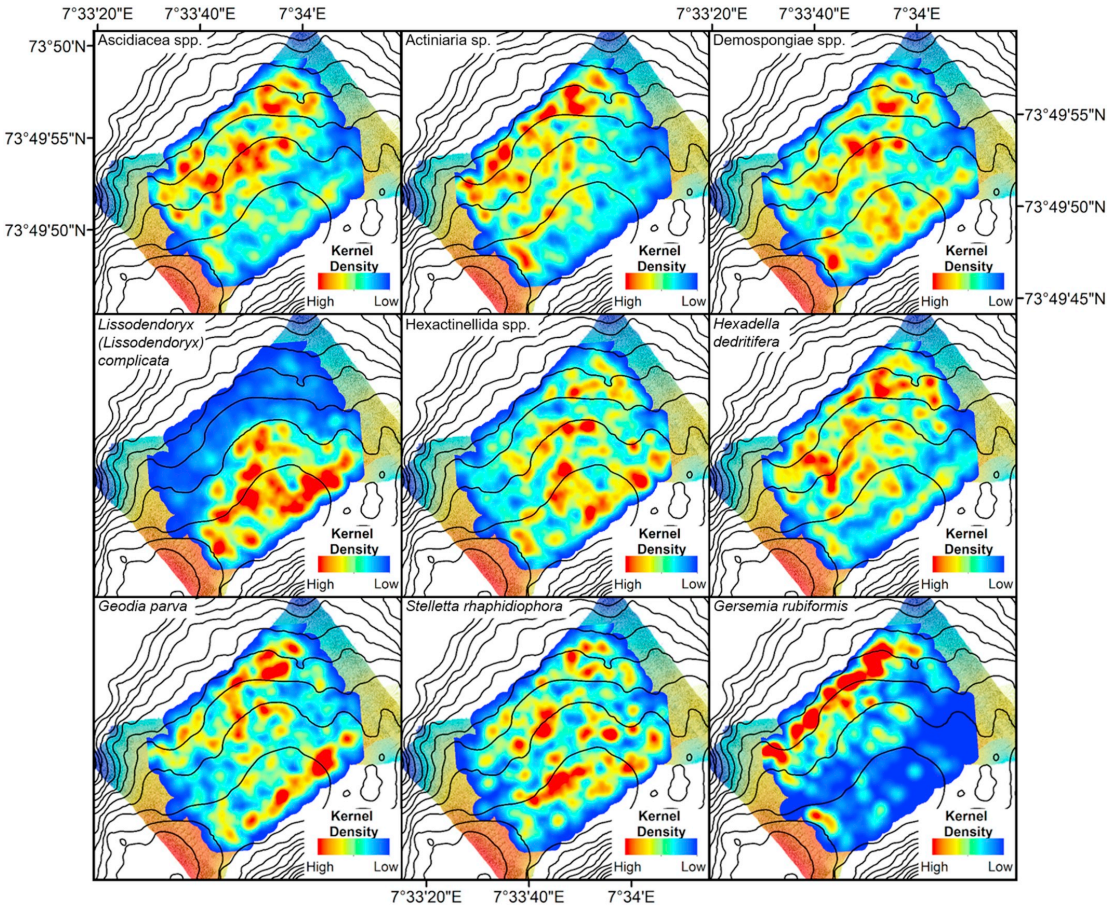

Fig. 4. Kernel density estimation plots of the most prominent megafauna on the Schulz Bank summit determined from the *Hugin 1000* imagery. Contour lines represent every 2 m and are as shown in Fig. 1. Kernel density values are normalized by the maximum densities occurring for each species.

significant positive trend with increasing water depth ($R^2 = 0.131$ $p < 0.001$).

The soft coral, *G. rubiformis* had a very patchy distribution and was only present in the north-western edges of the sample area. It became more abundant at depths greater than 586 m, and demonstrated a positive exponential relationship with depth (Nonlinear Least Squares: $p < 0.001$; Fig. 5).

3.4. Demersal fish on the summit

The summit was inhabited by three observable demersal fish species (n = 708 individuals) (Fig. 6), which were present within 662 images (11.8 % of optimal images). In any given image, there was a maximum of three individuals present.

The most common species was the Roughhead Grenadier (*Macrourus berglax*, Fig. 3G), which accounted for approximately 68.2% of the total observed fish abundance (n = 483 individuals). *Macrourus berglax* were always observed above the substrate and in motion. It was unclear whether there was a change in behaviour between images that contained the same individual.

The second most abundant species was a commonly targeted commercial species, the Greenland Halibut (*Reinhardtius hippoglossoides*, Fig. 3I), which accounted for approximately 25.0% of the total fish population. *Reinhardtius hippoglossoides* were observed swimming (n = 110 individuals) more often than non-swimming (n = 67 individuals).

The Arctic Skate (*Amblyraja hyperborea*, Fig. 3M) was the least abundant fish observed and accounted for 6.8% of the population (n = 48 individuals), and 27% of the skates observed were juveniles (Fig. 3L). Overlapping images that contained the same *A. hyperborea* individuals were separated by approximately 5 min. The individuals were seemingly undisturbed by the AUV because they did not move between images. All fish species appeared to be randomly distributed on the summit and displayed little spatial preference, and no specific epifaunal taxa association or depth (linear regression: $p > 0.01$; S15).

Amblyraja hyperborea egg cases were regularly observed throughout the sample area, often directly on the spicule mat (Fig. 6). They were present in 49.3% of all optimal images with a total abundance of 4061 eggs (n = 2769 images). The highest abundance of eggs in a single image was 6 eggs (n = 3 images), though most images only contained 1 egg (n = 1840 images). There appeared to be higher accumulations of eggs in the south-eastern region, the shallower section, of the sample area. However, the skate eggs displayed a weak relationship with depth ($R^2 = 0.030$, $p < 0.001$; S15).

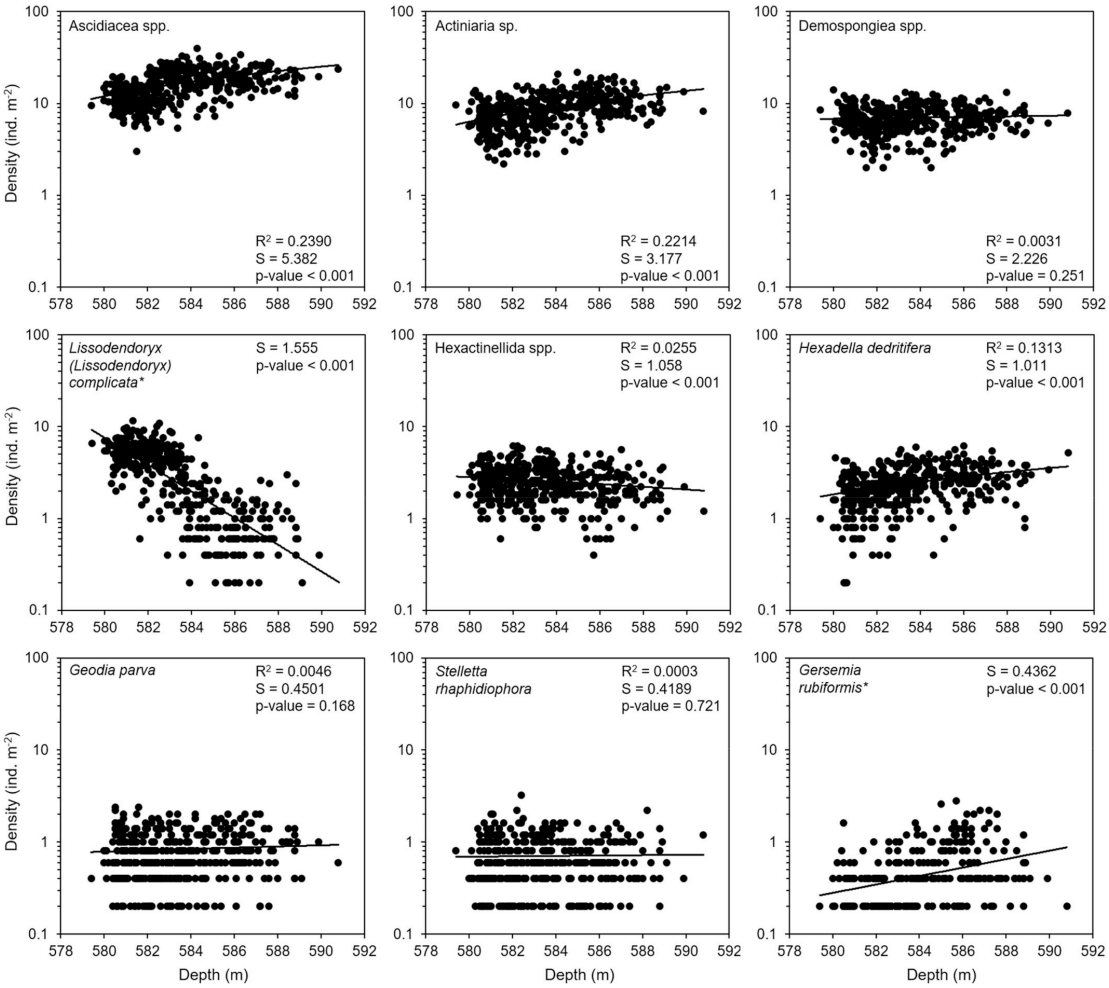

Fig. 5. Regression plots of density (ind. m^{-2}) against depth (m) for the most prominent megafauna on the Schulz Bank. Y-axes have been semi-logged to standardize the differences in densities between megafauna. Residual standard error (S) and R-squared show the statistical correlation of the relationship between density and depth. Asterisks (*) denotes taxa which had a non-linear relationship with depth.

4. Discussion

To the authors' knowledge, this study is the first that has utilised an AUV to map a deep-sea sponge ground in the North Atlantic and one of the very few studies to use an AUV to study the spatial distribution of deep-sea fish assemblages (Milligan et al., 2016; Powell et al., 2018). The AUV imagery provided insight of the major megafauna taxa inhabiting the sponge ground and detected the spatial patterns of the most prominent megafauna and demersal fish species. The presence of *Amblyraja hyperborea* egg cases and juveniles suggests the area may be used as a nursery ground.

4.1. Sponge ground on the summit

Geodia species are commonly the primary structure-forming sponge species found in sponge grounds in the North Atlantic (Klitgaard and Tendal, 2004; Cárdenas et al., 2013; Howell et al., 2016). Several species that were observed in the present study have previously been classified as indicator species or habitat builders of arctic sponge grounds (Cárdenas et al., 2013; Maldonado et al., 2016; Murillo et al., 2018). For example, Murillo et al. (2018) suggested that *G. hentscheli*, *G. parva*, and *S. rhaphidiophora* are indicative of arctic sponge grounds, and *L. complicata* can be considered an indicator of arctic slope sponge habitats (Mayer and Piepenburg, 1996). Additionally, as observed on the Schulz Bank, the hexactinellid sponge species *T. borealis* and *S. rosea,* are common in arctic sponge grounds (Maldonado et al., 2016).

The densities of the primary structure-forming sponges fit within all of the sponge ground definitions that have been previously suggested, where there are at least one sponge occurring every 1–30 m^2 (ICES, 2009), the sample area does contain 0.5–1 sponge per m^2 to 1 sponge per 10–30 m^2 (Hogg et al., 2010; Kutti et al., 2013), and the sponges are occurring in a continuous or semi-continuous fashion (Beazley et al., 2013). Based on the stated variables and presence of common arctic sponge ground species (Murillo et al., 2018), it is clear that the sample

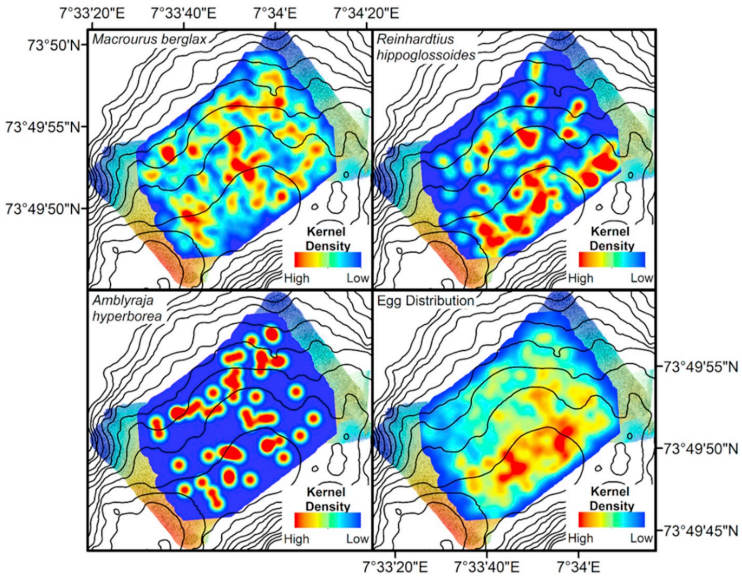

Fig. 6. Kernel density estimation plots of the demersal fish and *Amblyraja hyperborea* egg cases on the Schulz Bank summit determined from the *Hugin 1000* imagery. Contour lines represent every 2 m and are as shown in Fig. 1. Kernel density values are normalized by the maximum densities occurring for each species.

area is situated within a sponge ground. The full spatial extent of the habitat is unknown at this point. However it is likely to extend to a depth of at least 700 m, based on previous results from the Schulz Bank (Roberts et al., 2018).

4.2. Environmental conditions

The measured abiotic variables (temperature, salinity, slope, aspect, and rugosity), with the exception of depth, appeared to have little influence on the patterns displayed by the prominent megafauna. This is unsurprising given the low environmental variability that was observed on the seamount summit during the survey. Temperature and salinity are known to be important variables in the distribution of deep-sea sponge grounds over broad spatial scales (Beazley et al., 2015, 2018; Howell et al., 2016). But over smaller scales, studies have reported depth as the most important variable for demersal communities when compared to other parameters like temperature (Johannesen et al., 2017; Serrano et al., 2017). However, because depth can act as a proxy for many other abiotic variables (Howell et al., 2016), it is possible that unmeasured variables (e.g. local hydrodynamics, suspended matter, and substrate type) that are more sensitive to small-scale variability than the collected parameters are responsible for the patterns observed in the present study.

Roberts et al. (2018) found that the sponge ground on the summit of the Schulz Bank coincided with the boundary between two water masses, Upper Norwegian Deep Water and Norwegian Arctic Intermediate Water. The boundary was particularly dynamic owing to internal waves with a diurnal tidal periodicity and it was concluded that this may benefit the sponges through regular flushing with warmer, oxygen-enriched water from above, the supply of inorganic nutrients and DIC from below by turbulent mixing, and the provision of mechanisms for food supply and the prevention of smothering by sedimentation. The distribution of such 'benefits' over the seamount summit may be uneven as the broader scale seamount hydrodynamics interact with local scale topographic features (e.g. ridges and steep slopes) and this could influence the spatial patterns observed in individual taxa abiotically in ways not resolved by the present study.

Irrespective of this, given that variability is reduced at small scales (i.e. spatial autocorrelation), it can be hypothesised that community patterns are less likely to be influenced solely by the environment at such scales (Milligan et al., 2016). In such cases, ecological influences like biotic interactions, competition, food and substrate availability, reproduction strategies, and niche partitioning are thought to be major factors driving trends in small-scale community patterns (Mayer and Piepenburg, 1996; Kutti et al., 2013; Sell and Kröncke, 2013; Beazley et al., 2015; Johannesen et al., 2017). Yet, without a more comprehensive study on the influence of the localised environmental and ecological conditions on the individual species spatial patterns, it remains unclear.

4.3. Fine-scale patterns in the megafauna

The *Hugin 1000* AUV proved useful for capturing spatial patterns of the more prominent megafauna such as the ascidians, anemones, hexactinellids, larger demosponges, and fish. The majority of the megafauna were evenly distributed within the small survey area, with the exception of the ascidians, anemones, *L. complicata,* and *G. rubiformis*.

Ascidians and anemones are common inhabitants of sponge grounds (Klitgaard and Tendal, 2004; Hogg et al., 2010; Henry and Roberts, 2014). While the ascidians were often settled directly on the sediments, the anemones were frequently observed growing on the ascidians, large demosponges, and any other available substrate.

The most noteworthy pattern was observed for *L. complicata*, where its density rapidly diminished at depths greater than 586 m. *Lissodendoryx (Lissodendoryx) complicata* is common in arctic slope sponge communities (Mayer and Piepenburg, 1996; Murillo et al., 2018), and has been observed at depths exceeding 1470 m in the Davis Strait (Tompkins et al., 2017), and on the flanks of the Schulz Bank down to 3000 m (Rapp pers. obs.). The clear boundary within the sample area is most likely attributed to random patchiness or biological factors that have yet to be explored.

The lack of distinct spatial patterns produced by the major structure-forming sponges like *G. parva* and *S. rhaphidiophora* is to be expected.

They have a very wide depth range and have been found at depths up to 1997 m on the Schulz Bank in previous surveys (Cárdenas et al., 2013; Roberts et al., 2018). The large demosponges are common hosts to other sponge epibionts, like *H. dedritifera* (Cárdenas et al., 2013). It is likely that some of the other sessile megafaunal spatial patterns are influenced by the large demosponges, as the abundance of structure-forming sponges of the same genera was found to be an important variable in epibenthic megafaunal distribution at the Sackville Spur by Beazley et al. (2015). As an encrusting sponge, *H. dedritifera* is thought to carefully select its host, and therefore its distribution is likely influenced by the host species, substrate type, or the minimum nearest neighbour distance (Cárdenas et al., 2013; Beazley et al., 2015; McIntyre et al., 2016; Hawkes et al., 2019).

Gersemia rubiformis generally occurred in low densities and became more common at the north-western edges of the sample area, though it is common in the arctic benthic ecosystems (Sswat et al., 2015) and has been previously observed in regions dominated by *Geodia* spp. (Jørgensen et al., 2016; Murillo et al., 2016a). Similar to the other prominent megafauna within the sample area, *G. rubiformis* has a wide depth range and it has been documented from 1 m to 3600 m within the northern polar regions (Henry et al., 2003; Murillo et al., 2011, 2016a; Jørgensen et al., 2016). Patchy distribution patterns displayed by *G. rubiformis* in the Atlantic are rather common (Henry et al., 2003) and are thought to be a result of the juvenile settling process where juveniles aggregate at the base of parent colonies on substrate that has already been found to be hospitable by the adults. However, as the species was observed in low quantities, it remains unclear if similar mechanisms or random patchiness are driving the spatial distribution of *G. rubiformis* on the Schulz Bank.

4.4. Demersal fish in sponge grounds

Aggregations of demersal fish are commonly documented on seamounts (Clark et al., 2010) and around sponge grounds (Klitgaard and Tendal, 2004; Kenchington et al., 2013). In the present study, *Macrourus berglax, Reinhardtius hippoglossoides*, and *Amblyraja hyperborea* were consistently observed throughout the sample area and have been reported in other areas dominated by geodiids (Klitgaard and Tendal, 2004; Kenchington et al., 2013; Murillo et al., 2016b). Similar to the findings of Håpnes (2015), these fish species did not display spatial preference for any one particular area of the sponge ground and all fish species were widely and evenly distributed within the sample area.

Since very little is known about *A. hyperborea*, the results from the present survey give some insight on its biogeography and life-history. This skate species is a cold-water species found worldwide and has been observed in sloped regions of the Arctic from depths of 300–1500 m (Skjæraasen and Bergstad, 2001; Doglov et al., 2005; Lynghammar et al., 2013), though it has been reported in low abundances as deep as 1800 m (Stein et al., 2005). Videos collected from ROV surveys conducted on the Schulz Bank showed that *A. hyperborea* and its egg cases are present in lower densities on the flanks of the seamount (unpublished data). *Amblyraja hyperborea* egg cases were consistently observed in high numbers throughout the sample area, though it is uncertain how many egg cases were viable or in the process of degradation at the time of the survey. The presence of skate eggs and juveniles suggests that the area may act as a nursery for *A. hyperborea*, but further research is required to determine habitat specificity.

There is limited understanding of how demersal fish may use sponge grounds. Johannesen et al. (2017) suggest that while sponge grounds do not form feeding links for the fish present, they are likely to be important habitats for fish. Sponge-dominated seamounts have been described as essential habitats for fish species (Sánchez et al., 2008; Sell and Kröncke, 2013; García-Alegre et al., 2014), and evidence suggests that commercial fish catches can be influenced by the presence of such habitats (Rodríguez-Cabello et al., 2009). *Reinhardtius hippoglossoides* is a valued groundfish species that has been commonly associated with sponge grounds in the past (Kenchington et al., 2013; Beazley et al., 2015; Murillo et al., 2016b), and *A. hyperborea* is a common bycatch within the Greenland Halibut fishery (Peklova et al., 2014).

4.5. Limitations

Similar to findings from Håpnes (2015), the photomosaic facilitated the detection of several megafaunal morphotypes and demersal fish species. However, due to the surveying altitude, image resolution, or the size of the sample area (Sánchez et al., 2008, 2009; Williams et al., 2015), it is likely that the megafaunal densities and species richness were underestimated. Identifying benthic fauna solely with images becomes difficult as the camera lens moves further away from the substrate (Singh et al., 2004), which is consistent with the imagery collected here. Image surveys tend to have poor taxonomic resolution, where many individuals are either too small or cryptic to identify from images alone. This was the case for *G. parva* and *S. rhaphidiophora* as they were often hidden within the spicule mat. A combination of visual and corroborative extractive techniques would allow for a more reliable description of deep-sea habitats and is recommended wherever possible (Howell et al., 2014).

The impact of *Hugin 1000* on the behaviour of the mobile fish species is unknown. Like most visual-based surveying techniques, AUVs are suspected to generate behavioural responses during their surveys and may cause biases from noise or strobe lighting (Raymond and Widder, 2007). This can subsequently impact density estimates of mobile fauna (Stoner et al., 2008; Sánchez et al., 2009; Milligan et al., 2016). However, determining the extent of the impact and type of behavioural response is difficult since it can occur outside of the field of view, and avoidance behaviour may not be accurately captured by still imagery. Therefore, it is critical to heed caution when estimating fish population through imagery data. It is interesting to note that there were numerous incidences of *A. hyperborea* being seemingly unperturbed by the passage of the AUV.

4.6. Conclusion

This study provides insight into community patterns that are often overlooked when surveying deep-sea habitats. Not only were the fine-scale spatial patterns of important arctic sponge ground taxa like *Geodia parva*, *Stelletta rhaphidiophora, Lissodendoryx (Lissodendoryx) complicata*, and hexactinellid sponges visible, the images also showed demersal fish present in the entire sample area and *Amblyraja hyperborea* potentially using it as a nursery ground. Visual-based surveys are a non-extractive and non-destructive method that allow for the visualisation and characterisation of benthic habitats and give insight into drivers that occur over small-scales (<10's m). Such surveys improve the overall understanding of key species, their fine-scale spatial distribution, and structural habitat of importance to demersal fish (i.e. for nursery grounds), and are thus highly valuable to fisheries, management, and conservation efforts.

Data availability statement

The datasets presented in this article are available at https://doi.org/10.1594/PANGAEA.906904.

Declaration of competing interest

None to declare.

Acknowledgements

The work leading to this publication has received funding from the European Union's Horizon 2020 research and innovation programme through the SponGES project (grant agreement No 679849). This

document reflects only the authors' view and the Executive Agency for Small and Medium-sized Enterprises (EASME) is not responsible for any use that may be made of the information it contains. The University of Bergen, Bangor University, and the crew of *RV G.O. Sars* are acknowledged for their contribution to the project for collecting and providing the AUV imagery data for processing. Gokul Raj Krishna is recognised for assisting in the initial processing of the fish survey.

Appendix A. Supplementary data

Supplementary data to this article can be found online at https://doi.org/10.1016/j.dsr.2019.103137.

References

Beazley, L.I., Kenchington, E.L., Murillo, F.J., del Mar Sacau, M., 2013. Deep-sea sponge grounds enhance diversity and abundance of epibenthic megafauna in the Northwest Atlantic. ICES J. Mar. Sci. 70 (7), 1471–1490. https://doi.org/10.1093/icesjms/fst124.

Beazley, L., Kenchington, E., Yashayaev, I., Murillo, F.J., 2015. Drivers of epibenthic megafaunal composition in the sponge grounds of the Sackville Spur, northwest Atlantic. Deep-Sea Res. Part I Oceanogr. Res. Pap. 98, 102–114. https://doi.org/10.1016/j.dsr.2014.11.016.

Beazley, L.I., Wang, Z., Kenchington, E.L., Yashayaev, I., Rapp, H.T., Xavier, J.R., Murillo, F.J., Fenton, D., Fuller, S.D., 2018. Predicted distribution and climatic tolerance of the glass sponge *Vazella pourtalesi* on the Scotian Shelf and its persistence in the face of climatic variability. PLoS One 13 (10), e0205505. https://doi.org/10.1371/journal.pone.0205505.

Bell, J.J., 2008. The functional roles of marine sponges. Estuar. Coast Shelf Sci. 79, 341–353. https://doi.org/10.1016/j.ecss.2008.05.002.

Bell, J.B., Alt, C.H.S., Jones, D.O.B., 2016. Benthic megafauna on steep slopes at the northern mid-atlantic ridge. Mar. Ecol. 37, 1290–1302. https://doi.org/10.1111/maec.12319.

Bett, B.J., Rice, A.L., 1992. The influence of hexactinellid sponge (*Pheronema carpenteri*) spicules on the patchy distribution of macrobenthos in the Porcupine Seabight (bathyal NE Atlantic). Ophelia 36, 217–226. https://doi.org/10.1080/00785326.1992.10430372.

Buhl-Mortensen, L., Vanreusel, A., Gooday, A.J., Levin, L.A., Priede, I.G., Buhl-Mortensen, P., Gheerardyn, H., King, N.J., Raes, M., 2010. Biological structures as a source of habitat heterogeneity and biodiversity on the deep ocean margins. Mar. Ecol. 31, 21–50. https://doi.org/10.1111/j.1439-0485.2010.00359.x.

Cárdenas, P., Xavier, J.R., Reveillaud, J., Schander, C., Rapp, H.T., 2011. Molecular phylogeny of the Astrophorida (Porifera, *Demospongiae*[P]) reveals an unexpected high level of spicule homoplasy. PLoS One 6 (4), e18318. https://doi.org/10.1371/journal.pone.0018318.

Cárdenas, P., Rapp, H.T., Klitgaard, A.B., Best, M., Thollesson, M., Tendal, O.S., 2013. Taxonomy, biogeography and DNA barcodes of Geodia species (Porifera, Demospongiae, Tetractinellida) in the Atlantic boreo-arctic region. Zool. J. Linn. Soc-Lond. 169, 251–331. https://doi.org/10.1111/zoj.12056.

Cathalot, C., Van Oevelen, D., Cox, T.J.S., Kutti, T., Lavaleye, M., Duineveld, G., Meysman, F.J.R., 2015. Cold-water coral reefs and adjacent sponge grounds: hotspots of benthic respiration and organic carbon cycling in the deep sea. Front. Mar. Sci. 2 (37), 1–12. https://doi.org/10.3389/fmars.2015.00037.

Clark, M.R., Rowden, A.A., Schlacher, T., Williams, A., Consalvey, M., Stocks, K.I., Rogers, A.D., O'Hara, T.D., White, M., Shank, T.M., Hall-Spencer, J.M., 2010. The ecology of seamounts: structure, function, and human impacts. Annu. Rev. Mar. Sci. 2, 253–278. https://doi.org/10.1146/annurev-marine-120308-081109.

Costello, M.J., McCrea, M., Freiwald, A., Lundälv, T., Jonsson, L., Bett, B.J., Van Weering, T.C.E., De Haas, H., Roberts, J.M., Allen, D., 2005. Role of cold-water *Lophelia pertusa* coral reefs as fish habitat in the NE Atlantic. In: Freiwald, A., Roberts, J.M. (Eds.), Cold-water Corals and Ecosystems. Springer-Verlag, Berlin Heidelberg, pp. 771–805.

Danovaro, R., Snelgrove, P.V., Tyler, P., 2014. Challenging the paradigms of deep-sea ecology. Trends Ecol. Evol. 29, 465–475. https://doi.org/10.1016/j.tree.2014.06.002.

de Goeij, J.M., van Duyl, F.C., 2007. Coral cavities are sinks of dissolved organic carbon (DOC). Limnol. Oceanogr. 52 (6), 2608–2717. https://doi.org/10.4319/lo.2007.52.6.2608.

de Goeij, J.M., van Oevelen, D., Vermeij, M.J.A., Osinga, R., Middelburg, J.J., de Goeij, A.F.P.M., Admiraal, W., 2013. Surviving in a marine desert: the sponge loop retains resources within coral reefs. Science 342 (6154), 108–110. https://doi.org/10.1126/science.1241981.

Doglov, A.V., Grekov, A.A., Shestopal, I.P., Sokolov, K.M., 2005. By-catch of skates in trawl and long-line fisheries in the Barents Sea. J. Northwest Atl. Fish. Sci. 35, 357–366. https://doi.org/10.2960/J.v35.m524.

FAO, 2009. International Guidelines for the Management of Deep-Sea Fisheries in the High Seas. Rome.

Fox, J., Weisberg, S., 2011. An {R} Companion to Applied Regression, second ed. Sage, Thousand Oaks, California. Retrieved from. http://socserv.socsci.mcmaster.ca/jfox/Books/Companion.

García-Alegre, A., Sánchez, F., Gómez-Ballesteros, M., Hinz, H., Serrano, A., Parra, S., 2014. Modelling and mapping the local distribution of representative species on the le danois bank, el cachucho marine protected area (cantabrian sea). Deep-Sea Res. Part I Oceanogr. Res. Pap. 106, 151–164. https://doi.org/10.1016/j.dsr2.2013.12.012.

Grasmueck, M., Eberli, G.P., Viggiano, D.A., Correa, T., Rathwell, G., Luo, J., 2006. Autonomous underwater vehicle (AUV) mapping reveals coral mound distribution, morphology, and oceanography in deep water of the Straits of Florida. Geophys. Res. Lett. 33, L23616. https://doi.org/10.1029/2006GL027734.

Hansen, B., Østerhus, S., 2000. North Atlantic-nordic seas exchanges. Prog. Oceanogr. 45 (2), 109–208. https://doi.org/10.1016/S0079-6611(99)00052-X.

Harrell Jr., F.E., 2018. Package hmisc. Retrived from. https://cran.r-project.org/web/packages/Hmisc/index.html.

Hawkes, N., Korabik, M., Beazley, L., Rapp, H.T., Xavier, J.R., Kenchington, E.L., 2019. Glass sponge grounds on the Scotian Shelf and their associated biodiversity. Mar. Ecol. Prog. Ser. https://doi.org/10.3354/meps12903.

Henry, L.A., Roberts, J.M., 2014. Applying the OSPAR Habitat Definition of Deep-Sea Sponge Aggregations to Verify Suspected Records of the Habitat in UK Waters. JNCC Report. No. 508.

Henry, L.A., Kenchington, E.L.R., Silvaggio, A., 2003. Effects of mechanical experimental disturbance on aspects of colony responses, reproduction, and regeneration in the cold-water octocoral *Gersemia rubiformis*. Can. J. Zool. 81 (10), 1691–1701. https://doi.org/10.1139/z03-161.

Hogg, M.M., Tendal, O.S., Conway, K.W., Pomponi, S.A., van Soest, R.W.M., Gutt, J., Krautter, M., Roberts, J.M., 2010. Deep-sea Sponge Grounds: Reservoirs of Biodiversity. UNEP-WCMC Biodiversity Series. No. 32. Cambridge.

Hopkins, T.S., 1991. The GIN Sea – a synthesis of its physical oceanography and literature 1972-1985. Earth Sci. Rev. 30, 175–318. https://doi.org/10.1016/00128252(91)90001-V.

Howell, K.L., Bullimore, R.D., Foster, N.L., 2014. Quality assurance in the identification of deep-sea taxa from video and image analysis: response to Henry and Roberts. ICES J. Mar. Sci. 71 (4), 899–906. https://doi.org/10.1093/icesjms/fsu052.

Howell, K.L., Piechaud, N., Downie, A.L., Kenny, A., 2016. The distribution of deep-sea sponge aggregations in the North Atlantic and implications for their effective spatial management. Deep-Sea Res. Part I Oceanogr. Res. Pap. 115, 309–320. https://doi.org/10.1016/j.dsr.2016.07.005.

Huvenne, V.A.I., Bett, B.J., Masson, D.G., Le Bas, T.P., Wheeler, A.J., 2016. Effectiveness of a deep-sea cold-water coral Marine Protected Area, following eight years of fisheries closure. Biol. Conserv. 200, 60–69. https://doi.org/10.1016/j.biocon.2016.05.030.

Håpnes, S.J.H., 2015. Mapping of Demersal Fish and Benthos by Autonomous Underwater Vehicle Equipped with Optical and Acoustic Imagers at 600 Meters Depth in Trondheimsfjorden. MSc thesis. Norwegian University of Science and Technology, Trondheim, Norway.

ICES, 2009. Report of the ICES-NAFO Joint Working Group on Deep-Water Ecology (WGDEC), 9–13 March 2009, vol. 23, p. 94. ICES CM 2009\ACOM.

Jeansson, E., Olsen, A., Jutterström, S., 2017. Arctic intermediate water in the nordic seas, 1991–2009. Deep-sea res. Part I: oceanogr. Res. Pap. SO 128, 82–97. https://doi.org/10.1016/j.dsr.2017.08.013.

Jenness, J., 2013. DEM Surface Tools. Jenness Enterprises, Flagstaff.

Johannesen, E., Jørgensen, L.L., Fossheim, M., Primicerio, R., Greenacre, M., Ljubin, P. A., Dolgov, A.V., Ingvaldsen, R.B., Anisimova, N.A., Munhshin, I.E., 2017. Large-scale patterns in community structure of benthos and fish in the Barent Sea. Polar Biol. 40, 237–246. https://doi.org/10.1007/s00300-016-1946-6.

Jørgensen, L.L., Planque, B., Thangstad, T.H., Certain, G., 2016. Vulnerability of megabenthic species to trawling in the Barents Sea. ICES J. Mar. Sci. 73, i84–i97. https://doi.org/10.1093/icesjms/fsv107.

Kelly, D.S., Delaney, J.R., Juniper, S.K., 2014. Establishing a new era of submarine volcanic observatories: cabling axial seamount and the endeavour segment of the Juan de Fuca Ridge. Mar. Geol. 352, 426–450. https://doi.org/10.1016/j.margeo.2014.03.010.

Kenchington, E., Power, D., Koen-Alonso, M., 2013. Association of demersal fish with sponge grounds on the continental slopes of the northwest Atlantic. Mar. Ecol. Prog. Ser. 477, 217–230. https://doi.org/10.3354/meps10127.

Kenchington, E., Murillo, F.J., Lirette, C., Sacau, M., Koen-Alonso, M., Kenny, A., Ollerhead, N., Wareham, V., Beazley, L., 2014. Kernel density surface modelling as a means to identify significant concentrations of vulnerable marine ecosystem indicators. PLoS One 9 (10), e109365. https://doi.org/10.1371/journal.pone.0109365.

Klitgaard, A.B., Tendal, O.S., Westerberg, H., 1997. Mass occurrences of large sponges (Porifera) in Faroe Island (NE Atlantic) Shelf and slope areas: characteristics, distribution and possible causes. In: The Responses of Marine Organisms to Their Environments. Southampton Ocenography Centre, University of Southampton, England, pp. 129–142.

Klitgaard, A.B., Tendal, O.S., 2004. Distribution and species composition of mass occurrences of large-sized sponges in the northeast Atlantic. Prog. Oceanogr. 61, 57–98. https://doi.org/10.1016/j.pocean.2004.06.002.

Knudby, A., Kenchington, E., Murillo, F.J., 2013. Modeling the distribution of *Geodia* sponges and sponge grounds in the Northwest Atlantic. PLoS One 8 (12), e82306. https://doi.org/10.1371/journal.pone.0082306.

Kutti, T., Bannister, R.J., Fosså, J.H., 2013. Community structure and ecological function of deep-water sponge grounds in the Traenadypet MPA – northern Norwegian continental shelf. Cont. Shelf Res. 69, 21–30. https://doi.org/10.1016/j.csr.2013.09.011.

Ludvigsen, M., Sortland, B., Johnsen, G., Singh, H., 2007. Applications of geo-referenced underwater photo mosaics in marine biology and archaeology. Oceanography 20 (4), 140–149. https://doi.org/10.5670/oceanog.2007.14.

Lynghammar, A., Christiansen, J.S., Mecklenburg, C.W., Karamushko, O.V., Møller, P.R., Gallucci, V.F., 2013. Species richness and distribution of chondrichthyan fishes in the Arctic Ocean and adjacent seas. Biodiversity 14 (1), 57–66. https://doi.org/10.1080/14888386.2012.706198.

Maldonado, M., Aguilar, R., Bannister, R.J., Bell, J.J., Conway, K.W., Dayton, P.K., Díaz, C., Gutt, J., Kelly, M., Kenchington, E.L.R., Leys, S.P., Pomponi, S.A., Rapp, H. T., Rützler, K., Tendal, O.S., Vacelet, J., Young, C.M., 2016. Sponge grounds as key marine habitats: a synthetic review of types, structure, functional roles, and conservation concerns. In: Rossi, S., Bramanti, L., Gori, A., Orejas, C. (Eds.), Marine Animal Forests: the Ecology of Benthic Biodiversity Hotspots. Springer, Switzerland, pp. 1–39.

Marsh, L., Copley, J.T., Huvenne, V.A.I., Tyler, P.A., 2013. Getting the bigger picture: using precision remotely operated vehicle (ROV) videography to acquire high-definition mosaic images of newly discovered hydrothermal vents in the Southern Ocean. Deep-Sea Res. Part I Oceanogr. Res. Pap. 92, 124–135. https://doi.org/10.1016/j.dsr2.2013.02.007.

Mauritzen, C., 1996. Production of dense overflow waters feeding the North Atlantic across the Greenland-Scotland Ridge. Part 1: evidence for a revised circulation scheme. Deep-Sea Res. Part I Oceanogr. Res. Pap. 43 (6), 769–806. https://doi.org/10.1016/09670637(96)00037-4.

Mayer, M., Piepenburg, D., 1996. Epibenthic community patterns on the continental slope off East Greenland at 75°N. Mar. Ecol. Prog. Ser. 143, 151–164.

McIntyre, F.D., Neat, F., Collie, N., Stewart, M., Fernandes, P.G., 2015. Visual surveys can reveal rather different 'pictures' of fish densities: comparison of trawl and video camera surveys in the Rockall Bank, NE Atlantic Ocean. Deep-Sea Res. Part I Oceanogr. Res. Pap. 95, 67–74. https://doi.org/10.1016/j.dsr.2014.09.005.

McIntyre, F.D., Drewery, J., Eerkes-Medrano, D., Neat, F.C., 2016. Distribution and diversity of Deep-sea sponge grounds on the rosemary bank seamount, NE atlantic. Mar. Biol. 163 (143) https://doi.org/10.1007/s00227-016-2913-z.

Milligan, R.J., Morris, K.J., Bett, B.J., Durden, J.M., Jones, D.O.B., Robert, K., Ruhl, H.A., Bailey, D.M., 2016. High resolution study of the spatial distributions of abyssal fishes by autonomous underwater vehicle. Sci. Rep. 6, 26095. https://doi.org/10.1038/srep26095.

Morris, K.J., Bett, B.J., Durden, J.M., Huvenne, V.A., Milligan, R., Jones, D.O.B., McPhail, S., Robert, K., Bailey, D.M., Ruhl, H.A., 2014. A new method for ecological surveying of the abyss using autonomous underwater vehicle photography. Limnol Oceanogr. Methods 12, 795–809. https://doi.org/10.4319/lom.2014.12.795.

Murillo, F.J., Durán Muñoz, P., Altuna, A., Serrano, A., 2011. Distribution of deep-water corals of the flemish Cap, flemish pass, and the grand banks of newfoundland (Northwest Atlantic ocean): interaction with fishing activities. ICES J. Mar. Sci. 68 (2), 319–332. https://doi.org/10.1093/icesjms/fsq071.

Murillo, F.J., Durán Muñoz, P., Cristobo, J., Ríos, P., González, C., Kenchington, E., Serrano, A., 2012. deep-sea sponge grounds of the flemish Cap, flemish pass and the grand banks of newfoundland (Northwest Atlantic ocean): distribution and species composition. Mar. Biol. 8 (9), 842–854. https://doi.org/10.1080/17451000.2012.682583.

Murillo, F.J., Serrano, A., Kenchington, E., Mora, J., 2016. Epibenthic assemblages of the Tail of the Grand Bank and Flemish Cap (northwest Atlantic) in relation to environmental parameters and trawling intensity. Deep-Sea Res. Part I Oceanogr. Res. Pap. 109, 99–122. https://doi.org/10.1016/j.dsr.2015.08.006.

Murillo, F.J., Kenchington, E., Lawson, J.M., Li, G., Piper, D.J.W., 2016. Ancient Deep-sea sponge grounds on the flemish Cap and grand bank, Northwest Atlantic. Mar. Biol. 163, 63. https://dx.doi.org/10.1007%2Fs00227-016-2839-5.

Murillo, F.J., Kenchington, E., Tompkins, G., Beazley, L., Baker, E., Knudby, A., Walkusz, W., 2018. Sponge assemblages and predicted archetypes in the eastern Canadian Arctic. Mar. Ecol. Prog. Ser. 597, 115–135. https://doi.org/10.3354/meps12589.

Olsen, B.R., Troedsson, C., Hadziavdic, K., Pederson, R.B., Rapp, H.T., 2015. The influence of vent systems on pelagic eukaryotic micro-organism composition in the Nordic Seas. Polar Biol. 38, 547–558. https://doi.org/10.1007/s00300-014-1621-8.

Orvik, K.A., Niiler, P., 2002. Major pathways of atlantic water in the northern North Atlantic and nordic seas toward arctic. Geophys. Res. Lett. 29 (19), 1896. https://doi.org/10.1029/2002GL015002.

OSPAR, 2008. OSPAR List of Threatened And/or Declining Species and Habitats (Reference Number: 2008-6). London.

Pedersen, R.B., Rapp, H.T., Thorseth, I.H., Lilley, M.D., Barriga, F.J.A.S., Baumberger, T., Flesland, K., Fonseca, R., Früh-Green, G.L., Jorgensen, S.L., 2010. Discovery of a black smoker vent field and vent fauna at the Arctic Mid-Ocean Ridge. Nat. Commun. 1, 123. https://doi.org/10.1038/ncomms1124.

Peklova, I., Hussey, N.E., Hedges, K.J., Treble, M.A., Fisk, A.T., 2014. Movement, depth and temperature preferences of an important bycatch species, Arctic skate *Amblyraja hyperborea*. In: Cumberland Sound, Canadian Arctic. Endanger. Species Res, vol.23, pp. 229–240. https://doi.org/10.3354/esr00563.

Plotkin, A., Gerasimova, E., Rapp, H.T., 2018. Polymastiidae (Porifera: Demospongiae) of the nordic and siberian seas. J. Mar. Biol. Assoc. U. K. 98 (6), 1273–1335. https://doi.org/10.1017/S0025315417000285.

Powell, A., Clarke, M.E., Fruh, E., Chaytor, J.D., Reiswig, H.M., Whitmire, C.E., 2018. Characterizing the sponge grounds of grays canyon, Washington, USA. Deep-Sea Res. Part II Top. Stud. Oceanogr. 150, 146–155. https://doi.org/10.1016/j.dsr2.2018.01.004.

Raymond, E.H., Widder, E.A., 2007. Behavioral responses of two deep-sea fish species to red, far-red, and white light. Mar. Ecol. Prog. Ser. 350, 291–298. https://doi.org/10.3354/meps07196.

Rodríguez-Cabello, C., Sánchez, F., Ortiz de Zarate, V., Barreiro, S., 2009. Does le danois bank (el cachucho) influence albacore catches in the cantabrian sea? Cont. Shelf Res. 29 (8), 1205–1212. https://doi.org/10.1016/j.csr.2008.12.018.

Robert, K., Jones, D.O.B., Huvenne, V.A., 2014. Megafaunal distribution and biodiversity in a heterogeneous landscape: the iceberg-scoured Rockall Bank, NE Atlantic. Mar. Ecol. Prog. Ser. 501, 67–88. https://doi.org/10.3354/meps10677.

Robert, K., Huvenne, V.A.I., Georgiopoulou, A., Jones, D.O.B., Marsh, L., Cater, G.D.O., Chaumillon, L., 2017. New approaches to high-resolution mapping of marine vertical structures. Sci. Rep. 7, 9005. https://doi.org/10.1038/s41598-017-09382-z.

Roberts, E.M., Mienis, F., Rapp, H.T., Hanz, U., Meyer, H.K., Davies, A.J., 2018. Oceanographic setting and short-timescale environmental variability at an Arctic seamount sponge ground. Deep-Sea Res. Part I Oceanogr. Res. Pap. 138, 98–113. https://doi.org/10.1016/j.dsr.2018.06.007.

RStudio Team, 2016. RStudio. Integrated Development for R. RStudio, Inc., Boston, Massachusetts. Retrieved from. http://www.rstudio.com/.

Sánchez, F., Serrano, A., Parra, S., Ballesteros, M., Cartes, J.E., 2008. Habitat characteristics as determinant of the structure and spatial distribution of epibenthic and demersal communities of Le Danois Bank (Cantabrian Sea, N. Spain). J. Mar. Syst. 72, 64–86. https://doi.org/10.1016/j.jmarsys.2007.04.008.

Sánchez, F., Serrano, A., Ballesteros, M.G., 2009. Photogrammetric quantitative study of habitat and benthic communities of deep Cantabrian Sea hard grounds. Cont. Shelf Res. 29, 1174–1188. https://doi.org/10.1016/j.csr.2009.01.004.

Sell, A.F., Kröncke, I., 2013. Correlations between benthic habitats and demersal fish assemblages – a case study on the Dogger Bank (North Sea). J. Sea Res. 80, 12–24. https://doi.org/10.1016/j.seares.2013.01.007.

Serrano, A., Cartes, J.E., Papiol, V., Punzón, A., Garciá-Alegre, A., Arronte, J.C., Ríos, P., Lourido, A., Frutos, I., Blanco, M., 2017. Epibenthic communities of sedimentary habitats in a NE Atlantic deep-seamount (Galicia Bank). J. Sea Res. 130, 154–165. https://doi.org/10.1016/j.seares.2017.03.004.

Silverman, B.W., 1986. Density Estimation for Statistics and Data Analysis. Chapman and Hall, New York.

Singh, H., Armstrong, R., Gilbes, F., Eustice, R., Roman, C., Pizarro, O., Torres, J., 2004. Imaging coral I: imaging coral habitats with the SeaBED AUV. P. Soc. Photo-Opt. Ins. 5 (1), 25–42. https://doi.org/10.1023/B:SSTA.0000018445.25977.f3.

Skjæraasen, J.E., Bergstad, O.A., 2001. Notes on the distribution and length composition of *Raja lintea, R. fyllae, R. hyperborea*, and *Bathyraja spinicauda* (Pisces: rajidae) in the deep northeastern North Sea and on the slope of the eastern Norwegian Sea. ICES J. Mar. Sci. 58, 21–28. https://doi.org/10.1006/jmsc.2000.0985.

Sswat, M., Gulliksen, B., Menn, I., Sweetman, A.K., Piepenburg, D., 2015. Distribution and composition of the epibenthic megafauna north of Svalbard (Arctic). Polar Biol. 38, 861–877. https://doi.org/10.1007/s00300-015-1645-8.

Statham, P.J., Connelly, D.P., German, C.R., Brand, T., Overnell, J.O., Bulukin, E., Millard, N., McPhail, S., Pebody, M., Perrett, J., Squire, M., Stevenson, P., Webb, A., 2005. Spatially complex distribution of dissolved manganese in a fjord as revealed by high-resolution in situ sensing using the autonomous underwater vehicle Autosub. Environ. Sci. Technol. 39 (24), 9440–9445. https://doi.org/10.1021/es050980t.

Steen, I.H., Dahle, H., Stokke, R., Roalkvam, I., Daae, F.L., Rapp, H.T., Pedersen, R.B., Thorseth, I.H., 2016. Novel barite chimneys at the Loki's Castle Vent Field shed light on key factors shaping microbial communities and functions in hydrothermal systems. Front. Microbiol. 6 https://doi.org/10.3389/fmicb.2015.01510 article 1510.

Stein, D.L., Felley, J.D., Vecchione, M., 2005. ROV observations of benthic fishes in the northwind and Canada basins, arctic ocean. Polar Biol. 28, 232–237. https://doi.org/10.1007/s00300-004-0696-z.

Stoner, A.W., Ryer, C.H., Parker, S.J., Auster, P.J., Wakefield, W.W., 2008. Evaluating the role of fish behaviour in surveys conducted with underwater vehicles. Can. J. Fish. Aquat. Sci. 65, 1230–1243. https://doi.org/10.1139/F08-032.

Thresher, R., Althaus, F., Adkins, J., Gowlett-Holmes, K., Alderslade, P., Dowdney, J., Cho, W., Gagnon, A., Staples, D., McEnnulty, F., Williams, A., 2014. Strong depth-related zonation of megabenthos on a rocky continental margin (~700-4000 m) off Southern Tasmania, Australia. PLoS One 9 (1), e85872. https://doi.org/10.1371/journal.pone.0085872.

Tompkins, G., Baker, E., Antsey, L., Walkusz, W., Siferd, T., Kenchington, E., 2017. Sponges from the 2010-2014 paamiut multispecies trawl surveys, eastern arctic and subarctic: class Demospongiae, subclass heteroscleromorpha, order poecilosclerida, family coelosphaeridae, genera *forcepia* and *Lissodendoryx*. Can. Tech. Rep. Fish. Aquat. Sci. No. 3224.

Williams, A., Althaus, F., Schlacher, T.A., 2015. Towed camera imagery and benthic sled catches provide different views of seamount benthic diversity. Limnol Oceanogr. Methods 13, 62–73. https://doi.org/10.1002/lom3.10007.

Wood, S.N., 2011. Fast stable restricted maximum likelihood and marginal estimation of semiparametric generalized linear models. J. R. Stat. Soc. B. 73 (1), 3–36.

Wynn, R.B., Huvenne, V.A.I., Le Bas, T.P., Murton, B.J., Connelly, D.P., Bett, B.J., Ruhl, H.A., Morris, K.J., Peakall, J., Parsons, D.R., Sumner, E.J., Darby, S.E., Dorrell, R.M., Hunt, J.E., 2014. Autonomous Underwater Vehicles (AUVs): their past, present and future contribution to the advancement of marine geoscience. Mar. Geol. 352, 451–468. https://doi.org/10.1016/j.margeo.2014.03.012.

Zuur, A.F., Ieno, E.N., Walker, N.J., Saveliev, A.A., Smith, G.M., 2009. Mixed Effect Models and Extensions in Ecology with R. Statistics for Biology and Health. Springer Science + Business Media, New York, p. 574.

S1. Spearman's rank correlation matrix of the abiotic variables and prominent megafauna density (ind. m^2) in the sample area. Abiotic variables are highlighted in red. Significance level is indicated by coloration, where: (1) light grey or red are $0.01 \leq p < 0.05$; (2) medium grey or red are $0.001 \leq p < 0.01$; and (3) dark grey or red are $p < 0.001$.

	Temperature (°C)	Salinity (psu)	Slope (°)	Aspect (°)	Topographic Roughness	Ascidian spp.	Hexactinellida spp.	Demospongiae spp.	*Stelletta rhaphidiophora*	*Geodia parva*	*Hexadella dedritifera*	*Lissodendoryx (Lissodendoryx) complicata*	Actiniaria sp.	*Gersemia rubiformis*
Depth (m)	-0.17	0.14	0.00	-0.03	0.12	0.55	-0.14	0.06	0.02	0.09	0.39	-0.77	0.49	0.43
Temperature (°C)		0.12	0.01	0.10	0.15	-0.16	0.10	0.05	0.03	0.18	-0.09	0.08	-0.13	0.01
Salinity (psu)			-0.04	0.03	0.01	0.03	-0.08	0.00	0.03	0.04	0.10	-0.11	0.09	0.03
Slope (°)				-0.04	0.10	0.04	-0.12	-0.04	-0.05	-0.07	0.00	-0.12	0.22	0.07
Aspect (°)					0.05	0.06	-0.04	-0.09	0.07	-0.06	-0.01	-0.01	0.01	0.02
Topographic Roughness						0.11	0.02	-0.01	-0.11	0.03	0.17	-0.14	0.10	0.14
Ascidian spp.							-0.17	0.29	-0.02	-0.05	0.40	-0.46	0.49	0.36
Hexactinellida spp.								0.00	0.06	0.13	0.05	0.25	-0.23	-0.20
Demospongiae spp.									-0.16	-0.01	0.09	-0.12	0.12	0.09
Stelletta rhaphidiophora										0.13	0.07	0.12	-0.03	-0.04
Geodia parva											0.06	-0.01	0.04	0.15
Hexadella dedritifera												-0.35	0.34	0.25
Lissodendoryx (Lissodendoryx) complicata													-0.50	-0.48
Actiniaria sp.														0.47

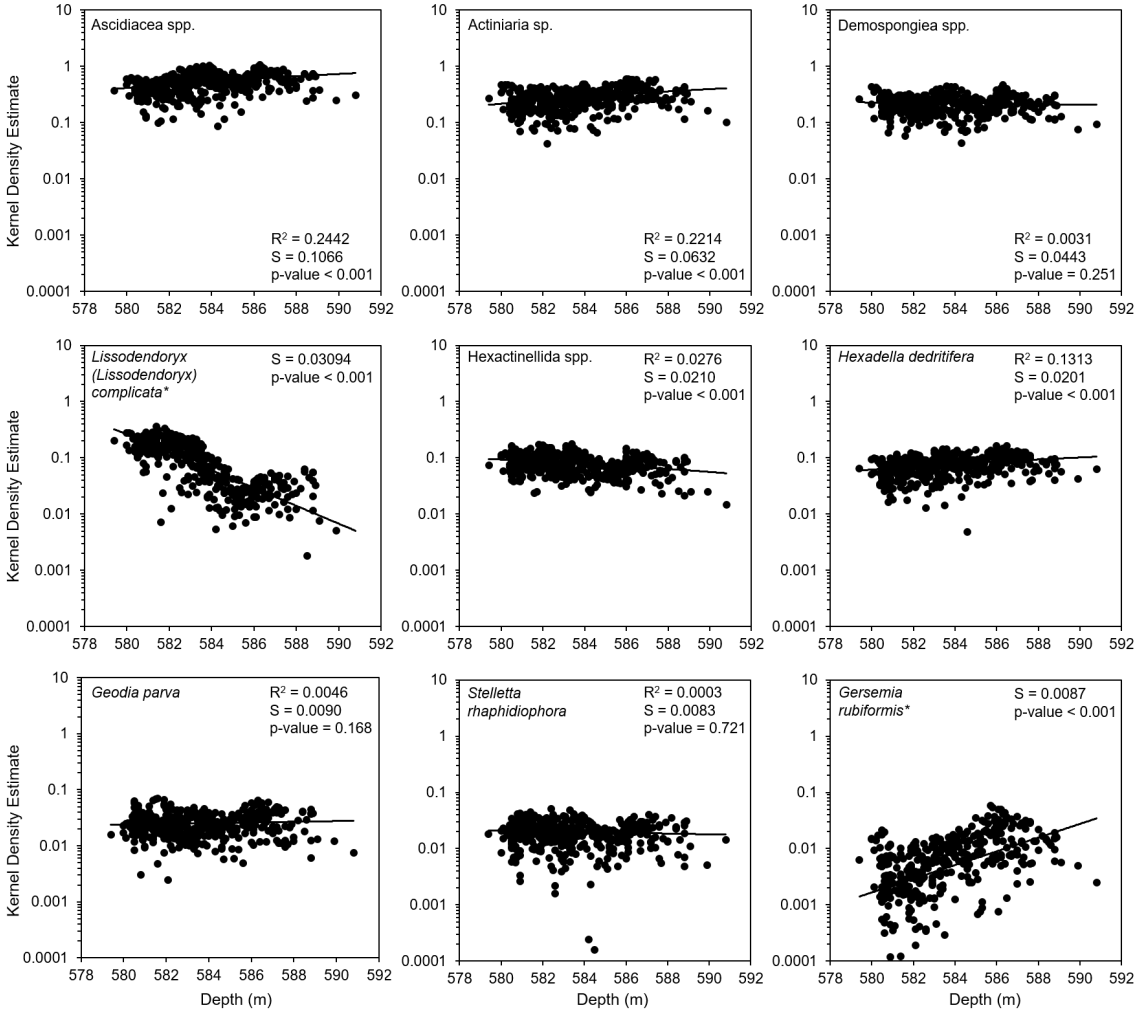

S2. Regression plots of kernel density estimates against depth (m) for the most prominent megafauna on the Schulz Bank. Y-axes have been semi-logged. Asterisks (*) denotes taxa which had a non-linear relationship with depth.

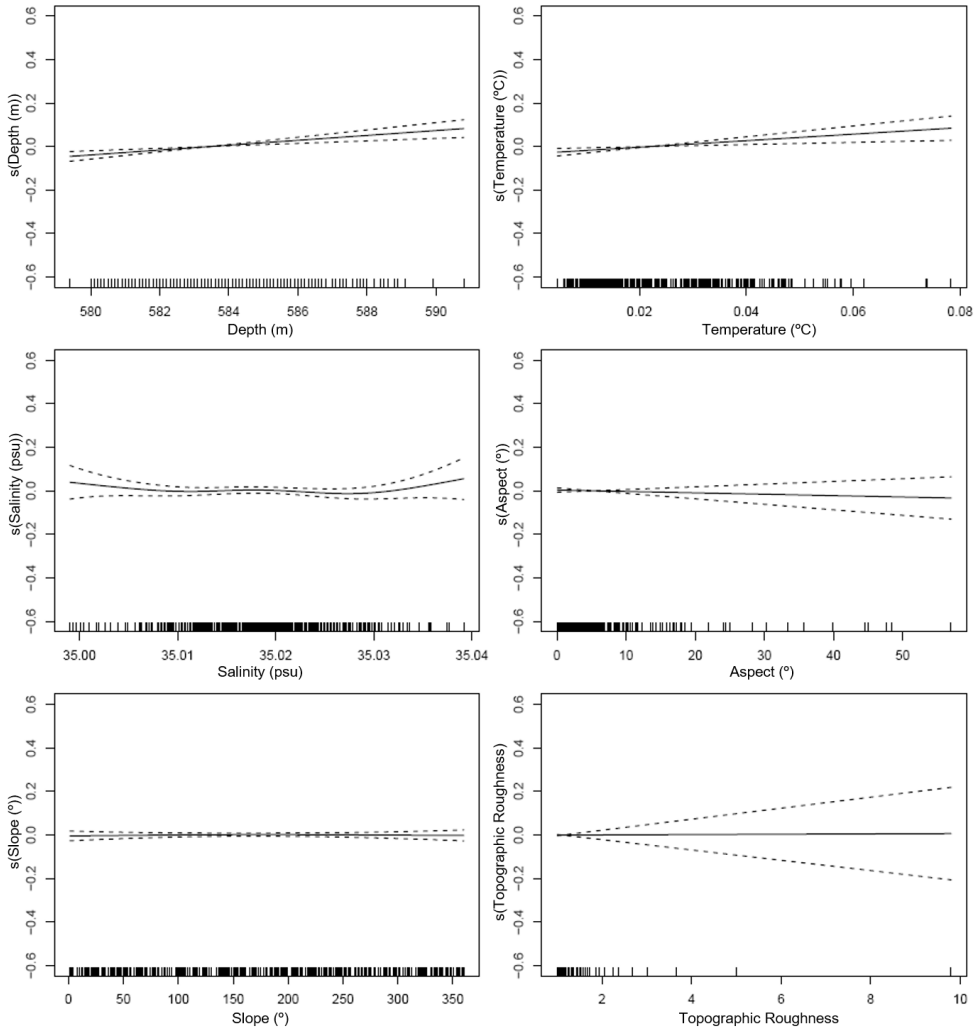

S3. Estimated smoothing curves obtained by the generalized additive model fitted to the species richness at each measured abiotic variable. The solid line indicates the smoothing curve and the dotted lines indicate the 95% point-wise confidence bands.

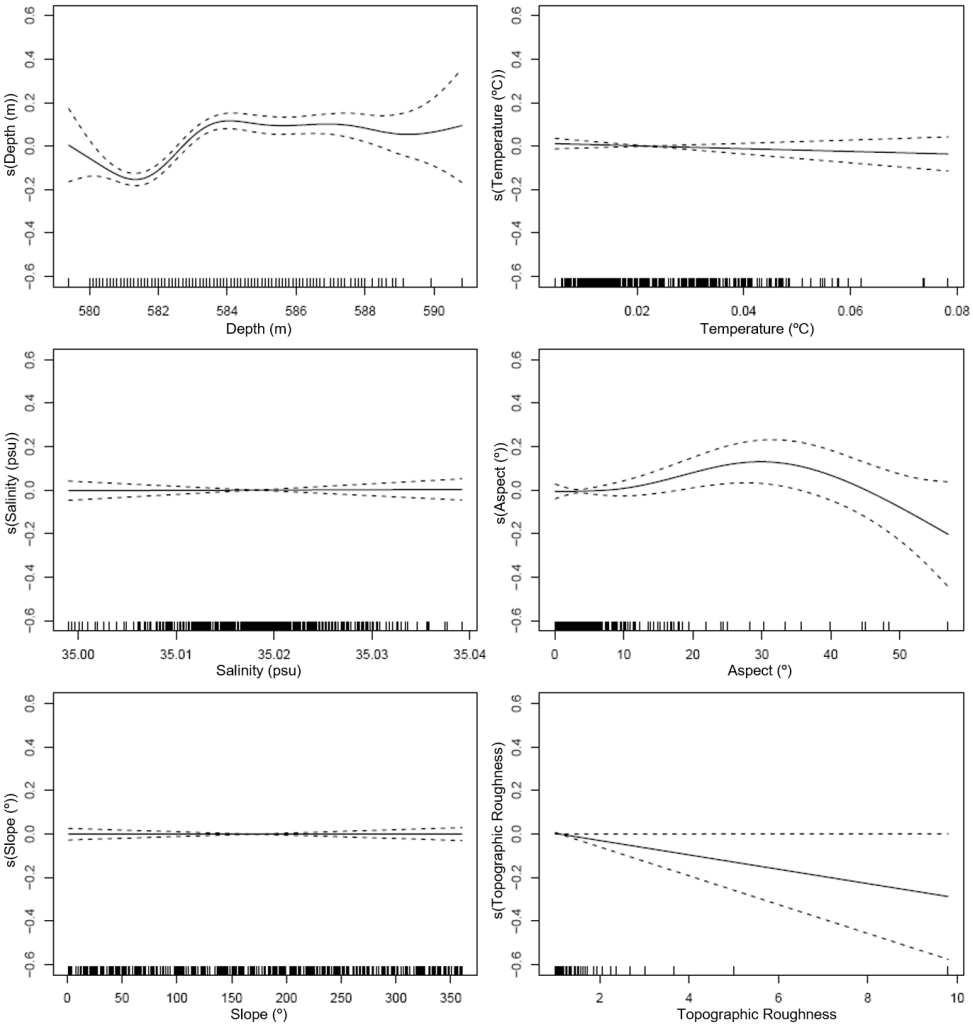

S4. Estimated smoothing curves obtained by the generalized additive model fitted to the total megafauna abundance at each measured abiotic variable. The solid line indicates the smoothing curve and the dotted lines indicate the 95% point-wise confidence bands.

S5. Summary statistics of the generalized additive models fitted to the most prominent megafauna abundance (negative binomial distribution, log link). Deviance explained (%) is the percent of null deviance in the data explained by the model. All abiotic variables contained a smoothing function.

Response	Explanatory	Deviance Explained (%)	R^2	P-value
Ascidiacea spp.	Depth (m)	37.60	0.3550	<0.001
	Temperature (ºC)	6.25	0.0619	<0.001
	Salinity (psu)	0.03	-0.0021	0.738
	Slope (º)	2.44	0.0135	0.251
	Aspect (º)	0.32	0.0009	0.228
	Topographic Roughness	0.23	-0.0005	0.283
Actiniaria sp.	Depth (m)	26.40	0.2680	<0.001
	Temperature (ºC)	8.68	0.0701	<0.001
	Salinity (psu)	1.18	0.0100	0.022
	Slope (º)	3.65	0.0342	0.002
	Aspect (º)	0.00	-0.0023	0.893
	Topographic Roughness	1.84	0.0084	0.002
Demospongiae spp.	Depth (m)	6.96	0.0595	<0.001
	Temperature (ºC)	0.35	0.0016	0.212
	Salinity (psu)	0.01	-0.0023	0.854
	Slope (º)	4.51	0.0290	0.006
	Aspect (º)	0.67	0.0049	0.082
	Topographic Roughness	0.08	-0.0015	0.534
Lissodendoryx (Lissodendoryx) complicata	Depth (m)	65.50	0.6300	<0.001
	Temperature (ºC)	5.44	0.0623	<0.001
	Salinity (psu)	0.65	0.0071	0.041
	Slope (º)	3.25	0.0339	0.015
	Aspect (º)	0.01	-0.0022	0.819
	Topographic Roughness	1.14	0.0077	0.397
Hexactinellida spp.	Depth (m)	2.81	0.0237	0.002
	Temperature (ºC)	1.44	0.0107	0.102
	Salinity (psu)	1.54	0.0114	0.141
	Slope (º)	0.97	0.0058	0.201
	Aspect (º)	0.31	0.0008	0.251
	Topographic Roughness	0.50	0.0025	0.135
Hexadella dedritifera	Depth (m)	15.40	0.1580	<0.001
	Temperature (ºC)	3.10	0.2740	0.014
	Salinity (psu)	0.41	0.0023	0.166
	Slope (º)	0.03	-0.0020	0.688
	Aspect (º)	0.03	-0.0020	0.717
	Topographic Roughness	2.32	0.0175	0.065
Geodia parva	Depth (m)	0.46	0.0028	0.142
	Temperature (ºC)	7.01	0.0708	<0.001
	Salinity (psu)	0.18	-0.0004	0.364
	Slope (º)	0.67	0.0036	0.334
	Aspect (º)	0.13	-0.0009	0.438
	Topographic Roughness	0.29	0.0011	0.233
Stelletta rhaphidiophora	Depth (m)	0.00	-0.0023	0.934
	Temperature (ºC)	0.05	-0.0018	0.614
	Salinity (psu)	0.94	0.0063	0.254
	Slope (º)	1.30	0.0075	0.630
	Aspect (º)	0.38	0.0019	0.167
	Topographic Roughness	1.39	0.0035	0.416
Gersemia rubiformis	Depth (m)	23.30	0.2280	<0.001
	Temperature (ºC)	5.84	0.0617	0.007
	Salinity (psu)	0.83	0.0060	0.057
	Slope (º)	0.76	0.0093	0.090
	Aspect (º)	0.32	0.0007	0.236
	Topographic Roughness	0.33	-0.0017	0.239

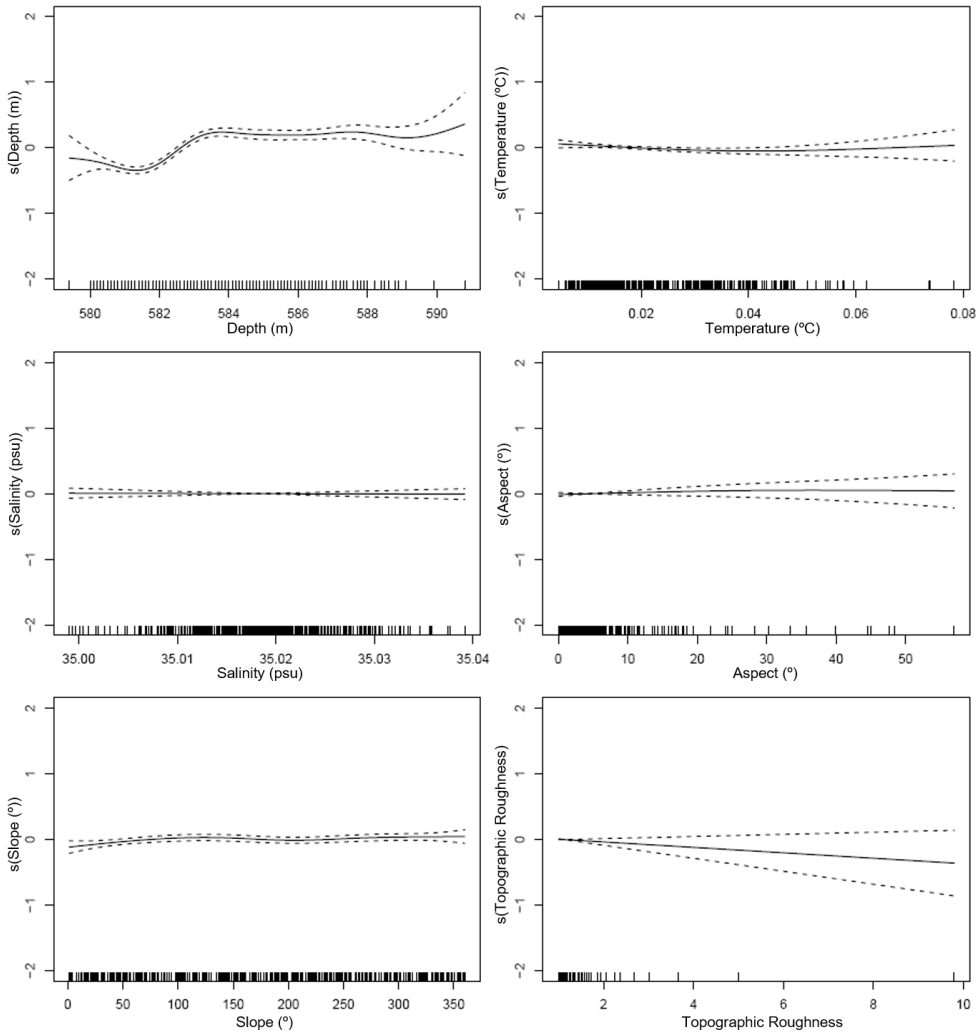

S6. Estimated smoothing curves obtained by the generalized additive model fitted to the Ascidiacea spp. abundance at each measured abiotic variable. The solid line indicates the smoothing curve and the dotted lines indicate the 95% point-wise confidence bands.

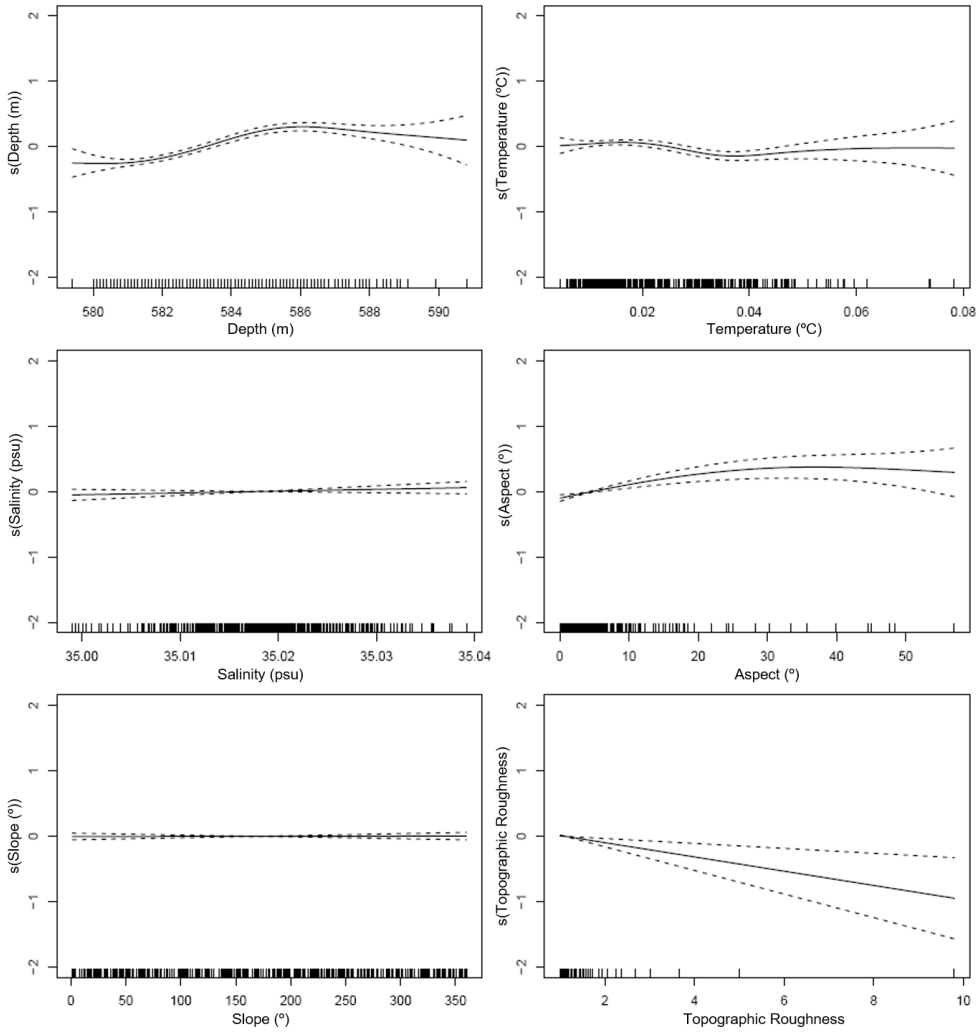

S7. Estimated smoothing curves obtained by the generalized additive model fitted to the Actiniaria sp. abundance at each measured abiotic variable. The solid line indicates the smoothing curve and the dotted lines indicate the 95% point-wise confidence bands.

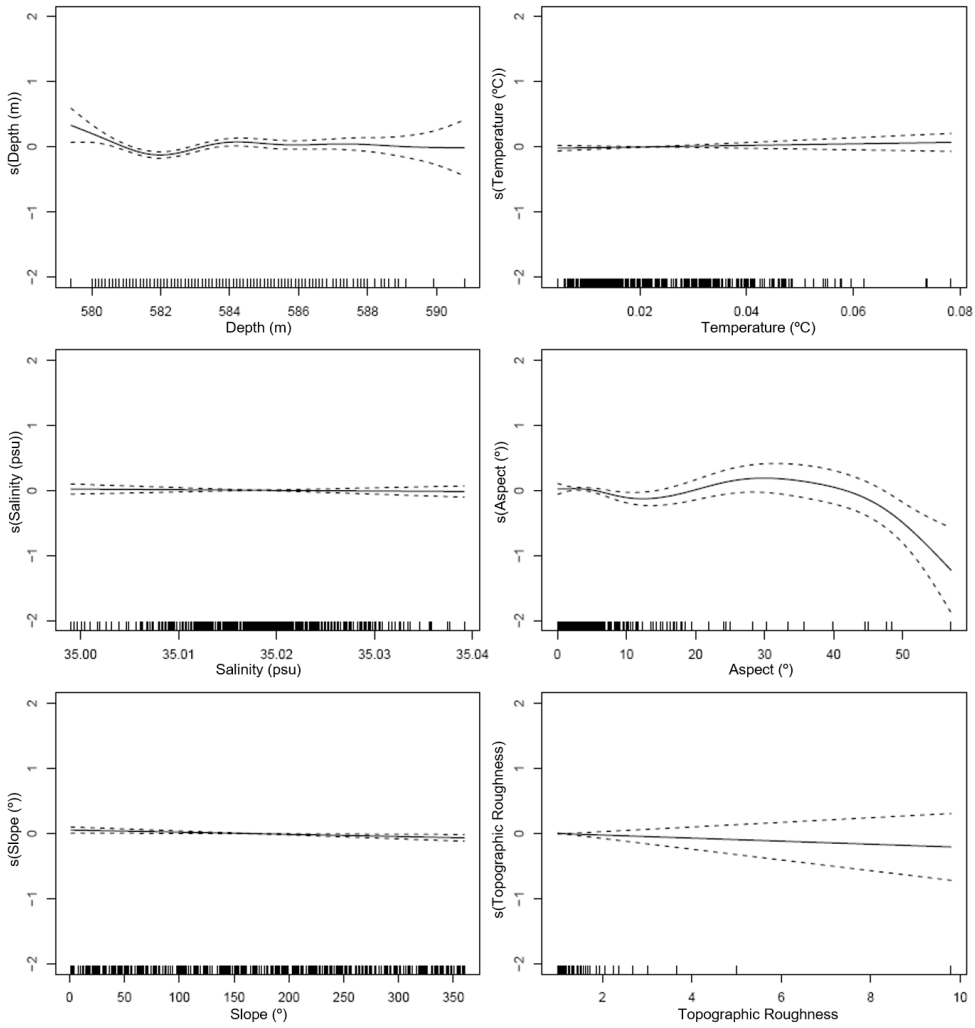

S8. Estimated smoothing curves obtained by the generalized additive model fitted to the Demospongiae spp. abundance at each measured abiotic variable. The solid line indicates the smoothing curve and the dotted lines indicate the 95% point-wise confidence bands.

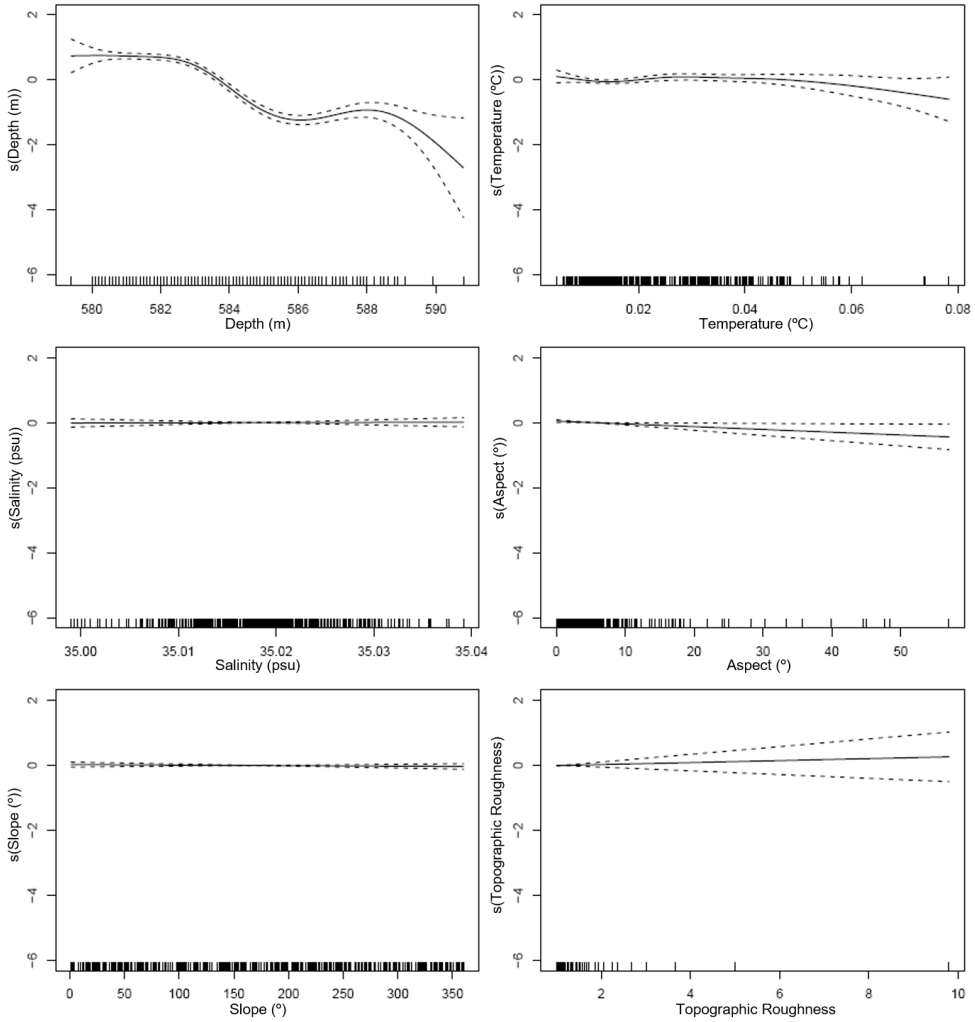

S9. Estimated smoothing curves obtained by the generalized additive model fitted to the *Lissodendoryx (Lissodendoryx) complicata* abundance at each measured abiotic variable. The solid line indicates the smoothing curve and the dotted lines indicate the 95% point-wise confidence bands.

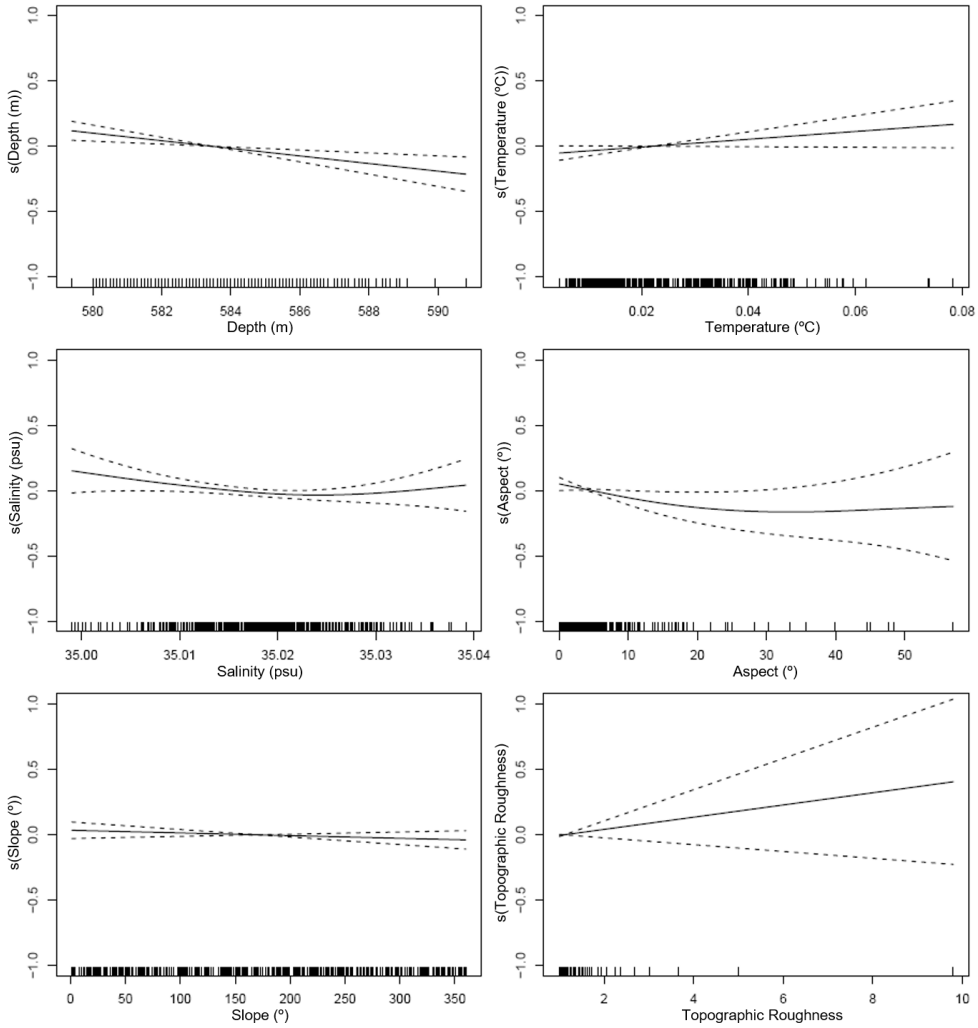

S10. Estimated smoothing curves obtained by the generalized additive model fitted to the Hexactinellida spp. abundance at each measured abiotic variable. The solid line indicates the smoothing curve and the dotted lines indicate the 95% point-wise confidence bands.

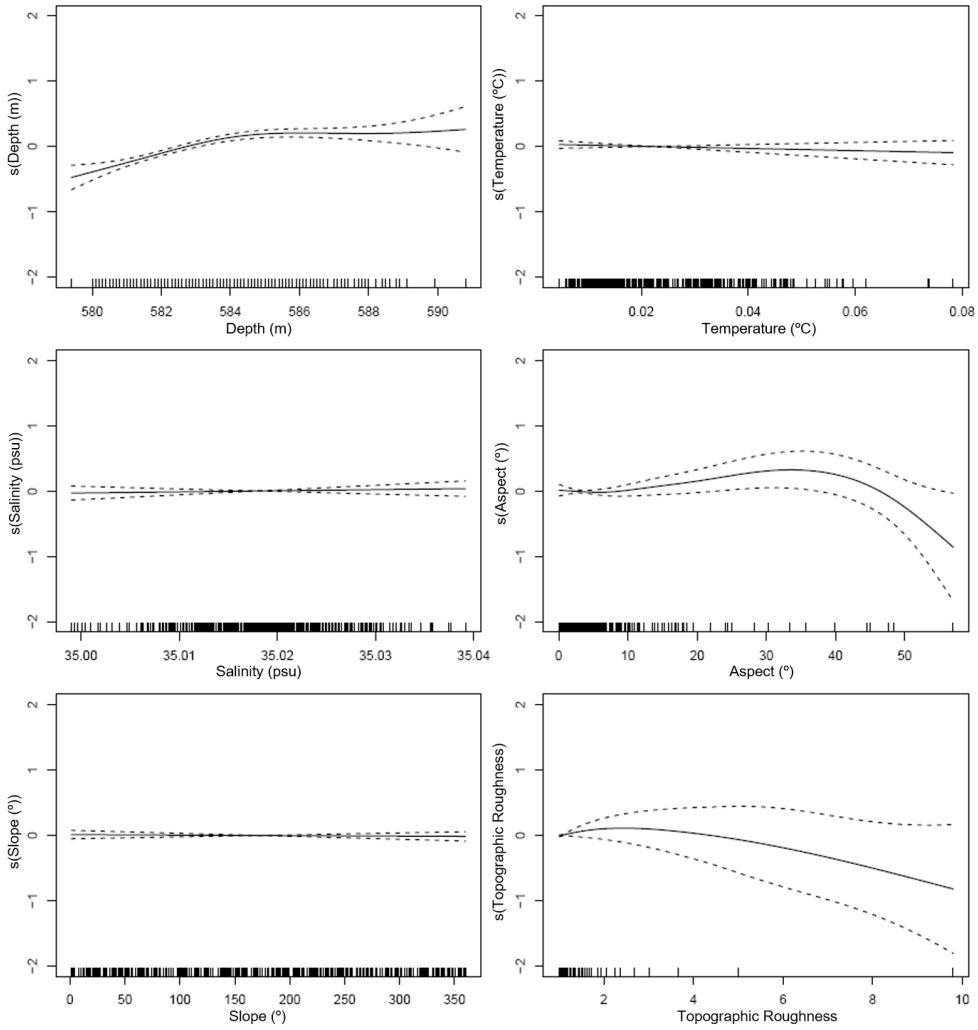

S11. Estimated smoothing curves obtained by the generalized additive model fitted to the *Hexadella dedritifera* abundance at each measured abiotic variable. The solid line indicates the smoothing curve and the dotted lines indicate the 95% point-wise confidence bands.

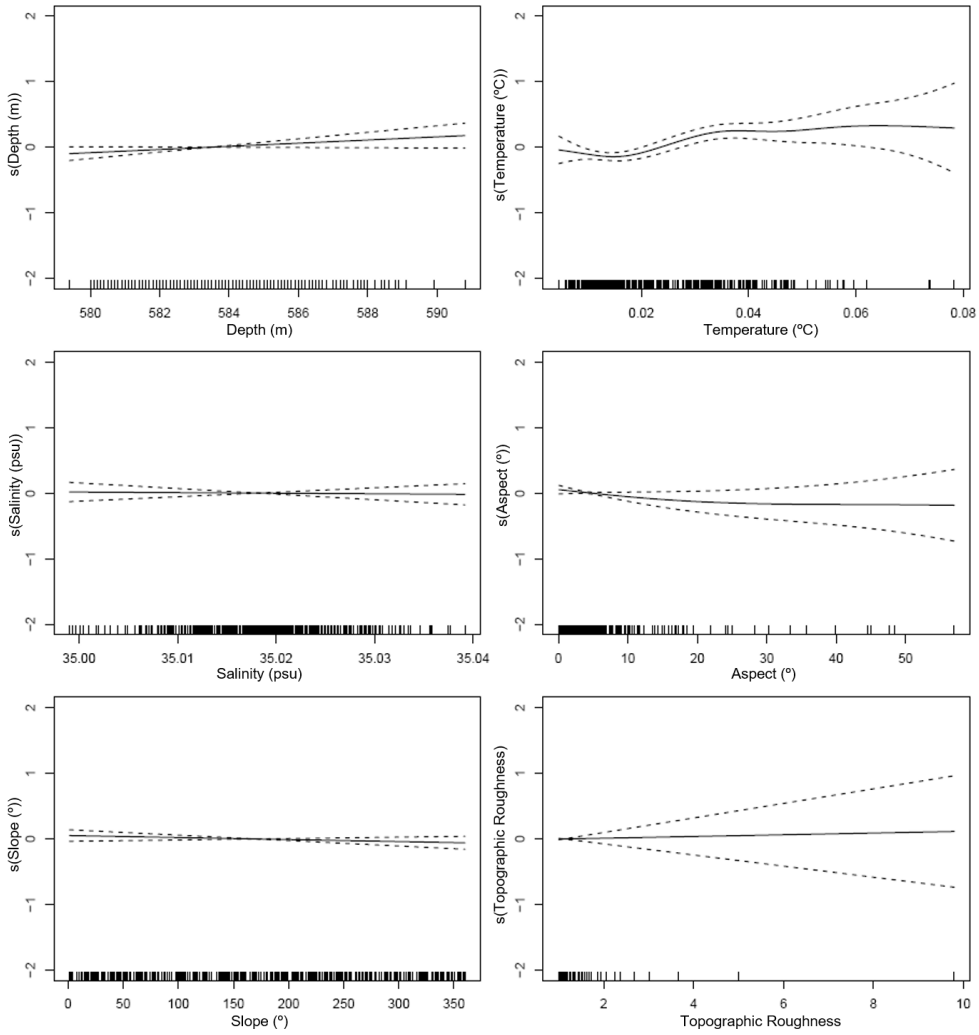

S12. Estimated smoothing curves obtained by the generalized additive model fitted to the *Geodia parva* abundance at each measured abiotic variable. The solid line indicates the smoothing curve and the dotted lines indicate the 95% point-wise confidence bands.

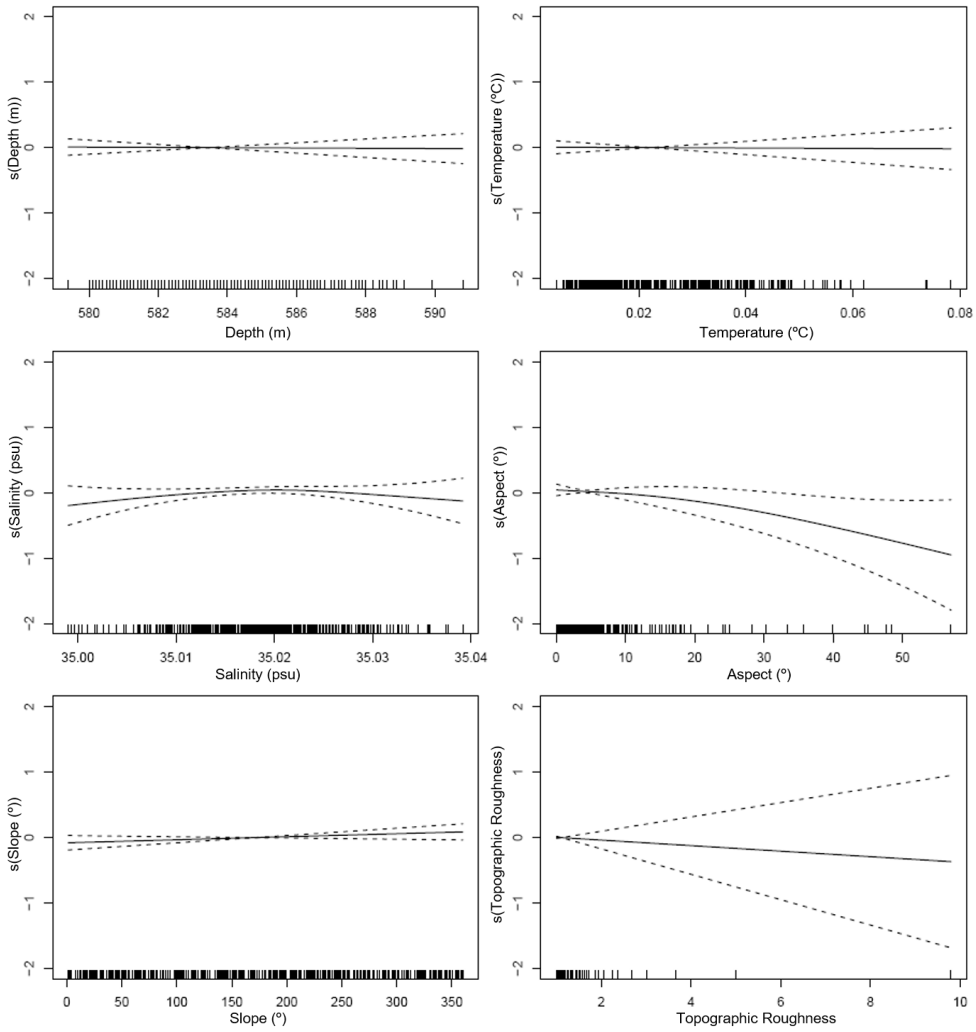

S13. Estimated smoothing curves obtained by the generalized additive model fitted to the *Stelletta rhaphidiophora* abundance at each measured abiotic variable. The solid line indicates the smoothing curve and the dotted lines indicate the 95% point-wise confidence bands.

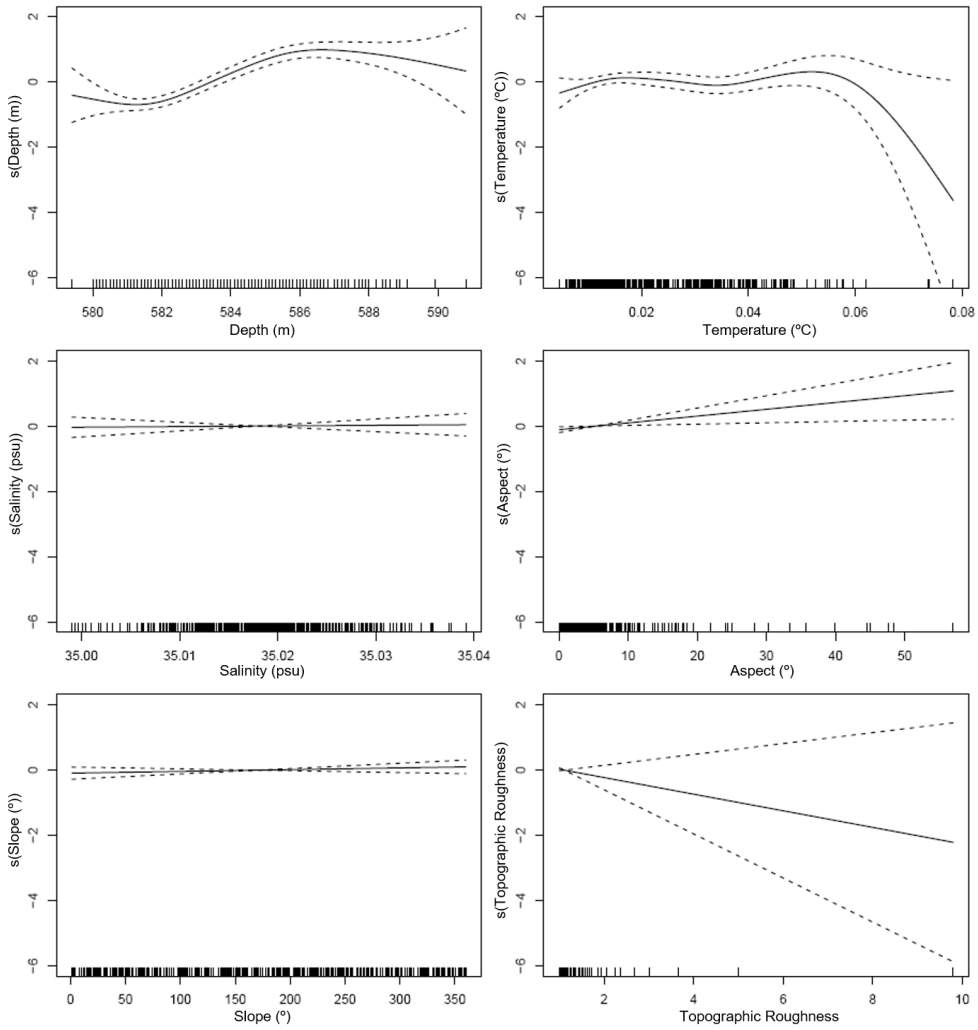

S14. Estimated smoothing curves obtained by the generalized additive model fitted to the *Gersemia rubiformis* abundance at each measured abiotic variable. The solid line indicates the smoothing curve and the dotted lines indicate the 95% point-wise confidence bands.

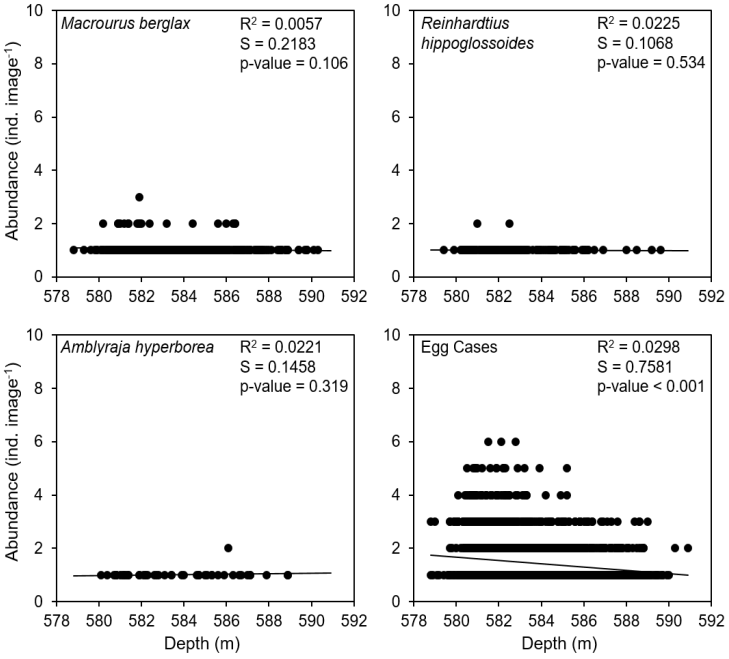

S15. Regression plots of the abundance (ind. image^{-1}) against depth (m) for the demersal fish and *Amblyraja hyperborea* egg cases on the Schulz Bank. Residual standard error (S) and R-squared show the statistical correlation of the relationship between density and depth.

Paper 3

frontiers in Marine Science

ORIGINAL RESEARCH
published: 09 June 2020
doi: 10.3389/fmars.2020.00393

Drivers of Megabenthic Community Structure in One of the World's Deepest Silled-Fjords, Sognefjord (Western Norway)

Heidi K. Meyer[1], Emyr M. Roberts[1], Furu Mienis[2] and Hans T. Rapp[1,3†]*

[1] Department of Biological Sciences and K.G. Jebsen Centre for Deep-Sea Research, University of Bergen, Bergen, Norway, [2] Department of Ocean Systems, Royal Netherlands Institute for Sea Research and Utrecht University, Den Burg, Netherlands, [3] NORCE, Norwegian Research Centre, NORCE Environment, Bergen, Norway

OPEN ACCESS

Edited by:
Thomas Wernberg,
University of Western Australia, Australia

Reviewed by:
Giorgio Bavestrello,
University of Genoa, Italy
Torstein Pedersen,
UiT The Arctic University of Norway, Norway

****Correspondence:***
Heidi K. Meyer
Heidi.Meyer@uib.no

†Deceased

Specialty section:
This article was submitted to Global Change and the Future Ocean, a section of the journal Frontiers in Marine Science

Received: *13 December 2019*
Accepted: *07 May 2020*
Published: *09 June 2020*

Citation:
Meyer HK, Roberts EM, Mienis F and Rapp HT (2020) Drivers of Megabenthic Community Structure in One of the World's Deepest Silled-Fjords, Sognefjord (Western Norway). Front. Mar. Sci. 7:393. doi: 10.3389/fmars.2020.00393

The Sognefjord is the longest (205 km) and deepest (1308 m) fjord in Norway, and the second-longest in the world. Coast-fjord exchange in Sognefjord is limited by a seaward sill at 170 m water depth, which causes a clear stratification between water masses as the dense oxygen-poor basin water mixes slowly with the well-oxygenated water directly above from the coastal ocean. Due to the homogeneity and limited variability in the deep-water, the deep slopes of Sognefjord represent the ideal setting to study how abiotic factors influence the deep-water benthic community structure. During the summer of 2017, two remotely operated vehicle (ROV) video transects were performed to compare the megabenthic community behind the sill (water depth: 1230 to 55 m; transect length: 1.39 km; distance from sill: ∼17 km) and within the central fjord (water depth: 1155–85 m; transect length: 2.43 km; distance from sill: ∼79 km). Accompanying conductivity–temperature–depth (CTD) deployments were made to measure the *in situ* abiotic factors and nutrient concentrations at each transect location, while the substrate characteristics (percent cover of soft and hard exposed substrate) were documented from the video footage. Here, Sognefjord's megabenthic community composition, distribution, and species richness were analyzed in relation to abiotic factors (e.g., depth, salinity, dissolved oxygen, chlorophyll *a* concentration, and percent cover of hard and soft substrata) within the fjord. Basin communities were homogeneous and characterized by sponges, echinoderms, and crustaceans, whereas the shallower regions were dominated by mobile scavengers. Contrary to other fjord-based studies, species richness and diversity were stable in the fjord basin and decreased with proximity to the sill, decreasing water depth, and at the boundary between intermediate and basin water. The findings demonstrate that highly stratified fjords support stable communities in their basins; however, further research is needed to investigate the influence water mass dynamics have on silled-fjord megafauna communities.

Keywords: fjord fauna, glass sponges, megafauna, Sognefjord, Norwegian fjords, remotely operated vehicles, extreme habitats

INTRODUCTION

Deep fjords are valuable study areas because they allow easy access to habitats that share similarities with continental shelf or deep-sea communities found in the open ocean (Bernd, 1993; Sweetman and Witte, 2008; Storesund et al., 2017). Their accessibility allows researchers to study the influence of abiotic factors on the shelf or deep-sea community ecology whilst reducing the limitations of cost and transportation that is often problematic for deep-sea research.

It is well documented that fjord communities are influenced by both the coast-fjord and/or depth gradients (Buhl-Mortensen and Høisaeter, 1993; Holte et al., 2004; Włodarska-Kowalczuk and Pearson, 2004; Storesund et al., 2017; Molina et al., 2019). The interaction between the ocean water and the fjord system helps carry seawater into the fjord, which aids in the distribution of fauna, organic nutrients, and inorganic material (Buhl-Mortensen and Høisaeter, 1993; Holte et al., 2004). However, within silled-fjords, the exchange of seawater between the coastal and fjord systems is reduced. The sill height, fjord topography, and freshwater input influences the transport of nutrients, pelagic larvae, organic matter, and dissolved oxygen, where benthic communities toward the inner fjord regions are negatively impacted due to the decreased access to resources (e.g., dissolved oxygen, organic carbon, nutrients) (Buhl-Mortensen and Høisaeter, 1993; Blanchard et al., 2010; Storesund et al., 2017). Density stratification between upper and bottom water masses is often observed and the inner basin(s) below the sill depth becomes isolated from the adjacent coastal system. This stratification leads to relatively stable temperatures and salinities within the basins (Renaud et al., 2007; Drewnik et al., 2016; Molina et al., 2019). With limited mixing within the water column, dissolved oxygen levels tend to decrease with depth, distance from the sill, and over time until a renewal event occurs, whereby more oxygenated ocean water mixes with fjord water. In general, faunal diversity and species richness is seen to decrease with increasing distance from the coastal regions and increasing water depth (Buhl-Mortensen and Høisaeter, 1993; Holte et al., 2004; Molina et al., 2019).

Deep-water stagnation is thought have a major influence on fjord basin communities, where lower oxygen concentrations can negatively impact the community structure and species composition (Blanchard et al., 2010; Molina et al., 2019), resulting in lower species richness with lower oxygen levels (Buhl-Mortensen and Høisaeter, 1993). In periods of hypoxic and anoxic conditions, where the oxygen concentration is <2.1 mL L^{-1}, defaunation of macrofauna and changes in faunal assemblages have been observed within the basin (Holte et al., 2005; Molina et al., 2019). In extreme cases of deoxygenation and strong stratification, a rise of acidification within fjord basins can occur (Jantzen et al., 2013), particularly if water exchange with adjacent coastal systems is insufficient.

Sognefjord is Norway's longest and deepest fjord. It is host to numerous towns and villages and has become a sought-out destination for many cruise ships, where thousands of tourists visit the fjord each year. There is concern on how these anthropogenic influences impact the fjord's marine habitat (Manzetti and Stenersen, 2010). Numerous studies in recent years have been conducted primarily on the microbial community (Poremba and Jeskulke, 1995; Storesund et al., 2017) or the influence of phytodetrital pulses on the macrofaunal community (Witte et al., 2003). Despite the accessibility of Sognefjord, the epibenthic megafauna community has been poorly studied, especially in recent years (Bernd, 1993). Bernd (1993) found that the central fjord and shallower adjacent side-fjord, Høyangsfjord, were primarily dominated by soft-bottom dwelling burrowing decapods (*Munida sarsi* and *Munida tenuimana*), holothurians (*Bathyplotes natans* and *Parastichopus tremulus*), and anthozoans. Høyangsfjord was found to have a lower megafaunal density compared to the main fjord. However, besides depth and general observations of substrate type, no thorough analysis was conducted on the influence of abiotic variables on the megafaunal community, especially over a horizontal or vertical gradient. In recent years several expeditions by the University of Bergen and the Institute for Marine Research in Norway, have taken place in the main- as well as the side-fjords, and knowledge about the fauna and benthic communities in Sognefjord is expected to increase rapidly when new data are made available over the coming years (Buhl-Mortensen et al., 2017; H. Glenner, personal communication).

In the present study, we used visual data collected with the remotely operated vehicle (ROV) *AEgir 6000* to investigate the benthic megafaunal community diversity and distribution in Sognefjord and the influence of abiotic variables on the community structure at two locations in the fjord. It is expected that the communities would be less diverse and dense with increasing distance from the sill due to the extremely stable conditions identified by Storesund et al. (2017) (see the section "Study Area" for site description). For this study, we had three main objectives: (1) characterize the benthic community structure based on their depth and distance from the sill, (2) detect any response in community structure and diversity to changes in water mass characteristics above and below the sill, and (3) examine the relationships between environmental conditions and community composition and diversity (using generalized linear models, or GLMs).

MATERIALS AND METHODS

Study Area

Sognefjord is located on the western Norwegian coast, extends to about 205 km and has a maximum water depth of 1308 m (Poremba and Jeskulke, 1995; Storesund et al., 2017). The fjord has a 3-layer water column structure (Svendsen, 2006; Storesund et al., 2017): the top layer is brackish water (salinity $\leq$ 33 psu), formed by the mixture of freshwater runoff and seawater, and moves out of the fjord; the intermediate layer (salinity between 33 and 35 psu) is well-oxygenated, owing to exchanges with the Norwegian Coastal Current above the sill depth, and hosts compensatory flows that may be in-fjord or out-fjord; and the bottom, or basin, water below the sill depth (salinity $>$ 35 psu after deep-water renewal) originates from Atlantic water and becomes gradually less dense between renewal events because

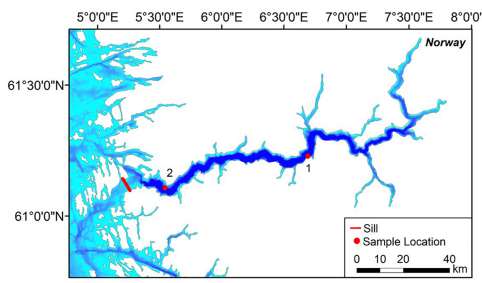

FIGURE 1 | Location of the two *AEgir 6000* transects in Sognefjord, Norway. Digital bathymetry with a resolution of 1/16 × 1/16 arc min was extracted from EMODnet Bathymetry Consortium (2018). ArcGIS (version 10.4; Environmental Systems Research Institute [ESRI], 2016) was used to map the transects.

of diffusion and mixing with the layer above, driven by tidal forcing. Whilst the shallow sill (170 m) at the mouth of the fjord allows for some exchange of water between the fjord system and the adjacent coastal water, the mixing is fairly reduced and strong stratification occurs because of the influx of terrestrial runoff (Storesund et al., 2017). Renewal of the basin water occurs approximately every 8 years (Buhl-Mortensen et al., 2020).

Conditions within the fjord basin below sill depth are fairly stable and homogeneous. Water temperature is consistently around 7.4°C and the salinity is generally greater than 35.0 psu (Witte et al., 2003; Storesund et al., 2017). Oxygen concentrations have been found to decrease with increasing distance from the sill and with depth, where Storesund et al. (2017) found the inner fjord and lower basin water to have oxygen concentrations below 4.5 mL L^{-1} in May and November 2012.

Data Collection

Two video transects were performed with the work-class ROV *Ægir 6000* in Sognefjord in July 2017 during a SponGES cruise with the R.V. *G.O. Sars* (**Figure 1**). Dive 1 (D1) was conducted within the central fjord (1155 – 85 m; 61° 6′ N, 6° 39′ E) and Dive 2 (D2) was located near the sill (1230 – 55 m; 61° 3′ N, 5° 22′ E), respectively. D1 and D2 had approximate transect lengths of 2.43 km and 1.39 km, and were located approximately 79 km and 17 km away from the sill, respectively. The approximate fjord side slopes for D1 and D2 are 43° and 44° inclined to the horizontal plane. Physical samples were collected by the ROV during the transects to help confirm identifications of fauna.

One ship-based conductivity–temperature–depth (CTD) sensor package cast was conducted for each transect to profile temperature (°C), salinity (psu), dissolved oxygen (mL L^{-1}) and chlorophyll *a* concentration (μg L^{-1}) throughout the water column. The bottom depths of the CTD casts corresponding to D1 and D2 were 1017 m and 1223 m, respectively. In addition, water samples were collected (using a rosette water sampler, on which the CTD package was mounted) from the different water masses for nutrient analysis. From the video footage, the percent cover of exposed hard substrate and soft sediment was estimated for each image analyzed.

Nutrient Content Analysis

Seawater samples for the analysis of inorganic dissolved nutrients (Si, PO_4, NH_4, NO_3, and NO_2) were collected with the CTD-rosette from selected depths. Sample depths were selected based on the profile of the CTD downcast, whereby samples were collected from five different depths. Subsamples were collected in 50 mL syringes, which were rinsed three times with water from the niskin bottles of the CTD rosette before being filled. After sampling on deck, samples were filtered through 0.2 μm filters and instantly sub-sampled into two vials, one of which was used for samples of ortho-phosphate (PO_4), ammonium (NH_4), nitrate (NO_3), and nitrite (NO_2), stored at −20°C and the other for silicate (Si), stored at 4°C. Nutrients were analyzed at NIOZ with a QuAAtro Gas Segmented Continuous Flow Analyzer. Measurements were made simultaneously on four channels for PO_4 (Murphy and Riley, 1962), NH_4 (Helder and De Vries, 1979), NO_2, and NO_3 (Grasshoff et al., 1983). Si was measured during a separate run (Strickland and Parsons, 1968). All measurements were calibrated with standards diluted in low nutrient seawater. For a detailed description of the sampling procedure we refer to Roberts et al. (2018).

Video Annotation

Still images were extracted from the videos approximately every 30 s to ensure there was no spatial overlap between images during analysis. Due to fluctuations in ROV altitude and changes in turbidity or topography, some areas of the transects were not suitable for analysis. Images were excluded if they contained any of the following characteristics: (1) image area obscured by part of the ROV or suspended material, (2) ROV was collecting physical specimens, (3) ROV was too far from the substrate (>10 m), (4) camera angle was not seabed-facing, (5) image contained poor light visibility, (6) image was blurred, and (7) overlapping image area. Videos were rescanned during image annotation to help identify individuals that were difficult to decipher in the stills alone, and in some cases, new stills were extracted if a more suitable image was present ±5 s from the original still. This was mostly the case for images that were blurred or contained poor light visibility and more suitable images of the same area were available within 5 s of the original image extracted. Parallel lasers of known separation (which project spots onto the seabed in order to determine image scale) were only active for the first hour of D1. It was therefore not possible to determine area (m^2) and density (individuals m^{-2}) for the survey and megafauna were enumerated based on individuals per image.

ImageJ (version 1.52) was used to annotate the extracted imagery. A virtual grid with 496 cells was overlaid on each image in ImageJ. The grid size was selected because the cells completely overlapped the images. Percent cover of substrate type was estimated by counting the number of grid cells that contained that particular substrate type, then calculating the percentage of the total number of grid cells represented by that value. The grid resolution was selected such that the cells were small enough to minimize the number containing multiple substrate types as

a proportion of total number of cells (and thereby increase the precision in the percent cover estimates) and large enough that the gridlines were not so dense as to obscure the fauna present in the image. In cases where cells contained multiple substrate types, the cell was characterized as the substrate that covered more than half of the cell. All epibenthic megafauna individuals that were easily visible within the imagery were counted and identified to the lowest taxonomic level. Due to fluctuations in altitude during video transects, some fauna had to be identified based on gross morphology (e.g., white sponge 1, yellow sponge 2, etc.). Taxa were classified as rare if represented by three or less individuals.

Statistical Analysis

Data Preparation

Based on the description of the Sognefjord water mass structure by Storesund et al. (2017), the biotic and abiotic data were assigned to three depth zones to identify any depth-related changes in the benthic community structure: "Above Sill" ($\leq$170 m), "Intermediate" (>170 to $\leq$300 m), and "Basin" (>300 m). No data from the surface brackish top-layer (1–10 m) was included. Due to differences in sampling frequency between the CTD profiling and image annotation, the abiotic variables were interpolated at 10 m depth intervals in Rstudio (version 1.2.5; RStudio Team, 2019). Nutrient composition was sampled with low frequency and was thereby excluded from statistical analysis. The megafauna abundances were summed into 10 m depth intervals. To account for missing data in the biotic dataset, certain depth intervals were removed from the abiotic dataset prior to statistical analysis. All multivariate statistical analysis was conducted in Primer (version 7) unless otherwise specified.

Environmental Variables

The environmental variables of D1 (central) and D2 (near-sill) were plotted against each other (e.g., temperatures from D1 vs. temperatures, at corresponding depths, from D2) to identify any notable differences in abiotic conditions between dives (**Supplementary Figure S1**). Furthermore, a correlation matrix was generated in Rstudio with package "corrplot" (version 0.84; Wei and Simko, 2017) to identify which abiotic variables were correlated (**Supplementary Figure S2**). Temperature had a strong negative correlation with salinity and positive correlation with dissolved oxygen (rho > 0.9), and was thereby dropped from further analysis. While depth was significantly correlated with the majority of the abiotic variables (p-value < 0.05) and had a moderately strong positive correlation with salinity and negative correlation with dissolved oxygen (rho > 0.7), it was selected to remain since it often acts as a proxy for other abiotic variables that were not measured in the present study. The remaining variables were normalized in Primer prior to multivariate analysis due to the different units used for each variable. A principal component analysis (PCA) of the selected abiotic variables was used to examine the environmental conditions within each depth zone per dive.

Community Composition and Diversity

Due to the lack of lasers throughout most of the dives, the abundances were converted to presence-absence data. A Sørensen similarity matrix between the two dives was calculated on the presence-absence dataset. Non-metric multidimensional scaling (nMDS) plots were constructed for each dive to identify differences between the community structure within each depth zone. An analysis of similarities (ANOSIM) was generated to identify significant differences between the depth zones and dives. SIMPER was used to determine which taxa were considered indicator organisms for each depth zone.

Diversity indices such as species richness and Shannon-Wiener diversity were calculated from the megafauna presence-absence data for the depth zones in both dives to compare the changes in species richness and diversity over the vertical and horizontal gradients. In SPSS (version 25), a Levene's test of homogeneity of variances was used to determine if the diversity indices were homogeneous prior to running a one-way analysis of variance (ANOVA) to determine if there were significant differences for each index. A Tukey honestly significant difference (HSD) *post hoc* test on the diversity indices was used to identify which depth zones were significantly different for each dive.

To examine which environmental variables best explained the variance in species richness and Shannon-Wiener diversity indices, GLMs were generated in Rstudio. The residual deviance was larger than the residual degrees of freedom, therefore a quasi-Poisson error was fitted to the GLMs to account for overdispersion (Zuur et al., 2009). Depth, salinity, dissolved oxygen, chlorophyll *a*, percent cover of exposed hard substrate and soft sediment were included in the GLMs.

RESULTS

Environmental Conditions

In general, the water was slightly warmer, more saline, and more oxygenated in the water column below the sill at D2 (near-sill), relative to the same depths in D1 (central). The top layer of water was made up of warm brackish water (**Figure 2**), and a sub-surface chlorophyll maximum occurred at the halocline between the brackish surface water and intermediate water (approximately at 20 to 30 m). At approximately 80 to 100 m, dissolved oxygen decreased. Dissolved oxygen levels recovered in the intermediate water just below the sill depth. There was a gradual transition between the intermediate water mass and basin water until about 300 m, where a drop in temperature and dissolved oxygen levels occurred. The basin water was fairly homogeneous and there was not much difference in the water properties between the dives, where temperature was around 7.5°C, salinity at 35.06 psu, and dissolved oxygen around 4.2 mL L^{-1}. D1 was frequently covered in soft sediment with exposed hard substrate patches throughout the transect, whereas D2 had distinct regions of solely soft sediment (e.g., bottom of fjord basin) and exposed hard substrate (e.g., along slopes and cliffs). Within the Intermediate Zone, small boulders and rocks became more frequent, and the sediment type became more coarse.

Inorganic nutrient concentrations increased with depth (**Table 1**), showing highest concentrations below 450 m water depth, while lowest concentrations were measured in surface

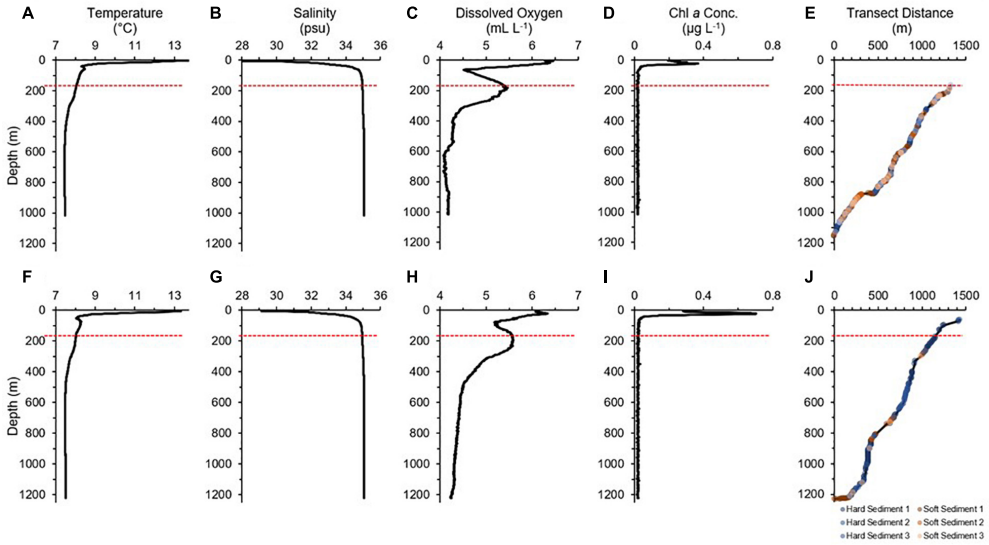

FIGURE 2 | CTD profiles and substrate type for Dive 1 **(A–E)** and Dive 2 **(F–J)** in Sognefjord, Norway. Red dashed line indicates the approximate sill depth (170 m). In **(E,J)**, sediment type 1 to 3 correspond with percent cover, where 1 = 100–91%; 2 = 90–71%; 3 = 70–51%.

TABLE 1 | Concentration of nutrients over depth for Dive 1 (central) and Dive 2 (near-sill) in Sognefjord, Norway.

Dive	*Depth (m)*	*Si* (µmol L(1L-1))	PO_4 ($\mu mol\ L^{-1}$)	NH_4 ($\mu mol\ L^{-1}$)	NO_3 ($\mu mol\ L^{-1}$)	NO_2 ($\mu mol\ L^{-1}$)
1	1028	16.67	1.158	0.202	14.87	0.034
	799	16.85	1.161	0.139	15.05	0.017
	500	14.63	1.114	0.135	14.95	0.019
	150	6.223	0.778	0.153	11.11	0.108
	6	0.153	0.046	0.139	0.135	0.066
2	1237	16.78	1.144	0.221	14.41	0.077
	800	14.52	1.091	0.173	14.39	0.028
	500	13.49	1.07	0.172	14.04	0.034
	150	5.46	0.726	0.112	10.48	0.021
	10	0.097	0.033	0.119	0.073	0.036

waters at both sites. Nutrient concentrations did not show large differences between the two sites.

In D1, from the suspended particulates observed in the video footage, predominately vertical settling appeared to occur. In these regions, sessile fauna and vertical rock walls were covered with a fine layer of particulate matter. However, D2 had higher observed turbidity throughout the dive compared to D1, with the settling of particulate matter apparent and some evidence of horizontal flow based on the position of the feeding apparatus of filter feeders and particulate direction changes.

In the PCA ordination, the first two principal components (PC) represented approximately 76% of the environmental variability within the two dives combined (47.1% and 28.6% for PC1 and PC2, respectively) (**Figure 3**). The PCA ordination showed that the images within the Basin Zones of both D1 and D2 were clearly distinguishable from the Intermediate and Above Sill Zones along the axes of PC1 and PC2. Dissolved oxygen (Eigenvector = 0.503), salinity (Eigenvector = −0.498), and depth (Eigenvector = −0.490) had the strongest influence on PC1. Percent cover of soft sediment (Eigenvector = −0.623) and exposed hard substrate (Eigenvector = 0.613) most strongly influenced PC2.

Sognefjord Megafauna Composition

In total, D1 had 79 taxa with a total of 11557 individuals and D2 had 89 taxa with a total of 10615 individuals (**Table 2**). After rare taxa were excluded from the dataset, there was a total of 22105 individuals and 72 taxa identified within 511 images, where D1 had 11528 individuals and 57 taxa and D2 had 10577 individuals and 63 taxa. Porifera made up the majority of the taxa (24),

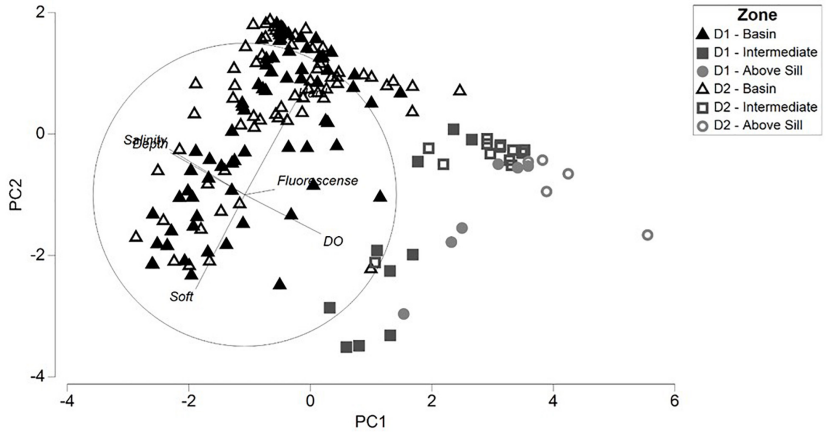

FIGURE 3 | Principal component plot of the abiotic variables for the depth zones within Dive 1 (closed) and Dive 2 (open), with the direction of the respective abiotic variables and their component score influence.

followed by Echinodermata (16), and Cnidaria (10). The Above Sill Zone for both D1 and D2 had the lowest total abundances and number of species compared to the other zones.

The top 10 most abundant taxa for D1 were White Encrusting Sponge 1, *Psolus squamatus* (O.F. Müller, 1776), *Hymedesmia* sp., Brachiopoda 1, *Munida tenuimana* Sars, 1872, *Gracilechinus acutus* (Lamarck, 1816), *Polymastia nivea* (Hansen, 1885), *Gracilechinus elegans* (Düben & Koren, 1844), Yellow Encrusting Sponge 1, and *Stylocordyla borealis* (Lovén, 1868). For D2, the top 10 most abundant taxa were the White Encrusting Sponge 1, Echinoidea 1, *P. squamatus*, *Hymedesmia* sp., *G. acutus*, *M. tenuimana*, Yellow Encrusting Sponge 1, *G. elegans*, *Acesta excavata* (Fabricius, 1779), and *Phakellia* spp.

Community Trends and Observations

Within the Basin Zone, exposed hard substrate was often covered with polychaete tubes, the bivalve *A. excavata*, cnidarians, and encrusting sponges (**Figure 4**). *Acesta excavata* was present in high densities when observed on vertical rocky walls, often with juveniles and dense accumulations of encrusting polychaetes nearby. The octocoral *Anthomastus grandiflorus* (Verril, 1878) (**Figure 4b**) and large glass sponges *Asconema* aff. *foliatum* (Fristedt, 1887) (**Figure 4e**) occurred only on vertical rock walls. In D1, *A.* aff. *foliatum* was covered by a fine layer of suspended particulate matter (**Figure 4e**).

Soft bottom areas were characterized by the enigmatic asteroid *Hymenodiscus coronata* (Sars, 1871), *M. tenuimana*, *Bathyplotes natans* (Sars, 1868), *Mesothuria intestinalis* (Ascanius, 1805), *Psilaster andromeda* (Müller & Troschel, 1842), small patches of *Kophobelemnon stelliferum* (Müller, 1776) and carnivorous sponges, and in rare cases, *Virgularia mirabilis* (Müller, 1776). Signs of lebensspuren such as burrows containing *M. tenuimana* within or nearby were observed throughout both dives (**Figures 4n,p**).

In regions with mixed substrate types (e.g., exposed hard substrate and soft sediment), *Psolus squamatus* was often observed concentrated at breaks in the slope or protruding surfaces. *Phakellia* spp., *Phakellia ventilabrum* (Linnaeus, 1767), and *Axinella infundibuliformis* (Linnaeus, 1759) were commonly positioned along slopes, aligned with the direction of observed horizontal particle flow (**Figure 4m**). Large anemones like *Bolocera tuediae* (Johnston, 1832) were observed residing on exposed hard substrate walls with soft sediment surrounding the substrate.

In the Intermediate and Above Sill Zone of D2, it should also be noted that there was a sudden occurrence of Echinoidea 1 in large quantities (max. 859 individuals per image) from 240 m to 60 m water depth (**Figure 4u**). For D2, the Above Sill Zone had a higher proportion of echinoderms present (**Figures 4v,y**). Numerous fish species, including *Chimaera monstrosa* (Linnaeus, 1758), *Sebastes viviparus* (Krøyer, 1845) (**Figure 4v**), and *Coryphaenoides rupestris* (Gunnerus, 1765), were observed within the upper regions of D1 and D2. Anthropogenic waste was found in the D1 Above Sill Zone (**Figure 4w**).

Community Structure

The community composition of the non-rare taxa showed significant differences between the depth zones and dives (ANOSIM Global R: 0.261, $p = 0.001$) (**Figure 5**). For D1, the nMDS plots and pairwise ANOSIM test indicated that the Basin and Intermediate Zones shared a similar community composition ($p > 0.05$). All other zones showed significant differences in community composition.

The SIMPER analysis revealed that for both dives, all zones except for D2-Above Sill had *P. squamatus*, *Hymedesmia* sp., and White Encrusting Sponge 1 within the top five contributing taxa (**Table 3**). Taxa from the Echinodermata were more common in D2 than D1. For both dives, the Basin and Above Sill

TABLE 2 | The presence (x) of all megafauna within each depth zone for Dive 1 (left) and Dive 2 (right) in Sognefjord, Norway.

				D1				*D2*			
Phylum	***Class (subclass*)***	***Taxon***	**Figure 4 *plate #***	***Basin***	***Intermediate***	***Above sill***	***Total %***	***Basin***	***Intermediate***	***Above sill***	***Total %***
Annelida	Echiura*	*Bonellia viridis* (Rolando, 1822)*	j	x			0.03				
		Maxmuelleria faex (Selenka, 1885)		x			0.17	x	x		0.16
	Sedentaria*	Serpulidae 1		x	x	x	0.36	x			0.22
		Serpulidae 2**	g					x			0.05
		Serpulidae 3**						x			0.01
	Undetermined	**Polychaeta 1***		x			0.03				
Arthropoda	Malacostraca	*Munida tenuimana* Sars, 1872	b, n, o, p	x	x		3.89	x			3.16
		Decapod 1	g	x	x		0.43	x			0.24
		Decapod 2		x			0.09		x		0.01
		Decapod 3**						x	x		0.21
		Decapod 4**						x			0.05
		Decapod 5*		x	x		0.03				
		Decapod 6		x	x		0.13	x			0.01
Brachiopoda		Brachiopoda 1	i	x	x		8.85	x			0.53
Chordata	Ascidiacea	Ascidiacea 1*		x			0.08				
	Holocephali	***Chimaera monstrosa* (Linnaeus, 1758)**		x			0.01		x		0.02
	Actinopterygii	***Sebastes viviparus* (Krøyer, 1845)****	v						x		0.02
		Coryphaenoides rupestris* (Gunnerus, 1765)*						x			0.01
	Undetermined	**Pisces 1***		x			0.01				
		Pisces 2*			x		0.01				
		Pisces 3**	x							x	0.01
		Pisces 4**								x	0.02
Cnidaria	Hexacorallia*	*Bolocera tuediae* (Johnston, 1832)		x	x		0.34	x	x		0.18
		Sagartia sp.	k	x	x		0.86	x			0.75
		Protanthea simplex* (Carlgren, 1891)*						x			0.01
		Actiniaria 1	h, s	x	x	x	0.35		x		0.07
		Actiniaria 2*		x			0.11				
		Actiniaria 3**						x	x		0.84
		Actiniaria 4**						x			0.04
		Actiniaria 5**								x	0.05
		Actiniaria 6**						x			0.12
	Octocorallia*	*Anthomastus grandiflorus* (Verrill, 1878)	b	x			0.29	x			0.34
		Kophobelemnon stelliferum (Müller, 1776)	q	x			0.08	x	x		0.03
		Virgularia mirabilis* (Müller, 1776)	r	x			0.01				
		Octocorallia 1**						x			0.02
		Octocorallia 2**						x			0.02
		Octocorallia 3*		x			0.02				
Echinodermata	Asteroidea	*Ctenodiscus crispatus* (Bruzelius, 1805)*		x	x	x	0.04				
		Henricia spp.		x	x	x	0.06	x	x	x	0.44
		Hymenodiscus coronata (Sars, 1871)	o	x			0.17	x			0.34

(Continued)

fmars-07-00393 June 6, 2020 Time: 15:25 # 7

TABLE 2 | Continued

				D1				D2			
Phylum	***Class (subclass*)***	***Taxon***	**Figure 4 *plate #***	***Basin***	***Intermediate***	***Above sill***	***Total %***	***Basin***	***Intermediate***	***Above sill***	***Total %***
		Poraniomorpha (Poraniomorpha) hispida* (M. Sars, 1872)*	f					x			0.01
		Pseudarchaster parellii (Düben & Koren, 1846)**							x	x	0.07
		Psilaster andromeda (Müller & Troschel, 1842)		x	x		0.04	x			0.01
		Pteraster militaris (O.F. Müller, 1776)		x	x	x	0.15	x	x	x	0.09
		Pteraster* sp.*						x			0.01
		Asteroidea 1	c	x			0.02	x			0.02
		Asteroidea 2**						x	x		0.02
		Asteroidea 3	i	x			0.01	x			0.02
		Asteroidea 4				x	0.01	x	x		0.02
		Asteroidea 5**						x		x	0.02
	Echinoidea	*Gracilechinus acutus* (Lamarck, 1816)	t, v, y	x	x	x	2.30	x	x	x	5.62
		Gracilechinus elegans (Düben & Koren, 1844)	s, x	x	x	x	1.83	x	x	x	1.26
		Echinoidea 1**	u					x	x	x	21.35
	Holothuroidea	*Bathyplotes natans* (M. Sars, 1868)		x			0.48	x			0.06
		Mesothuria intestinalis (Ascanius, 1805)		x	x		0.53	x			0.14
		Parastichopus tremulus (Gunnerus, 1767)	l, p, y	x	x	x	0.54	x	x	x	0.67
		Psolus squamatus (O.F. Müller, 1776)	e, j, m	x	x	x	23.09	x	x	x	19.31
	Ophiuroidea	*Ophiura albida* (Forbes, 1839)	g	x			0.02	x			0.03
		Ophiuroidea 1		x	x		0.37	x	x		0.18
		Ophiuroidea 2*		x			0.01				
		Ophiuroidea 3		x			0.01	x			0.01
Mollusca	Bivalvia	*Acesta excavata* (Fabricius, 1779)	d	x			0.11	x			1.27
	Polyplacophora	Polyplacophora 1*		x			0.01				
		Polyplacophora 2**						x			0.01
Porifera	Demospongiae	*Axinella infundibuliformis* (Linnaeus, 1759)	f	x		x	0.22	x	x		0.24
		Axinella rugosa (Bowerbank, 1866)		x	x		0.16	x			0.08
		Haliclona (Haliclona) urceolus (Rathke & Vahl, 1806)	t	x	x		0.90	x			0.25
		Hexadella dedritifera (Topsent, 1913)	g	x		x	0.01	x	x		0.84
		Hymedesmia sp.	g	x	x	x	11.34	x	x	x	7.98
		Phakellia ventilabrum (Linnaeus, 1767)	x	x	x	x	0.62	x	x		0.13
		Phakellia spp.	s, w	x	x	x	0.50	x			1.06
		Polymastia nivea (Hansen, 1885)		x	x	x	2.14	x	x		0.59
		Stryphnus fortis* (Vosmaer, 1885)		x			0.01				
		Stylocordyla borealis (Lovén, 1868)		x	x		0.97	X			0.14
		Thenea sp.*		x			0.02				
		Carnivorous Sponge 1*		x			0.04				
	Hexactinellida	*Asconema* aff. *foliatum* (Fristedt, 1887)	e	x			0.01	x			0.04
	Undetermined	**Orange Encrusting Sponge 1****						x			0.03
		White Encrusting Sponge 1	b, g	x	x	x	32.21	x	x	x	26.66
		Yellow Encrusting Sponge 1	g	x	x	x	1.48	x	x	x	2.26

(Continued)

TABLE 2 | Continued

				D1				D2			
Phylum	***Class (subclass*)***	***Taxon***	**Figure 4 *plate #***	***Basin***	***Intermediate***	***Above sill***	***Total %***	***Basin***	***Intermediate***	***Above sill***	***Total %***
		Brown Globular Sponge 1		x	x		0.09		x		0.01
		White Globular Sponge 1		x	x		0.17	x			0.06
		White Globular Sponge 2		x			0.03	x			0.03
		White Globular Sponge 3**						x			0.14
		Infundibuliform Sponge 1		x			0.02	x			0.02
		Infundibuliform Sponge 2		x	x		0.41	x			0.14
		Infundibuliform Sponge 3		x	x		0.03	x			0.03
		Infundibuliform Sponge 4**						x			0.01
		White Massive Sponge 1		x	x	x	0.72		x		0.03
		White Massive Sponge 2		x			0.12	x			0.05
		White Massive Sponge 3**						x			0.05
		Yellow Massive Sponge 1**						x			0.04
		Stalked Sponge 1		x	x		0.73	x			0.11
		White Verrucose Sponge 1**	a					x			0.08
		Indet Sponge 1*			x		0.01				
		Indet Sponge 2*		x			0.02				
		Indet Sponge 3*		x			0.02				
		Indet Sponge 4*		x			0.01				
Other		Unidentified 1*		x			0.13				
		Unidentified 2		x			0.04	x			0.01
		Unidentified 3		x		x	0.07	x			0.03
		Unidentified 4*		x			0.07				
		Unidentified 5*		x	x		0.54				
		Unidentified 6		x			0.05	x			0.31
		Unidentified 7**						x			0.14
		Unidentified 8**						x			0.06
		Unidentified 9*		x			0.01				
		Unidentified 10*		x			0.02				
		Unidentified 11*		x		x	0.03				
		Unidentified 12**						x			0.01
		Unidentified 13**						x			0.03
		Unidentified 14**						x			0.01
		Unidentified 15**						x			0.02
		Unidentified 16**						x			0.01
		Total abundance		9676	1449	432	11557	6837	3191	587	10615
		Total number of species		76	37	21	79	79	28	15	89
		Total number of images		275	32	13	320	165	18	8	191

*Total percentage (%) is the percentage of total abundance for each respective taxon. Asterisks denotes morphotaxa that were only observed within one dive, where * = Dive 1 and ** = Dive 2. Highlighted taxa are rare (<3 individuals) and dropped from statistical analyses.* ***Figure 4*** *plate reference indicates which* ***Figure 4*** *image plate that particular taxa can be found within. Bolded taxa are rare (<3 individuals) and dropped from statistical analyses.*

fmars-07-00393 June 6, 2020 Time: 15:25 # 9

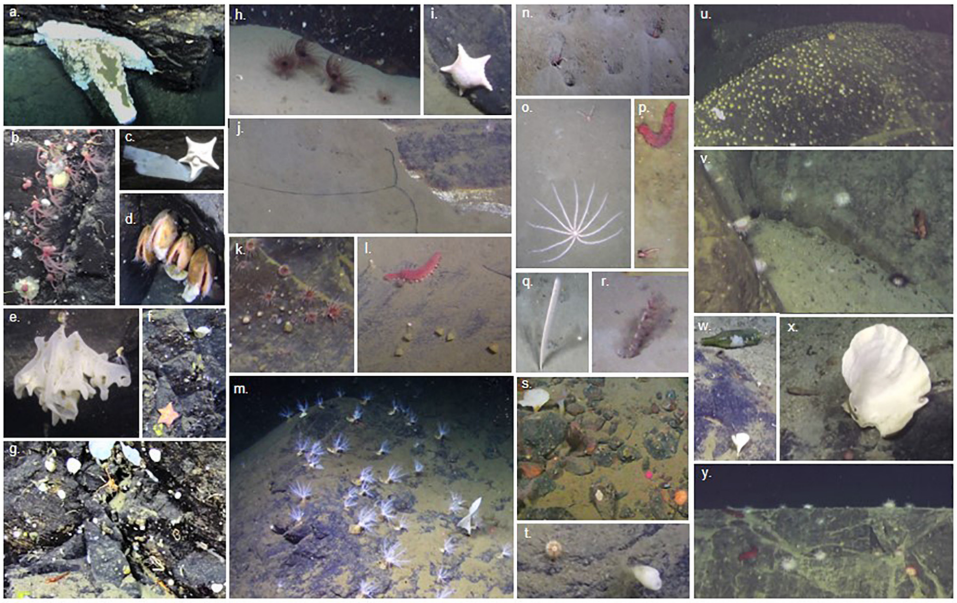

FIGURE 4 | Example of taxa and megafauna communities observed in Sognefjord, Norway. Panels **(a–g)** represents Basin Zone taxa on exposed hard substrate. Panels **(h–m)** displays Basin taxa in environments with both hard and soft substrate present. Panels **(n–r)** shows taxa common in soft sediment habitats. Panels **(s–u)** displays taxa within the Intermediate Zone. Panels **(v–y)** shows the Above Sill Zone. Refer to **Table 2** for the taxa identifications.

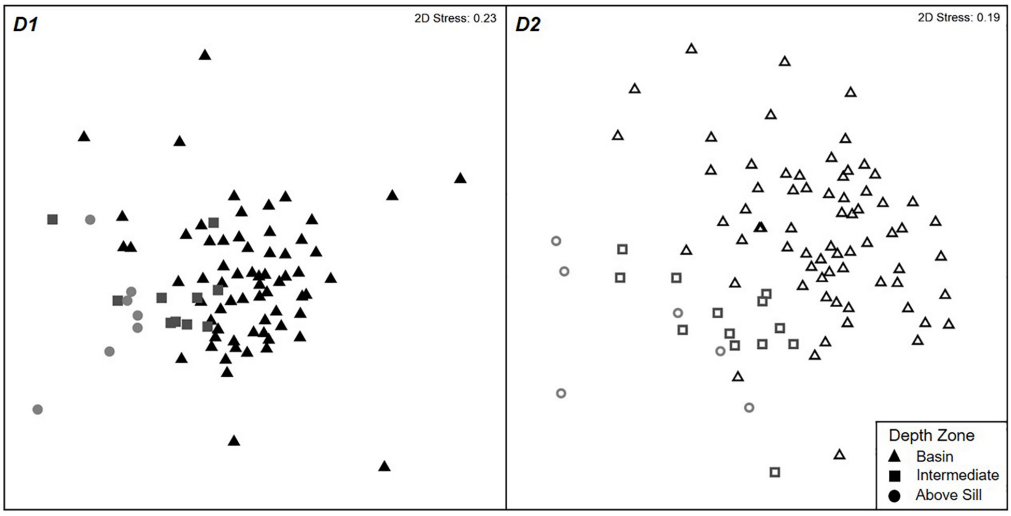

FIGURE 5 | Non-metric MDS ordination plots visualizing the Sørensen resemblances of the megafauna presence-absence data at different depth zones between Dive 1 (stress = 0.23; left) and Dive 2 (stress = 0.19; right). The distance between the points relates to the similarity of community composition at each depth, whereby the closer the points the more similar the community.

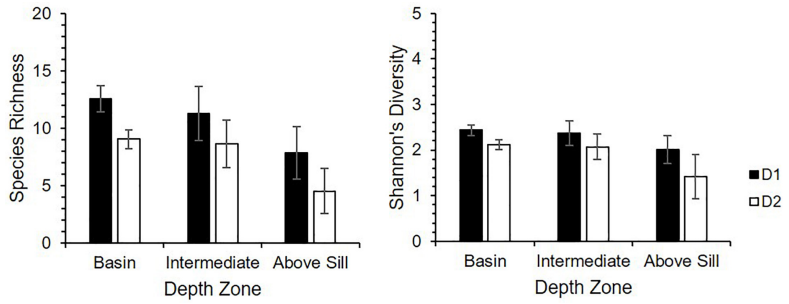

FIGURE 6 | Averaged diversity indices (species richness and Shannon-Wiener diversity index) per depth zone of the Dive 1 (D1; closed) and Dive 2 (D2; open) presence-absence community data in relation to the three depth zones in Sognefjord, Norway. Error bars represent 95% confidence intervals.

Zones had the largest difference in community composition (SIMPER, D1: Average dissimilarity = 63.03%; D2: Average dissimilarity = 78.87%). *Munida tenuimana*, *Parastichopus tremulus* (Gunnerus, 1767), Brachiopoda 1, *G. elegans*, and *Pteraster militaris* (O.F. Müller, 1776) contributed most to the differences between the Basin and Above Sill communities for D1. For D2, *M. tenuimana*, *P. squamatus*, *G. acutus*, *Hymedesmia* sp., and White Encrusting Sponge 1 contributed most to the differences between the two zones.

Diversity of Sognefjord's Megafauna Community

The diversity indices for the D2 (near-sill) zones were consistently lower than those of the corresponding zones in D1 (central) (**Figure 6**). For both dives, the diversity indices for the Above Sill Zones were lower than those of the deeper zones. The diversity indices all passed the Levene's test of homogeneity ($p > 0.05$), and the one-way ANOVA indicated that there were significant differences ($p < 0.001$) in the indices for D1 and D2 and their respective depth zones. The species richness and diversity were statistically significantly different between the D1 and D2 respective Basin Zones (Tukey HSD: $p < 0.01$). There was a significant difference in species richness between the Basin and Above Sill Zones for D1 (Tukey HSD: $p = 0.03$) and trend toward significant difference between the Basin and Above Sill Zones for D2 (Tukey HSD: $p = 0.069$). For the Shannon-Wiener diversity index, there was a significant difference between the Basin and Above Sill Zones for D2 (Tukey HSD: $p = 0.005$), and a significant difference between the Intermediate and Above Sill Zones (Tukey HSD: $p = 0.047$).

Environmental Influence on the Megafauna Community

Salinity and dissolved oxygen were the most influential variables on the diversity indices when considered separately, as revealed by GLMs (**Table 4** and **Supplementary Figure S3**), and depth had little influence alone. For species richness, the combination of depth and dissolved oxygen explained 10.85% of the deviance within the dataset. For diversity, the combination of depth, salinity, and dissolved oxygen explained 19.01% of the deviance in the dataset.

DISCUSSION

The present study provides a more recent overview of the Sognefjord megabenthic community composition than Bernd (1993) and focuses on the abiotic conditions more than was recently published by Buhl-Mortensen et al. (2017, 2020). The observations were similar to the findings from Bernd, where the deeper regions were characterized by sponges, holothurians and *Munida tenuimana*; however, in addition to sponges and holothurians, the shallower regions, particularly above the sill, had a higher abundance of urchins and anemones present.

Sognefjord shares some of the same fauna elements found in Hardangerfjord (Buhl-Mortensen and Buhl-Mortensen, 2014; Buhl-Mortensen et al., 2020). Both fjords are dominated by *Munida* sp., *Parastichopus tremulus*, *Psolus squamatus*, and *Phakellia* species. However, as stated by Buhl-Mortensen et al. (2020), and as was observed in this study, many of the taxa observed in Sognefjord are not present in Hardangerfjord.

As is common for fjord systems, many of the taxa observed are continental slope or deep-water species. For example, *Anthomastus grandiflorus* (Verril, 1878), which is considered a deep-sea species with a distribution of 457–1760 m (Molodtsova et al., 2008), was observed in small clusters on vertical rock walls at depths below 540 m, and *Kophobelemnon stelliferum* and *Virgularia mirabilis* (Müller, 1776) were both observed in low quantities in soft bottom regions at depths below 630 and 500 m, respectively. *Coryphaenoides rupestris* was observed in the Basin Zone of D2, a deep-water fish that has been found to have isolated subpopulations within Sognefjord (Delaval et al., 2018). A peculiar finding was the presence of very large specimens (up to 140 cm long) of the hexactinellid (glass) sponge *Asconema* aff. *foliatum* on vertical cliffs below 800 m depth at both dive sites, representing a group of species normally confined to deep and cold waters on the outer shelf off Northern Norway, or along the Reykjanes or Arctic Mid-Ocean Ridges (e.g., Tabachnick and Menshenina, 2007; Maldonado et al., 2016; Roberts et al., 2018).

TABLE 3 | Taxa responsible for the differences in the top 10 highest contributing megafauna within each zone identified in the similarity percentage analysis (SIMPER) for Dive 1 (Left) and Dive 2 (Right).

D1	*Morphotaxa*	*Sim/SD*	*%*	*Cumulative %*	*D2*	*Morphotaxa*	*Sim/SD*	*%*	*Cumulative %*
	Basin								
	*Psolus squamatus**	**1.99**	15.3	15.3		*Psolus squamatus**	**1.64**	20.2	20.2
	White Encrusting Sponge 1*	**1.78**	13.7	29.0		White Encrusting Sponge 1*	1.39	18.0	38.2
	*Munida tenuimana**	**1.67**	13.3	42.3		*Hymedesmia* sp.*	1.42	17.6	55.7
	Hymedesmia sp.*	**1.68**	12.3	54.6		*Munida tenuimana**	1.15	17.3	73.0
	Brachiopoda 1	0.91	7.8	62.4		Yellow Encrusting Sponge 1*	0.53	5.2	78.2
	Yellow Encrusting Sponge 1*	0.65	4.5	67.0		*Phakellia* spp.*	0.47	4.4	82.6
	Phakellia spp.*	0.63	4.5	71.5		*Gracilechinus acutus*	0.38	3.7	86.3
	Stylocordyla borealis	0.60	4.1	75.5		*Parastichopus tremulus*	0.23	1.6	87.9
	Haliclona (Haliclona) urceolus	0.56	3.6	79.2		Decapod 1	0.26	1.5	89.5
	Polymastia nivea	0.49	3.0	82.2		*Gracilechinus elegans*	0.26	1.5	91.0
	Intermediate								
	*Psolus squamatus**	**4.48**	16.6	16.6		*Parastichopus tremulus*	**1.99**	18.8	18.8
	White Encrusting Sponge 1*	**4.48**	16.6	33.1		White Encrusting Sponge 1*	1.4	15.2	34.1
	*Gracilechinus elegans**	**1.76**	13.4	46.5		*Gracilechinus acutus**	1.08	13.4	47.4
	Hymedesmia sp.*	**1.92**	12.0	58.5		*Psolus squamatus**	1.08	12.9	60.3
	Yellow Encrusting Sponge 1*	1.25	9.0	67.5		*Bolocera tuediae*	0.88	10.9	71.3
	Phakellia spp.	0.91	7.0	74.5		*Gracilechinus elegans**	0.87	9.7	81.0
	*Gracilechinus acutus**	0.91	6.8	81.3		*Hymedesmia* sp.*	0.73	6.8	87.7
	Polymastia nivea	0.69	4.8	86.1		Yellow Encrusting Sponge 1*	0.48	3.7	91.4
	Parastichopus tremulus	0.52	3.4	89.5		Echinoidea 1	0.36	3.5	94.9
	Haliclona (Haliclona) urceolus	0.53	3.2	92.6		Ophiuroidea 1	0.2	0.9	95.8
	Above Sill								
	White Encrusting Sponge 1*	**4.72**	23.4	23.4		*Gracilechinus acutus*	**3.55**	51.9	51.9
	Hymedesmia sp.*	**1.44**	16.0	39.4		Echinoidea 1	0.78	16.1	68.0
	*Parastichopus tremulus**	**1.46**	15.6	54.9		*Parastichopus tremulus**	0.46	12.7	80.7
	Gracilechinus elegans	**1.46**	15.6	70.5		Actiniaria 5	0.48	7.8	88.5
	Psolus squamatus	0.91	9.8	80.3		*Henricia* spp.	0.26	4.2	92.7
	Pteraster militaris	0.61	5.9	86.2		White Encrusting Sponge 1*	0.26	2.7	95.3
	Yellow Encrusting Sponge 1*	0.61	5.9	92.1		Yellow Encrusting Sponge 1*	0.26	2.4	97.8
	Phakellia spp.	0.62	5.2	97.2		*Hymedesmia* sp.*	0.26	2.2	100.0
	White Massive Sponge 1	0.22	1.1	98.4					
	Polymastia nivea	0.22	0.8	99.2					

Bolded taxa have the highest similarity (SIM)/standard deviation values (< 1.5). Asterisks (*) indicate taxa that were present in the respective depth zone for both dives.

Now we address each of this study's objectives in turn.

Community Patterns With Depth and Distance From the Sill

In general, much of the same taxa composition was observed in both dives for depth zones below the sill depth. The largest difference in megabenthic community composition was found between the deepest and shallowest zones for both dives, and similar trends have been observed in other surveys (Starmans et al., 1999; Sswat et al., 2015; Molina et al., 2019). In the present study, the Basin Zone was characterized more by sessile fauna (e.g., *P. squamatus, Acesta excavata, Hymenodiscus coronata*, and sponges) and *M. tenuimana*, whereas the Above Sill Zone was more dominated by echinoderms and anemones.

Contrary to numerous fjord and shelf-based studies (Buhl-Mortensen and Høisaeter, 1993; Holte et al., 2004; Webb et al., 2009; Włodarska-Kowalczuk et al., 2012; Sswat et al., 2015; Gasbarro et al., 2018; Molina et al., 2019), we find that communities at the shallowest depths (Above Sill Zone) and in closer proximity to the sill (D2) have the lowest number of species and diversity. Buhl-Mortensen et al. (2017, 2020) observed a similar trend in relation to the proximity to sill, where the outer region in Sognefjord had lower species richness compared to the middle region (Buhl-Mortensen et al., 2017, 2020). However, Buhl-Mortensen et al. (2020) observed a trend of decreasing species richness with increasing depth, which was not observed in the present study. The trends observed in the present study are more consistent with shelf community patterns observed by Starmans et al. (1999), where shallower regions contained a lower number of highly abundant taxa than the deeper stations and diversity increased with increasing water depth. This reduction in species richness and diversity in D2 (near-sill) and the areas above the sill could be driven by changes in water mass characteristics or increased physical stress on the

TABLE 4 | Summary statistics of the generalized linear models (GLMs) fitted to species richness and Shannon-Wiener diversity (Poisson distribution, quasi-Poisson error).

Diversity index	*Variable*	*Explained deviance*	*Residual deviance*	*% Explained*	*Pr(>|t|)*
Total number of species	Null		320.65		
	Depth (m)	0.99	319.66	0.31	0.461
	Salinity (psu)	14.75	305.90	4.60	0.006
	Dissolved oxygen (mL L^{-1})	22.13	298.52	6.90	0.001
	Chlorophyll *a* concentration ($\mu g\ L^{-1}$)	0.00	320.65	0.00	0.980
	Exposed hard substrate (%)	5.31	315.34	1.66	0.089
	Soft sediment (%)	2.43	318.22	0.76	0.245
	Silicon ($\mu mol\ L^{-1}$)	1.43	319.22	0.45	1.245
	Phosphate ($\mu mol\ L^{-1}$)	0.43	320.22	0.13	2.245
	Ammonium ($\mu mol\ L^{-1}$)	−0.57	321.22	−0.18	3.245
	Nitrate ($\mu mol\ L^{-1}$)	−1.57	322.22	−0.49	4.245
	Nitrogen dioxide ($\mu mol\ L^{-1}$)	−2.57	323.22	−0.80	5.245
	Best combination				
	Depth + dissolved oxygen	34.78	285.87	10.85	
Shannon-Wiener diversity	Null		21.09		
	Depth (m)	0.08	21.01	0.38	0.396
	Salinity (psu)	0.98	20.11	4.65	0.003
	Dissolved oxygen (mL L^{-1}	1.05	20.03	4.99	0.002
	Chlorophyll *a* concentration ($\mu g\ L^{-1}$)	0.00	21.08	0.01	0.865
	Exposed hard substrate (%)	0.41	20.68	1.95	0.056
	Soft sediment (%)	0.02	21.07	0.08	0.712
	Silicon ($\mu mol\ L^{-1}$)	1.43	319.22	0.45	1.245
	Phosphate ($\mu mol\ L^{-1}$)	0.43	320.22	0.13	2.245
	Ammonium ($\mu mol\ L^{-1}$)	−0.57	321.22	−0.18	3.245
	Nitrate ($\mu mol\ L^{-1}$)	−1.57	322.22	−0.49	4.245
	Nitrogen dioxide ($\mu mol\ L^{-1}$)	−2.57	323.22	−0.80	5.245
	Best combination				
	Depth + salinity + dissolved oxygen	2.07	19.01	9.83	

Percentage (%) explained is the percentage of null deviance in the data explained by the model.

benthic communities as the environmental conditions become less stable (Starmans et al., 1999; Jones et al., 2007).

Influence of Water Mass Properties and Sill Depth

The basin waters of both dives were fairly homogeneous (Storesund et al., 2017) and likely contributed to the homogeneity observed in the species composition in the deeper regions. Water mass properties (e.g., temperature, salinity, dissolved oxygen) play a significant role in megabenthic community composition (Buhl-Mortensen and Høisaeter, 1993; Williams et al., 2010; Meyer et al., 2015), which appears to be the case for Sognefjord as well. The changes in species composition appear to gradually occur around the transition between the basin and intermediate water masses, which is at approximately 300 m (Storesund et al., 2017), and more clearly near the sill depth. Studies have shown that sills affect water mass dynamics in ways that are critical to the structuring of benthic communities (Strømgren, 1970; Rüggeberg et al., 2011).

As Buhl-Mortensen and Høisaeter (1993) stated, the environment in fjord basins is influenced by the sill depth. With shallow sills, organic matter becomes trapped within the inner fjord below the sill depth and is not flushed out readily by the adjacent coastal water (Klitgaard-Kristensen and Buhl-Mortensen, 1999). As such, it is possible that organic input from renewal events and terrestrial sources (e.g., rivers, runoff, snowmelt, etc.) accumulates and has longer residence times in fjord basins (relative to shallower waters), providing food and nutrients to the benthic fauna below the sill depth. In a recent study of the Sognefjord by Buhl-Mortensen et al. (2020), the authors observed continuous detritus cover on sloping bedrocks at depths greater than 400 m and terrestrial organic material mixed in with the basin's soft sediment. The observed higher species richness and presence of deposit-feeding holothurians (*Bathyplotes natans* and *Mesothuria intestinalis*) and suspension-feeding *Hymenodiscus coronata* in the Basin Zone's soft bottom regions indicate availability of organic matter to the basin floor (Roberts and Moore, 1997; Flach et al., 1998; Amaro et al., 2015).

The vertical-falling particulate matter along the rocky walls observed in D1 is likely an important food source for many of the filter- and suspension-feeders (e.g., encrusting sponges, *Asconema* aff. *foliatum*, encrusting polychaetes, and *Acesta exacta*) residing on the vertical rock walls or under overhangs. Areas of flow acceleration owing to irregular topography (e.g., ridges, peaks, and other elevated substrate) experience increased

particle fluxes and are also likely important for suspension feeders (e.g., *Psolus squamatus*, *Phakellia* spp., *Phakellia ventilabrum*, and *Axinella infundibuliformis*) (Flach et al., 1998; Buhl-Mortensen et al., 2020). As is common in fjord environments, it is likely that the quality of food is lower in the basin and inner fjord compared to regions nearer to the sill (Klitgaard-Kristensen and Buhl-Mortensen, 1999). However, the higher species richness and presence of suspension- and deposit-feeders within the basin suggests the fauna may be adapted to the low quality of food, or that this is compensated by the stability of the basin environment. It is clear that a more rigorous study should be conducted to quantify and assess the quality of the organic matter supplied to the basin communities.

Environmental Dynamics

Depth, salinity, and dissolved oxygen were highlighted as important variables for the diversity indices. Depth acts as a proxy for other factors and it is likely that parameters which were not accounted for in the present study (e.g., food availability, particulate organic matter, localized hydrodynamics, pollution) are also influencing the patterns observed (Jones et al., 2007; Webb et al., 2009; Williams et al., 2010). Dissolved oxygen and percentage cover of substrate type varied most between the two dives, both of which are known to be critical for many benthic habitats (Holte et al., 2005; Williams et al., 2010; Sswat et al., 2015). The availability of hard substrate is important for sessile invertebrates (Williams et al., 2010; Buhl-Mortensen et al., 2012), and in this study, regions with exposed hard substrate were often covered with sponges, serpulid worm tubes, bivalves, and holothurians, similar to observations made by Gasbarro et al. (2018). However, for the Sognefjord megafauna community, there was not much difference in diversity and species richness between percent cover of hard substrate, soft bottom or mixed substrates. Therefore, it is possible that other factors like environmental dynamics or food availability is driving the patterns observed.

The megafauna communities at the mouth of the fjord (D2) showed lower diversity and species richness compared to central fjord (D1) communities. The central fjord environment is more stable than that of the fjord mouth, which is subjected to greater temporal variability (Storesund et al., 2017) due to exchange with the coastal ocean. Differences between the two dives are likely to be largely a result of horizontal environmental gradients along the fjord set up by biogeochemical and physical processes. For example, dissolved oxygen concentrations at the interface between the basin and intermediate water and at the sill depth differed slightly between dives (**Supplementary Figure S1**), the water being more oxygenated toward the sill (D2) because of the influence of coastal water. Dissolved oxygen concentrations at these depths are likely diminished with distance up-fjord by diffusion to and entrainment of vertically adjacent, less oxygenated waters and by the cumulative effects of (bacterial) respiration with distance from the sill (Storesund et al., 2017).

Areas with high environmental disturbance are characterized by an increase in mobile species, decrease in sessile fauna, and overall lower diversity (Włodarska-Kowalczuk et al., 2005; Jones et al., 2006; Webb et al., 2009; Hughes et al., 2010; Włodarska-Kowalczuk et al., 2012), as was observed in D2 and regions above the sill depth. The higher turbidity observed in D2 may have impacted the fjord benthic communities. Sessile suspension-feeding invertebrates are at a risk of smothering in areas with high quantities of suspended material in the water column (Jones et al., 2006; Kutti et al., 2015; Meyer et al., 2015). Fauna that are not limited by such conditions can persist (Rygg, 1985; Włodarska-Kowalczuk et al., 2005, 2012; Gasbarro et al., 2018), sometimes in high abundances, which could contribute to the increased abundance of echinoderms and reduced occurrences of sponges and sessile holothurians in the shallower regions of the fjord. Buhl-Mortensen et al. (2020) also noted that the shallower and silled regions of the fjord have relatively strong currents, whereas, the bottom currents in the basin were weak. This supports the general picture of gradients in environmental variability and stress within the fjord.

Future Implications

The environmental conditions in Sognefjord are affected by anthropogenic influences, such as cruise ships, fish farms, hydroelectric stations, and pollution (Manzetti and Stenersen, 2010). There is limited information concerning how such influences impact the Sognefjord community, though fish stocks have seen a considerable reduction (see Manzetti and Stenersen, 2010) and the shellfish community showed increased diarrhetic shellfish poisoning toxins with increased distance into the fjord (Ramstad et al., 2001).

A study by Rygg (1985) found that fjords with high pollutant concentrations were characterized by opportunistic species. Additional organic input from anthropogenic sources like fish farming or nutrient runoff may lead to hypoxic conditions in the fjord basin (Levin et al., 2009; Johansen et al., 2018). Johansen et al. (2018) predicted that increased organic matter within Norwegian fjord basins will lead to a dominance of deposit feeders, while the presence of suspension feeders will decline. Similar to the findings of Rygg (1985), Johansen et al. (2018) also found a shift in the community structure toward opportunistic species as a result of oxygen depletion and increased temperatures. Coastal water temperatures have been rising (Aure, 2016), which has led to increased temperatures within fjord basins (Johansen et al., 2018), resulting in changes in stratification and reduced oxygen supply. Long-time series temperature and organic input data are not readily available for Sognefjord, but if its environmental conditions follow the trajectories of other Norwegian fjords it is possible to predict a similar shift toward more opportunistic species. The present study does not include any temporal replication and the impact and future implications of anthropogenic-derived environmental change on the system is largely unknown and requires more research.

CONCLUSION

This study provides a recent overview of Sognefjord's megabenthic community near the sill of the fjord and the central fjord. Megafauna community composition was homogeneous within the fjord basin; however, species richness and diversity declined with proximity to the sill and with decreasing

water depth, particularly at the boundary between basin and intermediate water and at the sill depth. The fjord basin was characterized by *Psolus squamatus*, *Munida tenuimana*, *Phakellia* sp., *Acesta excavata*, and encrusting sponges. At shallower depths, the fjord was dominated by echinoderms, particularly in the dive closest to the sill. It is clear that more research is needed to understand the influence of shallow sills and water mass structure on fjord communities, as this study shows these features are important to Sognefjord's megabenthic communities. The clear stratification occurring between the basin water and intermediate water within Sognefjord would make it well suited for future surveys designed to monitor a wider range of environmental conditions or to understand future scenarios with stratification changes or deoxygenation.

DATA AVAILABILITY STATEMENT

The datasets generated for this study can be found at PANGAEA: https://doi.pangaea.de/10.1594/PANGAEA.914801.

AUTHOR CONTRIBUTIONS

HR, ER, and FM collected the video footage, CTD casts, and nutrient data for the study. HM annotated the video footage. HR provided fauna identifications. ER interpreted the *in situ* abiotic conditions and calculated the slope and distance from the sill for the transects. HM performed the statistical analysis. FM provided the sampling design, analysis and description for the nutrient contents. HM wrote the manuscript. All the authors read, edited, and approved the final manuscript.

FUNDING

The work leading to this publication has received funding from the European Union's Horizon 2020 Research and Innovation Programme through the SponGES project (Grant Agreement No. 679849). This document reflects only the authors' view and the Executive Agency for Small and Medium-sized Enterprises (EASME) is not responsible for any use that may be made of the information it contains. FM is supported by the Innovational Research Incentives Scheme of the Netherlands Organisation for Scientific Research (NWOVIDI Grant No. 016.161.360).

ACKNOWLEDGMENTS

The video footage and CTD casts were collected in 2017 on the RV *G.O. Sars* during a SponGES cruise, therefore, the crew of the RV *G.O. Sars* and the ROV *AEgir 6000* as well as participating SponGES team are thanked for their contribution to this project. EMODnet Bathymetry Consortium (2018) is acknowledged for the use of high-resolution bathymetry map for Sognefjord. The work presented here is dedicated to the memory of our friend and mentor HR, who spent his life improving global understanding of deep-sea sponges.

SUPPLEMENTARY MATERIAL

The Supplementary Material for this article can be found online at: https://www.frontiersin.org/articles/10.3389/fmars.2020.00393/full#supplementary-material

REFERENCES

Amaro, T., de Stigter, H., Lavaleye, M., and Duineveld, G. (2015). Organic matter enrichment in the whittard channel; its origin and possible effects on benthic megafauna. *Deep Sea Res. Part I Oceanogr. Res. Pap.* 102, 90–100. doi: 10.1016/j.dsr.2015.04.014

Aure, J. (2016). *Kystklima. Havforskningsrapporten-2016. Fisken Havet Særnummer 1-2016*. Bergen: Institute of Marine Research.

Bernd, C. (1993). A television and photographic survey of megafaunal abundance in Central Sognefjorden, Western Norway. *Sarsia* 78, 1–8. doi: 10.1080/00364827.1993.10413515

Blanchard, A. L., Feder, H. M., and Hoberg, M. K. (2010). Temporal variability of benthic communities in an Alaskan glacial fjord, 1971-2007. *Mar. Environ. Res.* 69, 95–107. doi: 10.1016/j.marenvres.2009.08.005

Buhl-Mortensen, L., Buhl-Mortensen, P., Dolan, M. F. J., Dannheim, J., Bellec, V., and Holte, B. (2012). Habitat complexity and bottom fauna composition at different scales on the continental shelf and slope of northern Norway. *Hydrobiologia* 685, 191–219. doi: 10.1007/s10750-011-0988-986

Buhl-Mortensen, L., Buhl-Mortensen, P., Glenner, H., and Båmstedt, U. (2017). Dyphavshabitater langt inn i landet: nye undersøkelser av havbunnen i sognefjorden. *Naturen* 6, 246–251.

Buhl-Mortensen, L., Buhl-Mortensen, P., Glenner, H., Båmstedt, U., and Bakkeplass, K. (2020). Chapter 19 -The inland deep sea - benthic biotopes in the Sognefjord. *Seafloor Geomorphol. Benthic Habit.* 5, 355–372. doi: 10.1016/B978-0-12-814960-7.00019-11

Buhl-Mortensen, L., and Høisaeter, T. (1993). Mollusc fauna along an offshore-fjord gradient. *Mar. Ecol. Prog. Ser.* 97, 209–224. doi: 10.3354/meps097209

Buhl-Mortensen, P., and Buhl-Mortensen, L. (2014). Diverse and vulnerable deep-water biotopes in the Hardangerfjord. *Mar. Biol. Res.* 10, 253–273. doi: 10.1080/17451000.2013.810759

Delaval, A., Dahle, G., Knutsen, H., Devine, J., and Salvanes, A. G. V. (2018). Norwegian fjords contain sub-populations of roundnose grenadier, Coryphaenoides rupestris, a deep-water fish. *Mar. Ecol. Prog. Ser.* 586, 181–192. doi: 10.3354/meps12400

Drewnik, A., Wêsławski, J. M., Włodarska-Kowalczuk, M., Łącka, M., Promińska, A., Zaborska, A., et al. (2016). From the worm's point of view. I: environmental settings of benthic ecosystems in Arctic fjord (Hornsund, Spitsbergen). *Polar Biol.* 39, 1411–1424. doi: 10.1007/s00300-015-1867-1869

EMODnet Bathymetry Consortium (2018). *EMODnet Digital Bathymetry (2018).* Available online at: https://www.emodnet-bathymetry.eu/data-products/acknowledgement-in-publications

Environmental Systems Research Institute [ESRI], (2016). *ArcGIS Release 10.4*. Redlands, CA: ESRI.

Flach, E., Lavaleye, M., de Stigter, H., and Thomsen, L. (1998). Feeding types of benthic community and particle transport across the N.W. European continental margin (Goban Spur). *Prog. Oceanogr.* 42, 209–231. doi: 10.1016/S0079-6611(98)00035-34

Gasbarro, R., Wan, D., and Tunnicliffe, V. (2018). Composition and functional diversity of macrofaunal assemblages on vertical walls of a deep northeast Pacific fjord. *Mar. Ecol. Prog. Ser.* 597, 47–64. doi: 10.3354/meps12599

Grasshoff, K., Erhardt, M., and Kremling, K. V. (1983). *Methods of Seawater Analysis*. Weinheim: John Wiley & Sons.

Helder, W., and De Vries, R. T. P. (1979). An automatic phenol-hypochlorite method for determination of ammonia in sea- and brackish waters. *Neth. J. Sea Res.* 13, 154–160. doi: 10.1016/0077-7579(79)90038-90033

Holte, B., Oug, E., and Cochrane, S. (2004). Depth-related benthic macrofaunal biodiversity patterns in three undisturbed north Norwegian fjords. *Sarsia* 89, 91–101. doi: 10.1080/00364820410003496

Holte, B., Oug, E., and Dahle, S. (2005). Soft-bottom fauna and oxygen minima in sub-arctic north Norwegian sill basins. *Mar. Biol. Res.* 1, 85–96. doi: 10.1080/17451000510019033

Hughes, S. J. M., Jones, D. O. B., Hauton, C., Gates, A. R., and Hawkins, L. E. (2010). An assessment of drilling disturbance on *Echinus acutus* var. *norvegicus* based on in-situ observations and experiments using a remotely operated vehicle (ROV). *J. Exp. Mar. Bio. Ecol.* 395, 37–47. doi: 10.1016/j.jembe.2010.08.012

Jantzen, C., Haussermann, V., Forsterra, G., Laudien, J., Ardelan, M., Maier, S., et al. (2013). Occurrence of a cold-water coral along natural pH gradients (Patagonia, Chile). *Mar. Biol.* 160, 2597–2607. doi: 10.1007/s00227-013-2254-2250

Johansen, P.-O., Isaksen, T. E., Bye-Ingebrigtsen, E., Haave, M., Dahlgren, T. G., Kvalø, S. E., et al. (2018). Temporal changes in benthic macrofauna on the west coast of Norway resulting from human activities. *Mar. Pollut. Bull.* 128, 483–495. doi: 10.1016/j.marpolbul.2018.01.063

Jones, D. O. B., Bett, B. J., and Tyler, P. A. (2007). Depth-related changes in the arctic epibenthic megafaunal assemblages of Kangerdlugssuaq, East Greenland. *Mar. Biol. Res.* 3, 191–204. doi: 10.1080/17451000701455287

Jones, D. O. B., Hudson, I. R., and Bett, B. J. (2006). Effects of physical disturbance on the cold-water megafaunal communities of the Faroe-Shetland Channel. *Mar. Ecol. Prog. Ser.* 319, 43–54. doi: 10.3354/meps319043

Klitgaard-Kristensen, D., and Buhl-Mortensen, L. (1999). Benthic foraminifera along an offs.hore-fjord gradient: a comparison with amphipods and molluscs. *J. Nat. Hist.* 33, 317–350. doi: 10.1080/002229399300281

Kutti, T., Bannister, R. J., Fossa, J. H., Krogness, C. M., Tjensvoll, I., and Sovik, G. (2015). Metabolic responses of the deep-water sponge *Geodia barretti* to suspended bottom sediment, simulated mine tailings and drill cuttings. *J. Exp. Mar. Biol. Ecol.* 473, 64–72. doi: 10.1016/j.jembe.2015.07.017

Levin, L. A., Ekau, W., Gooday, A. J., Jorissen, F., Middelburg, J. J., Naqvi, S. W. A., et al. (2009). Effects of natural and human-induced hypoxia on coastal benthos. *Biogeosciences* 6, 2063–2098. doi: 10.5194/bg-6-2063-2009

Maldonado, M., Aguilar, R., Bannister, R. J., Bell, J. J., Conway, K. W., Dayton, P. K., et al. (2016). "Sponge grounds as key marine habitats: a synthetic review of types, structure, functional roles, and conservation concerns," in *Marine Animal Forests: the Ecology of Benthic Biodiversity Hotspots*, eds S. Rossi, L. Bramanti, A. Gori, and C. Orejas. (Springer: Switzerland), 1–39.

Manzetti, S., and Stenersen, J. H. V. (2010). A critical view of the environmental condition of the Sognefjord. *Mar. Pollut. Bull.* 60, 2167–2174. doi: 10.1016/j.marpolbul.2010.09.019

Meyer, K. S., Sweetman, A. K., Young, C. M., and Renaud, P. E. (2015). Environmental factors structuring Arctic megabenthos – a case study from a shelf and two fjords. *Front. Mar. Sci.* 2:22. doi: 10.3389/fmars.2015.00022

Molina, E. J., Silberberger, M. J., Kokarev, V., and Reiss, H. (2019). Environmental drivers of benthic community structure in a deep sub-arctic fjord system. *Estuar. Coast. Shelf Sci.* 225:106239. doi: 10.1016/j.ecss.2019.05.021

Molodtsova, T. N., Sanamyan, N. P., and Keller, N. B. (2008). Anthozoa from the northern mid-atlantic ridge and charlie-gibbs fracture zone. *Mar. Biol. Res.* 4, 112–130. doi: 10.1080/17451000701821744

Murphy, J., and Riley, J. P. (1962). A modified single solution method for the determination of phosphate in natural waters. *Anal. Chim. Acta* 27, 31–36. doi: 10.1016/S0003-2670(00)88444-88445

Poremba, K., and Jeskulke, K. (1995). Microbial activity in the sediment of the Sognefjord (Norway). Helgoländ. Meeresuntersuchun. 49, 169-176.

RStudio Team (2019). *RStudio: Integrated Development.* Boston: R. RStudio, Inc. Available online at: http://www.rstudio.com/

Ramstad, H., Hovgaard, P., Yasumoto, T., Larsen, S., and Aune, T. (2001). Monthly variations in diarrhetic toxins and yessotoxin in shellfish from coast to inner part of the Sognefjord, Norway. *Toxicon.* 39, 1035–1043. doi: 10.1016/S0041-0101(00)00243-249

Renaud, P. E., Włodarska-Kowalczuk, M., Trannum, H., Holte, B., Wêsławski, J. M., Cochrane, S., et al. (2007). Multidecadal stability of benthic community structure in a high-Arctic glacial fjord (van Mijenfjord, Spitsbergen). *Polar Biol.* 30, 295–305. doi: 10.1007/s00300-006-0183-189

Roberts, D., and Moore, H. M. (1997). Tentacular diversity in deep-sea deposit-feeding holothurians: implications for biodiversity in the deep sea. *Biodivers. Conserv.* 6, 1487–1505. doi: 10.2307/1543510

Roberts, E. M., Mienis, F., Rapp, H. T., Hanz, U., Meyer, H. K., and Davies, A. J. (2018). Oceanographic setting and short-timescale environmental variability at an Arctic seamount sponge ground. *Deep Sea Res. Part I Oceanogr. Res. Pap.* 138, 98–113. doi: 10.1016/j.dsr.2018.06.007

Rüggeberg, A., Flögel, S., Dullo, W.-C., Hissmann, K., and Freiwald, A. (2011). Water mass characteristics and sill dynamics in a subpolar cold-water coral reef setting at Stjernsund, northern Norway. *Mar. Geol.* 282, 5–12. doi: 10.1016/j.margeo.2010.05.009

Rygg, B. (1985). Distribution of species along pollution-induced diversity gradients in benthic communities in Norwegian fjords. *Mar. Pollut. Bull.* 16, 469–474. doi: 10.1016/0025-326X(85)90378-90379

Sswat, M., Gulliksen, B., Menn, I., Sweetman, A. K., and Piepenburg, D. (2015). Distribution and composition of the epibenthic megafauna north of Svalbard (Arctic). *Polar Biol.* 38, 861–877. doi: 10.1007/s00300-015-1645-1648

Starmans, A., Gutt, J., and Arntz, W. E. (1999). Mega-epibenthic communities in Arctic and Antarctic shelf areas. *Mar. Biol.* 135, 269–280. doi: 10.1007/s002270050624

Storesund, J. E., Sandaa, R. A., Thingstad, T. F., Asplin, L., Albretsen, J., and Erga, S. R. (2017). Linking bacterial community structure to advection and environmental impact along a coast-fjord gradient of the Sognefjord, western Norway. *Prog. Oceanogr.* 159, 13–30. doi: 10.1016/j.pocean.2017.09.002

Strickland, J. D. H., and Parsons, T. R. (1968). A practical handbook of seawater analysis. *Bull. Fish. Res. Board Canada* 167, 1–31.

Strømgren, T. (1970). Emergence of *Paramuricea placomus* (L.) and *Primnoa resedaeformis* (Gunn.) in the inner part of *Trondheimsfjord* (West coast of Norway). *K. Norske Vidensk. Selsk. Skr.* 70, 1–5.

Svendsen, S. W. (2006). *Stratification and Circulation in Sognefjorden*. Master's thesis, University of Bergen, Bergen.

Sweetman, A. K., and Witte, U. (2008). Macrofaunal response to phytodetritus in a bathyal Norwegian fjord. *Deep Sea Res. Part I Oceanogr. Res. Pap.* 55, 1503–1514. doi: 10.1016/j.dsr.2008.06.004

Tabachnick, K. R., and Menshenina, L. L. (2007). Revision of the genus *Asconema* (Porifera : Hexactinellida : Rossellidae). *J. Mar. Biol. Assoc. U. K.* 87, 1403–1429.

Webb, K. E., Barnes, D. K. A., and Gray, J. S. (2009). Benthic ecology of pockmarks in the Inner Oslofjord, Norway. *Mar. Ecol. Prog. Ser.* 387, 15–25. doi: 10.3354/meps08079

Wei, T., and Simko, V. (2017). *R Package "Corrplot": Visualization of a Correlation Matrix (Version 0.84)*. Available online at: https://github.com/taiyun/corrplot

Williams, A., Althaus, F., Dunstan, P. K., Poore, G. C. B., Bax, N. J., Kloser, R. J., et al. (2010). Scales of habitat heterogeneity and megabenthos biodiversity on an extensive Australian continental margin (100-1100-m depths). *Mar. Ecol.* 31, 222–236. doi: 10.1111/j.1439-0485.2009.00355.x

Witte, U., Aberle, N., Sand, M., and Wenzhöfer, F. (2003). Rapid response of a deep-sea benthic community to POM enrichment: an in situ experimental study. *Mar. Ecol. Prog. Ser.* 251, 27–36. doi: 10.3354/meps251027

Włodarska-Kowalczuk, M., and Pearson, T. H. (2004). Soft-bottom macrobenthic faunal associations and factors affecting species distributions in an Arctic glacial fjord (Kongsfjord, Spitsbergen). *Polar Biol.* 27, 155–167. doi: 10.1007/s00300-003-0568-y

Włodarska-Kowalczuk, M., Pearson, T. H., and Kendall, M. A. (2005). Benthic response to chronic natural physical disturbance by glacial sedimentation in an Arctic fjord. *Mar. Ecol. Prog. Ser.* 303, 31–41.

Włodarska-Kowalczuk, M., Renaud, P. E., W?sławski, J. M., Cochrane, S. K. J., and Denisenko, S. G. (2012). Species diversity, functional complexity and rarity in Arctic fjordic versus open shelf benthic systems. *Mar. Ecol. Prog. Ser.* 463, 73–87. doi: 10.3354/meps09858

Zuur, A. F., Ieno, E. N., Walker, N. J., Saveliev, A. A., and Smith, G. M. (2009). *Mixed Effect Models and Extensions in Ecology with R. Statistics for Biology and Health*. New York, NY: Springer.

Conflict of Interest: The authors declare that the research was conducted in the absence of any commercial or financial relationships that could be construed as a potential conflict of interest.

frontiers

Supplementary Material

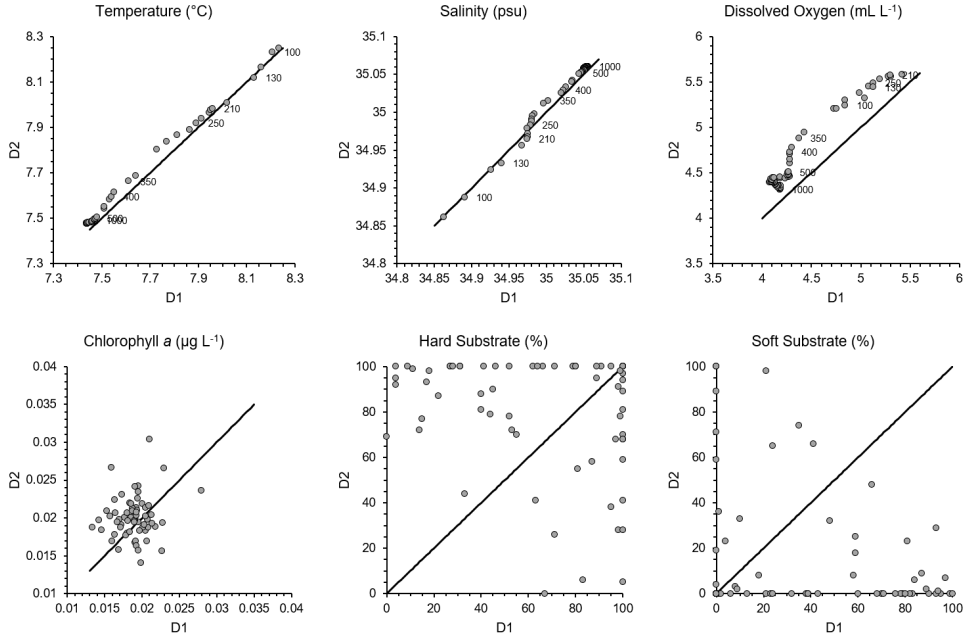

Supplementary Figure 1. Pairwise plot comparisons of temperature, salinity, dissolved oxygen, chlorophyll, percent exposed hard substrate, and percent soft sediment at corresponding depths in Dive 1 (D1) and Dive 2 (D2).

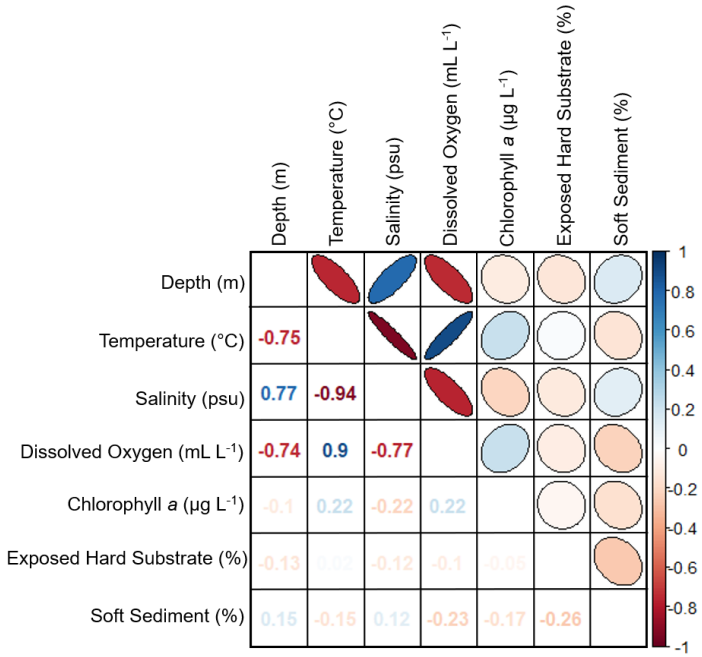

Supplementary Figure 2. Correlation matrix of the abiotic variables in Sognefjord, Norway.

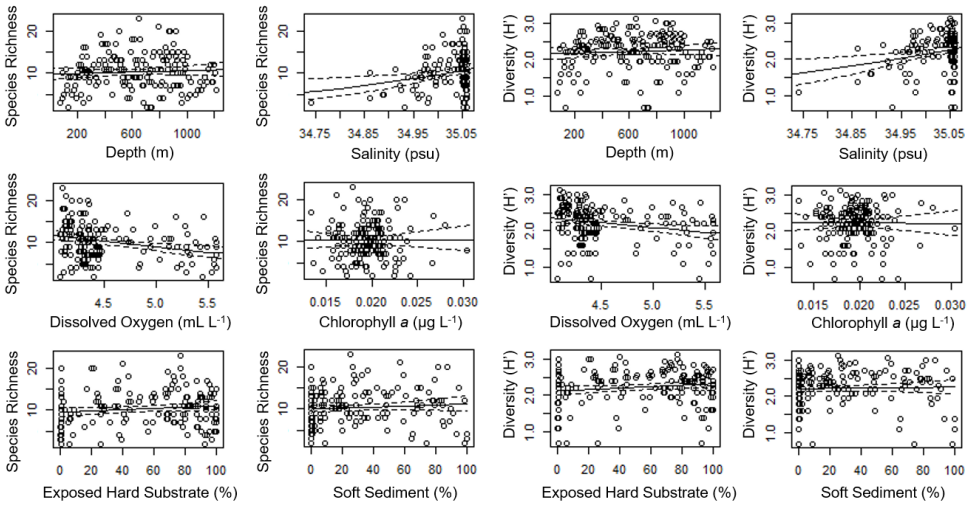

Supplementary Figure 3. Regression plots of the generalised linear models (GLMs; Poisson distribution, Quasipoisson error) fitted to species richness and Shannon Wiener diversity against the depth, salinity, dissolved oxygen, chlorophyll concentration, and percent cover of exposed hard substrate and soft sediment.

Paper 4

Graphic design: Communication Division, UiB / Print: Skipnes Kommunikasjon AS

uib.no

ISBN: 9788230865118 (print)
9788230859087 (PDF)